



Thèse présentée pour obtenir le grade de
Docteur de l'Université de Strasbourg

Discipline : Sciences Chimiques

Par Cristina CARPANESE

Utilisation simultanée de liaisons hydrogène et de coordination en tectonique moléculaire

Soutenue le 15 Juillet 2010 devant la commission d'examen :

Prof. Emmanuel Cadot (Université de Versailles St-Quentin)

Rapporteur externe

Dr. Joël Patarin (Université de Haute Alsace)

Rapporteur externe

Dr. Philippe Gros (Université Henri Poincaré – Nancy 1)

Examineur

Dr. Pierre Rabu (IPCMS CNRS – Strasbourg)

Examineur

Prof. Mir Wais Hosseini (Université de Strasbourg, IUF)

Co-directeur de thèse

Dr. Sylvie Ferlay-Charitat (Université de Strasbourg)

Co-directeur de thèse



Thèse présentée pour obtenir le grade de
Docteur de l'Université de Strasbourg

Discipline : Sciences Chimiques

Par Cristina CARPANESE

Simultaneous use of hydrogen and coordination bonds in molecular tectonics

Soutenue le 15 Juillet 2010 devant la commission d'examen :

Prof. Emmanuel Cadot (Université de Versailles St-Quentin)

Dr. Joël Patarin (Université de Haute Alsace)

Dr. Philippe Gros (Université Henri Poincaré – Nancy 1)

Dr. Pierre Rabu (IPCMS CNRS – Strasbourg)

Prof. Mir Wais Hosseini (Université de Strasbourg, IUF)

Dr. Sylvie Ferlay-Charitat (Université de Strasbourg)

Rapporteur externe

Rapporteur externe

Examineur

Examineur

Co-directeur de thèse

Co-directeur de thèse

“Era proprio idrogeno, dunque: lo stesso che brucia nel sole e nelle stelle,
e dalla cui condensazione si formano in eterno silenzio gli universi.”

Primo Levi, *Il sistema periodico*; 1975

“And so it was hydrogen, indeed: the very one that burns inside the sun and the stars,
the one from whom condensation the universe takes form in timeless silence.”

Dedicato ai miei nonni che
guardano le stelle e il formarsi degli universi:

Maria, Emilio, Assunta e Vincenzo

Aknowledgments

First of all I would like to thank Prof. Emmanuel Cadot, Dr. Joël Patarin, Dr. Philippe Gros and Dr. Pierre Rabu for their agreement to judge this work.

I would like to thank my supervisors: Prof. Mir Wais Hosseini for giving me the opportunity to work in his laboratory in Strasbourg and for his support, and Dr. Sylvie Ferlay for her patience, her willingness to listen and the many advices about scientific writing.

I would like to thank all the people that supported me during this, almost, four years Ph.D., especially for motivating and cheering me up during the difficult periods. First of all the colleagues I shared the office with, especially, my dear friend Dr. Elisabeth Kühn who shared with me many confidences and many bedrooms; the almost doctor Dmitry Pogozhev for the many chocolate tablets he gave me and for helping me with billion of informatics problems, as well as Thomas Lang who has my same passion for coffee and is all the time kind, calm and positive.

As well as, I would like to thank Dr. Fabrice Eckes for being the exact contrary of a Swiss watch! Dr. Stephan Baudron who is able to take pictures that make me appear gorgeous and for his good 'fluid' on the crystal growth. Dr. Aurélie Guenet for her kindness and for being a master in 'zen' philosophy. Dr. Cory Black for his support, nice chats and all tips about English language. Nicolas Delcey for his willingness and for being a lavish storyteller, Catherine Bronner for her discretion, kindness and sweetness and Dr. Marina Koziakova, from Russia for chemistry and for love.

In a random order, thank to All the students that, over these years, have traveled through the lab: Claude Wolter, Diana Salem, Aude Bartel, Alexandre Gehin, David Pocic, Mei-Jin Lin, Nicolas Zigon, Patrick Larpent, Fabien Sguerra, Alexander (Sasha) Ovsyannikov, Catalin Maxim, Julien Bourlier, Pierre Dechambenoit, Akram Hijazi, Jerome Ehrhart, Brandon Kilduff, Christy Lee, Yusuke (Suzuki) Yoshida, Katia Nchimi Nono, Arnaud Poirel, Domingo Salazar-Mendoza, Manuela Callari (my first student!), Gaetano (Tano) Di Stefano, Riccardo, Thibaut, Sébastien, Eric, Sarah, Antoine, Bertrand and all the others.

I would like to thank all the other members of the lab: Dr. Abdelaziz Jouaiti,, Dr. Mohamedally Kurmoo, for their scientific advice and the teatime chats, Dr. Ernest Graf, Dr. Stephan Baudron, Dr. Pierre Mobian for their scientific advice and their kindness, as well as Prof. Véronique Bulach for all support in meeting organization, Prof. Jean-Marc Planeix for teaching me how to take photo with a microscope and Prof. Marc Henry for his collaboration to my article. How to forget Nathalie Kyritsakas-Gruber both for teaching me how to use the XRD machine and for the patience dealing with my invisible, needle shaped crystals. I would like to thank also Françoise Rothut for all her administrative help when I arrived in Strasbourg and Valérie Rey for all the administrative help after I was in Strasbourg, their willingness and kindness.

I would like to thank the NMR services of the Université de Strasbourg, in particular Dr. Lionel Allouche and Jean-Daniel Sauer, and the MS service, in particular Dr. H  l  ne Nierengarten and Romain, for their scientific support.

And finally, I would like to thank the European Marie Curie Early Stage Training (EST) programme for financial support during the first three years of my Ph.D and all the students and professors of FuMaSSEC network in Barcelona and Nottingham for having made of all our meetings a great human experience.

I also would like to thank the people of SUAPS in particular all the students, teachers and friends of the climbing team for the nice moments spent in the gymnasium and for the ways climbed on artificial and rock cliffs, for having make me feeling well accepted and always at home. Thank you thus to Fr  d  ric Fauvet , Thomas Kedinger, Herv   Martz, Pascal, Henry, Alan, Meri, Lionel, Chlo  , Manon, Christine, G.-B., Aurelian, Mit-mat and many many others.

Thanks to Catherine and Marc-Andr   and all the people of the Chemin Neuf community of Strasbourg and, last but not the least, I do thank my dear Achille for his continuous psychological support and for believing in me and in my qualities. Grazie, senza di te non ce la avrei mai fatta!

This work was financially supported by the Marie-Curie Early Stage Training program.



Résumé de thèse

Utilisation simultanée de liaisons hydrogène et de coordination en tectonique moléculaire

Ce travail est centré sur la conception, la synthèse ainsi que l'étude structurale d'architectures supramoléculaires obtenues dans des conditions d'auto-assemblage, en utilisant les concepts de la "*tectonique moléculaire*", branche de la chimie supramoléculaire qui s'occupe de la conception et synthèse de nouveaux solides cristallins étendus à partir des syntons unitaires préalablement choisis. Un des enjeux de la chimie supramoléculaire¹ est la construction d'assemblées moléculaires en utilisant les phénomènes de reconnaissance moléculaire. Ces architectures, qui possèdent une organisation périodique à l'échelle microscopique, sont formées par association spontanée de composants moléculaires appelés "briques moléculaires de construction" ou tectons.

La conception et la construction de réseaux moléculaires hybrides *i.e.* comprenant à la fois des entités purement organiques et métalliques ou organo-métalliques suscitent beaucoup d'intérêt depuis quelques années. De très nombreuses assemblées, obtenues à partir de la mise en réseau de composants moléculaires, ont été reportées ces vingt dernières années, certaines d'entre elles présentant des propriétés physiques.²

Parmi les interactions intermoléculaires faibles utilisées pour l'assemblage des briques entre elles, la liaison hydrogène joue un rôle fondamental³ et exerce une grande influence sur l'organisation spontanée des matériaux moléculaires à l'état solide obtenus à partir de briques indépendantes. Ceci est lié à la sélectivité, la directionalité ainsi que la réversibilité de la liaison hydrogène, qui est devenue maintenant une interaction prépondérante dans le domaine de "l'ingénierie cristalline". Lorsqu'il s'agit de créer des réseaux moléculaires de plus en plus robustes, il devient important de combiner la liaison hydrogène avec des interactions électrostatiques fortes, donnant ainsi lieu à des "*liaisons hydrogène assistées par des charges*". Dans la littérature, plusieurs réseaux moléculaires construits à partir de liaisons hydrogène assistées par des charges ont déjà été décrits.^{4,5}

Une des motivations de ce projet de recherche est de préparer et d'analyser d'un point de vue structural de nouvelles architectures moléculaires hybrides organiques/inorganiques assemblées simultanément par des liaisons hydrogène et des liaisons de coordination. En effet, l'insertion de métaux de transition dans des systèmes supramoléculaires est très prometteur, grâce aux propriétés telles que l'oxydation/réduction, les propriétés optiques ou magnétiques.⁶

Pour ce faire, notre choix pour la construction de ces architectures portera, dans un premier temps, sur la reconnaissance de la paire cations bisamidinium (donneurs de liaison hydrogène) / anions carboxylates (accepteurs de liaison hydrogène). Sur

cette base, de nouveaux tectons organiques, des complexes métalliques et des réseaux assemblés par liaison de coordination et liaison hydrogène ont été synthétisés et sont décrits dans ce travail.

En particulier, il a été montré que les tectons cationiques organiques portant une ou plusieurs fonctions amidines protonées sont particulièrement bien adaptés pour la formation de réseaux moléculaires lorsqu'ils sont assemblés avec des tectons anioniques de type carboxylates, sulfonates ou polycyanometallates.⁷ Dans notre travail, les métaux de transition vont être introduits dans les réseaux sous forme de complexes métalliques obtenus à partir de ligands bifonctionnels présentant à la fois des sites de coordinations vis à vis des métaux ainsi que des sites de reconnaissance anioniques vis à vis des fonctions amidines, comme les carboxylates [fig.1]. Une autre voie explorée consistera à placer les fonctions amidines en périphérie du complexe métallique.

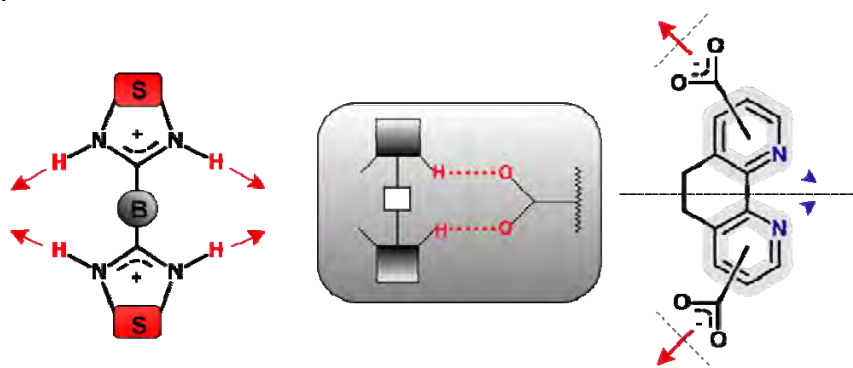


Figure 1. Représentation schématique de la reconnaissance moléculaire entre les tectons anioniques et les tectons cationiques.

Dans un deuxième temps, la reconnaissance plus complexe entre les fonctions carboxyliques et polypyridylamidique sera entreprise.

Ce travail sera ainsi structuré en trois chapitres, illustrant les différentes stratégies adoptées pour atteindre nos objectifs. La première et deuxième partie seront consacrée à la conception et synthèse préliminaire des complexes métalliques (metallatectons) ainsi que des ligands organiques (accepteurs de liaison hydrogène) et des cations bis-amidinium (donateurs de liaison hydrogène) utilisés comme tectons pour la formation des réseaux. L'étude structurale des réseaux comportant un nombre de composants allant de 2 à 4 sera effectuée. La troisième partie, enfin, sera consacrée au développement d'une nouvelle famille de ligands.

I. Tectons pour la construction de réseaux hybrides par liaison hydrogène

a) Tectons organiques

Afin de générer des réseaux moléculaires hybrides, une série de ligands N donneurs à partir de squelettes bipyridine, biquinoline, phenanthroline, présentant des

groupements carboxyliques à leur périphérie pouvant être engagés dans des liaisons hydrogène a été synthétisée.

De même, une famille de cations symétriques bisamidinium [fig. 2] a été utilisée, contenant différents espaceurs (S) [voir fig. 1] entre deux atomes d'azote de chaque groupement amidine cyclique ainsi que différents espaceurs (B) [voir fig. 1] pontant les deux groupements amidines. L'espaceur B éthylène (ou éthène), est particulièrement bien adapté d'un point de vue métrique pour la reconnaissance des espèces anioniques carboxylates, par liaison hydrogène en mode dihapto [voir fig. 1].^{8,9}

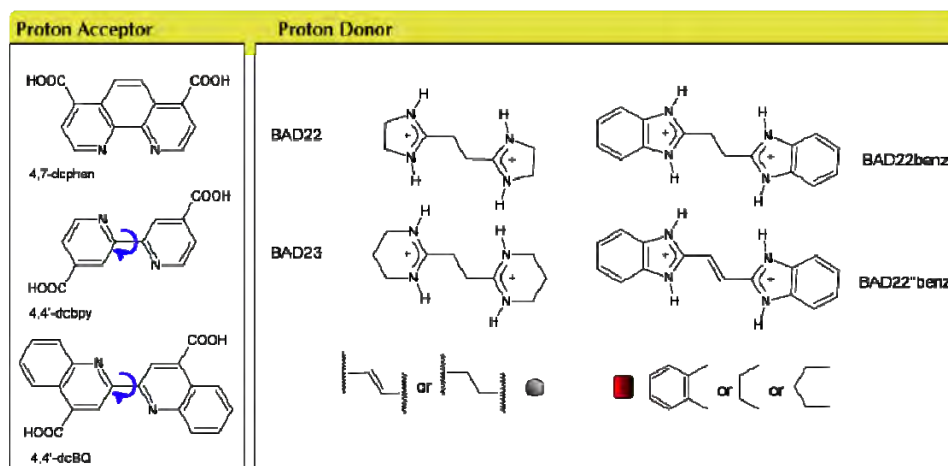


Figure 2. Association de ligands anioniques accepteurs de liaisons hydrogène /cations donneurs de liaisons hydrogène pour la formation de réseaux moléculaires.

La reconnaissance mutuelle de deux composants organiques a été tout d'abord testée pour la création de réseaux purement organiques dans le but de vérifier leur affinité. Par exemple, en combinant ce ligand avec le cation bisamidinium BAD23, un réseau monodimensionnel, assemblé par liaison hydrogène a été obtenu [cf fig. 6a].

Une deuxième stratégie consistant à insérer un groupement donneur de liaison hydrogène à la périphérie des ligands N donneurs a été entreprise. Le groupement choisi est bien évidemment un groupement amidine, qui pourra ensuite être utilisé avec des tectons organiques comportant des fonctions carboxylates (figure 3). Une stratégie analogue a déjà été explorée par Nocera *et al.*¹²

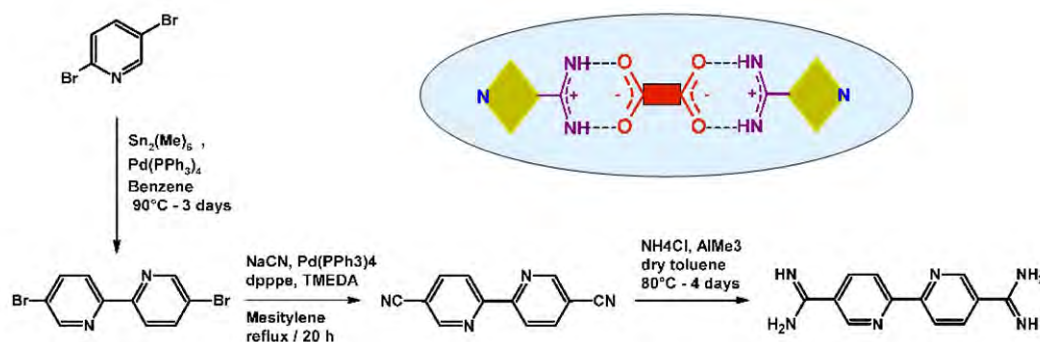


Figure 3. Schéma synthétique pour la formation de ligands comportant des fonctions amidines à la périphérie.

La synthèse d'un ligand dérivé de la 2,2'-bipyridine a été mise au point, où deux fonctions amidines en position 5 et 5' ont été greffées [fig. 3]. Ce ligand sera d'abord utilisé pour la formation de réseaux organiques avec des espèces dicarboxylates et ensuite pour la formation de réseaux hybrides en présence d'un métal.

b) Tectons métalliques

Une première stratégie synthétique envisagée pour la construction des réseaux consiste à générer dans un premier temps des espèces métalliques discrètes comportant à leur périphérie des accepteurs de liaisons hydrogènes (comme les carboxylates), qui, pour la formation de réseaux moléculaires hybrides, seront dans un deuxième temps combinés avec des tectons donneurs de liaisons hydrogène¹⁰.

Ainsi, de nouveaux complexes métalliques, obtenus à partir de ligands mono et di-carboxylate dérivés de 2,2'-bipyridine, de 4,7-phenanthroline ou de 2,2'-biquinoline, ont été synthétisés. Toute une série de complexes mononucléaires mono, di et trisubstitués par ces ligands mono- ou bis-carboxyl -ates (-iques) a été obtenue [voir fig. 4].

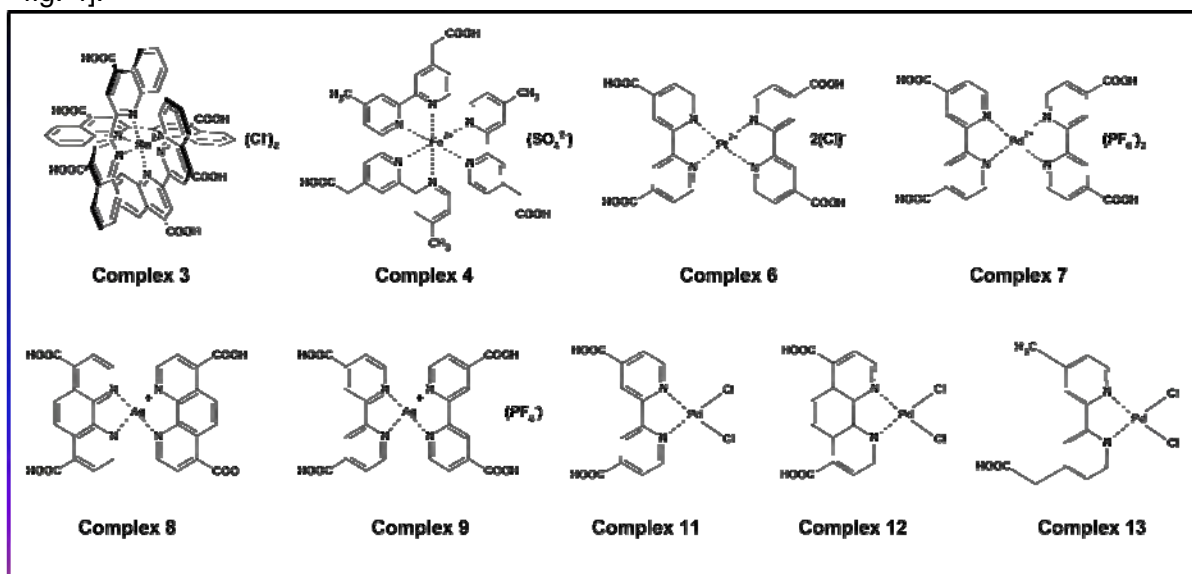


Figure 4. Famille de complexes obtenus, utilisés ensuite comme tectons pour la formations de réseaux par liaisons hydrogène.

Ces entités métalloganiques seront ensuite testées pour leur capacité à former des réseaux par liaison hydrogène lorsqu'elles sont combinées à des cations de type amidinium. Cette stratégie n'a malheureusement pas abouti aux résultats attendus.

c) Synthèse de réseaux moléculaires "one-pot"

La stratégie présentée ci-dessus implique l'utilisation séquentielle des différents composants (tectons). Une autre alternative peut reposer sur la synthèse "one pot" qui consiste à utiliser de manière simultanée tous les éléments à assembler de façon à générer une architecture périodique par une technique "d'auto-assemblage". Cette

méthode a été testée avec un ligand N donneur bifonctionnel symétrique: acide 1,10-phenanthroline-4,7-dicarboxylique et acide 2,2'-bipyridine-4,4'-dicarboxylique. Ces deux espèces diffèrent par le degré de libre rotation de la jonction entre les deux entités pyridine pour le ligand bipyridine [fig. 5].

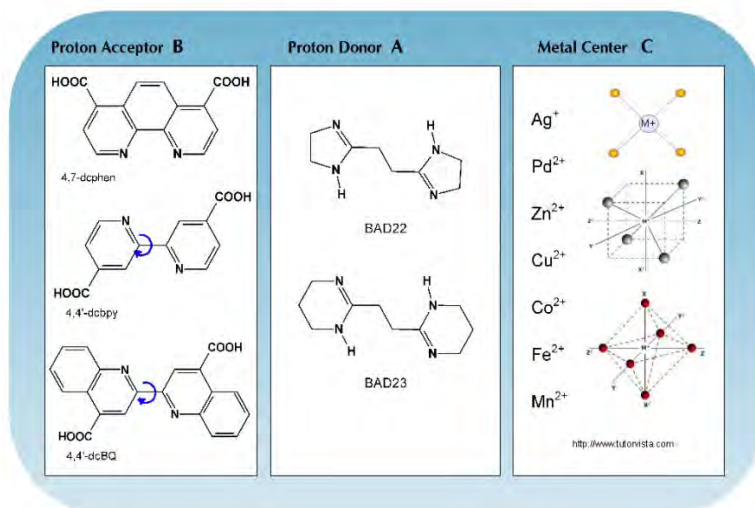


Figure 5. Les trois tectons utilisés pour la formation de réseaux hybrides utilisant la méthode 'one-pot'.

Un système à trois composants a donc été utilisé, combinant un tecton cationique de type bisamidinium (BAD23), un ligand N donneur comportant deux fonctions carboxylates ainsi qu'un sel métallique ; de cette manière des architectures bidimensionnelles à liaison hydrogène et à quatre composants ont été obtenues.

Afin de comprendre le mécanisme de formation de telles entités étendues, les différents nœuds de la structure ont été reproduits indépendamment (figure 6). Ensuite, en combinant le ligand acide 1,10-phenanthroline-4,7-dicarboxylique avec un sel d'argent, un complexe (complexe 8, figure 4) a été obtenu et caractérisé du point de vue structural, mettant en évidence une stœchiométrie métal/ligand égale à 2 [fig. 6].

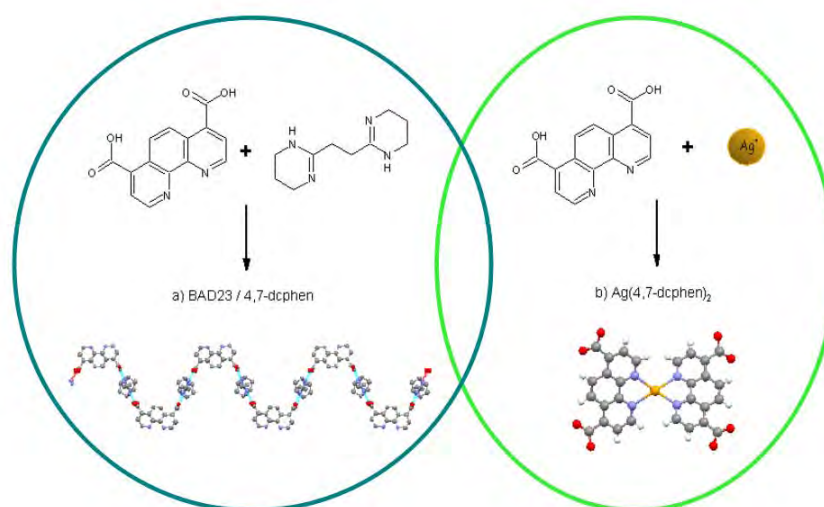


Figure 6. a) Réseau moléculaire purement organique à partir de cation organique et du ligand anionique; b) Complexe métallique (Ag) obtenu à partir du ligand anionique.

Ainsi, la formation de réseaux bidimensionnels assemblés par liaisons hydrogène, à partir de trois composants indépendants, est reliée à la reconnaissance individuelle des 3 composants entre eux (complexe d'argent en géométrie carré plan ainsi que le réseau organique 1D assemblé par liaisons hydrogène). L'intervention de ce complexe comportant 4 unités carboxylates coplanaires conduit à un réseau moléculaire bidimensionnel cationique [fig. 7].

La validité de ce principe de construction a été montrée par l'utilisation de différents sels d'argent (AgMF_6 , $M = \text{As}, \text{Sb}$ or P) et l'obtention et la caractérisation de trois réseaux isostructuraux assemblés par liaisons de coordination et liaisons hydrogènes¹¹, formés à partir de quatre composants.

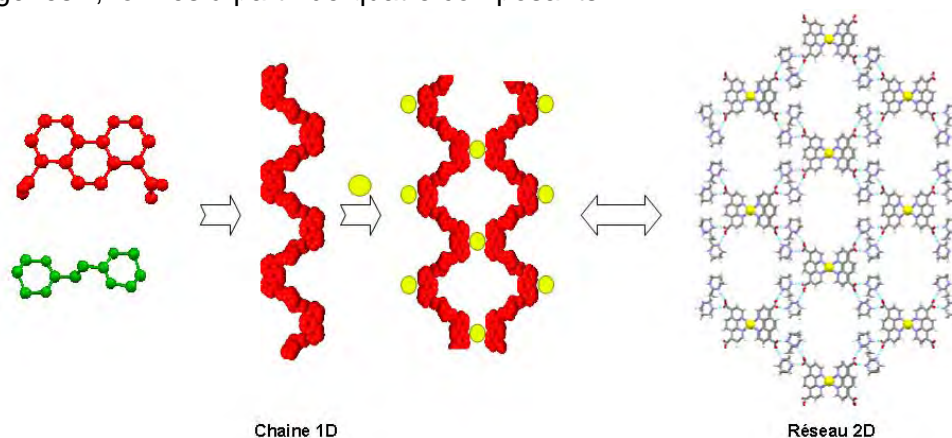


Figure 7. Schéma de formation du réseau bidimensionnel assemblé en "one-pot" à partir de trois composants individuels: Ag(I) , 4,7-dcphen, BAD23.

Un autre exemple de tel réseau à trois composants est donné dans ce travail : une architecture tridimensionnelle triplement interpénétrée est formée à partir du ligand anionique 1,10-phenanthroline-4,7-dicarboxylate, le dication bisamidinium et le cation Cu^{2+} . Un polymère de coordination 1D est obtenu à partir du cation cuivre et du ligand anionique, ces chaînes étant ensuite connectées par le dication bisamidinium. (fig. 8)

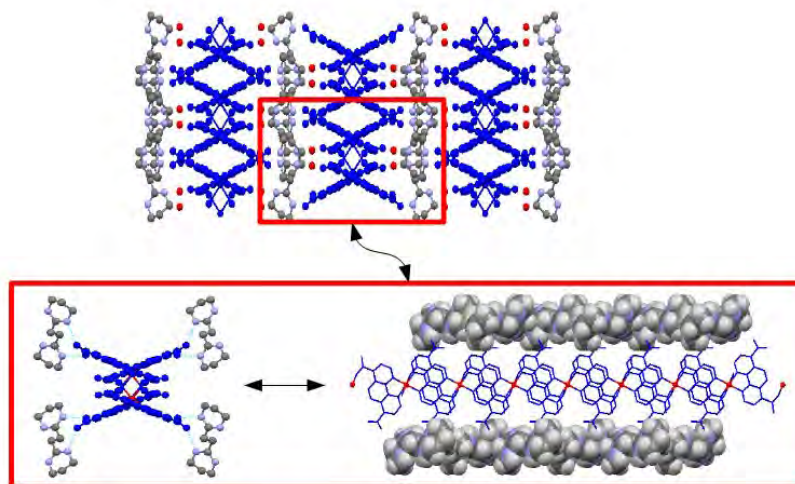


Figure 8. Schéma de formation du réseau tridimensionnel assemblé en "one-pot" à partir de trois composants individuels: Cu(II) , 4,7-dcphen, BAD23.

II. Autres réseaux moléculaires hybrides basés sur des complexes de carboxylates

Dans la deuxième partie, afin d'étudier le rôle joué par la position ortho (par rapport à N) de la fonction carboxylate dans les ligands anioniques N donneurs étudiés précédemment, ce qui autorise notamment la présence de carboxylates dans la sphère de coordination du métal, deux ligands à charpente hétérocyclique ont ainsi été synthétisés, basés sur l'entité 2,2'-bipyridine (acide 2,2'-bipyridine-6,6'-dicarboxylique) ou phenanthroline (acide 4,7-phenanthroline-2,9-dicarboxylique). La coordination des cations métalliques Zn(II), Cu(I/II) and Ag(I) par ces ligands 6,6'-dcbpy ou 2,9-dcphen ainsi que la formation de réseaux moléculaires en présence ou non d'une base ont été étudiées.

Nous avons pu obtenir une série de réseaux hybrides 1D et 2D basés sur la liaison hydrogène et formés à partir de complexes discrets. Figure 9 sont rassemblés les différentes géométries des complexes obtenus utilisés ensuite comme brique de construction en vue de la formation de réseaux cristallins.

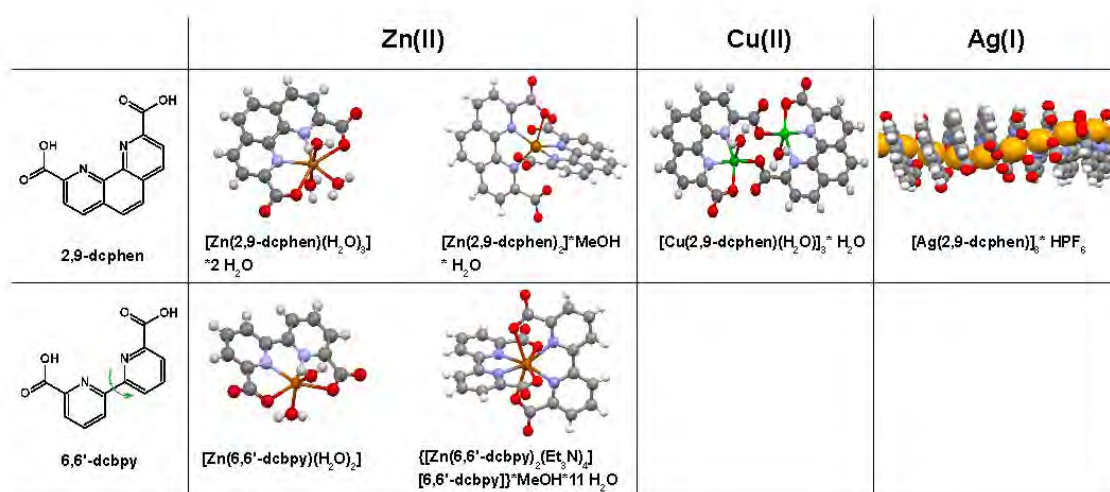


Figure 9. Complexes servant comme briques de construction pour des réseaux type liaison de coordination-liaison hydrogène et obtenus par combinaison de Zn(II), Cu(II) et Ag(I) avec les ligands acide 1,10-phenanthroline-2,9-dicarboxylique et acide 2,2'-bipyridine-6,6'-dicarboxylique.

L'utilisation du cation bisamidinium pour la formation de réseaux à trois composants n'a pas donné des résultats encourageants avec ce type de système, néanmoins par combinaison avec d'autres bases comme la triéthylamine, nous avons pu confirmer la formation d'un réseau moléculaire à trois composants.

De plus, la combinaison du ligand (2,9-dicarboxy-1,10-phenanthroline) avec un sel d'argent, ne conduit pas à la formation d'un complexe isolé, mais à la formation d'un polymère de coordination monodimensionnel basé sur des interactions Ag-Ag [fig. 10]. Dans cette architecture hélicoïdale remarquable, les distances Ag-Ag ($d_{Ag-Ag} \approx 3 \text{ \AA}$) sont très faibles et témoignent d'interactions d^{10} - d^{10} . Ces réseaux, dont les cristaux

sont stables, vont être étudiés pour leur propriétés des mesures de conductivité à l'état solide.

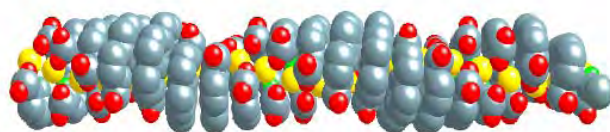


Figure 10. Réseau monodimensionnel hélicoïdal obtenu à partir de la coordination de l'acide 1,10-phenanthroline-2,9-dicarboxylique avec un sel d'argent.

III. Réseaux et complexes basés sur des ligands polypyridylamidiques

Enfin, dans une troisième et dernière partie, nous nous sommes intéressés à une nouvelle famille de ligands symétriques donneurs/accepteurs de liaisons hydrogènes basés sur des squelettes de type 2,2'-bipyridine, 2,2'-biquinoline ou 1,8-naphthyridine portant des groupements pyridyles. Ces ligands N donneurs sont chélatant vis à vis des métaux de transition [Zone 1 en figure 11a], et présentent des sites de reconnaissance pour les groupements organiques de type acide carboxylique^{13,14,15} [Zone 2 en figure 11a], ces deux motifs pouvant être particulièrement intéressants pour la formation de réseaux hybrides.

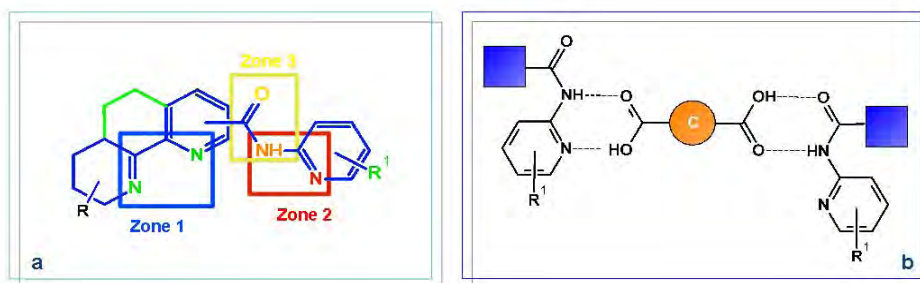


Figure 11. Stratégie de conception de ligands polypyridylamidiques N donneurs et schéma de reconnaissance par liaison hydrogène entre groupements acides carboxyliques et N-pyridyl amine en vue de la construction de réseaux moléculaires.

Cette dernière stratégie, illustrant de formation de réseaux moléculaires assemblés à partir de liaisons hydrogène, repose sur l'augmentation de la denticité des ligands organiques en synthétisant de nouvelles espèces polypyridylamidiques symétriques [fig. 12].

Comme ceux précédemment décrits, ces ligands seront ensuite utilisés: 1) pour la formation de réseaux purement organiques à deux composants par auto reconnaissance avec des diacides carboxyliques; 2) pour la formation de complexes discrets à base de métaux de transition; 3) pour la formation de réseaux hybrides organiques/inorganiques.

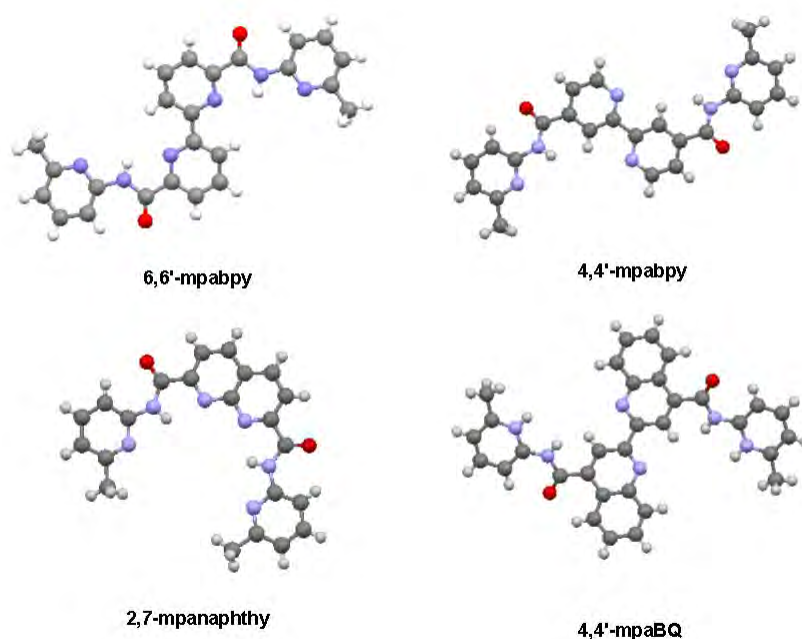


Figure 12. Ligands N donneurs polypyridylamidiques synthésés et utilisés pour la reconnaissance par liaison hydrogène de groupements carboxylates

Chaque nouveau ligand a été caractérisé par les méthodes classiques ainsi qu'à l'état solide par rayons X pour obtenir des informations conformationnelles. Entre autres, la formation d'un réseau hélicoïdal racémique entre le ligand 4,4'-bis-[N-(6-méthylpyridin-2-yl)carbamoyl]2,2'-bipyridine et l'acide ferrocène dicarboxylique représente un premier résultat significatif.

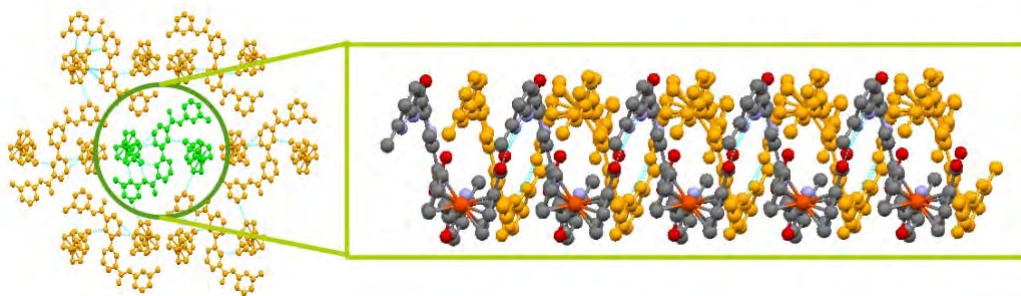


Figure 13. Double chaîne monodimensionnelle hélicoïdale entrelacée, formée par $\{[4,4\text{-dcbpy}]_2[\text{Ferroxdc}]_2\}$

Références

1. J. M. Lehn; *Supramolecular chemistry: concepts and perspectives*; VCH, **1995**
2. A. M. Beatty; *Coord. Chem. Rev.* **2003**, *246*, 131-143
3. G. R. Desiraju; *Angew. Chem.*, **1995**, *107*, 2541-2558
4. J.C. MacDonald, P.C. Dorrestein, M.M. Pilley, M.M. Foote, J.L. Lundburg, R.W. Henning, A.J. Schultz, J.L. Manson; *J. Am. Chem. Soc.*, **2000**, *122*, 11692-11702
5. A. Moghimi, M. Ranjbar, H. Aghabozorg, F. Jalali, M. Shamsipur, G.P.A. Yap, H. Rahbarnoohi; *J. Molec. Structure*, **2002**, *605*, 133-149
6. S. L. James; *Chem. Soc. Rev.*, **2003**, *32*, 276-288
7. M. W. Hosseini; *Acc. Chem. Res.* **2005**, *38*, 313-323
8. O. Felix, M. W. Hosseini, A. De Cian; J. Fischer, *New J. Chem.*, **1998**, 1389-1393
9. Olivier Felix; Thèse de doctorat, Univ. Louis Pasteur, **1999**
10. D. Braga, L. Maini, F. Grepioni, A. De Cian, O. Felix, J. Fischer, M.W. Hosseini; *New J. Chem.*, **2000**, *24*, 547-553
11. C. Carpanese, S. Ferlay, N. Kyrtsakas, M. Henry, M. W. Hosseini; *Chem. Comm.*, **2009**, 6786-6788
12. J. Rosenthal, J.M. Hodgkiss, E.R. Young, D.G. Nocera et al., *J. Am. Chem. Soc.*, **2006**, *128*, 10474-10483
13. T. Kato, O. Ihata, S. Ujiie, M. Tokita, J. Watanabe; *Macromolecules*, **1998**, *31*, 3551-3555
14. B. König, O. Möller, P. Bubenitschek; *J. Org. Chem.*, **1995**, *60*, 4291-4293
15. S. J. Geib, C. Vicent, E. Fan, A. D. Hamilton; *Angew. Chem. Int. Ed.*, **1993**, *32*, 119-121

Table of contents

Table of contents

Chapter 1 – Introduction.....	1
I.1 Introduction: Supramolecular chemistry and its context.....	4
I.1.1 Definition and historical background.....	4
I.1.2 Basic concepts in supramolecular chemistry.....	7
I.1.2.1 Molecular recognition.....	7
I.1.2.2 Self-assembly and self-organization.....	8
I.1.2.3 Supramolecular interactions.....	9
I.2 Molecular Tectonics vs Crystal Engineering.....	12
I.3 Molecular Tectonics and molecular networks.....	12
I.3.1 Definition and concepts in molecular tectonics.....	12
I.3.2 Generalities and dimensionality of molecular networks.....	13
I.3.2.1 O-D discrete assemblies.....	15
I.3.2.2 1-D networks.....	16
I.3.2.3 2-D networks.....	18
I.3.2.4 3-D networks.....	19
I.4 Crystal engineering and design of tectons.....	21
I.4.1 Analysis and assembly prediction.....	22
I.4.1.1 Coordination networks: prediction.....	22
I.4.1.2 Hydrogen bonded networks: prediction.....	23
I.4.2 Crystal formation process.....	25
I.4.2.1 Crystal nucleation.....	25
I.4.2.2 Crystal growth.....	26
I.4.2.3 Polymorphism: a thermodynamic approach.....	27
I.5 Hydrogen and coordination bonding in molecular networks.....	29
I.5.1 Functional networks based on coordination bond.....	29
I.5.1.1 Generalities.....	29
I.5.1.2 Examples of multifunctional networks.....	29
I.5.2 Functional networks based on hydrogen bond.....	31
I.5.2.1 Generalities.....	31
I.5.2.2 The role of hydrogen bond in molecular recognition.....	32
I.5.2.3 Functional organic networks based on hydrogen bond.....	33
I.5.2.4 Functional networks based on mixed coordination bond and H-bond.....	34
I.6 Purpose of this work.....	36
Chapter 2 – Tectons for H-bonded hybrid networks and isolated complexes.....	37
II.1 Generalities, objectives and strategies.....	39
II.2 State of the art in the literature.....	41
II.2.1 Two component systems: Self-complementary metallic complexes.....	42

II.2.2 Three component systems.....	45
II.2.2.1 Pyridinedicarboxylates based assemblies.....	45
II.2.2.2 Imidazole based assemblies.....	46
II.2.2.3 Other assemblies.....	46
II.2.3 Earlier work in the lab.....	47
II.2.3.1 Two components systems.....	47
II.2.3.2 Three components systems.....	49
II.3 Chosen components and nodes	51
II.3.1 Component A: Bisamidinium cation, H bond donor	51
II.3.1.1 Description of the tecton.....	51
II.3.1.2 Bisamidine and bisamidinium synthesis.....	54
II.3.2 Component B: General considerations about amidinium/carboxylate recognition events.....	57
II.3.3 Component B: Carboxylates bearing ligands, H-bond acceptor.....	58
II.3.3.1 Description of the tectons.....	58
II.3.3.2 Synthesis of the tectons.....	59
II.3.3.3 Characterization of the tectons.....	60
II.3.4 Component B: Amidine bearing ligands, H-bond donor.....	62
II.3.4.1 Synthesis of the tecton.....	62
II.3.4.2 Characterization of the tecton.....	63
II.3.5 Component C: Metal core.....	64
II.4 Synthesis of transition metallatectons.....	65
II.4.1 Mono-substituted metallatectons $M^{\text{II}}LX_2$	65
II.4.1.1 General description.....	65
II.4.1.2 Literature outcome.....	66
II.4.1.3 Obtained results.....	68
II.4.2 Di-substituted tectons $M^{\text{II}}L_2 \cdot X_2$	69
II.4.2.1 General description.....	69
II.4.2.2 Literature outcome.....	69
II.4.2.3 Obtained results.....	71
II.4.3 Tri-substituted tectons.....	73
II.4.3.1 General description.....	73
II.4.3.2 Literature outcome.....	73
II.4.3.3 Obtained results.....	74
II.4.4 Tetra-substituted tectons.....	75
II.4.5 Metallatectons as building blocks for H-bonded coordination networks: some conclusions.....	77
II.5 Formation of two components assemblies.....	77
II.5.1 Choice and description of the nodes - Choice of bis-amidinium tectons.....	78
II.5.2 Formed Organic H-bonded networks.....	79
II.5.2.1 1D-network obtained upon combination of BAD23 with [4,4'-dcBQ]...80	

II.5.2.2 1D-network obtained upon combination of BAD23 with [4,7-dcphen].....	81
II.5.2.3 2D-network obtained upon combination of Bad22 with [4,4'-dcbpy].....	82
I.5.2.4 General conclusion concerning the (A+B) formation.....	83
II.6 Hybrid organic/inorganic networks	84
II.6.1 Network conception	84
II.6.2 2-D networks with BAD23, 4,7-dcphen and Ag(I).....	85
II.6.2.1 Structural analysis.....	85
II.6.2.2 XRPD and thermal studies.....	88
II.6.3 3-D network with BAD23, 4,7-dcphen and Cu(II).....	89
II.6.3.1 Structural analysis.....	90
II.6.4 Conclusions on the presented three components hybrid networks.....	92
II.7 General conclusions.....	92

Chapter 3 – Hybrid networks based on carboxylates complexes.....93

III.1 Coordination abilities of the used tectons.....	95
III.2 Literature background.....	96
III.2.1 Coordination complexes and networks based on 6,6'-dcbpy.....	96
III.2.2 Coordination complexes and networks based on 2,9-dcphen.....	98
III.2.2.1 Networks based on metal + ligand.....	98
III.2.2.2 Networks based on metal + ligand +base.....	100
III.3 Used tectons for coordination complexes and networks formation.....	101
III.3.1 Ligand synthesis.....	101
III.3.2 Structural characterization.....	101
III.4 Hybrid Networks based on Carboxylates Complexes.....	103
III.4.1 Context.....	103
III.4.1.1 Network summary.....	104
III.4.2 Structural Analysis.....	104
III. 4.2.1 Hybrid networks based on zinc(II).....	104
III. 4.2.2 Hybrid network based on Copper(II).....	109
III. 4.2.3 Coordination network based on Silver(I).....	112
III.5 Conclusions.....	114

Chapter 4 – Networks and complexes based on polyamides ligands.....117

IV.1 Aim of the work.....	119
IV.2 Design of ligands and networks conception.....	119
IV.2.1 Ligand design.....	119
IV.2.2 Networks conception.....	120
IV.2.2.1 Combination with dicarboxylic units as H bond acceptors.....	121

IV.2.2.2	Combination with transition metal ions.....	122
IV.2.2.3	Combination with transitions metal ions and dicarboxylic acids H bond acceptors.....	122
IV.2.3	Project.....	122
IV.3	Literature examples.....	123
IV.3.1	Purely organic systems with pyridine carboxamide and carboxylic acids.....	123
IV.3.2	Systems involving transition metals.....	124
IV.4	Target polyamides ligands.....	125
IV.4.1	Ligands synthesis.....	125
IV.4.1.1	[4,4'-mpabpy] and [6,6'-mpabpy].....	126
IV.4.1.2	[2,7-mpanaphthy].....	127
IV.4.1.3	[4,4'-mpaBQ].....	127
IV.5	Structural study of the four ligands.....	128
IV.5.1	Ligand 2,7-Bis-[N-(6-methylpyridin-2-yl)carbamoyl]-1,8-naphthyridine - [2,7-mpanaphthy].....	128
IV.5.2	Ligand 4,4'-Bis-[N-(6-methylpyridin-2-yl)carbamoyl]-2,2'-bipyridine - [4,4'-mpabpy].....	130
IV.5.3	Ligand 6,6'-Bis-[N-(6-methylpyridin-2-yl)carbamoyl]-2,2'-bipyridine - [6,6'-mpabpy].....	131
IV.5.4	Ligand 4,4'-Bis-[N-(6-methylpyridin-2-yl)carbamoyl]-2,2'-biquinoline - [4,4'-mpaBQ].....	132
IV.5.5	Some conclusions.....	133
IV.6	Structural study of the ligands with dicarboxylic acids.....	134
IV.6.1	[4,4'-mpabpy] and Ferrocenedicarboxylic acid.....	135
IV.7	Structural study of the ligands with transition metals.....	137
IV.7.1	[2,7-mpanaphthy] and Cu(II).....	137
IV.7.2	[4,4'-mpabpy] and Mn(II).....	138
IV.7.3	[4,4'-mpabpy] and Pt(II).....	140
IV.8	Conclusions.....	141
Chapter 5 – General conclusions and perspectives.....		143
V.1	General conclusions and perspectives.....	145
V.1.1	Hybrid networks based on carboxylates ligands and bisamidinium cations (Chapter II and III).....	145
V.1.2	Hybrid networks based on polyamides ligands (Chapter IV).....	149
Chapter 6 – Experimental section.....		151
VI.1	Generalities.....	153
VI.2	Synthesis of ligands.....	156

VI.3 Synthesis of complexes.....179

Annexes.....197

Annexe A - Crystal structures - Chapter II.....199
Annexe A - Crystal structures - Chapter III.....226
Annexe A - Crystal structures - Chapter IV.....237
Annexe B - Abbreviations.....247
Annexe C - Communications.....249

Chapter I

Introduction

“Do you remember Mr Spiegelman, the mechanic? Your father suspects he has a gastric ulcer, and sent him here for a medical control. He is going to have a ‘meal’ based on barium.”

(freely translated from *Uncle Tungsten*, by Oliver Sacks)

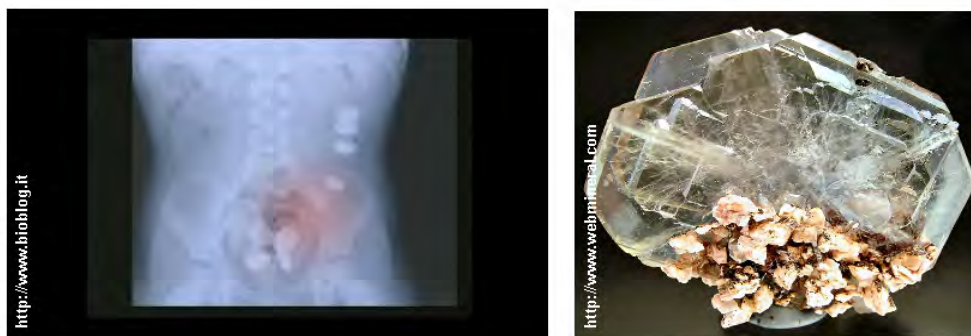


Figure 1. X-ray of the digestive system (left) and crystals of barite ($BaSO_4$) (right).

The great human discoveries are often born from little intuitions and from the observation of the phenomena of the surrounding nature. So in 1895, Roentgen discovers X ray nearly by chance realizing that if he placed his own hand between a cathode rays tube and a fluorescent screen, he could see the bony skeleton; from that moment X ray have entered in our everyday life, as everybody knows the importance of a radiography [Fig. 1], and more and more they are in our everyday scientific life ranging from the structural work dealing with proteins up to the study of minerals or materials.

Nature is a primary inspiration spring for all those who are interested in ‘architecture’, the discovery and elucidation of the structure of the DNA double helix (that incidentally was proved through the fundamental X ray diffraction data) based on hydrogen bonded DeoxyriboNucleic Acid nucleobases changed the vision of chemists which became no more based on atoms or molecules but based on *supermolecules*.

The comprehension of these phenomena and the creation of new architectures became the subject of a new field around the end of sixties, spreading out rapidly to different disciplines, such as biology and material sciences. This field is known as Supramolecular Chemistry.

In this introductory section, after a general overview of the subject, will be presented some of the basic concepts of Supramolecular Chemistry. Furthermore we will introduce few open topics such as hydrogen bonding, crystallisation and network design. Finally, inherent literature examples representing the challenges of this work will be described.

I.1 Introduction: Supramolecular chemistry and its context

I.1.1 Definition and historical background

The term Supramolecular Chemistry has been introduced in 1978 by Jean Marie Lehn, awarded with the Nobel Prize in 1987 with Donald J. Cram and Charles J. Pedersen. The following definition has been given for Supramolecular Chemistry¹ “the chemistry of molecular assemblies and of the intermolecular bond”, another definition is given by Jean Marie Lehn: “one can define supramolecular chemistry as *the chemistry beyond the molecule*, founded on more complex entities that spring from the association of at least two chemical species bound by intermolecular forces”.

While molecular chemistry is related to covalent bonds, supramolecular chemistry^{2,3} deals with weak interactions, or ‘secondary’ interactions that allow the formation of supermolecules: oligomolecular systems composed of limited number of entities organized into assemblies composed of different entities.

The fundamentals of Supramolecular Chemistry date back to the late 19th century and the early 20th century when some of the basic concepts of this developing research field were first argued, the concepts of coordination chemistry and the principle of lock-and-key. The roots of supramolecular chemistry are firmly anchored to the ground of traditional chemistry where it represents a connection among different fields and at the same time an enhancement. Although supramolecular chemistry is based on ‘older’ chemical concepts, it represents an innovation in terms of a new way to figure out the matter. We often need an old language to describe new scientific acquisition, so that the noteworthy comparison put forth by Roland Barthes⁴ between the chemistry and the language helps us to better figure out the landscape in which supramolecular chemistry is situated.

According to Barthes, like the letters in languages make the words and the words make the sentences and those sentences build up a speech, as well as in chemistry atoms make molecules, and molecules make supermolecules that form ordered supramolecular buildings (see figure 2).

¹ a) J.-M. Lehn, *Pure Appl. Chem.*; **1978**, *50*, 871-875; b) J.-M. Lehn, *Acc. Chem. Res.*; **1978**, *11*, 49-57

² J.-M. Lehn, *Supramolecular Chemistry: Concepts and Perspectives*, VCH, **1995**

³ a) J. W. Steed, J. L. Atwood, *Supramolecular Chemistry*, Wiley, **2000** ; b) J. W. Steed, D. R. Turner, K. J. Wallace; *Core Concepts in Supramolecular Chemistry*; Wiley, Chichester, **2007**

⁴ R. Barthes, *Leçon Inaugurale*, Collège de France, **1977**

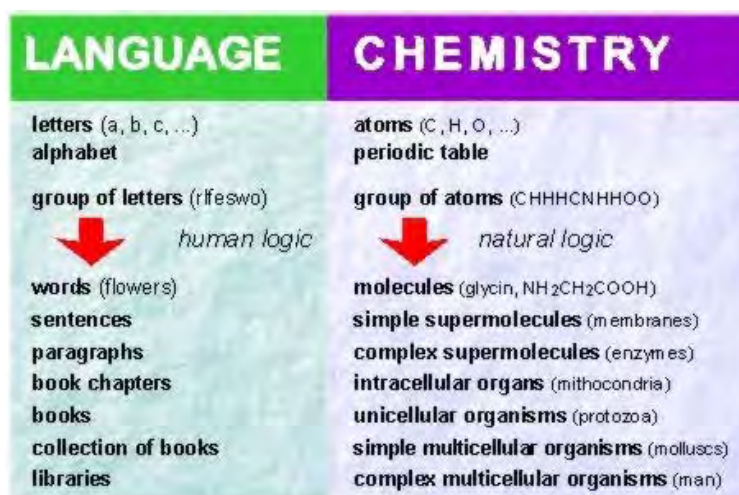


Figure 2. *Parallelism between chemistry and language*⁵.

Even if based on already known physical phenomena governing the matter, supramolecular chemistry contributes to illustrate many new ways in which the matter may organize and opens multiple perspectives concerning methods for studying these new assemblies, this also produces new molecules as new materials with new properties together with a new challenge that is to say, to be able to master the non-covalent bonding exactly as molecular synthetic chemistry masters the covalent one.

The field of supramolecular chemistry covers different domains and could be roughly divided into three representative fields that will be briefly presented below through examples: the host-guest chemistry, the chemistry of molecular devices and *crystal engineering*, where the so called *molecular tectonics* (§ 1.3) is one of its branch strictly related to molecular networks.

The host-guest chemistry is the first developed branch of supramolecular chemistry. In the host-guest relationship, usually a *host* is a large molecule or molecular aggregate that houses another molecule or ion, a *guest*, according to an effective visual definition by Steed and Atwood: “the host-guest binding event may be likened to catching a ball in the hand”. More formally it involves a complementary stereo-electronic arrangement of binding sites where the host is defined as any molecule or ion whose binding sites *converge* in the complex (e.g., Lewis donor atoms, hydrogen bond donors...), the guest component is defined as any molecule or ion whose binding sites *diverge* in the complex. Host-guest chemistry is the chemistry of the crown ethers⁶, cryptands⁷, cavitands (e.g., calixarenes⁸, cyclophanes,⁹

⁵ From the Inaugural Lecture of the Academic Year hold by Professor V. Balzani, Bologna, 17 October **1997**

⁶ C. J. Pedersen; *Organic Syntheses*, Coll. Vol. 6, p.395 (1988); Vol. 52, p.66 (1972).

⁷ B. Dietrich, *Cryptate Complexes in Inclusion Compounds*, J. L. Atwood, J. E. D. Davies, D. D. McNicol, Academic Press Ed., **1984**

cyclodextrins¹⁰...), but also of inclusion compounds such as clathrates (e.g. zeolites and MOF¹¹) and is at the base of transmembrane transport of cations in biological systems. A nice example of host-guest chemistry is proposed by Zhang and co-workers¹² where a cyclodextrin host as drug scavenger for transportation of a molecule of a steroid used as medical anaesthetic [Fig. 3a].

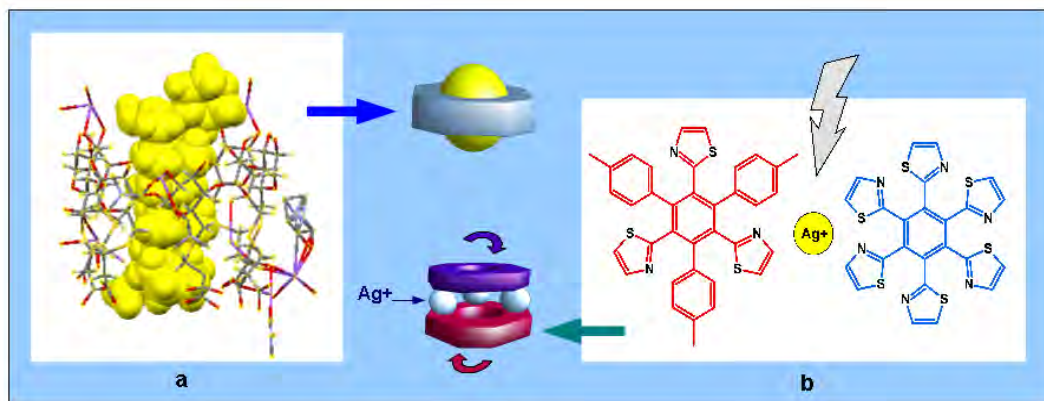


Figure 3. System from supramolecular chemistry: a) a molecule of rocuronium steroid (anaesthetic) encapsulated by a cyclodextrin derivative (ref 12); b) ligand exchange leading to an intramolecular rotational motion in this heterotopic sandwich complex of Ag^+ (ref 14).

The second branch of supramolecular chemistry is the one of supramolecular devices; we can define a molecular machine or device¹³ as a molecule at the nanometric level conceived to produce a work usually in a reversible way. A molecular machine is assembled with interacting components. Light-induced processes are of fundamental importance in this field as light is one of the most exploited energy sources for this kind of devices, but also electrochemical or magnetic impulse are used. This is the chemistry of catenanes, rotaxanes, non linear optical materials, dendrimers. One example of supramolecular device is from Hiraoka, and Shionoya¹⁴ that have

⁸ a) A. Ikeda, S. Shinkai; *Chem. Rev.*, **1997**, 97, 1713-1734 ; b) P. Schmitt, P. D. Beer, M. G. B. Drew, P. D. Sheen; *Angew. Chem. Int. Ed.*, **1997**, 36, 1840-1842 ; c) L. R. Nassimbeni, *Acc. Chem. Res.*, **2003**, 36, 631-637

⁹ B. J. Whitlock, H. W. Whitlock; *J. Am. Chem. Soc.*, **1994**, 116, 2301-2311

¹⁰ a) J. Szejtli, *J. Chem. Rev.*, **1998**, 98, 1743-1754 ; b) S. A. Nepogodiev, J. F. Stoddart; *J. Chem. Rev.*, **1998**, 98, 1959-1976 ; c) Kenneth A. Connors; **1997**, 97, 1325-1358

¹¹ S. L. James, *Chem. Soc. Rev.*, **2003**, 32, 276-288

¹² A. Bom, M. Bradley, K. Cameron, J. K. Clark, J. van Egmond, H. Feilden, E. J. MacLean, A. W. Muir, R. Palin, D. C. Rees, M.-Q. Zhang; *Angew. Chem. Int. Ed.*, **2002**, 41, 265-270

¹³ a) W. R. Browne, B. L. Feringa, *Nature Nanotechnology* , **2006**, 1, 25-35 ; b) V. Balzani, M. Gomez-Lopez, J. F. Stoddart, "Molecular Machines", *Acc. Chem. Res.* **1999**, 31, 405-414 ; c) V. Balzani, M. Gomez-Lopez, J. F. Stoddart, *Acc. Chem. Res.*, **1998**, 31, 405-414 ; d) M. C. T. Fyfe, J. F. Stoddart, *Acc. Chem. Res.*, **1997**, 30, 393-401

¹⁴ S. Hiraoka, M. Shiro, M. Shionoya; *J. Am. Chem. Soc.*, **2004**, 126 , 1214-1218

created a molecular ball-bearing assembling two disc-shaped molecules that rotate relative to each other on silver ions (Ag^+) sandwiched in between [Fig. 3b].

The third branch is represented by crystal engineering that we'll go into thoroughly afterwards (see § 1.4.). In the next sections, a general view of the main concepts in supramolecular chemistry will be given, focusing our attention on crystal engineering and in particular on molecular tectonics.

1.1.2 Basic concepts in supramolecular chemistry

1.1.2.1 Molecular recognition

Molecular recognition is intimately at the origin of supramolecular phenomena, architectures or devices. From biochemistry processes like DNA folding to host-guest interaction, template effect, self-assembly and self-replication, supramolecular devices are all based on molecular recognition. In the lock-and-key model put on by Emil Fischer in 1894 to describe the receptor-substrate interaction in the enzymes, the key factor for recognition are the geometry and size of the binding cavity and the shape complementarity between the substrate and the enzyme binding site.

On his turn, complementarity could be a complex process involving not a single event but a series of cooperative actions among complementary binding sites and the additional contribution of multiple weak interactions; an host must be able to discriminate between different guests like a free spot in a puzzle frame can be filled only with his appropriate part, like it happens in biological systems [Fig. 4].

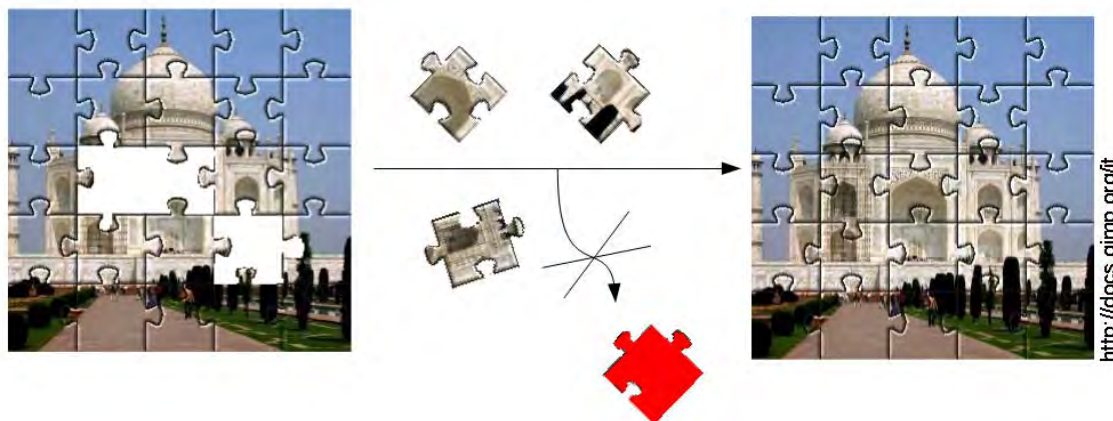


Figure 4. Schematic representation of the molecular recognition events based on complementarity between components.

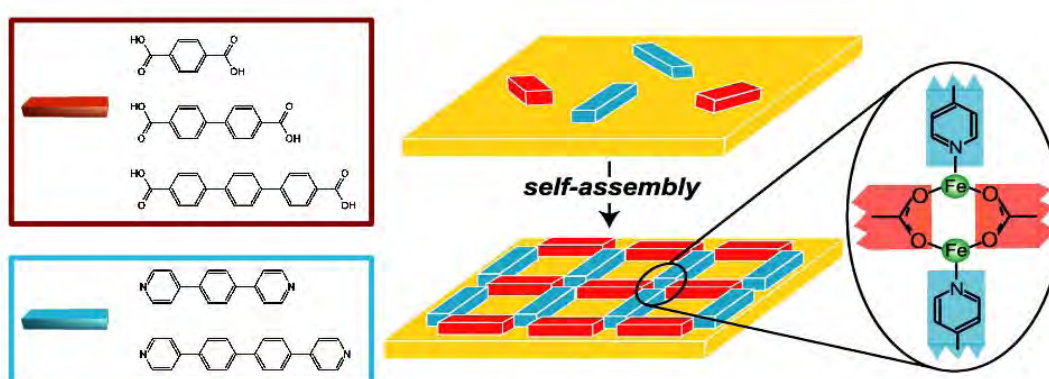
Better is the complementarity between supramolecular components higher is the related “binding” energy. This refers not only to a single non covalent bond but includes the shape and the whole electrostatic surface of the recognition sites, it requires a combination of sterical fit, good match of the local and bulk charge distribution, a

suitable space arrangement thus maximising the attractive and minimising the repulsive forces.

1.1.2.2 Self-assembly and self-organization

Supramolecular self-assembly¹⁵ is a direct consequence of molecular recognition and could be defined as the process of spontaneous aggregation of two or more components possessing complementary characteristics. Self-assembly is at the base of organization in the crystal lattice, host-guest formation or receptor-substrate binding in enzymatic catalysis, and all these processes are driven by thermodynamic stability enhancement *i.e.*, an accurate balance between entropic and enthalpic contributions. Closely linked to the idea of self-assembly is the concept of self-replication, the ability to produce a copy of itself, and self-organisation.

Self-assembly is the particular and localized process of recognition while self-organisation can be considered as the general assembly of the whole architecture. Self-assembly and self-organization are both multi-steps processes, they use the reversibility of kinetically labile interactions as fundamental instrument to sift through the energetics of the system and choose the most thermodynamically favourable free energy conformation. The kinetic lability gives to the auto-assembled systems some specific feature such as self-repairing, on the contrary systems that are not kinetically labile cannot repair their mistakes and their defaults are permanent. One significant example of self-recognition is the self-assembly on surface of a multicomponent system presented by Kern *et al.*¹⁶ [Fig. 5]. The ligands coordinate with iron atoms on a copper substrate to form rectangular compartments of well ordered arrays from redundant ligand mixtures by molecular self-recognition and selection, enabled by efficient error correction and cooperativity.



¹⁵ a) Whitesides, G. M., Mathias, J. P., Seto, T. *Science*, **1991**, *254*, 1312-1319; b) J. S. Lindsey, *New J. Chem.*, **1991**, *15*, 153-180 ; b) D. Philp, J. F. Stoddart, *Synlett*, **1991**, 445-458 ; c) M. Eigen, *Naturwissenschaften*, **1971**, *33a*, 465-523

¹⁶ A. Langner, S. L. Tait, N. Lin, C. Rajadurai, M. Ruben, K. Kern; *PNAS*, **2007**, *104*, 17927-17930

Figure 5. Self-organization of different dicarboxylate and bipyridyl ligand around Fe atom on a copper surface to form a rectangular network; the coordination arrangement at each node is detailed (ref. 16)

Molecular recognition and self-assembly are possible thanks to weak non-covalent interactions that are the core of supramolecular chemistry, we cannot exempt in the next section to give a general overview of these forces, their energy range and some key characteristics.

1.1.2.3 Supramolecular interactions

We can identify different types of interactions depending on their energy, their directionality, their metrics and their geometry. These interactions are summarized in figure 6 and listed below.

Non-covalent bond ranges from coordinative bond and columbic interactions, with a strength of several hundreds kJ/mol (1 cal = 4.184 J) comparable to weak covalent bonding, to weak van der Waals interactions that worth only a few kJ/mol.

100-350 kJ/mol: Ionic interactions are the strongest among the weak electrostatic interactions. They have a distance dependence of the potential energy (E_p) as $1/r$ and depend on the dielectric constant of the medium. There is no particular directionality in the ion-ion interaction and they can be considered as long-range interactions.

50-200 kJ/mol: Interactions between ions and dipoles that are somewhat weaker with a distance dependence in $1/r^2$. One example is the interaction of metal cations in crown ethers, so they can be considered directional forces with a medium range of influence.

4-65 kJ/mol: Hydrogen bond, fundamental in biochemistry, is also largely employed in supramolecular chemistry, it can be considered as a special case of dipole-dipole interaction where a hydrogen atom connected to a electron withdrawing atom or group, interacts with a near dipole. It is generally more energetic than a normal dipole-dipole interaction (between 4 and 65 KJ/mol for neutral molecules can reach 120 kJ/mol for Charge Assisted Hydrogen Bond) and it has some characteristic features such as directionality¹⁷ that make of it a precious tool for the design of assemblies. Moreover, it exhibits a short range influence. Particular attention will be dedicated to the hydrogen bond further into the chapter.

¹⁷ J. D. Duniz, A. Gavezzotti, *Angew. Chem. Int. Ed.*, **2005**, *44*, 1766-1787

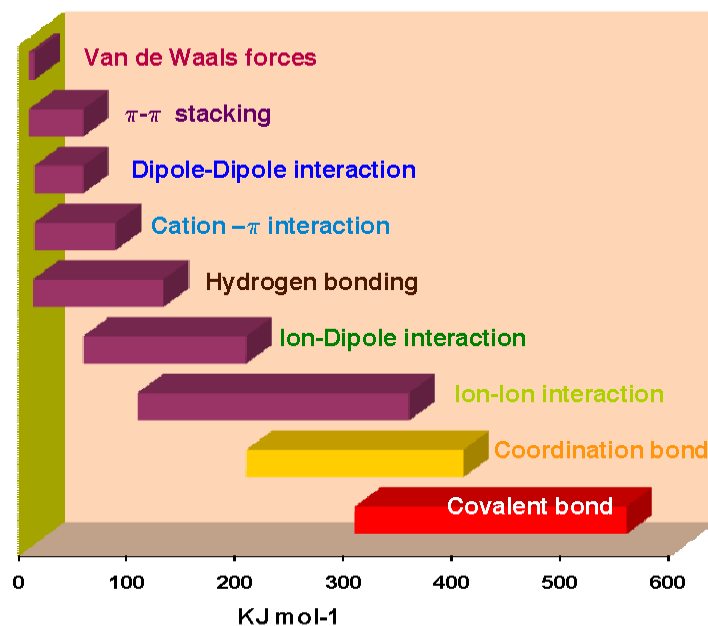


Figure 6. Scale of energy of the supramolecular weak interactions used in supramolecular assemblies compared with coordination and covalent bonds.

5-50 kJ/mol: Dipole-dipole interactions, also called Keesom interactions, are caused by permanent dipoles in molecules with a distance dependence in $1/r^3$ or even $1/r^6$ for rotating polar molecules so their influence is over a short range and again the orientation of the two interacting dipoles plays an important role, so they are directional forces. This interaction is present, for example, in compounds containing carbonyl groups.

0-80 kJ/mol: Non-covalent forces involve also π -systems¹⁸, which can interact with cations or other π -systems. They can be divided into cation- π interactions (5-80 KJ mol⁻¹) and π - π interactions (0-50 KJ mol⁻¹). Aromatic rings such as benzene bear a quadrupole moment with a partially positive σ -scaffold and a partially negative π -cloud above and below the ring plane¹⁹. Consequently, alkali metals and other cations can form an attractive interactions when located above the centre of the aromatic ring or olefin, examples are the interactions of a K⁺ cation with a benzene ring that in the gas phase has an energy of 80 KJ mol⁻¹ and benzene-Ag⁺ interactions with a partial covalent characters.

The π - π interaction is usually called π -stacking and may occur in different positions: face-to-face and edge-to-face. Two similarly electron-rich or electron-poor π -systems (e.g., benzene ring) tend not to interact in a perfect face-to-face manner²⁰ but in shifted one, because the two partially negative π -clouds would repulse each other.

¹⁸ C. A. Hunter, *Chem. Soc. Rev.*, **1994**, 101-109

¹⁹ J. C. Ma, D. A. Dougherty, *Chem. Rev.*, **1997**, 97, 1303-1324

²⁰ C. A. Hunter, J. K. M. Sanders, *J. Am. Chem. Soc.*, **1990**, 112, 5525-5534

Benzene rings prefer an edge-to-face orientation. When two aromatics interact and one of which is electron-rich and one is electron-deficient the face-to-face disposition is preferred.

Less than 5 kJ/mol. van der Waals forces are the weakest interactions and arise from the interaction of polarized electron clouds by the proximity of adjacent nuclei. These forces have an attractive contribution and a negative contribution that avoid collapsing and a distance dependence in $1/r^6$ for attractive dispersion interactions or in $1/r^{12}$ for repulsive interactions.

In particular we can distinguish two attractive components: from dipole-induced dipole (Debye induction) or from induced dipole-dipole (London dispersion). They are usually non directional, and the strength is proportional to the area of the contact surface.

Next to these interactions, considered as the most important, there are other important effects that affect network formation in the solid state: (i) the hydrophobic effect, which consists in the minimization of the energetically unfavorable surface between polar/protic and unpolar/aprotic molecules; (ii) the forces between multipoles²¹; (iii) the weak interactions between nitrogen and halogen atoms²²; (iv) the dihydrogen bridges²³ between metal hydrides and hydrogen bond donors; and, to conclude, (v) the close packing that, according to Kitaigorodski²⁴, is related to the maximization of favourable van der Waals interactions and thus represents an important force in crystallization and crystal engineering

Intermolecular forces are usually weaker than covalent bonds so that supramolecular species are generally thermodynamically less stable, kinetically more labile, more flexible and dynamic, than their covalent counterparts. If we consider the possibility of assembly of a discrete number of components, the richness of supramolecular chemistry resides in the multiple mixing of these forces and the variety of possible combinations,. This further increased if we consider the assembly of an infinite number of components.

Along this line, our work deals with the branch of supramolecular chemistry concerned by infinite assembly in the crystalline state. This domain is called *molecular tectonics*. In the following section, we will introduce *molecular tectonics* together with the concept of molecular networks.

²¹ R. Paulini, K. Müller,, F. Diederich, *Angew. Chem. Int. Ed.*, **2005**, *44*, 1788-1805

²² P. Auffinger, F. A. Hays, E. Westhof, P. S. Ho, *Proc. Natl. Acad. Sci. USA*, **2004**, *101*, 16789-16794

²³ R. H. Crabtree, P. E. M. Stegbahn, O. Eisenstein, A. L. Rheingold, T. F. Koetzle, *Acc. Chem. Res.*, **1996**, *29*, 348 354

²⁴ A. I. Kitaigorodski, *Molecular Crystals and Molecules*, Academic Press, New York, **1973**

1.2 Molecular Tectonics vs Crystal Engineering

Molecular tectonics is an approach derived from *crystal engineering* (see § 1.4); in this section, we analyse thoroughly the key features of molecular tectonics, that represent the guideline at the base of this work, and we focus on the design of the building blocks for the generation of infinite architectures. We will return after to crystal engineering to deal more specifically with some common problems of supramolecular chemistry such as crystal design and growth.

Both approaches are strictly interconnected. Molecular tectonics²⁵ is a more intuitive approach based on specific recognition patterns and on the use of specific molecular components programmed for molecular recognition and self-assembly. To describe molecular tectonics, we borrow the definition given by Wuest²⁶: in 1997: “*Tectons are molecules whose interactions are dominated by specific attractive forces that induce the assembly of aggregates with controlled geometries, and molecular tectonics is the art and science of supramolecular construction using tectonic subunits*”.

Conversely, crystal engineering tries to rationalise the network formation in order to predict the crystal growth in terms of connectivity, topology, short and long range interactions supported by computational methods. Crystal engineering²⁷, has been defined by Jerry Atwood as “*the design and preparation of a crystalline material based on a knowledge or, at least, consideration of a steric, topological and intermolecular bonding capabilities of the constituent building blocks*”²⁸.

In the following sections, the molecular tectonics and the crystal engineering approaches will be tackled in relation with some topics connected to this work.

1.3 Molecular Tectonics and molecular networks

1.3.1 Definition and concepts in molecular tectonics

Molecular tectonics [from the greek *tektoniké*, composed by *téchnè*, art and *tektòn*, carpenter or builder] is therefore based on molecular recognition events and their iteration in order to build molecular networks in a rational way. We can identify a first phase of analysis of existing crystal structure to point out recurrent recognition motives and a second phase dealing with design and preparation of molecular synthons (tectons). The final goal is to synthesized molecular networks in the

²⁵ a) M. Simard, D. Su, J. D. Wuest; *J. Am. Chem.*; **1991**, *113*, 4696-4698 ; b) J. M. Thomas; *Nature*; **1981**, 289, 633-634 ; c) M. W. Hosseini, *Acc. Chem. Res.*, **2005**, *38*, 313-323 ; d) M. W. Hosseini, *Chem. Commun.*, **2005**, 5825-5829

²⁶ P. Brunet, M. Simard, J. D. Wuest; *J. Am. Chem. Soc.*, **1997**, *119*, 2737-2738

²⁷ a) M. J. Zaworotko, *Chem. Soc. Rev.*, **1994**, 283-288 ; b) D. Braga, F. Grepioni, G. Desiraju, *Chem. Rev.*, **1998**, *98*, 1375-1405

²⁸ J. W. Steed, J. L. Atwood, *Supramolecular Chemistry*, Wiley, **2000**, p.392

crystalline phase that are infinite periodic molecular assemblies formed under self-assembly conditions between self-complementary tectons.

The words tecton, synthon and building block are often used as synonym to indicate each building bricks that compose the final architecture: they bear the required recognition sites in order to make the local recognition process that constitutes the assembling node. They are recurrent, local assemblies of different components using weak, directional interactions, mainly coordination bond and hydrogen bond, in this way the network can be seen as a translational repetition of the same motif.

According to the prevalent interaction dominating the network, purely coordination networks, in the presence of metal/ligand, or purely hydrogen bonded networks, using only organic components, may be obtained. When both interactions occur, the formed networks may be called "hybrid networks".

1.3.2 Generalities and dimensionality of molecular networks

If the supramolecular architecture is formed only by one single molecule bearing one or more sites for recognition the final assembly is called *homomeric* and we speak about self-complementary tectons; if the structure is composed of one or more tectons, it is called *heteromeric* (see figure 7). There is no theoretical limit to the number of involved building blocks but as their number increases, the control and predictability of their assembly in the network decrease.

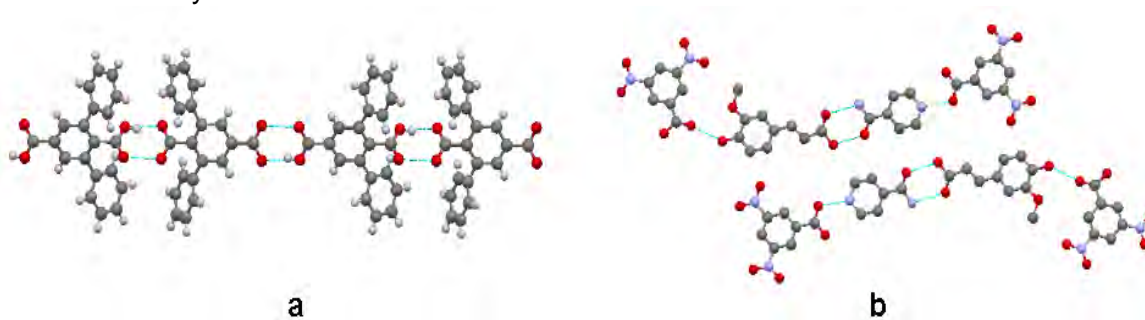


Figure 7. Homomeric, one tecton²⁹ (a) and heteromeric, three tectons³⁰ (b), molecular networks.

Depending on the nature of the involved tectons (position of their interaction sites), the final architecture can be either finite or infinite; in the first case we talk of isolated supramolecular assemblies and for the second we talk about supramolecular networks and the dimensionality may be: mono-dimensional (1D), when the repetition occurs in one space direction, bi-dimensional (2D), when the repetition occurs in two

²⁹ D. A. Dickie, M. C. Jennings, H. A. Jenkins, J. A. C. Clayburne, *Inorg. Chem.*, **2005**, *44*, 828-834

³⁰ C. B. Aakeröy, A. M. Beatty, B. A. Helfrich; *Angew. Chem. Int. Ed.*, **2001**, *40*, 3240-3242

space directions or three-dimensional (3D) networks, with repetition in the three space directions.

This is strongly related to the shape, number, position and orientation of the binding sites on the building blocks. Generally we can distinguish *endo*-receptors (molecule presenting a convergent orientation of the binding sites) from *exo*-receptors (molecule presenting a divergent orientation of the binding sites). The use of *endo*-receptors will lead to finite, discrete assembly as for the inclusion complexes [Fig. 8a], whereas *exo*-receptor when associated with a molecule bearing only one interaction site leads to a cap-complex [Fig. 8b] or with a tecton bearing two interaction sites leads to infinite networks [Fig. 8c].

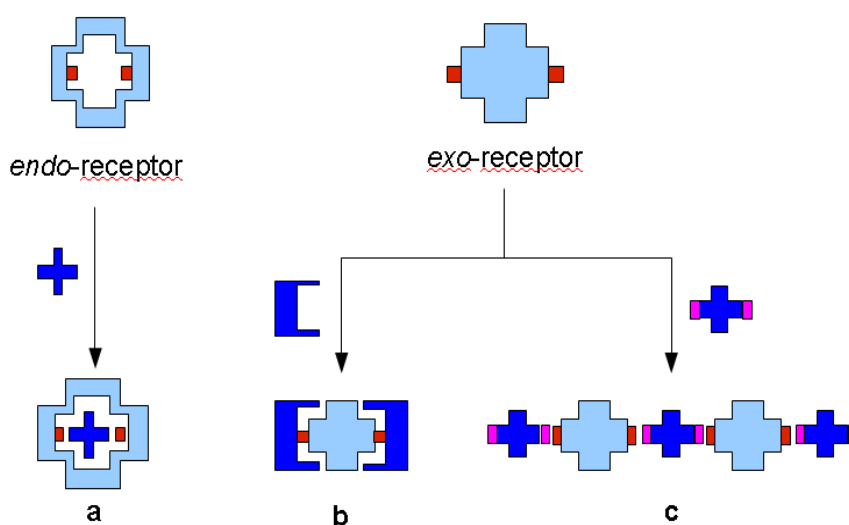


Figure 8. Schematic representation of *endo*- and *exo*-receptors. a) Convergent binding sites lead to inclusion complexes, b) divergent binding sites lead to a capped complexes or c) to infinite molecular networks.

The dimensionality of a infinite molecular networks depends on the number of spatial translations (dimensions) of the recognition node. If we want to obtain a network with a dimensionality equals to n , the connectivity of at least one or all the involved tectons has to be $n+1$, so, for example, to obtain a 1D network the tecton has to bear at least two recognition sites divergently oriented.

For the same set of building blocks bearing more than one interaction sites, different architectures may be obtained: this is called structural supramolecular isomerism³¹ and polymorphism in the solid state (see § 1.3.3.2).

The dimensionality of networks will be illustrated in the following sections by some selected examples however without being exhaustive; examples will describe both coordination networks and hydrogen bonded assemblies.

³¹ a) B. Moulton, M. J. Zaworotko, *Chem. Rev.*, **2001**, *101*, 1629-1658 ; b) A. M. Beatty, *Coord. Chem. Rev.*, **2003**, *246*, 131-143

I.3.2.1 O-D discrete assemblies

Discrete assemblies³² are obtained for instance when a building block bearing convergent interaction sites is associated with a molecule bearing divergent binding sites, that is the case for the host-guest supermolecules or an inclusion complexes as shown in figure 8a.

When a tecton is equipped with two interaction sites with an appropriate angle between them, dimeric, trimeric or tetrameric complexes may be obtained [Fig.9a/9b], but also 0-D discrete assemblies such as cubes or bipyramids, as illustrated in figure 9c.

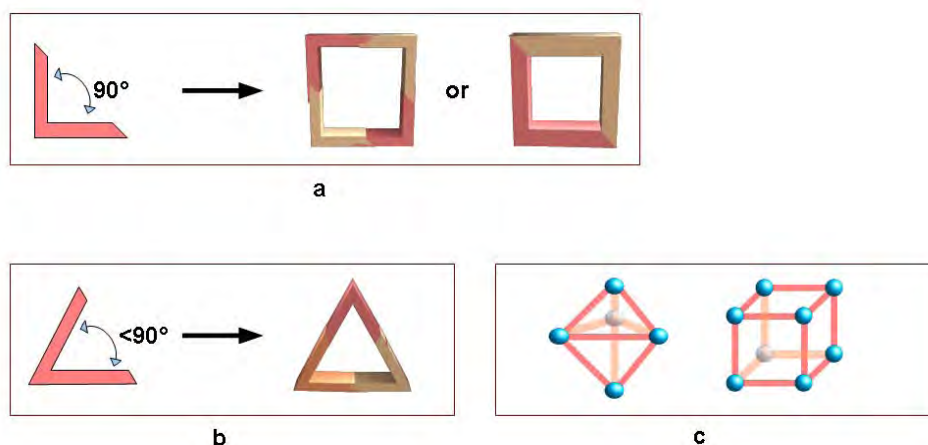


Figure 9. Possible supramolecular discrete assemblies: a) Supramolecular dimers and tetramers, b) supramolecular trimers, and c) bi-pyramidal and cubic architectures.

These are only some examples of the manifold possible architectures; some real examples are illustrated below for self-assembling coordination compounds such as the triangular macrocycle of Mirkin *et al.*³³ based on an homochiral binaphthyl derivative, $\text{Cu}(\text{OAc})_2$ as the taping metal and pyridine filling the inner cavities [fig. 10a]. Another example is given by the well known tetranuclear square complex reported by Fujita³⁴ composed of *cis*-protected $\text{Pd}(\text{II})(\text{en})_2$ building blocks, at the edge, linked by 4,4'-bipyridine. Fujita was also the first to develop three dimensional supramolecular macrocycles as the square based bipyramid cage based on a 2,4,6-tripyridinyl-1,3,5-triazine³⁵ [fig. 10b and 10c], all these networks have been conceived basing on some simple prediction criteria (as discussed in § I.4.1.1). The search for discrete assemblies

³² M. Schmittel, V. Kalsani; *Functional, Discrete, Nanoscale Supramolecular Assemblies*, in Topics in current chemistry, Vol. 245, Springer Berlin/Heidelberg, **2005**

³³ J. Heo, Y.-M. Jeon, C. A. Mirkin, *J. Am. Chem. Soc.*, **2007**, *129*, 7712-7713

³⁴ a) M. Fujita, O. Sasaki, T. Mitsuhashi, T. Fujita, J. Yazaki, K. Yamaguchi, K. Ogura, *Chem. Commun.*, **1996**, 1535-1536 ; b) M. Fujita, *Chem. Soc. Rev.*, **1998**, *27*, 417-425

³⁵ a) F. Ibukuro, T. Kusakawa, M. Fujita, *J. Am. Chem. Soc.*, **1998**, *120*, 8561-8562 ; b) M. Fujita, S. Nagao, K. Ogura, *J. Am. Chem. Soc.*, **1995**, *117*, 1649-1650

has increased with time due to the interest concerning molecular nano-chemistry and nano-devices; for example, cages and boxes, like the supramolecular cube by Lang *et al.*³⁶ built using W(Cp)-S-Cu cluster at the apex of the cube and Cu-CN-Cu as edges on each face [Fig. 10d].

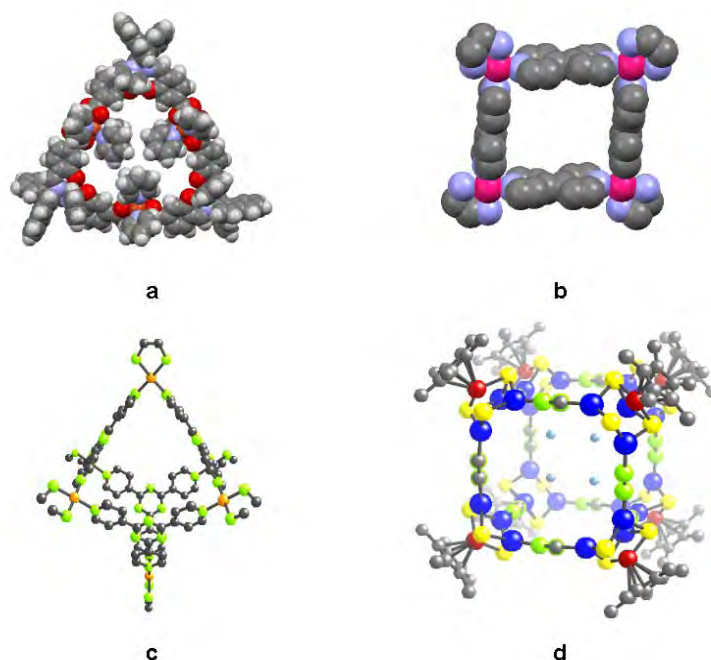


Figure 10 Examples of a) a homochiral (*S,S,S*) triangular complex (ref. 33), b) a square complex and two nanosized cages(ref.34) c) with the shape of square bi-pyramid (ref.35) and d) with the shape of a cube (ref. 36).

1.3.2.2 1-D networks

When the building blocks offer at least two *exo*-connecting sites, homomeric or heteromeric mono-dimensional networks may be obtained, upon translating the nodes in one space direction. The networks can adopt different geometries: from the simplest linear shape to the more complex helicoidal shape, passing through three common non-linear geometries: wavy, zig-zag and crenellated. In these cases the networks are constituted by a single string [Fig. 11 a,b,c,d].

We also may have 1-D network formed by two paired strings, in this option usually they are interconnected at the level of one recognition node to generate a ladder network [Fig. 11f]. Moreover it is possible to have networks composed of a building block bearing two divergent sites and the coordination node (usually a metal) substituted with another building block with convergent interaction sites. In that case, a 1D network of the rack type is obtained [Fig. 11e].

³⁶ J. -P. Lang, Q.-F. Xu, Z.-N. Chen, B. F. Abrahams; *J. Am. Chem. Soc.*, **2003**, *125*, 12682-12683

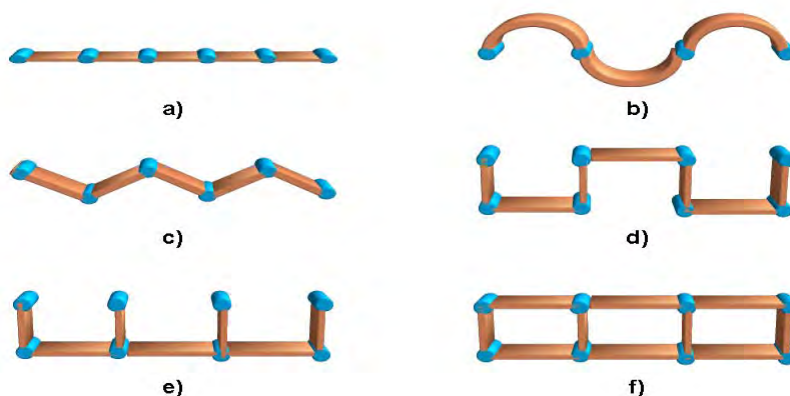


Figure 11. Some examples of the possible geometries for 1D networks: a) linear, b) waved, c) zig-zag, d) crenellated, e) rack and f) ladder.

Many examples of one dimensional networks dealing with both coordination polymers and hydrogen bonded architectures have been reported. Interesting is the case of the waved chain presented by Ciani *et al.*³⁷, which is a 1D coordination network with parallel interlacing forming a polyrotaxane layer of composition $[M_2(L)_3(SO_4)_2]$ (where $M = Zn$ and Cd and $L = 1,4$ -bis(imidazol-1-ylmethyl)benzene) [Fig. 12a].

Field and Venkataraman³⁸ explored the control of supramolecular topology through an homomeric hydrogen bonded networks (N-derivative of dibenzoic acid). In particular while the secondary amine derivative leads to a zig-zag chain, the tertiary amine, substituted with three benzene rings, leads to a helical chain [Fig. 12b].

Using a molecular building unit having a T-shape, interconnected double chain, or molecular ladders, like this example based on coordination polymers of bis(4-pyridyl)ethane were reported by Zavorotko *et al.*³⁹ [Fig. 12c].

³⁷a) L. Carlucci, G. Ciani, D. M. Proserpio; *Cryst. Growth Des.*, **2005**, 5, 37-39 ; b) L. Carlucci, G. Ciani, D. M. Proserpio, *Coord. Chem. Rev.*, **2003**, 246, 247-289

³⁸ J. E. Field, D. Venkataraman, *Chem. Comm.*, **2002**, 306-307

³⁹ T. L. Hennigar, D. C. MacQuarrie, P. Loiseau, R. D. Rogers, M. J. Zavorotko, *Angew. Chem. Int. Ed.*, **1997**, 36, 972-973

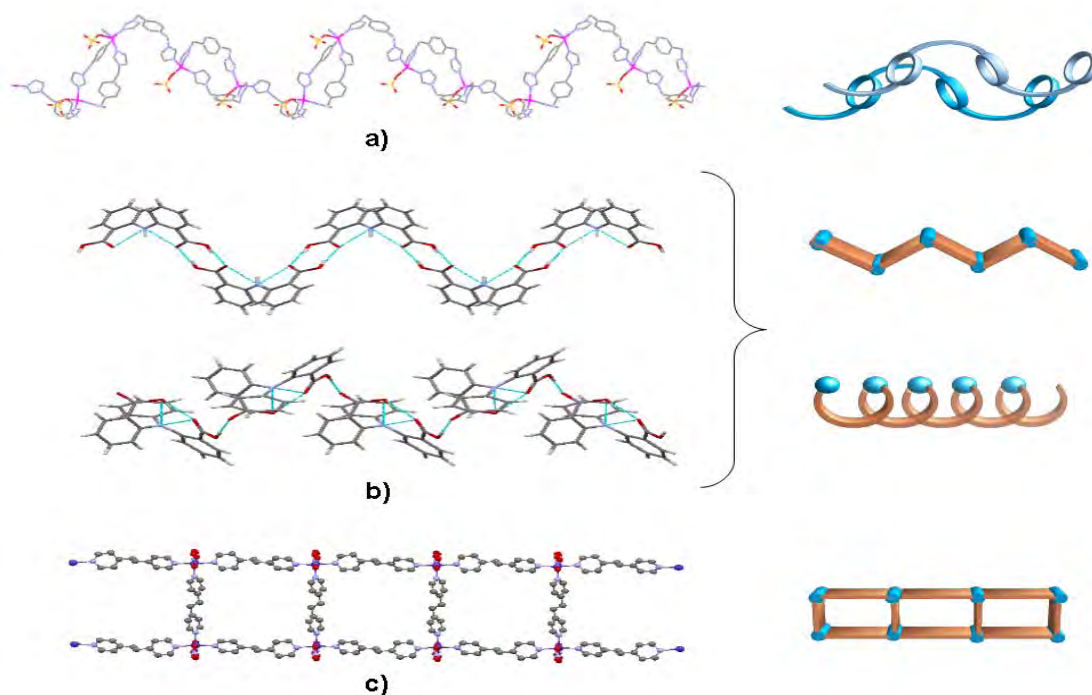


Figure 12. Examples of mono-dimensionnal systems : a) a waved coordination network (ref.37), b) an helix versus zig-zag hydrogen bonded networks (ref.38) and c) a ladder coordination network (ref.39).

1.3.2.3 2-D networks

It is possible to extend the geometries of the 1-D networks along a second perpendicular axis in order to obtain the corresponding 2-D networks that offer a large variety of geometry.

We can distinguish square, rhomboidal or rectangular motives when the building blocks possess four exo-receptors leading to bi-dimensional grids [Fig. 13a,b,d,e], or hexagonal motives if the building blocks offer three exo-receptors, leading to honeycomb networks [fig. 13c].

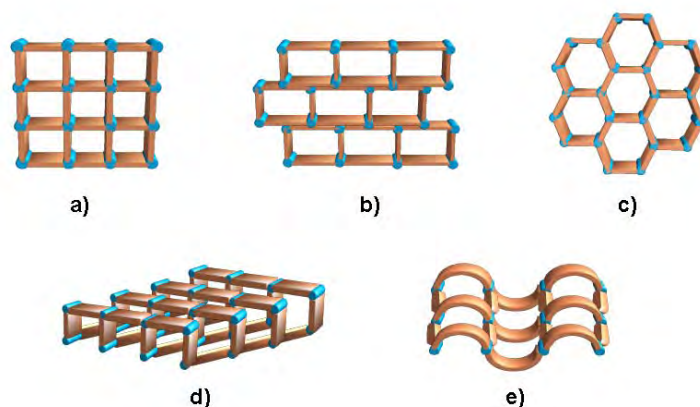


Figure 13. Some examples of the possible geometries for 2D networks: a) square grid, b) brick wall, c) hexagonal, d) bilayer, e) waved square grid.

The most encountered geometries are the square grid and the hexagonal (or honeycomb) grid. The former is illustrated by the hydrogen bonded network of aquazinc tetra(4-carboxyphenyl)porphyrin isolated by Goldberg *et al.*⁴⁰ [fig. 14a], the latter is represented by the structure of 1,3,5-trimesic acid, one of the most known example of honeycomb network obtained based on auto-complementary tectons⁴¹ [fig. 14b]. Otherwise, Rao *et al.*⁴² obtained 2-D hydrogen bonded networks combining *via* hydrogen bonding tri-thiocyanuric acid and 4,4'-bipyridine, leading to two types of grids as shown in figure 14c and d.

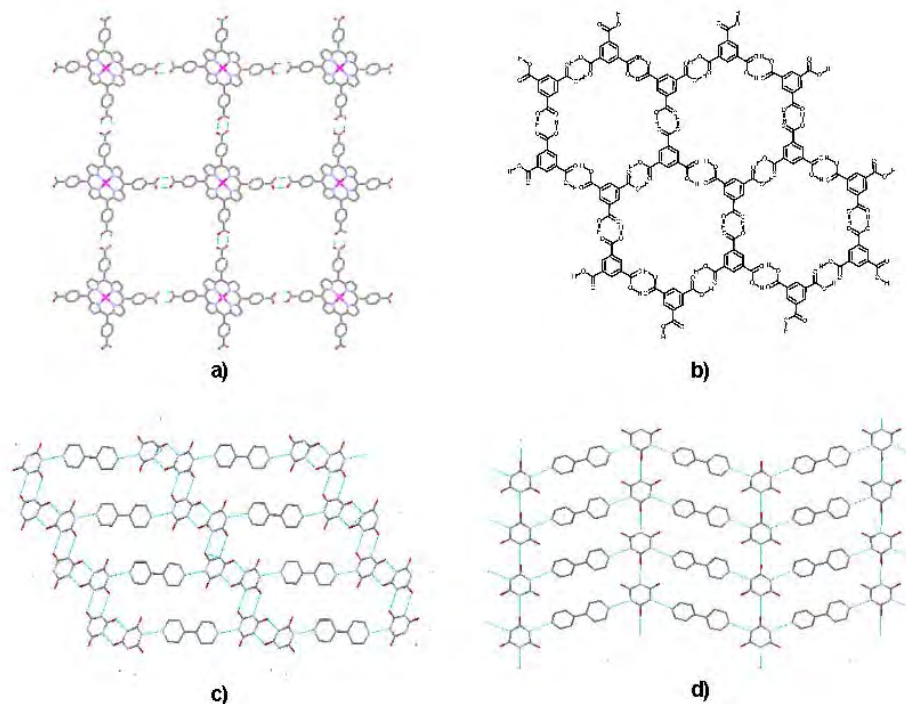


Figure 14. 2D networks: a) square grid (ref.40) b) hexagonal or honeycomb 2D network (ref.41), and rectangular 2D networks, linear c) and zig-zag d) (ref.42).

1.3.2.4 3-D networks

For three dimensional networks, the degree of complexity increases due to the multiple possible combinations between the different components. Among the many examples of 3-D networks, most of them are interpenetrated⁴³. The phenomenon of

⁴⁰ Y. Diskin.Posner, I. Goldberg, *Chem. Comm.*, **1999**, 1961-1962

⁴¹ a) D. J. Duchamp, R. E. Marsh, *Acta Crystall.*, **1999**, B25, 5-19; b) F. H. Herbstein, M. Kapon, G. M. Reisner, *J. Includ. Phenom.*, **1987**, 5, 211-214 ; c) F. H: Herbstein, *Top. Curr. Chem.*, **1987**, 140, 107-139

⁴² A. Ranganathan, V. R. Pedireddi, G. Sanjayan, K. N. Ganesh, C. N. R. Rao, *J. Mol. Struct.*, **2000**, 522, 87-94

⁴³ a) N. J. Burke, A. D. Burrows, M. F. Mahon, J. E. Warren, *CrystEngComm*, **2008**, 10, 15-18; b) L. Carlucci, G. Ciani, D. M. Proserpio, in *Making Crystals by Design: Methods, Techniques and Applications*, Chap.3 (Eds. D. Braga, F.Grepioni), Wiley, New York, **2006**; c) V. A. Blatov, L. Carlucci, G. Ciani, D. M. Proserpio; *CrystEngComm*, **2004**, 6, 378-395 ; d) S. R. Batten; *CrystEngComm*, **2001**, 18,

interpenetration is connected to the necessity of the maximum packing interaction energy and is generated by the topological entanglement of one network with one or more others through their respective voids so that they are inseparable without breaking bonds.

We can distinguish many different geometries for 3D networks, generally the most common are cuboid networks, based on tetrahedral nodes, and diamondoid networks, based on octahedral nodes, [Fig. 15a and b] but there are many others that have been observed in recent years, such as the quite rare and difficult to predict or even analyse giroid networks⁴⁴.

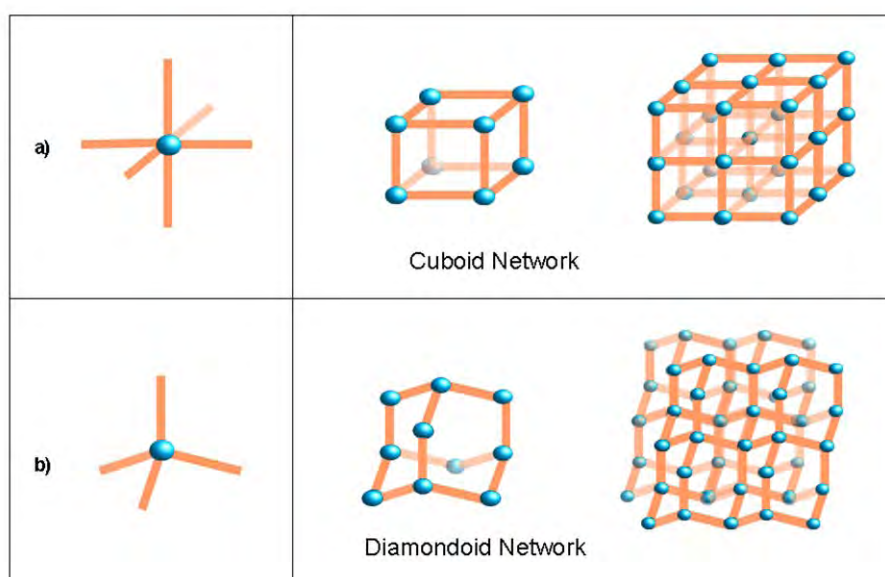


Figure 15. 3D networks with (a) cuboid and (b) diamond-like architectures.

Concerning the MOF's (Metal Organic Framework) and related families of porous networks, these are mostly based on cuboid networks [Fig. 15a] in which the nodes, presenting an octahedral geometry, are connected by organic pillars. Conversely the basic tecton for a diamondoid network⁴⁵ [Fig. 15b] is a tetradentate tetrahedral building block like the prototype adamantane-1,3,5,7-tetracarboxylic acid⁴⁶.

Different building blocks can lead to 3D network; examples are given with tectons having connecting sites pointing towards three or four directions, for instance, the hybrid coordination/H-bonded network based on nicotinamide silver complexes [Fig. 16a] developed by Aakeröy *et al.*⁴⁷, or the hybrid network based on the tetraresorcinol,

1-7 ; e) S. R. Batten, B. F. Hoskins, R. Robson, *Chem. Eur. J.*, **2000**, *6*, 156-161 ; f) S. R. Batten, R. Robson; *Angew. Chem. Int. Ed.*, **1998**, *37*, 1460-1494

⁴⁴ A. B. Mallik, S. Lee, E. B. Lobkovsky; *Cryst. Grow. Des.*, **2005**, *5*, 609-616

⁴⁵ M. J. Zaworotko, *Chem. Soc. Rev.*, **1994**, 283-288

⁴⁶ O. Ermer; *J. Am. Chem. Soc.*; **1988**, *110*, 3747-3754

⁴⁷ C. B. Aakeröy, A. M. Beatty, B. A. Helfrich, *J. Chem. Soc., Dalton Trans.*, **1998**, 1943-1945

a tetrahedric silicon derivative conceived to form diamondoid networks, by Wuest, Simard *et al.*⁴⁸ [Fig. 16b].

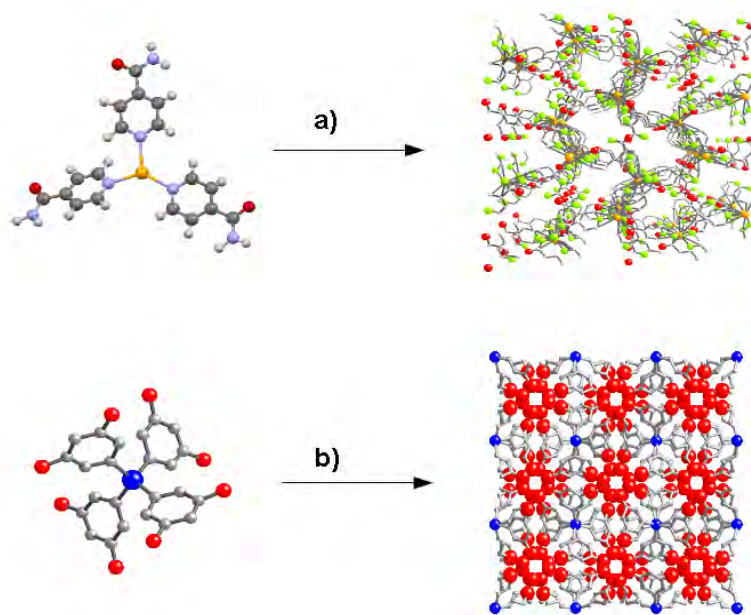


Figure 16. Examples of 3-D hydrogen bonded networks a) from a three substituted quasi-planar silver complex (ref.47) and b) from a tetrahedral tetra-substituted building block (ref.48).

1.4 Crystal engineering and design of tectons

Crystal engineering⁴⁹ takes into account molecular shape, topology⁵⁰, electronic properties, along with short- and long-range interactions, in order to design, select and prepare components that will be able to self assemble into the desired crystalline material. In a long term perspective and through computational methods⁵¹, crystal engineering has the objective to rationalize and predict crystal packing.

⁴⁸ a) O. Saied, T. Maris, X. Wang, M. Simard, J. D. Wuest, *J. Am. Chem. Soc.*, **2005**, *127*, 10008-10009 ; b) P. Brunet, M. Simard, J. D. Wuest; *J. Am. Chem. Soc.*, **1997**, *119*, 27-37-2738 ; c) X. Wang, M. Simard, J. D. Wuest, *J. Am. Chem. Soc.*, **1994**, *116*, 12119-12120 ; d) M. Simard, D. Su, J. D. Wuest, *J. Am. Chem. Soc.*, **1991**, *113*, 4696-4698

⁴⁹ a) C. B. Aakeröy, N. R. Champness, C. Janiak, *CrystEngComm.*, **2010**, *12*, 22-43; b) G. R. Desiraju; *Angew. Chem. Int. Ed.*, **2007**, *46*, 8342-8356; c) G. R. Desiraju; *Curr. Sci.*; **2005**, *88*, 374-380; d) D. Braga, L. Brammer, N. R. Champness, *CrystEngComm.*, **2005**, *7*, 1-19; e) G. R. Desiraju; *Angew. Chem.*; **1995**, *107*, 2541-2558; f) G. R. Desiraju; *Angew. Chem. Int. Ed. Engl.*; **1995**, *34*, 2311-2327; g) G. M. Whitesides, E. E. Simanek, J. P. Mathias, C. T. Seto, D. Chin, M. Mammen, D. M. Gordon; *Acc. Chem. Res.*; **1995**, *28*, 37-44; h) G. R. Desiraju; *Crystal Engineering. The Design of Organic Solids*; Elsevier, Amsterdam, **1989**; i) J.-M. Lehn; *Angew. Chem. Int. Ed. Engl.*; **1988**, *27*, 89-112

⁵⁰ S. J. Tauber, *J. Res. National Bureau of standards, A-Phys. Chem.*, **1963**, *67A*, 591-599

⁵¹ a) A. Gavezzotti; *Supramolecular interactions: energetic considerations* in 'Making crystals by design', Ed. D. Braga, F. Grepioni, Wiley-VCH, Weinheim **2006** ; b) A. Gavezzotti; *Acc.Chem.Res.*,**1994**, *27*, 309-314 ; c) G. R. Desiraju, A. Gavezzotti, *Acta Cryst.*,**1989**, *B45*, 473-475; d) A. Gavezzotti, *Molecular Shape and Crystal Packing Modes for Organic Molecules: a Computational Approach in Organic*

The synthesis of crystals is a much more difficult process to control than molecular synthesis since it involves weak, non-directional interactions with some still unknown aspects. Thus the prediction and hence the control of the structure of even simple crystal is still largely unfeasible. Consequently the obtention of solids with desired physical and chemical properties is still far from being achieved.

Coordination bond, hydrogen bond and other non-directional interactions define substructural patterns between building blocks, taking into account all these weak interactions involved in the crystal packing is extremely difficult, in this brief treatment will try to consider separately the role of the two major components, mainly coordination and hydrogen bonds.

1.4.1 Analysis and assembly prediction

The statistical analysis of experimental structures *via* the Cambridge Crystallographic Database (CSD) is an important tool for prediction of crystal packing; another very important tool is computational chemistry but a in-depth treatment lies outside the intention of this work.

We will give below three examples of predicting criteria developed in the recent years in attempts to organize and rationalise the structural data sorting out in some of empirical rules of easy application. This will be discussed again during the presentation of the results in the next chapters.

1.4.1.1 Coordination networks: prediction

Along this line, Fujita⁵² proposed a scheme related to the control of the self-assembly of discrete metallic coordination aggregates versus coordination polymeric species.

This simple scheme is built starting from the nature of the binding sites (see also endo- and exo-receptors in § 1 3 2). According to this scheme, as we can see in figure 17, if we combine a divergent component with a convergent component, we will obtain discrete aggregates, both using a naked, divergent metal centre with a convergent ligand able to envelop the metal [Fig. 17a], and using a divergent ligand after protecting the metal with a blocking ligand [Fig. 17b], conversely using two divergent synthons, we will obtain polymeric assemblies [Fig. 17c].

Materials for Non-linear Optics (Ed. R.A. Hann and D. Bloor) - Special Publ. N.69, Royal Soc. Chemistry, London **1989**.

⁵² a) M. Fujita, S. Nagao, K. Ogura, *J. Am. Chem. Soc.*, **1995**, *117*, 1649-1650 ; b) M. Fujita, D. Oguro, M. Miyazawa, *Nature*, **1995**, *378*, 469-471; b) D. L. Caulder, K. N. Raymond; *Acc. Chem. Res.*, **1999**, *32*, 975-982 ; c) S. Leininger, B. Olenyuk, P. J. Stang, *Chem. Rev.*, **2000**, *100*, 853-908

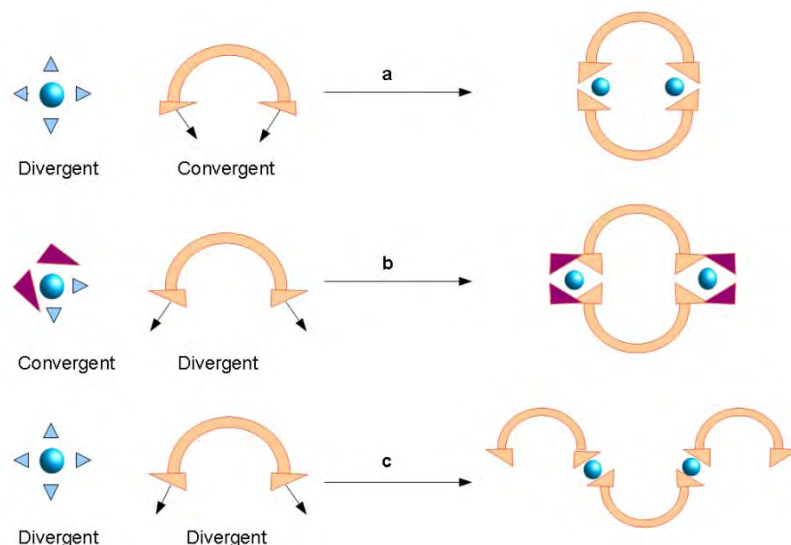


Figure 17. Fujita's scheme: a) and b) discrete assembly formation and c) extended infinite network formation using metals and ligands (ref.52a).

Other approaches to network prediction are, for instance, the Symmetry Interaction model by Raymond and Caulder^{52b} and the Molecular Library model by Stang *et al*^{52c}.

1.4.1.2 Hydrogen bonded networks: prediction

The second example is related to the prediction of hydrogen bond patterns and is known as the *Etter's rule of thumb*⁵³. These approach using CSD and applying a topological study of the hydrogen bonded arrays is based on graph set system⁵⁴. According to graph set system, an hydrogen bond motif is described by a $\mathbf{G}_d^a(\mathbf{n})$ notation where \mathbf{G} represent a graph set (D for Dimer, S for H-bond intramolecular, R for cycle, C for infinite chain), the superscript \mathbf{a} the number of acceptors, the subscript \mathbf{d} the number of donors and \mathbf{n} the number of atoms involved in the bond. For more complicated cases, when the same bond contains more than one motif, Etter distinguishes also a first and second order motif.

Some empirical rules have been established to determine the most favourable hydrogen bonding patterns. Three of these rule are general and state that i) when having the choice, hydrogen bonding occurs between better proton donor and acceptor; ii) the intramolecular six-membered hydrogen bond is the first to be formed and the most stable one [Fig. 18a]; iii) once the best donor-acceptor couples are formed, the formation of the second best donor and acceptor sets take place. The best proton donor, according to Etter's study are carboxylic acids, amides, ureas, anilines, imides, phenols.

⁵³ M. C. Etter, *Acc. Chem. Res.*, **1990**, 23, 120-126

⁵⁴ L. N. Kuleshova, P. M. Zorky, *Acta Crystallogr.*, **1980**, B36, 2113-2115

This has been illustrated, for example between carboxylic acid and 2-aminopyrimidine (2AP); in this case, CSD analysis leads to a preference for forming a cyclic $R^2_2(8)$ pattern [Fig. 18b] and, while for the naked 2AP both N atoms on the ring are the best acceptor, for a substituted 2AP there is a "priority" concerning the acceptor behaviour between both N atoms [Fig. 18c]. This represents one of the examples of prediction that follows the enounced rules, that, according to the authors, is doomed to quickly evolve with new available crystal data.

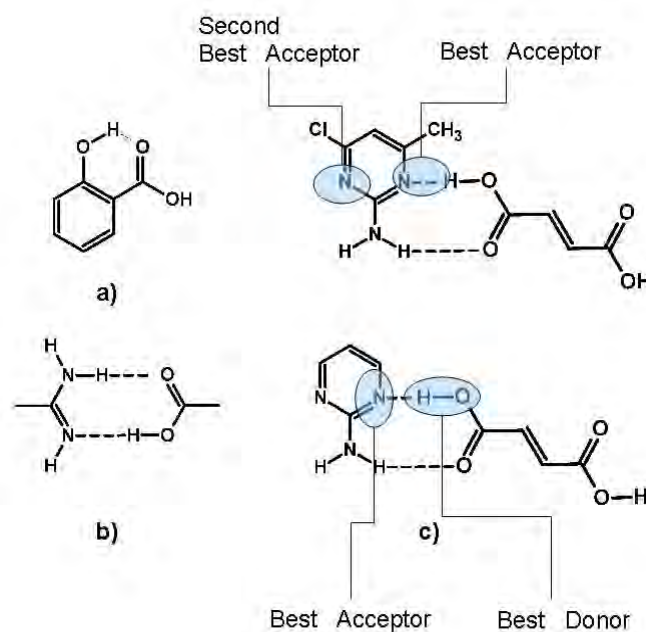


Figure 18. Etter's rules for (a) the intramolecular six-membered bonding, (b) intermolecular bonding forms a $R^2_2(8)$ pattern and (c) differentiation in the best donor and best acceptor for carboxylic acid and a 2AP (ref.53).

The last study that deserves to be described in the frame of crystal engineering, is made by the research group of Gilli⁵⁵ that built up a so called pK_a slide rule, or predicting hydrogen bond strengths from acid-base molecular properties. Based on extended bibliographic research, a wide library of pK_a values for most common classes of D-H donors and A acceptors in water has been set up leading to an empirical graphical evaluation for prediction of ΔpK_a . The "slide ruler" [Fig. 19] is based on the fact that the strength of D-H...A bond increases with decreasing ΔpK_a with a maximum for $\Delta pK_a = 0$ and was verified through gas-phase enthalpy evaluation and CSD data.

⁵⁵ P. Gilli, L. Pretto, V. Bertolasi, G. Gilli; *Acc. Chem. Res.*, **2009**, *42*, 33-44

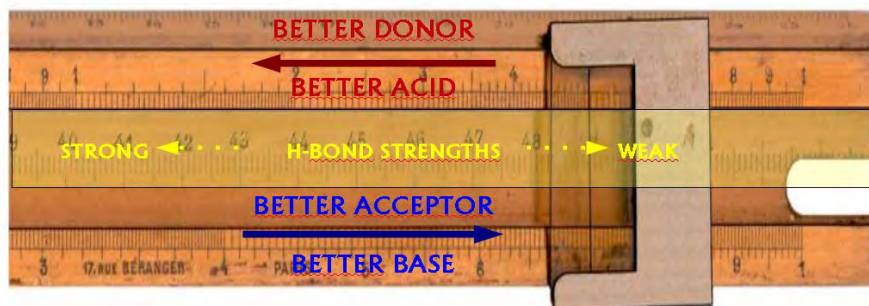


Figure 19. A wooden slide ruler illustrating the use of the rule for the prediction of acid-base association in hydrogen bonded network (ref.55).

Nevertheless the effort put in this subject, it still remains very challenging to predict the structure of crystalline solids from their chemical composition. The open subject of crystal growth process and polymorphs formation is very intriguing and, because this work deals with molecular networks in the solid state, will be briefly discussed below. Concerning the different crystallisation techniques used to obtain the studied crystals, they will be described in the Annexes.

I.4.2 Crystal formation process

For the analysis of molecular networks, crystal growth⁵⁶ is an intriguing field. Though often neglected in the network conception for his unpredictability⁵⁷, it represents one of the most interesting exploration area of crystal engineering.

Crystals are macroscopic objects showing a long-range order and bulk properties. But is it possible to anticipate the structure of a crystal from the isolated tectons? The formation of crystals results from different processes detailed below.

I.4.2.1 Crystal nucleation

The crystallisation process starts from the formation of an initial cluster (an aggregation with few units with ordering at the short range) in a supersaturated solution, the coalescence of these primordial aggregates in bigger subcritical particles that aggregate and re-dissolve constitutes the process of nucleation⁵⁸. Only once a critical, stable nucleus has formed, the veritable growth process begins with the ordering of a thick solution layer around the nucleus leading to a long range ordering. The free energy required to form the critical nucleus is affected by an unfavoured entropic factor because crystallisation introduces an ordering factor which is frequently

⁵⁶ a) J. Hulliger, *Angew. Chem. Int. Ed.*, **1994**, 33, 143-162 ; b) I. Sunagawa, *Growth, Morphology and Perfection*; Cambridge University Press, Cambridge, **2005**

⁵⁷ R. Banerjee, R. Mondal, J. A. K. Howard, G. R. Desirajul.; *Cryst. Growth Des.*; **2006**, 6, 999-1009

⁵⁸ R. J. Davies, K. Allen, N. Blagden, W. I. Cross, H. F. Liebermann, M. J. Quayle, S. Righini, L. Seton, G. J. T. Tiddy, *CrystEngComm*, **2002**, 4, 257-264

lowered by interactions with the reaction vessel surfaces or the presence of even very small impurities that act as aggregation nuclei.

McBride and Carter⁵⁹ demonstrate that crystal growth starts from only one crystallisation event by an interesting and elegant experiment. Starting from NaClO₃, that crystallise into a chiral space group usually in the statistic racemic mixture, they could prove that if the crystallisation is perturbed by stirring, only one enantiomorphous form is obtained. They filmed the precise moment where the first crystallisation nucleus was stroked by the stirrer bar spreading around into the solution invisible cluster fragments that give rise to many crystallisation nuclei over only 30 seconds and, incredibly, all the formed crystals were L-handed.

1.4.2.2 Crystal growth

The crystallisation process is, by definition, a self-assembly process (§ 1.1.2.2) because the different molecular components must find and recognise one each other and find their optimum orientation, the resulting aggregate must then grow further, resulting in a robust ordered nucleus.

In organic chemistry, crystallisation has been for a long time one of the most effective methods of purifying substances and separating racemates, most recently, under the impulse of industrial crystallisation⁶⁰ and materials research, new single-crystal growth methods have been developed or optimized. The crystallisation process is often made in solution⁶¹ but occurs also in gel⁶², via hydrothermal synthesis⁶³ or in the solid state⁶⁴ with different kinetics.

Crystallisation is fundamentally a non-equilibrium phenomenon in which both kinetics and thermodynamics aspects contribute to the final structure. Concerning coordination polymers, in order to avoid amorphous products, it is preferable to use a labile metal-ligand combination that allows the initially formed (kinetic) products, which may be mixtures, to have the opportunity to rearrange and give a single thermodynamically favoured product. When self-assembly in solution is thermodynamically controlled, the components are able to shift through a variety of possible structures, using self-reparation through decomplexation and re-complexation

⁵⁹ J. M. McBride, R.L. Carter, *Angew. Chem. Int. Ed.*, **1991**, *30*, 293-295

⁶⁰ W. A. Tiller, *The Science of Crystallisation* (Vol. I and II), Cambridge University Press, Cambridge, **1991**

⁶¹ a) G. Matz, *Kristallisation, Grundlagen und Technik*, Springer, Berlin, **1969**; b) R. A. Horne, *Water and Aqueous Solutions*, Wiley, New York, **1972**

⁶² A. Rabenau, *Angew. Chem. Int. Ed.*, **1985**, *24*, 1026-1040

⁶³ H. K. Heinisch, *Crystals in Gels and Liesegang Rings*, Cambridge University Press, Cambridge, **1988**

⁶⁴ T. Friščić, E. Meštrović, D. Škalec Šamec, B. Kaitner, L. Fábián, *Chem. Eur. J.*, **2009**, *15*, 12644-12652

steps until they find the one of the maximum stability and minimum of energy (see figure 19).

1.4.2.3 Polymorphism: a thermodynamic approach

Polymorphism for crystals can be considered like isomerism for supramolecular structures. The crystal packing depends in many cases on crystallisation conditions and polymorphic structures (crystals with the same synthons but different packing arrangements) are common. Predict polymorphism⁶⁵ is a difficult task and has great consequences concerning, for instance, the potential commercial application, the main interested fields are pharmaceutical⁶⁶ and pigment⁶⁷ industry.

Two main approaches have been proposed to rationalize the packing of organic molecular crystals: a thermodynamic and a kinetic one.

The one proposed by Kitaigorodskii⁶⁸ is more geometrical, assuming that interactions are weak and without directionality. In this *isotropic model*, crystal structures are governed by close packing rather than specific interactions, along with this theory the packing is based on the total system energy *i.e.*, in solution, the system is able to explore all the possible molecular combinations before selecting the one lowest in energy through already exposed crystal nucleation process, this leads to 'thermodynamic crystal' (see § 1.4.2) [Fig.20].

The *chemical model* was originally proposed by Etter⁶⁹, it implies that structural directionality dominates the crystal formation and is brought about by chemical factors. As hydrogen bonds become weaker, the anisotropic component of packing decreases but it never disappears completely. With this approach and forcing the simplification, a close look at the hydrogen bond pattern is enough to bring back to the final packing of what is considered the 'kinetic crystal' [Fig.20]. Following a kinetic model, structures that form faster will predominate over structures that are most stable. Considering to see crystallization as a supramolecular reaction, polymorphs are as alternative reaction products⁷⁰.

⁶⁵ a) J. D. Duniz, A. Gavezzotti, *Angew. Chem. Int. Ed.*, **2005**, *44*, 1766-1787 ; b) J. W. Steed, *CrystEngComm.*, **2003**, *5*, 169-179 ; c) A. Gavezzotti; *Cryst. Eng. Comm.*, **2002**, *4*, 343-347

⁶⁶ A. Bruger, *Topics in Pharmaceutical Sciences*, Elsevier,; Amsterdam, **1983**

⁶⁷ P. Erk, H. Helgelsberg, M. F. Haddow, R. Van Gelder, *CrysEngComm.*, **2004**, *6*, 674-679

⁶⁸ A. I. Kitaigorodski; *Molecular crystals and molecules*, Academic Press, New York, **1973**

⁶⁹ M. C: Etter, *Acc. Chem. Res.*, **1990**, *23*, 120-126

⁷⁰ G. R. Desiraju, *Nat. Mater.*, **2002**, *1*, 77-79

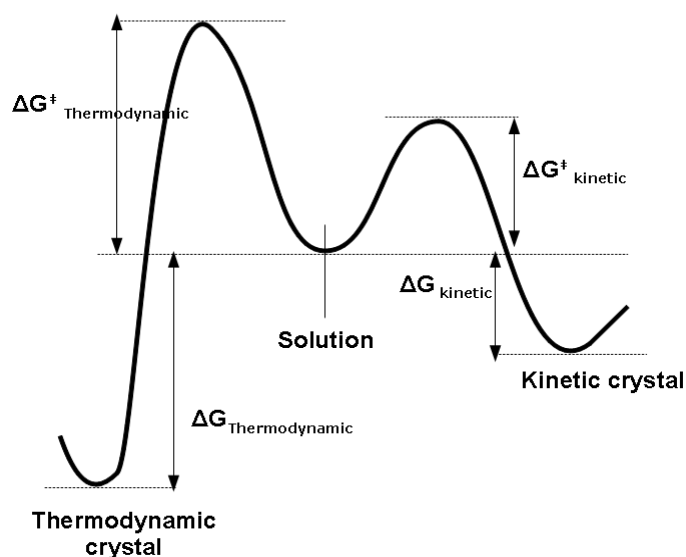


Figure 20. Energetic representation of the thermodynamic and kinetic products of crystallisation..

The supramolecular synthon concept is settled in the mid-way trying to combine both theories (geometric and hierarchical approach) in the real crystal life. The synthon formation in fact requires both interaction energies (anisotropy) and crystal packing energies (isotropy). Some examples describe kinetic and thermodynamic crystals⁷¹. We can consider a first example where the thermodynamic crystal is equivalent to the kinetic one. In this situation, polymorphism will certainly not be observed. When the kinetic and thermodynamic crystals are different, polymorphism is observed according to the kinetic or thermodynamic pathways chosen during crystallization process. Roughly, the thermodynamic crystal is the one with the best crystal packing but not necessary with the most favourable interactions and *vice versa* for the kinetic crystal. [Fig.20]

A major challenge is to establish general experimental protocols to obtain the thermodynamic crystal in any polymorphic system. This would mean, methods to slow down nucleation such as high-temperature and hydrothermal synthesis, gel growth, crystallization from supercritical fluids, or other methods unexplored up to now. A significant example is the case of 1,3,5-trinitrobenzene, where the thermodynamic crystal is three-dimensionally close-packed and was calculated to be 5.8 kcal mol⁻¹ more stable than its kinetic polymorphous crystal, but was discovered 125 years after⁷².

⁷¹ a) S. Roy, A. Nangia; *Cryst. Growth Des.*, **2007**, *7*, 2047-2058 ; b) G. R. Desiraju; *Angew. Chem. Int. Ed.*, **2007**, *46*, 8342-8356 ; c) A. Dey, G. R. Desiraju; *CrystEngComm*; **2006**, *8*, 478-482 ; d) A. Dey, M. T. Kirchner, V. R. Vangala, G. R. Desiraju, R. Moondal, J. A. K. Howard; *J. Am. Chem. Soc.*; **2005**, *127*, 10545-10559 ; e) K. Muller, F. Diederich, R. Paulini; *Angew. Chem.*; **2005**, *117*, 1820-1839; *Angew. Chem. Int. Ed.*; **2005**, *44*, 1788-1805 ; f) G. R. Desiraju; *CrystEngComm*; **2002**, *4*, 499

⁷² P. K. Thallapally, R. K. R. Jetti, A. K. Katz, H. L. Carrell, K. Singh, K. Lahiri, S. Kotha, R. Boese, G. R. Desiraju; *Angew. Chem. Int. Ed.*; **2004**, *43*, 1149-1155

Some of these techniques have been used in this work (see Annexes), from the most common solvent diffusion and evaporation of very diluted solution (10^{-3} - 10^{-4} M) to hydrothermal synthesis and gel growth, with different success.

I.5 Hydrogen and coordination bonding in molecular networks

There will be now presented some examples of functional networks conceived using concepts illustrated along this work (self-recognition, molecular tectonic and network conception, crystal engineering and crystal growth).

In particular we are going to distinguish coordination, hydrogen and hybrid networks, for each, we'll give a general introduction and we'll present some significant examples.

I.5.1 Functional networks based on coordination bond

I.5.1.1 Generalities

The coordination bond is one of the chief driving force to obtain infinite molecular architectures or coordination polymers⁷³. The advantage to use coordination bonds as driving force in the building of a supramolecular networks resides in the robustness of the final structure and in its highly directional feature, in fact, the binding energy of a dative bond is the highest among the weak interactions (see figure 5) and, at the same time, it is possible to play with its lability or inertness.

The use of metallic tecton offers the possibility to introduce within the architecture physical property such as photochemical, electrochemical or magnetic properties.

I.5.1.2 Examples of multifunctional networks

Coordination networks are investigated for their magnetic properties⁷⁴, optical properties⁷⁵, gas storage ability⁷⁶, sensing functionality⁷⁷ and electronic conduction⁷⁸,

⁷³ a) M. D. Ward, *Annu. Rep. Prog. Chem. Sect. A*, **2002**, 98, 285-320 ; b) S. L. James, *Chem. Soc. Rev.*, **2003**, 32, 276-288

⁷⁴ a) J. H. Nettleman, R. M. Supkowski, R. L. LaDuca; *J. Solid State Chem.*, **2010**, 183, 291-303; b) M. Clemente-Leon, E. Coronado, M. Lòpez-Jordà, G. Miinguez Espallargas, A. Soriano-Portillo, J. C. Waerenborgh; *Chem. Eur. J.*, **2010**, 16, 2207-2219 ; c) L. F. Ma, B. Liu, L.-Y. Wang, C.-P. Li, M. Du, Dalton Transactions, **2010**, 39, 2301-2308; d) M. Andruh, *Chem. Commun.*, **2007**, 2565-2567; e) E. Coronado, J. R. Galán-Mascarós, C. J. Gómez-García, V. Laukhin; *Nature*, **2000**, 408, 447-449 ; f) Miller, J. S. *Inorg. Chem.* **2000**, 39, 4392-4408

⁷⁵ a) Sliwa, M.; Letard, S.; Malfant, I.; Nierlich, M.; Lacroix, P. G.; Asahi, T.; Masuhara, H.; Yu, P.; Nakatani, K.; *Chem. Mater.* **2005**, 17, 4727-4735. ; b) Datta, A.; Pati, S. K.; *Chem. Soc. Rev.*, **2006**, 35, 1305-1323.; c) Cariati, E.; Macchi, R.; Robert, D.; Ugo, R.; Galli, S.; Casati, N.; Macchi, P.; Sironi, A.; Bogani, L.; Caneschi, A.; Gatteschi, D., *J. Am. Chem. Soc.* **2007**, 129, 9410-9420

sometime with a synergetic effect between these properties, leading to multifunctional materials.

As the only presented example related with molecular magnetism, we report a recent study, published by Miyasaka *et al.*⁷⁹, of a reversible photoswitching based on coordination assemblies of single-molecule magnets (SMMs) (see figure 21).

The compound is a monodimensional chain composed of mixed tetranuclear $[\text{Mn}^{\text{II}}_2\text{-Mn}^{\text{III}}_2]$ complexes linked by carboxylates extremities of a diarylethene ligand. The photochromic reaction in the solid state induces an isomerization of the ligand, as illustrated in figure 21, with a simultaneous magnetization of the Mn complex arrays.

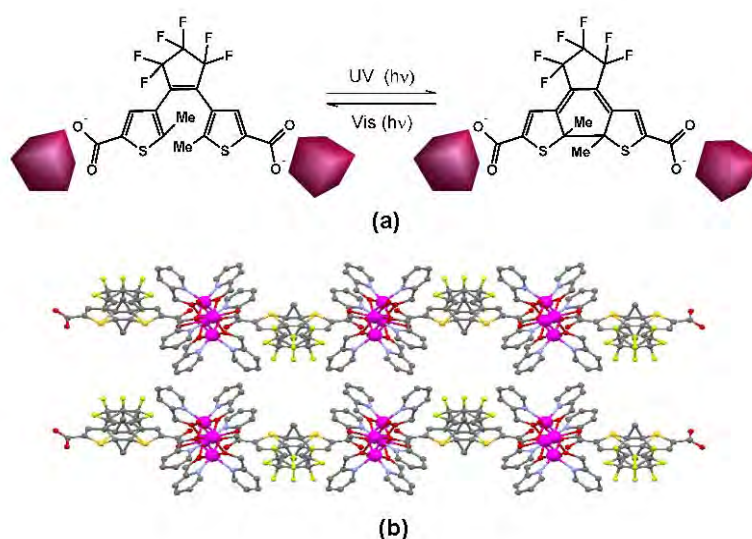


Figure 21. Example of multifunctional coordination network: a) photoswitchable isomerisation of the diarylethene ligand, b) single chain formed by the supramolecular assembly of SMMs linked by photochromic ligand (ref.79).

⁷⁶ a) Wang, X.-S.; Ma, S., Yuan, D.; Yoon, J. W.; Hwang, Y. K.; Chang, J.-S.; Wang, X.; Jorgensen, M. R.; Chen, Y.-S.; Zhou, H.-C., *Inorg. Chem.*, **2009**, *48*, 7519–7521 ; b) Jeon, Y.-M.; Armatas, G. S.; Heo, J.; Kanatzidis, M. G.; Mirkin, C. A.; *Advanced Materials* , **2008**, *20*, 2105-2110 ; c) T. K. Maji, S. Kitagawa, *Pure and Applied Chemistry*, **2007**, *79*, 2155-2177; d) Y. Kubota, M. Takata, R. Matsuda, R. Matsuda, R. Kitaura, S. Kitagawa, T. C. Kobayashi; *Angew. Chem. Int. Ed.*; **2006**, *45*, 4932-4936 ; e) J. L. Rowsell, O. M. Yaghi, *Angew. Chem. Int. Ed.*, **2005**, *44*, 4670-4675

⁷⁷ a) A. Kobayashi, H. Hara, S.-I. Noro, M. Kato, *Dalton Trans.*, **2010**, DOI: 10.1039/b91769d ; b) N. Iki, M. Ohta, T. Tanaka, T. Horiuchi, H. Hoshino, *N. J. Chem.*, **2009**, *33*, 23-25 ; c) M. Melegari, M. Suman, L. Pirondini, D. Moiani, C. Massera, F. Uguzzoli, E. Kalenius, P. Vainiotolo, J.-C. Pirater, J.-P. Dutasta; *Chem. Eur. J.*, **2008**, *14*, 5772-5779 ; d) F. Faridbod, M. R. Ganjali, R. Dinavard, P. Norouzi, S. Riahi, *Sensors*, **2008**, *8*, 1645-1703 ; e) C. Siering ; H. Kerschbaumer ; M. Nieger ; S. R. Waldvogel, *Organic Letters*, **2006**, *8*, 1471-1474

⁷⁸ a) H. Minemawari, T. Naito, T. Inabe; *Cryst. Growth. Des.*, **2009**, *9*, 4830-4833; b) J.-F. Gao, Z.-M. Li, Q.-j. Meng, Q. Yang; *Mat. Lett.*, **2008**, *62*, 3530-3532; c) E. Coronado, J. R. Galan-Mascaros, C. Gimenez-Saiz, C. J. Gomez-Garcia; *Mol. Cryst. Liq. Cryst. Sci. Tech., sect. A*; **1997**, *305*, 543-552

⁷⁹ M. Morimoto, H. Miyasaka, M. Yamashita, M. Irie, *J. Am. Chem. Soc.*, **2009**, *131*, 9823-9835

I.5.2. Functional networks based on hydrogen bond

I.5.2.1 Generalities

The importance of hydrogen bonding⁸⁰ is eminent concerning the structure, function and dynamics of a large number of chemical systems. The involved fields are very different and include mineralogy, material science, general inorganic and organic chemistry, supramolecular chemistry, biochemistry, molecular medicine as well as pharmacy. The hydrogen bond is the most important of all directional intermolecular weak interactions. Hydrogen bonding is useful for its directionality, flexibility and strength (see § I.1.2.3).

Hydrogen bonding in biological or chemical systems is complex and we can roughly distinguish between (i) strong hydrogen bonds, with binding energies of more than 60 kJ/mol and distances between 2.2 and 2.5 Å that are comparable with the sum of van der Waals radii, (ii) moderate hydrogen bonds, that are by far the most common particularly in biological systems, with energies between 15-60 kJ/mol and distances of 2.5-3.2 Å and (iii) very weak hydrogen bonds between poor acceptors and poor donors with energies <15 kJ/mol and distances of up to 4 Å.

The strongest hydrogen bonds have a major covalent contribution⁸¹, considering the O-H...O interaction in water, the intermolecular distance is shortened by around 1 Å compared to the sum of the van der Waals radii for the H and O atoms, which indicates that there is substantial overlap of electron orbitals to form three-centre four-electron bond. Medium-strong hydrogen bonding are usually assisted by an isotropic charge (electrostatic charge-assisted Hydrogen bond or CAHB), they can reach higher binding energies as, for example, the F-H...F⁻ hydrogen bond is one of the strongest ever known and has a bond energy around 160 kJ/mol, where the moderate and weak ones have a mainly isotropic electrostatic nature.

The correspondence length/strength in hydrogen bonding is still debated and not simple, it is important to consider a second parameter that is the D-H...A angles. The range of possible D-H...A angles changes and is narrow for the stronger, linear hydrogen bond (or σ -type with D-H...A angles of $\approx 180^\circ$) where the proton is shared almost equally between the two electronegative atoms (see figure 22 below), while the most frequent moderate hydrogen bonds are distorted or bent with an angle range of 130° - 180° that delimitates a 'cone of approach' of the donating D to the acceptor A species, ending up to 90° - 150° angles for the weakest ones (see figure 22).

⁸⁰ a) A. D. Buckingham, J.E. Del Bene, S. A. C. McDowell; *Chem. Phys. Letters*; **2008**, 463, 1-10 ; b) H.D. Lutz, *J. Mol. Struc.*, **2003**, 646, 227-236 ; c) T. Steiner; *Angew. Chem. Int. Ed.*; **2002**, 41, 48-76 ; d) T. Steiner, G. Koellner; *J. Mol. Biol.*; **2001**, 305, 535-557; e) G. R. Desiraju, T. Steiner; *The Weak Hydrogen Bond in Structural Chemistry and Biology*; OUP, Oxford, **1999** ; f) G. A. Jeffrey; *Introduction to Hydrogen Bonding*; OUP, Oxford, **1997**

⁸¹ P. Gilli, V. Bertolaso, V. Ferretti, G. Gilli, *J. Am. Chem. Soc.*, **1994**, 115, 909-919

Long-range interactions and short-range packing requirements in the case of crystals can change the structure of hydrogen bond by distorting it from linearity; bifurcated hydrogen bonds are another recurrent structural motif (figure 22). There is a correspondence between structure and strength of hydrogen bond, roughly the linear symmetric one is considered strong and the bifurcated non-linear one is relatively weak.

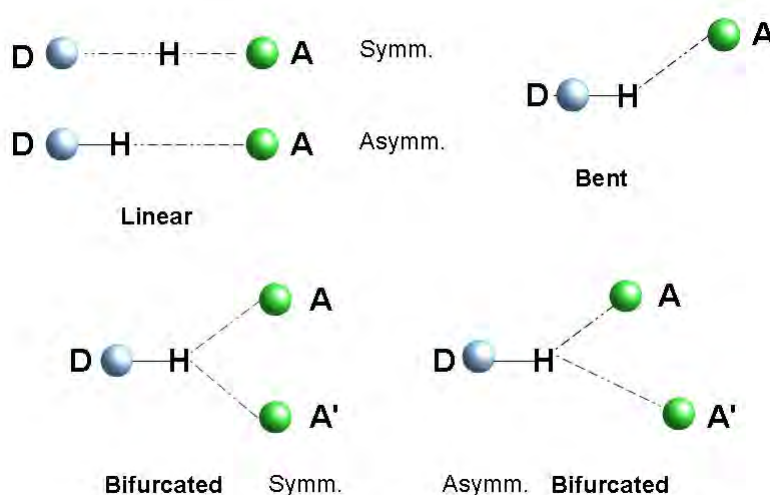


Figure 22. Symmetric and asymmetric hydrogen bonds, together with their different geometries.

About the techniques suited for studying hydrogen bonding in chemical systems, next to some classical ones like Infrared and Raman spectroscopy, or newer like Magic Angle Spinning NMR (MAS-NMR) the technique of excellence is the Inelastic Neutron Scattering (INS) that is the only instrumentation that can locate precisely the hydrogen position since the density of hydrogen atom is too low to be determined by XRD. X-ray diffraction will be the major technique used in this work. Nowadays X-ray crystallography is becoming an even more powerful technique with modern X-ray detectors, which enables to refine hydrogen position within the third decimal digit. In practical use, the position of the hydrogen is precisely localized through local density determination only for strong, highly directional hydrogen bonds, in the other case, hydrogen position is mathematically ensued starting from the hybridization of the linked atoms (sp , sp^2 , sp^3); but it is not possible to localize precisely their position in case of weak isotropic hydrogen bonds.

1.5.2.2. The role of hydrogen bond in molecular recognition

Hydrogen bonding is an eminent favourite for crystal design as is demonstrated by the large literature on the subject; as stated in § 1.4.1.2, the prediction concerning H bond pattern is possible, and Allen *et al.*⁸² have even determined a scale of probability

⁸² F. H. Allen, W. D. S., Motherwell, P. R. Raithby, G. P. Shields, R. Taylor, *New J. Chem.*, **1999**, 23, 25-34

of formation (P_m) for 75 bimolecular ring motifs, some of them being illustrated in figure 23, following the Etter's rules.

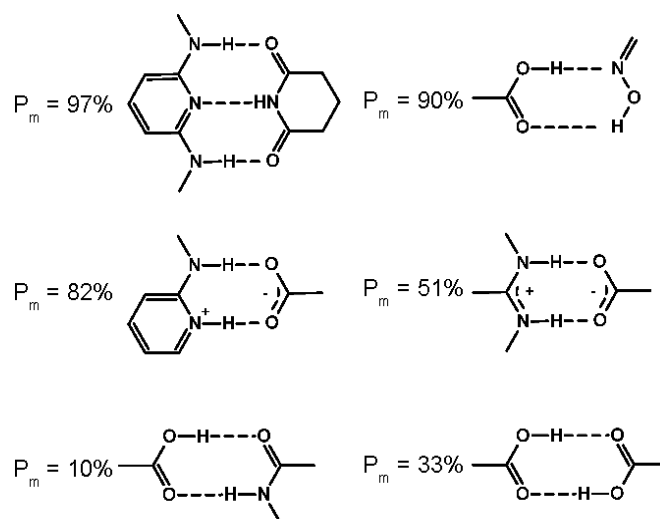


Figure 23. Some examples of estimated probability of formation (P_m) for cyclic hydrogen bond recognition patterns in organic H bonded networks (ref.82).

Charge assistance has long been recognized as a practical way to reinforce the hydrogen bond, and to allow the prediction of the patterns⁸³. This will be illustrated in the case of the interaction between bis-amidinium cations and anions (see § I.5.2.4 and § II.2.3).

In the recent years an increasing number of hydrogen bonded networks have been published with an increasing interest for functional networks⁸⁴. Here will be presented some examples of functional networks based on hydrogen bond alone and in combination with coordination bond.

I.5.2.3 Functional organic networks based on hydrogen bond

Many examples of organic H bonded networks have arisen from concepts of crystal engineering (see § I.3 and § I.4), some of them being functional.

Hydrogen bonded networks are sometimes investigated also for their ability to form amorphous compounds. Wuest *et al.*⁸⁵ studied derivatives of the aminotriazine, shown in figure 24b, looking for amorphous molecular glasses for use in optoelectronic devices. Derivatives of this substituted triazine forms hydrogen bonded networks as shown by the crystal structure of pentamethyl product [Fig. 24], when changing methyl with longer chain, they inhibit crystallisation in order to form glasses with high T_g (glass transition temperature) and electronic properties.

⁸³ M. D. Ward, *Chem. Commun.*, **2005**, 5838-5842

⁸⁴ a) C. B. Aakeröy, A. M. Beatty, *Aus. J. Chem.*, **2001**, *54*, 409-421 ; b) J. C. MacDonald, G. M. Whiteside, *Chem. Rev.*, **1994**, *94*, 2383-2420

⁸⁵ O. Lebel, T. Maris, M.-E. Perron, E. Demers, J. D. Wuest, *J. Am. Chem. Soc.*, **2006**, *128*, 10372-10373

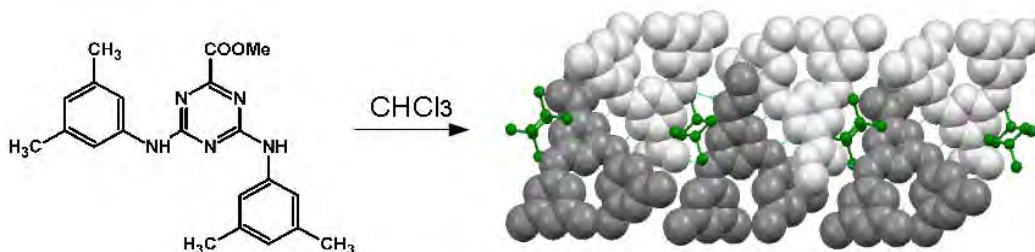


Figure 24. Bis(mexylamino)-triazine crystallized from chloroform (ref.85); its derivatives are exploited as glasses for optoelectronic devices for their low crystallisation tendency.

Hereafter are considered some examples of networks ensuing for the simultaneous use of H-bond and coordination bond, specially conceived for desired applications, other literature examples more strictly related to three component networks will be reported in the next chapter (§ II.2).

1.5.2.4 Functional networks based on mixed H-bond and coordination bond

Adding hydrogen bonding to coordination bond can lead to new topology for solid molecular network. Such networks appeared recently in the literature with an increasing number of examples in different fields: fluorescence, surface functionalisation, medicine and biomimetic materials, and electronics⁸⁶.

The photoluminescence properties are exploited in the case of hydrogen bonded arrays through pyridine dicarboxylic acid interactions to a core cluster of $[\text{Re}_6\text{Se}_8]^{2+}$ (see figure 25)⁸⁷. $[\text{Re}_6\text{Q}_8]^{n+}$ clusters, where (Q = S, Se, Te), are promising units as potential candidates⁸⁸ in multiple fields (chemical sensors, magnetic materials, drug carriers etc.)



⁸⁶ a) A. C. Laungani, M. Keller, J. M. Slattery, I. Krossing, B. Breit, *Chem. Eur. J.*, **2009**, *15*, 10405-10422; b) L. Fischer, M. Decossas, J.-P. Briand, C. Didierjean, G. Guichard, *Angew. Chem. Int. Ed.*, **2009**, *48*, 1625-1628; c) R. Madueno, M. T. Räisänen, C. Silien, M. Buck, *Nature*, **2008**, 618-621; d) J. De Girolamo, P. Reiss, A. Pron, *J. Phys. Chem. C*, **2007**, *111*, 14681-14688; e) J.-Z. Lu, J.-W. Huang, L.-F. Fan, J. Liu, X.-L. Chen, L.-N. Ji, *Inorg. Chem. Commun.*, **2004**, *7*, 1030-1033

⁸⁷ H. D. Selby, B. K. Roland, M. D. Carducci, Z. Zheng, *Inorg. Chem.*, **2003**, *42*, 1656-1662

⁸⁸ Y. Kim, V. E. Fedorov, S.-J. Kim; *J. Mater. Chem.*, **2009**, *19*, 7178-7190

Figure 25. 1D H-bonded arrays containing a cluster of $[Re_6Se_8]^{2+}$ and pyridine dicarboxylic acid (ref.87)

Another example has been developed inside the laboratory⁸⁹ exploiting a series of isomorphous compounds to stimulate the epitaxial growth *i.e.*, the crystal growth around another single crystal. This is one significant case of application of the crystal engineering principles; using a CAHB between $[Co(CN)_6]^{3-}$ or $[Fe(CN)_6]^{3-}$ salts and the organic bisamidinium dication BADbenz3 [Fig. 26] and exploiting a recurrent hydrogen bonding motif, leading to "crystals of crystals".

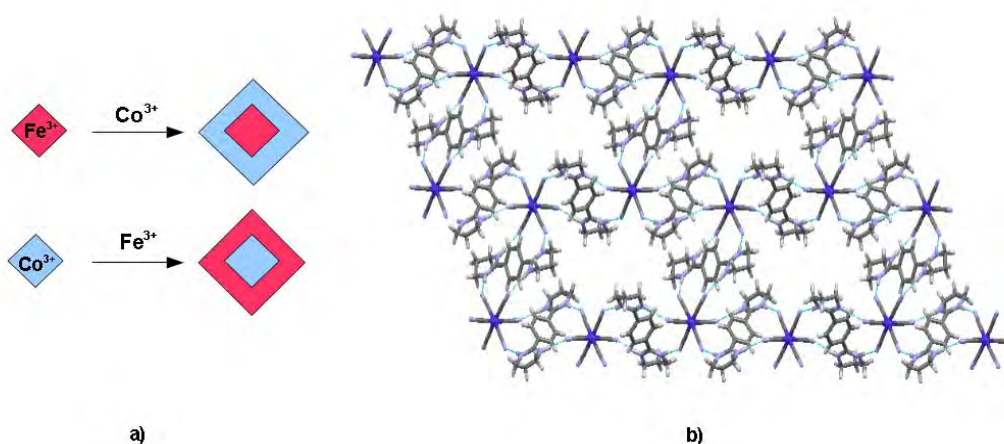


Figure 26. a) Schematic representation of the epitaxial growth and b) particular view of the crystal packing and coordination/hydrogen bonding interconnection of $[Co(CN)_6]_2(BADbenz3)_3$ (ref.89).

With the approaches and concepts developed in this first part and using the tools (weak hydrogen bonds and labile coordination bonds) a large variety of molecular networks have been obtained, and especially functional networks. This is the context where this project has been developed.

1.6 Purpose of this work

The most recent development of supramolecular chemistry⁹⁰ is related to the declared intent of controlling the formation of supramolecular assemblies and architectures by the use of molecular recognition processes: self-assembly and self-

⁸⁹ S. Ferlay, M. W. Hosseini, *Chem. Commun.*, **2004**, 788-789

⁹⁰ J.-M. Lehn, *Supramolecular Chemistry; concepts and perspectives*, VCH, **1995**

organisation. The supramolecular assembly of several molecular compounds results from the spontaneous association of the different tectons, induced by recognition events under the intermolecular control of non-covalent interactions in solution.

The purpose of this project is to prepare and analyse, from a structural point of view, new functional hybrid organic/inorganic networks based on self-recognition events and, more generally, to explore, better understand and develop the way to combine hydrogen and coordination bond together, in order to obtain reliable, reproducible assemblies that may present some physical properties. We manage to rationalize the way to obtain mono-, bi-, tri- dimensional architectures through the use of appropriate tectons.

The presented work finds his collocation into the field of *molecular tectonics*, in particular the self-assembly and self-organization of molecular tectons based on hydrogen bonding and coordination bond, and will be divided into three parts.

The first main part is related with the conception and synthesis of hybrid organic-inorganic molecular networks based on self-recognition between a specific H-bond acceptor (carboxylate anion) and a specific H-bond donor, a cyclic bisamidinium cation, developed into our research group.

In a second part we will present new hybrid self-assembled networks, in particular an Ag wire based on coordination bond between a silver salt and carboxylate anion, and in the third part will be discussed the development of a new class of polypyridine-amides ligands, their synthesis and their conception in order to exploit the self-recognition pattern between pyridine amide and carboxylic acid for the formation of helical hydrogen bonded assemblies toward mixed, hybrid organic-inorganic networks *via* coordination and hydrogen bonds.

Chapter II

Tectons for H-Bonded Hybrid Networks and Isolated Complexes

II.1 Generalities, objectives and strategies

The undertaken project focuses on the use of the hydrogen bonding interaction between carboxylate and bis-amidinium tecton in the formation of molecular networks involving coordination complexes. The introduction of a metal ion in such structures is also interesting for the combination of the rich physical properties of transition metals with potential application in optics, magnetism, conducting materials. The formation of reliable architectures with the possibility of varying the size of the inner pores is also a challenge.

Since the nineties, among all the chemical groups widely used in crystal engineering¹, carboxylates moieties are used in the coordination sphere of the metal as O-donor ligands, that is generally the case for topics like metal-organic frameworks², coordination networks on surfaces³, coordination polymers⁴; otherwise hydrogen bond is used as unique driving force for the architecture construction and the obtained structures are purely organic networks⁵.

Third point, considering the self-complementarity of the components, lots of supramolecular architectures reported are homomeric⁶, *i.e.*, built up from a unique self-complementary building block. Considering the last point, in fact, we have many examples of hydrogen bonded networks generated by self-assembling of a single

¹ a) D. Braga, L. Brammer, N. R. Champness, *CrystEngComm.*, **2005**, *7*, 1-19; b) L. Brammer, *Chem. Soc. Rev.*, **2004**, *33*, 476-489; c) N. A. J. M. Sommerdijk, *Angew. Chem., Int. Ed.*, **2003**, *42*, 3572-3574; d) D. Braga, G. R. Desiraju, J. S. Miller, A. G. Orpen, S. L. Price, *CrystEngComm.*, **2002**, *4*, 500-509; e) B. Moulton, M. J. Zaworotko, *Chem. Rev.*, **2001**, *101*, 1629-1658; f) D. Braga, F. Grepioni, *Acc. Chem. Res.*, **2000**, *33*, 601-608; g) C. B. Aakeröy, *Acta Crystallogr.*, **1997**, *B53*, 569-586

² a) J. R. Long, O. M. Yaghi; *Science*, **2010**, *327*, 846-850; b) L. Hamon, C. Serre, T. Devic, T. Loiseau, F. Millange, G. Ferey, G. De Weireld; *J. Am. Chem. Soc.*, **2009**, *131*, 8775-8777; c) D. J. Tranchemontagne, J. L. Mendoza-Cortes, M. O'Keefe, O. M. Yaghi, *Chem. Soc. Rev.*, **2009**, *38*, 1257-1283; d) S. Horike, S. Shimonura, S. Kitagawa, *Nature Chem.*, **2009**, *1*, 695-704; e) W. Yang, X. Lin, A. J. Blake, C. Wilson, P. Hubberstey, N. R. Champness, M. Schröder, *Inorg. Chem.*, **2009**, *48*, 11067-11078; f) S. L. James, *Chem. Soc. Rev.*, **2003**, *32*, 276-288

³ a) N. Lin, Langner, S. L. Tait, C. Rajadurai, M. Ruben, K. Kern, *Chem. Comm.*, **2007**, 4860-4862

⁴ a) N. R. Kelly, s. Goetz, S. R. Batten, P. E. Kruger, *CrystEngComm*, **2008**, *10*, 1018-1026; b) Q. Chu, G.-X. Liu, Y.-Q. Huang, X.-F. Wang, W.-Y. Sun, *Dalton Trans.*, **2007**, 4302-4311

⁵ a) C. B. Aakeröy, J. Desper, J. F. Urbina, *CrystEngComm*, **2005**, *7*, 193-201; b) A. Moghimi, M. Ranjbar, H. Aghabozorg, F. Jalali, M. Shamsipur, G. P. A. Yap, H. Rahbarnoohi, *J. Mol. Structure*, **2002**, *605*, 133-149; c) C. B. Aakeröy, A. M. Beatty, B. A. Helfrich, *Angew. Chem. Int. Ed.*, **2001**, *40*, 3240-3242; d) M. C. Etter, *J. Phys. Chem.*, **1991**, *95*, 4601-4610; e) M. C. Etter, *Acc. Chem. Res.*, **1990**, *23*, 120-126; f) M. C. Etter, G. M. Frankenbach, *Chem. Mater.*, **1989**, *1*, 10-12

⁶ J. D. Duniz in *Perspectives in Supramolecular Chemistry, Vol.2: The crystal as a Supramolecular Entity*, Wiley, New York, **1995**

carboxylic acid type tecton leading to mono-dimensional, bi-dimensional or tri-dimensional networks [see Introduction].

The originality of the project consists in: a) the use of a system with three components (an organic spacer **A**, a ligand **B** and a metal centre **C** [see Fig. 1]) instead of two components (a self-complementary ligand plus a metal centre or two complementary organic species), as in the majority of the existing examples; b) the carboxylate moieties placed at the periphery of the ligands and used as H-bond donor acceptor for hydrogen bonding; c) the attempt to achieve a controlled and selective use of two different bonds during the synthesis of the network.

Of course, due to the introduction of a supplementary tecton, the complexity⁷ of the system increases; passing from two to three components and using at least two different driving forces, charge assisted hydrogen bond and coordination bond, the combination possibilities of the components are statistically increased. That explains the intricacy to obtain this kind of networks.

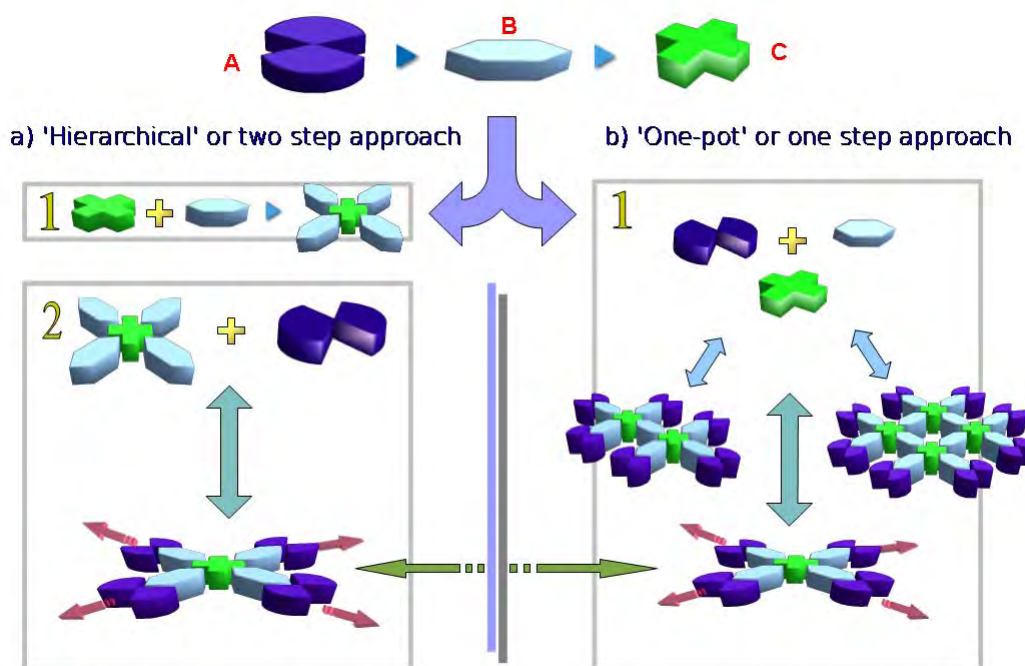


Figure 1. Schematic representation of both strategies carried out for the obtention of H bonded coordination networks : a) Hierarchical strategy, b) One-pot strategy.

In figure 1, we give a schematic representations of the components (three objects and two nodes) involved in the formation of the envisaged systems; component **A** represents cyclic bis-amidinium cation acting as a proton donor in charge assisted hydrogen bond and used as organic spacer; component **B** represents N-chelating type ligands based on bipyridine, biquinoline and phenanthroline backbones bearing one or

⁷ J.-M. Lehn, *Supramolecular Chemistry; concepts and perspectives*, p.201-202, [10.14]

two carboxylates (proton acceptor) moieties for hydrogen bonding [or vice-versa bearing two amidine moieties (proton donor) and in this case **A** is a dicarboxylic acid (proton acceptor)]; component **C** represents a metallic or semi-metallic centre. We can consider all the three independently [Fig.1b] or we can group two of them reducing in this way the number of possible spontaneous assemblies of the system [Fig.1a].

In a first strategy, following what we called a '*hierarchical approach*', we synthesised a series of tetra-, tri-, di- and mono-metallic complexes using N-chelating ligands of bipyridine type (**C** + **B**, forming a metallatecton). In a second step, these tectons were tested as building blocks *via* coupling with bis-amidinium cations (**B**, proton donor) in order to obtain networks with different dimensionalities. In this way, the coordination node is preformed and only in a second step the hydrogen bond will be set up. The idea subtended is to direct and pre-organize the system that, even if it contains three components, is handled as a two components one [Fig. 1a].

In the second adopted strategy, a *one-pot* self-assembly approach under mild conditions is performed mixing simultaneously the three components: the chelating ligand bearing carboxylates moieties (proton acceptor), the bis-amidinium cation (proton donor) and the metal salt. In this way both assembling nodes i) the coordination node, between metal and ligand, and ii) the hydrogen bonding node between the complementary carboxylate and amidinium, are set up together [Fig. 1b].

During this project, we will focus on solid state structural studies, thus the obtention of single crystals is crucial for the complete structural investigation.

The state of the art in the literature, regarding this type of architectures, will be examined in the following section.

II.2 State of the art in the literature

In this section some meaningful examples reported in literature of hybrid networks using coordination and hydrogen bond will be presented. They adopt both the *one-pot* or one-step method and the *hierarchical* approach; particularly we'll focus our attention on examples where the involved ligands are bearing carboxylate moieties because we choose to study this functional group. We will show some examples of systems based on two components (metal + ligand) and others based on three components (metal + ligand + connector), besides we will present the results obtained in our Laboratory. Example involving isolated complexes will be presented in a specific part (see § II.4).

All the provided examples are quite recent and demonstrate that the subject begins to be tackled only lately owing to its complexity.

II.2.1 Two component systems: self-complementary metallic complexes

The most common type of hybrid networks that we could find in the literature are the two components self-complementary networks based on metallic complexes. There are some examples of mixed coordination and hydrogen bonded networks where the ligand bears carboxylate moieties and is N-donor toward the metal. Four examples will be given here below. For the reported cases, the study have been performed in the crystalline state, using single crystal X ray diffraction, and in the last case, the studies have been performed in solution.

An interesting example of one-dimensional helical chains⁸ is based on hydrogen bonding between chiral AgL_2 tecton where **L** is the bifunctional ligand 4-(3-(2-pyridyl)pyrazol-1-ylmethyl)benzoic acid, which is self-complementary. The ligand includes either two nitrogen atoms for chelating a metal and a self-complementary hydrogen-bonding region.

In the reported networks, the AgL_2 tectons are hydrogen bonded together either directly, through two carboxylic acids, or in a mediated way by anions or solvent molecules leading to a 1-D helical systems or *meso*-helical depending on the nature of the counter ion, one example is illustrated in figure 2.

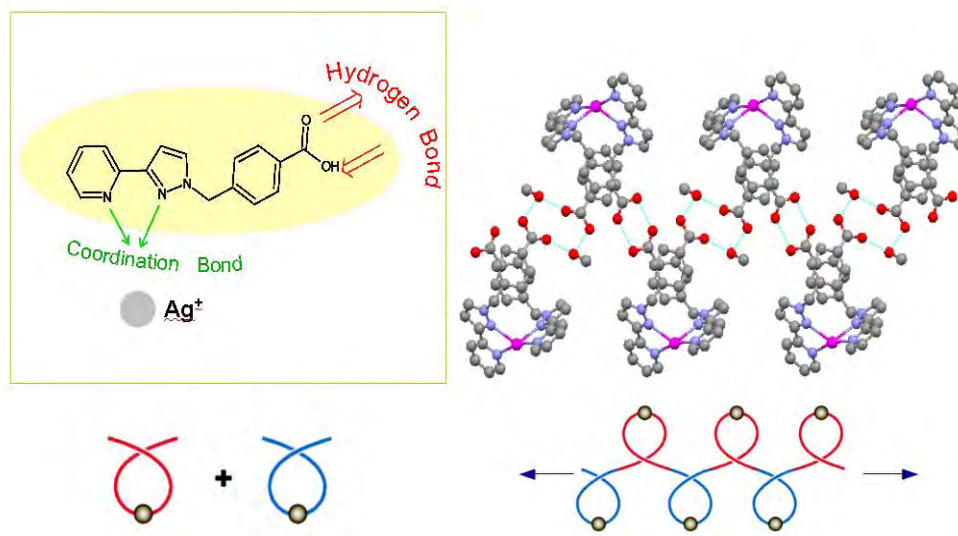


Figure 2. Schematic representation of the one-dimensional hydrogen bonded *meso*-helical chain of $[(\text{AgL}_2)\text{PF}_6]\cdot\text{CH}_3\text{OH}$ (ref. 8).

In a second example, Kruger *et al.*⁹ proposed the use of 4,4'-dicarboxy-2,2'-bipyridine to form monosubstituted Co(II) and Cu(II) complexes that lead to 3D

⁸ D. A. McMorran, *Inorg. Chem.*, **2008**, 47, 592-601

⁹ a) E. Tynan, P. Jensen, P. E. Kruger, A. C. Lees, M. Nieuwenhuyzen, *Dalton Trans.*, **2003**, 1223-1228 ; b) E. Tynan, P. Jensen, N. R. Kelly, P. E. Kruger, A. C. Lees, B. Moubaraki, K. S. Murray, *Dalton Trans.*, **2004**, 3440-3447 ; c) E. Tynan, P. Jensen, A. C. Lees, B. Moubaraki, K. S. Murray, P. E. Kruger, *CrystEngComm*, **2005**, 90-95

networks *via* hydrogen bonding between carboxylates, lattice water and coordinated water molecules. It is note worthy that depending on the protonation of the ligand and the nature of the metal, different dimensionalities may be obtained [Fig. 3].

Under basic conditions, when the ligands are fully deprotonated, *i.e.*, in the carboxylate form, hydrogen bonding undergoes between carboxylate and coordinated water or lattice water molecules and the whole network collapses after air exposure [Fig. 3a] or, in one other case, the carboxylic acid belongs, in acidic condition, to the coordination sphere of the metal [Fig. 3b], leading to a robust lattice through hydrogen bond interactions *via* carboxylic acid [Fig. 3c]. The example shows the importance of the pH during the formation of the network.

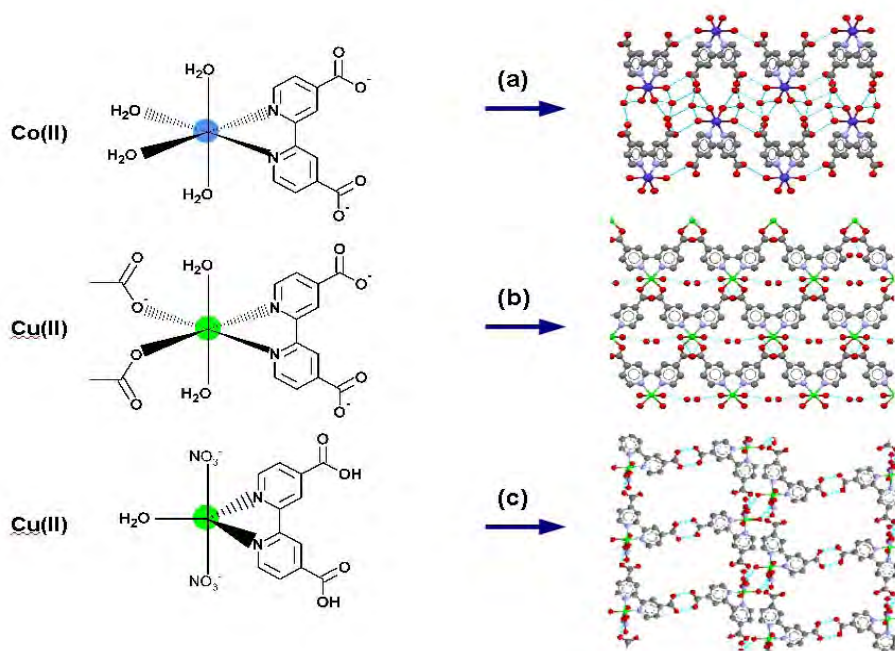


Figure 3. 3-D networks from monosubstituted complexes of 4,4'-dicarboxy-2,2'-bipyridine with Co(II) and Cu(II). The ligand is deprotonated for $[\text{Co}(\text{dcbpy})(\text{H}_2\text{O})_4] \cdot 4\text{H}_2\text{O}$ (a) and $\{[\text{Cu}(\text{dcbpy})(\text{H}_2\text{O})_2] \cdot 2\text{H}_2\text{O}\}_n$ (b) but remains fully protonated in $[\text{Cu}(\text{H}_2\text{dcbpy})(\text{NO}_3)_2(\text{H}_2\text{O})]$ (c)(ref. 9).

The interpenetrated rhombohedral networks¹⁰ derived from kinetically inert Co(III) and Rh(III) tri-substituted complexes with 5,5'-dicarboxy- and 4,4'-dicarboxy-2,2'-bipyridine are another example of self-complementary networks based on metallic complexes using a two components system [Fig. 4]. The complex bears three carboxylate to compensate the charge on the metal and three carboxylic acids. A 3-D cubic network is formed *via* recognition of carboxylate groups located at the periphery of bipyridine ligands.

¹⁰ a) P. G. Desmartin, A. F. Williams, G. Berardinelli, *New J. Chem.*, **1995**, *19*, 1109-1112 ; b) C. J. Matthews, M. R. J. Elsegood, G. Berardinelli, W. Clegg, A. F. Williams, *Dalton Trans.*, **2004**, 492-497

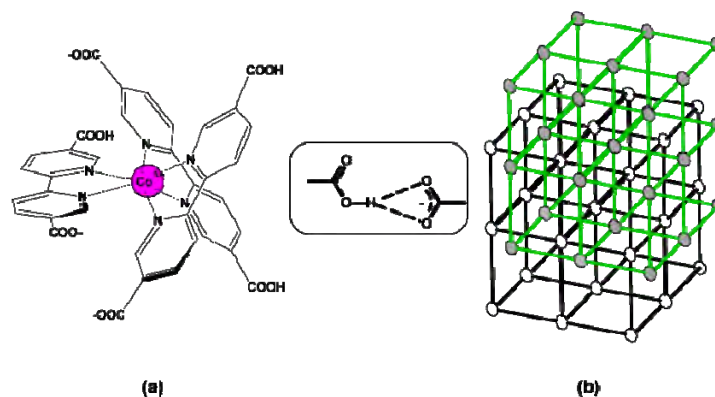


Figure 4. a) The hydrogen bonds between carboxylate in $\text{Co}(5,5'\text{-dcbpy})_3$ that forms b) 3D interpenetrating rhombohedral networks (ref. 10).

The fourth example illustrates the formation of a single stranded one-dimensional network based on Fe(II) and a terpyridine derivated ligand bearing a zwitterionic carboxylate-guanidinium functional group¹¹. The network formation, tracked by NMR, follows a different sequence of events, in fact, the dimerization of the zwitterionic ligand forms a ion pair, that is the first assembling node based on charge-assisted hydrogen bond, and concurrently the second node is assured by metal coordination of the tris-chelating terpyridine extremity following to the addition of FeCl_2 [Fig. 5].

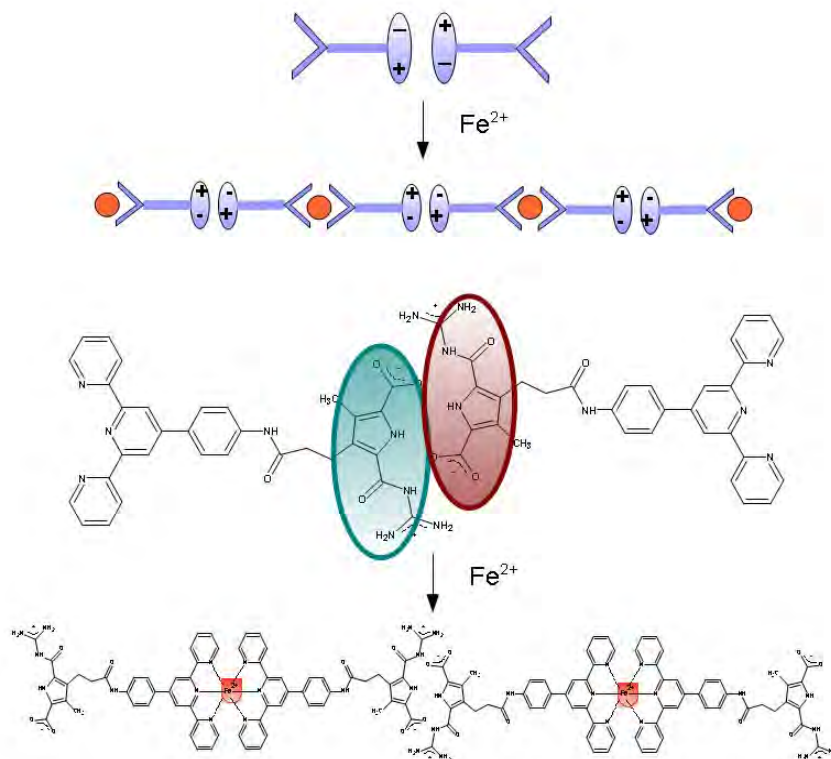


Figure 5. Single chain strand based on recognition between auto-complementary zwitterionic complexes (ref.11).

¹¹ G. Gröger, V. Stepanenko, F. Würthner, C. Schmuck, *Chem. Commun.*, **2009**, 698-700

II.2.2 Three component systems

If we consider solid state architectures composed of three different building blocks and including hydrogen bonding with carboxylate moieties, the related literature is scarce. In the following examples we collected which are, to the best of our knowledge, the only existing examples where three components, a metal core, a N-donor ligand (used as H bond acceptor/donor) and a spacer (used as H bond donor/acceptor), are used as tectons for network formation. For the given examples, we will distinguish if a 'hierarchical approach' or 'one-pot' strategy has been applied in order to obtain the assemblies.

In § II.2.2.1 are presented the examples where the ligand is bearing a H-bond donor functional group and the spacer is a H-bond acceptor. There are no examples where the ligand is an H-bond acceptor and the spacer is the H-bond donor.

II.2.2.1 Pyridinedicarboxylates based assemblies

The well documented study performed by MacDonald *et al.*¹² clearly illustrates the concept of formation of molecular networks using three components system and charge assisted hydrogen bonds.

Mixing up in a one-pot procedure, 2,6-pyridinedicarboxylic acid ligand, imidazole and different transition metals (Mn^{2+} , Co^{2+} , Ni^{2+} , Cu^{2+} , Zn^{2+}), they obtained a series of isostructural supramolecular networks based on three components [Fig. 6]. This study illustrate the "one-pot" approach.

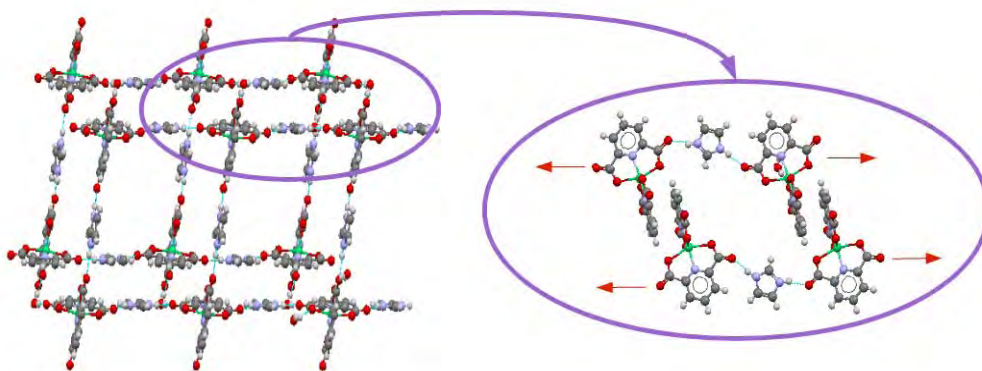


Figure 6. One example of bis(imidazolium-2,6-pyridinecarboxylate) $M(II)$ (where $M = Ni^{2+}$) isostructural networks reported by MacDonald *et al.* (ref. 12).

The charge mediated hydrogen bonding between imidazolium cations and pyridinedicarboxylate anions is the element that dominates the three dimensional crystal packing for these supramolecular structures. Bi-dimensional sheets are formed

¹² a) J. C. MacDonald, P. C. Dorrestein, M. M. Pilley, M. M. Foote, J. L. Lundburg, R. W. Henning, A. J. Schultz, J. L. Manson, *J. Am. Chem. Soc.*, **2000**, *122*, 11692-11702 ; b) J. C. MacDonald, P. C. Dorrestein, M. M. Pilley, *Cryst. Growth Design*, **2000**, *1*, 29-38

by total self-assembly *via* hydrogen bonding between bi-substituted $M(II)[2,6\text{-pyridinedicarboxylate}]_2$ complex and imidazolium cation; 2-D planes are bounded via pyridine rings π -stacking in the final 3-D structure. It represents an example of the aim to control molecular packing in crystalline materials using strong ionic hydrogen bonds in combination with metal-ligand coordination bonds.

II.2.2.2 Imidazole based assemblies

The hydrogen bond donor moiety may also be placed on the N donor ligand and, in this case, the spacer is a bi-carboxylate organic molecule; so did the authors in the following examples. Larsson and Öhrström¹³ reported a 3-D network connected *via* hydrogen bonds of $\text{Co(III)}(2,2'\text{-biimidazole})_3$ with terephthalate. Crystal structure results in a porous 3-D network five times interpenetrated [Fig. 7].

This studies covers the “hierarchical strategy” employed for the formation of robust molecular networks.

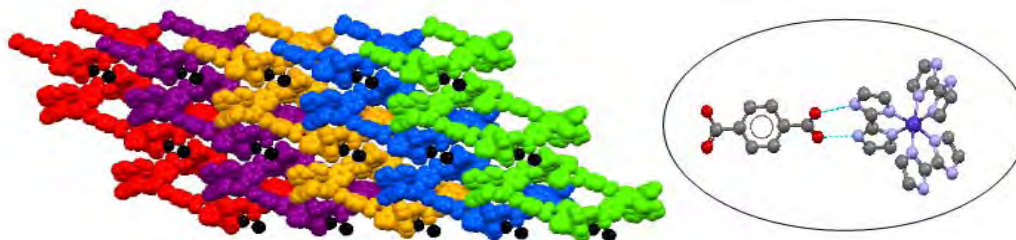


Figure 7. Representation of $\{\text{Co(III)}-(\text{biim-H})_2(\text{biim-H}_2)\}_2 (p\text{-COO-Ph-COOH})_2 \cdot \text{H}_2\text{O}$, interpenetrating network (left) and the recognition motif between biimidazole and terephthalate (right) (ref. 13).

II.2.2.3 Other assemblies

Daniel Nocera *et al.*¹⁴ studied photo-induced PCET within a donor-acceptor interface formed between an amidinium-carboxylates salt bridge [Fig. 8] in order to better understand the relationship electron transfer/proton motion that affects the rate of proton transfer in multiple biological systems.

The amidinium-purpurin conjugated macrocycle provides a general tool to locate a proton within PCET interfaces with carboxylate-dinitrobenzene or naphthalenediimide. The hydrogen bond formation is studied *via* NMR and UV-vis absorption and emission spectra in solution.

¹³ K. Larsson, L. Öhrström; *CrystEngComm*, **2004**, 6, 354-359

¹⁴ a) E. R. Young, J. Rosenthal, D. G. Nocera; *Chem. Comm.*, **2008**, 2322-2324; b) J. Rosenthal, J. M. Hodgkiss, E.R. Young, D. G. Nocera; *J. Am. Chem. Soc.*, **2006**, 128, 10474-10483 ; c) C. Turrò, C. K. Chang, G. E. Leroi, R. I. Cukier, D. G. Nocera; *J. Am. Chem. Soc.*, **1992**, 114, 4013-4015

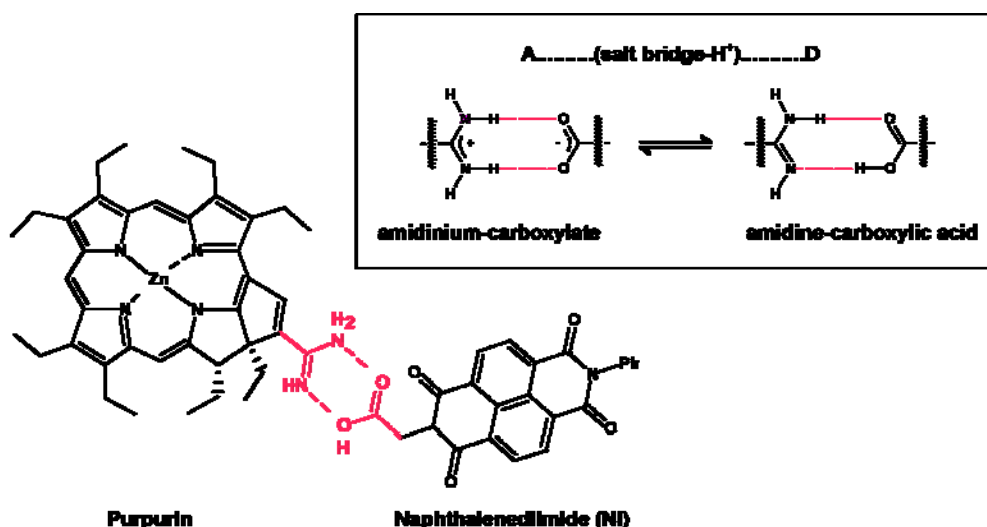


Figure 8. Purpurin-Chlorin donor/acceptor adducts used to determine the Proton Coupled Electron Transfer (PCET) between amidinium-carboxylate charged interface (ref. 14).

The general trend shown by the literature reported examples is an evolution from a purely structural investigation towards the development of networks as functional materials, in fact metal-organic frameworks with 4,4'-dicarboxybipyridine by Kruger *et al.* and 2,6-pyridine dicarboxylate by McDonald *et al.* are investigated for their magnetic properties, and mixed ligand complexes of Co(III) containing biimidazole have been recently studied by Nair *et al.*¹⁵ for their interaction *via* hydrogen bonding to DNA and development of the anticancer medical technology called photodynamic therapy.

II.2.3 Earlier work in the lab

The following two examples are related to the results previously obtained in our laboratory and focus on three component systems containing a particular hydrogen bond donor that is a bisamidinium cation, a peculiar building block that will be presented hereafter (§ II.3.1).

II.2.3.1 Two components systems

An organic-organometallic supramolecular assembly using organometallic ferrocene dicarboxylate and bisamidinium cations were obtained in our laboratory in collaboration with Braga's group¹⁶. Both building blocks were chosen, so that charge assisted N-H⁽⁺⁾...O⁽⁻⁾ hydrogen bonds may occur.

The reaction of the dicarboxylic organometallic acid $[(\eta^5\text{-C}_5\text{H}_4\text{COOH})_2\text{Fe}]$ with cyclic bis-amidines (BAD22, BAD23 and BAD23OH see table 1, § II.3.1.1) occurs *via*

¹⁵ R. Indumathy, T. Weyhermüller, B. U. Nair, *Dalton Trans.*, **2010**, 39, 2087-2097

¹⁶ D. Braga, L. Maini, F. Grepioni, A. De Cian, O. Felix, J. Fischer, M. W. Hosseini, *New. J. Chem.*, **2000**, 24, 547-553

proton transfer from the ferrocene dicarboxylic acid to the organic base. As expected, a 1-D structure results from recognition of carboxylic acid with BAD23-OH [Fig. 9], where the carboxylic groups are disposed in a divergent fashion. The charge-assisted bonding interaction $N-H^{(+)}\cdots O^{(-)}$ between carboxylate and amidinium presents the typical bis-dihapto motif as previously observed in crystals obtained from bis-amidines and organic acids¹⁷. The water molecules present in the crystal structures act as a bridge between the chains forming thus two-dimensional layers.

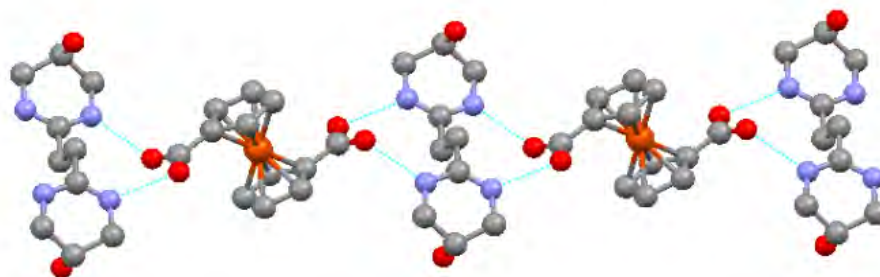


Figure 9. Crystalline single chain $[(\eta^5-C_5H_4COO)_2Fe][C_{10}H_{20}N_4O_2]$ between ferrocene dicarboxylic acid/BAD23OH 1:1 stoichiometric ratio. (ref. 16).

The use of a 2:1 stoichiometry induced a partial deprotonation of the ligand, leading to a mono-carboxylate organometallic anion and a di-protonated bisamidinium conducting to the formation a three-dimensional network between ferrocene dicarboxylic acid and BAD23 [Fig. 10]. The mono-deprotonation of the diacid seems to satisfy the requested equilibrium between donor and acceptor sites justifying the absence of solvent molecules in the crystal lattice.

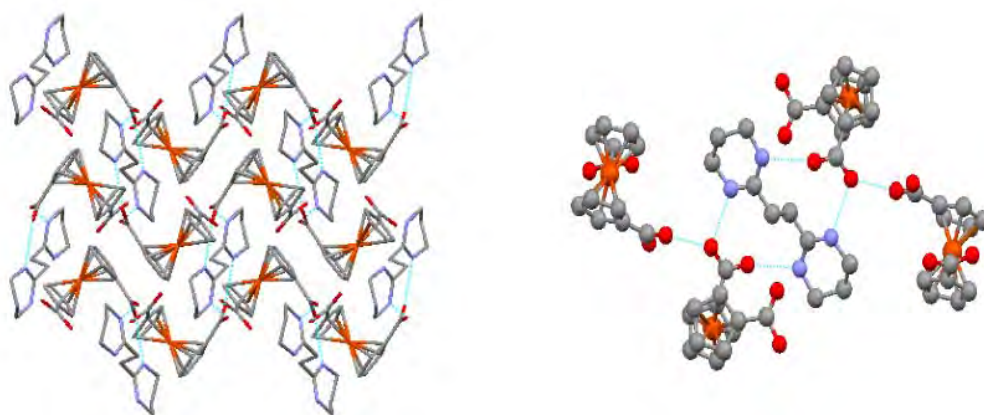


Figure 10. Crystalline 3D network $[(\eta^5-C_5H_4COO)(\eta^5-C_5H_4COOH)Fe]_2[C_{10}H_{20}N_4]$ between ferrocene dicarboxylic acid/BAD23 2:1stoichiometric ratio. On the right is shown the charge-assisted bonding interaction $N-H^{(+)}\cdots O^{(-)}$ between carboxylate and amidinium (ref. 16).

¹⁷ a) O. Felix, M. W. Hosseini, A. De Cian, J. Fischer, *New J. Chem.*, **1998**, 22, 1389-1393 ; b) O. Felix, M. W. Hosseini, A. De Cian, J. Fischer, *Angew. Chem. Int. Ed.*, **1997**, 36, 102-104 ; c) O. Felix, M. W. Hosseini, A. De Cian, J. Fischer, *Tetrahedron Lett.*, **1997**, 38, 1755-1758 ; d) O. Felix, M. W. Hosseini, A. De Cian, J. Fischer, *Tetrahedron Lett.*, **1997**, 38, 1933-1936

Further studies of the solid state behaviour of ferrocene di-carboxylate combined with organic bases like 1,4-phenylenediamine and guanidinium were carried out demonstrating the successfulness of this approach¹⁸ and, as well, inverting the donor-acceptor relative position *i.e.*, using ferrocene di-pyridyl and forming hybrid organic-organometallic networks with organic acids¹⁹.

II.2.3.2 Three components systems

The one-pot approach has been further developed in our laboratory using (i) a bisamidinium cation, (ii) 2,6-pyridinecarboxylate (pdca) or 2,4,6-pyridine tricarboxylate (ptca)²⁰ and (iii) different transition metal. A great variety of compounds were obtained using the 'one pot' approach, in a water/DMSO solution [Chart 1].

The use of di- and tri-substituted carboxylic acids makes particularly difficult to find appropriate crystallization conditions, in particular the limited solubility of carboxylic acid compounds restricts the range of solvent that can be used.

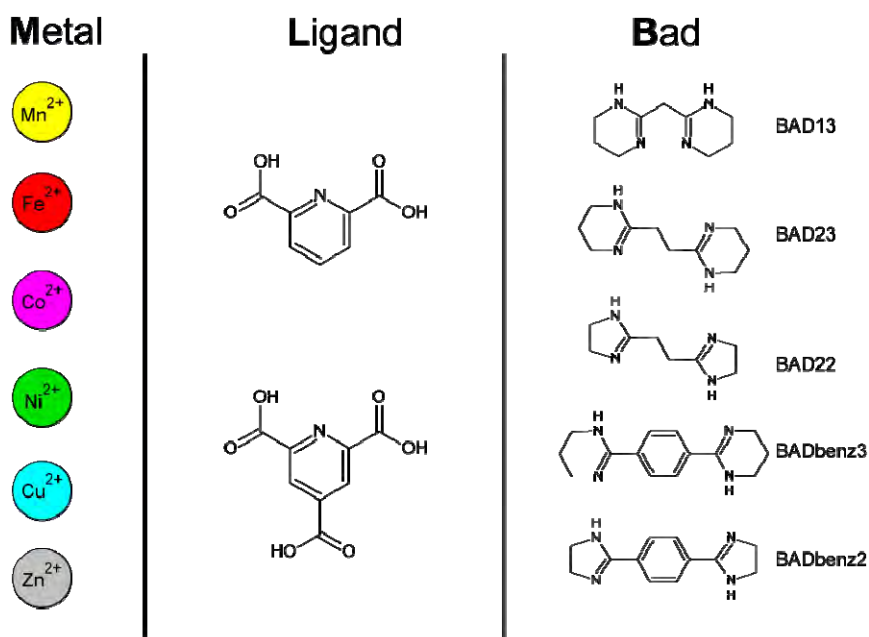


Chart 1. Components used to obtain hybrid coordination/hydrogen bonding networks based on metals, bisamidinium H-bond donor cations and pyridinecarboxylate derivatives.

Due to different bisamidinium shape and to different used metals, several systems were obtained, the resulting structures are mono-, bi- and tri-dimensional networks and some of them are presented below [Fig. 11].

¹⁸ D. Braga, L. Maini, M. Polito, L. Mirolo, F. Grepioni, *Chem. Eur. J.*, **2003**, 9, 4362-4370

¹⁹ D. Braga, S. L. Giaffreda, F. Grepioni, G. Palladino, M. Polito, *New J. Chem.*, **2008**, 32, 820-828

²⁰ G. Marinescu, S. Ferlay, M. W. Hosseini, unpublished results

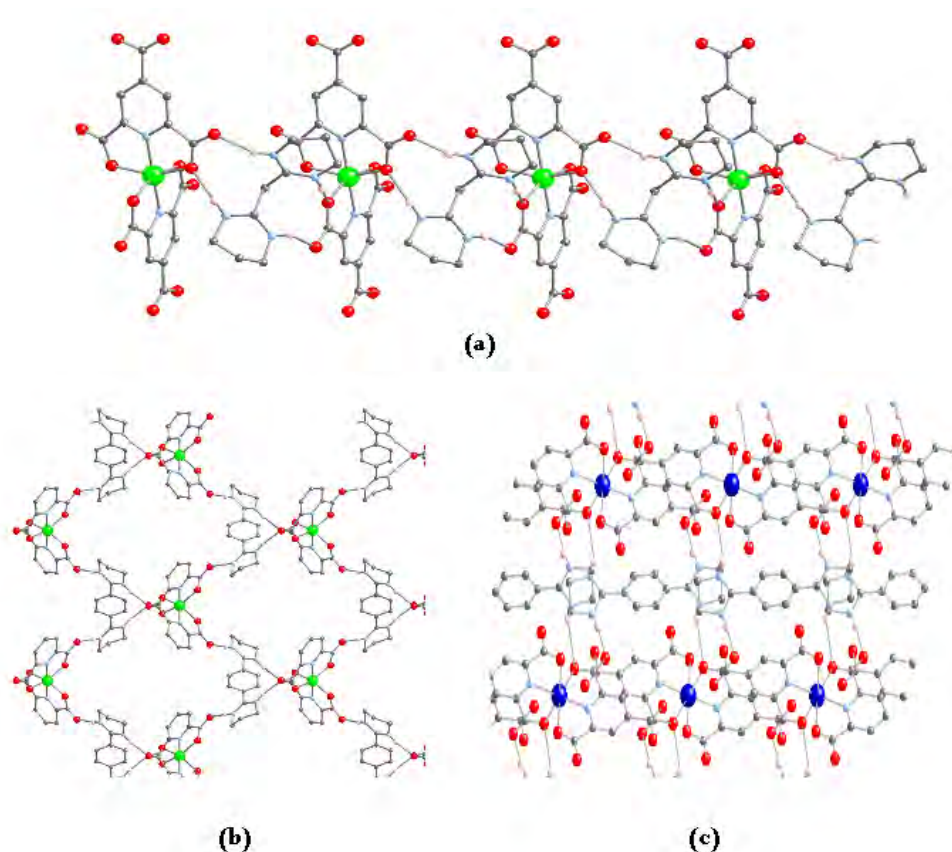


Figure 11. a) 1-D chain obtained with 2,4,6-pyridinetricarboxylic acid, BAD13 and $M(II)=Co, Cu, Ni, Zn$; b) 2-D sheet obtained with 2,6-pyridinedicarboxylic acid, BADbenz3 and $M(II)=Cu, Ni$; c) 3-D network obtained with 2,4,6-pyridine tricarboxylic acid, BADbenz2 and $M(II)=Co, Ni, Cu, Zn, Mn$ (solvent molecules are omitted for clarity), (ref. 20).

The rationalisation of these data seems rather difficult, different coordination modes have been observed for bisamidinium: bis-monohapto- η^2 and bis-dihapto- η^4 [Fig. 11a] bridging two molecules of complex, tris-monohapto- η^3 bridging two or three molecules or tetrakis-monohapto- η^4 bridging three molecules [Fig. 11b] or four molecules [Fig. 11c]. We can say that: i) the size of bis-amidinium infers on coordination mode in fact bis-dihapto is observed only for BAD22/BAD23 and tetrakis-monohapto only for BADbenz; ii) the carboxylic acid in *para*- position on ptca is not involved in hydrogen bond but only carboxylates in *ortho*- position and already coordinated to the metal; iii) the role of solvent included in the lattice is important in fact crystals are isostructural considering the same ligand, bisamidinium cation and the same number of water molecules included into the lattice.

All this proves the great versatility of bisamidinium cation but shows also that the role of number and position of moieties on the organic ligand is not easily predictable or explicable.

II.3 Chosen components and nodes

The tectons that will be used for assemblies formations will be described in details below. As stated in the introduction, there will be 3 tectons : (i) tecton A that may be considered as H bond donor (or a dicarboxylic acid, which will not be described here), (ii) tecton B which will be a N donor ligand bearing some H bond acceptor groups (or some H bond donor, in the second case), (ii) tecton C which is the metal center.

II.3.1 Component A: Bisamidinium cation, H bond donor



II.3.1.1 Description of the tecton

The amidine function has been widely studied in our laboratory, several cases of charge assisted hydrogen bonding have already been described, in particular it has been shown that protonated bis-amidinium based tectons are well suited for the generation of purely organic H-bonded molecular networks using anionic moieties such as carboxylates,²¹ sulfonates,²² phosphonates,²³ nitriles,²⁴ nitronyl-nitroxide,²⁵ or hybrid organic/inorganic networks with oxometallates,²⁶ cyanometallates²⁷ and thiocyanometallates²⁸ derivatives, affording a large variety of molecular networks²⁹.

²¹ a) M. W. Hosseini, R. Ruppert, P. Schaeffer, A. De Cian, N. Kyritsakas, J. Fischer, *Chem. Comm.*, **1994**, 2135-2136 ; b) O. Felix, M. W. Hosseini, A. De Cian, J. Fischer, *Tetrahedron Lett.*, **1997**, 38, 1755-1758 ; *Tetrahedron Lett.*, **1997**, 38, 1933-1936 ; *Angew. Chem. Int. Ed.*, **1997**, 36, 102-104 ; O. Felix, M. W. Hosseini, A. De Cian, J. Fischer, *New J. Chem.*, **1998**, 22, 1389-1393 ; c) O. Felix, M. W. Hosseini, A. De Cian, J. Fischer, *Chem. Comm.*, **2000**, 281-282 ; *J. Solid State Sciences*, **2001**, 3, 789-793

²² G. Brand, M. W. Hosseini, R. Ruppert, A. De Cian, J. Fischer, N. Kyritsakas; *New J. Chem.*, **1995**, 19, 9-13

²³ a) M. W. Hosseini, G. Brand, P. Schaeffer, R. Ruppert, A. De Cian, J. Fischer, *Tetrahedron Lett.*, **1996**, 37, 1405-1408 ; b) V. Ball, J.-M. Planeix, O. Felix, J. Hemmerle, P. Schaaf, M. W. Hosseini, J.-C. Voegel, *Cryst. Growth and Des.*, **2002**, 2, 489-492 ; c) J.-M. Planeix, T. Duhoo, J. Czernuszka, M. W. Hosseini, E. F. Brès, *J. Mat. Chem.*, **2003**, 13, 2521-2524

²⁴ D. M. Shacklady, S.-O. Lee, S. Ferlay, M. W. Hosseini, M. D. Ward, *Cryst. Growth & Design*, **2005**, 5, 2310-2312

²⁵ Olivier Felix, Ph. D. dissertation – Université Louis Pasteur, **1999**

²⁶ C. Paraschiv, S. Ferlay, M. W. Hosseini, N. Kyritsakas, J.-M. Planeix, M. Andruh, *Rev. Roum. Chim.*, **2007**, 52, 101-104

²⁷ a) S. Ferlay, O. Felix, M. W. Hosseini, J.-M. Planeix, N. Kyritsakas, *Chem. Comm.*, **2002**, 702-703 ; b) S. Ferlay, V. Bulach, O. Felix, J.-M. Planeix, M. W. Hosseini, N. Kyritsakas, *Cryst. Eng. Comm.*, **2002**, 4, 447-453 ; c) S. Ferlay, R. Holakovski, M. W. Hosseini, J.-M. Planeix, N. Kyritsakas, *Chem. Comm.*, **2003**, 1224-1225 ; d) C. Paraschiv, S. Ferlay, M. W. Hosseini, V. Bulach, J.-M. Planeix, *Chem. Comm.*, **2004**, 2270-2271 ; e) S. Ferlay, M. W. Hosseini, N. Kyritsakas, *Chem. Comm.*, **2004**, 787-788 ; f) P.

A specific hydrogen bond donor has been designed for the construction of molecular networks. The characteristic features of these molecules are illustrated in Figure 12. A typical bis-amidinium cation is a cyclic dication where the two positive charges are delocalised on three atoms (N-C-N) locked in the ring.

The molecule owns four N-H sites acting as directional hydrogen bonding donor and powered by the presence of delocalised charges, one can modulate the scaffold of this molecule in two points: i) the spacer **S** between the two bis-amidinium ions that will affect the distance (d_{N-N}) between two N-H bond and also the rigidity of the molecule, the substituent might be chosen for their flatness and rigidity (or physical properties) in order to have four coplanar hydrogen bonds (as benzene or polycondensate phenyl rings) or for their flexibility (alkyl chain) to let a certain degree of freedom ; ii) the bridge **B** between two nitrogen atom of the same amidine moiety both in the length of the carbon chain (ethylene, C2, propylene, C3 or more), that will affect the direction of the N-H bond and is related angle (Θ_{HNC}), and the possible presence of substituent on the bridge (see table1).

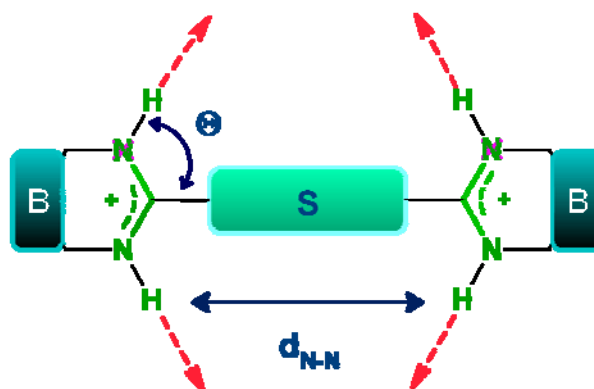


Figure 12. Schematic representation of a bis-amidinium dication.

The chemical modifications of the cyclic bisamidinium cation allow us to finely tune its characteristics in order to differentiate the recognition pattern with cyanometallates²⁷ or carboxylates²¹ and also to vary the potential applications (molecular crystals,³⁰ porous materials,³¹ liquid crystals³²), at this purpose, in table 1 are illustrated all the already obtained tectons by variation of **S** and **B**.

Dechambenoit, S. Ferlay, M. W. Hosseini, *Cryst. Growth & Design*, **2005**, *5*, 2310-2312 ; g) P. Dechambenoit, S. Ferlay, M. W. Hosseini, J.-M. Planeix, N. Kyritsakas, *New. J. Chem.*, **2006**, *30*, 1403-1410; h) P. Dechambenoit, S. Ferlay, M. W. Hosseini, N. Kyritsakas, *Chem. Comm.*, **2007**, 4626-4628

²⁸ G. Marinescu, S. Ferlay, N. Kyritsakas, M. W. Hosseini, *Dalton. Trans.*, **2008**, 615-619

²⁹ M. W. Hosseini; *Actualité Chimique*, **2005**, 290-291, 59-71; *Chem. Comm.*, **2005**, 5825-5829 ; *Cryst. Eng. Comm.*, **2004**, *6*, 318-322 ; *Coord. Chem. Rev.* **2003**, *240*, 157-166

³⁰ E. F. Brès, S. Ferlay, P. Dechambenoit, H. Leroux, M. W. Hosseini, S. Reyntjens, *J. Mat. Chem.*, **2007**, 1559-1562

³¹ P. Dechambenoit, S. Ferlay, N. Kyritsakas, M. W. Hosseini, *J. Am. Chem. Soc.*, **2008**, *130*, 17106-17113 ; *Chem. Comm.*, **2009**, 1559-1561; *Chem. Comm.*, **2009**, 6798-6800

A nomenclature has been developed to name simply the different molecules: the main part of the name consists in the shortening of Bis-amidine to obtain the word BAD, then the spacer between the two moieties is described, the third part describes the substituent on the cyclic amidine. In this way the 1,2-Bis(-2'-imidazolyl)ethane with a $-(\text{CH}_2-\text{CH}_2)-$ spacer and a imidazoline ring is condensed in BAD22 and is related dication BAD22-2H^+ .

Concerning BAD22benz and BAD2d2benz, they are bearing a benzene ring condensed to the five member cyclic amidine ring, this expedient should stabilize, by conjugation, the cyclic amidine towards hydrolysis, furthermore introducing an aromatic ring into the structure also add other properties to the molecule such as luminescence, or strengthen the assembling *via* π -stacking.

Spacer / Bridge	Spacer	Bridge	Spacer	Bridge	Spacer	Bridge

Table 1. Examples of bisamidinium cations already synthesized and the possible differentiation.

³² M. W. Hosseini, D. Tsiourvas, J.-M. Planeix, Z. Sideratou, N. Thomas, C. M. Paleos, *Collec. Czech. Chem. Comm.*, **2004**, *69*, 1161-1168

A bis-amidinium cation is a four site H-bond donor, the formed hydrogen bond may be described with μ_n which is the number of neighbours involved in hydrogen bonds, and (η^n) which is the number of donating sites effectively interacting with an acceptor site (hapticity). In our case, a bis-amidinium cation can use one, two, three or four N-H bonds so may be mono-, bi-, tri- or tetrahapto-; we can also specify if it uses one or more bonds to bind the same acceptor centre, in this case it may be considered as bis-monohapto (two different sites) or mono-dihapto (the same site).

Another way to describe the hydrogen bond within a network has been proposed by Kuleshova and Zorkii³³ and developed by Etter³⁴, as already described in § I.4.1.2. In this work we will use the first example of nomenclature that seems to be more intuitive.

II.3.1.2 Bisamidine and bisamidinium synthesis

The synthesis of the amidine function has been largely studied in organic chemistry,³⁵ and the reactions to form amidine and amidinium have been carried out starting with nitriles,³⁶ aldehydes,³⁷ thioamides,³⁸ or carboxylic acids³⁹. Below we will focus on the tectons that have been used in this study.

Synthetic general methods for cyclic bis-amidine/bis-amidinium synthesis has been already developed, adapted and optimized in the laboratory in precedent works^{25,40}.

The general method to obtain bis-amidinium cation, for BAD22, BAD23 and BADbenz, follows the one proposed by Oxley and Short²⁸ in which a di-nitrile was condensed with a monotosylate diamine salt in order to obtain the corresponding stable

³³ a) L. N. Kuleshova, P. M. Zorsky, *Acta Crystallogr.*, **1980**, B36, 2113-2115 ; b) L. N. Kuleshova, P. M. Zorsky, *Zh. Strukt. Khim.*, **1980**, 22, 153-156

³⁴ a) M. C.. Etter, *Isr. J. Chem.*, **1985**, 25, 312-319; b) M. C.. Etter, *Acc. Chem. Res.*, **1990**, 23, 120-126; c) M. C.. Etter *J. Phys. Chem.*, **1991**, 95, 4601-4610 ; d) M. C.. Etter, J. B. Bernstein, J. M. MacDonald, *Acta Cryst.*, **1990**, B46, 256-262

³⁵ S. Patai, *The chemistry of amidines and Imidates*, Wiley, London, **1995**

³⁶ a) P. Oxley, W. F. Short, *J. Chem. Soc.*, **1946**, 147-150; *J. Chem. Soc.*, **1947**, 382-389 ; *J. Chem. Soc.*, **1948**, 1514-1527 ; b) P. Oxley, M. W. Partridge, T. D. Robson, W. F. Short, *J. Chem. Soc.*, **1946**, 763-771; c) M. W. Partridge, W. F. Short, *J. Chem. Soc.*, **1947**, 390-394 ; d) R. P. Hullin, J. Miller, W. F. Short, *J. Chem. Soc.*, **1947**, 394-396 ; e) P. Oxley, M. W. Partridge, W. F. Short, *J. Chem. Soc.*, **1947**, 1110-1116; *J. Chem. Soc.*, **1948**, 303-309 ; f) W. H. Graham, *J. Am. Chem. Soc.*, **1965**, 4396-4397

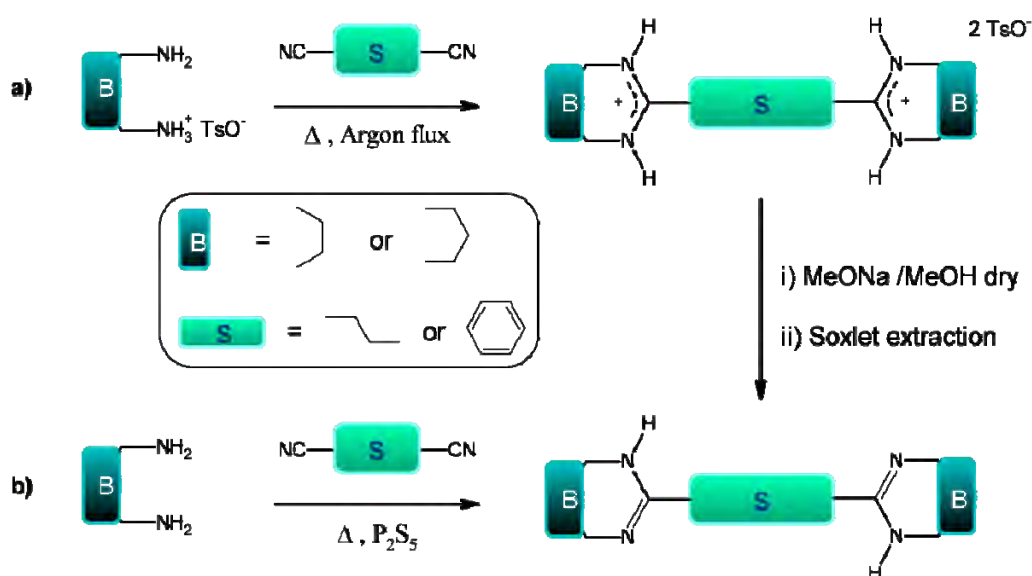
³⁷ a) H. Fujioka, K. Murai, Y. Ohba, A. Hiramatsu, Y. Kita, *Tetrahedron Lett.*, **2005**, 46, 2197-2199 ; b) Mirkhami, *Tetrahedron Lett.*, **2006**, 47, 2129-2132 ; c) M. Ishihara, H. Togo, *Synlett*, **2006**, 227-230; *Tetrahedron Lett.*, **2007**, 1474-1480 ; *Synthesis*, **2007**, 1939-1942 ; d) S. Sayama, *Synlett*, **2006**, 1479-1484

³⁸ J. Spychała, *Catalysis Letters*, **2006**, 109, 55-60

³⁹ V. B. Piskov, V. P. Kasperovich, L. M. Yakovleva; *Russian J. Chem. Eng. Ed.*, **1976**, 917-923

⁴⁰ a) Wojciech Jaunky, Ph. D. dissertation – Université Louis Pasteur, **2001** ; b) Pierre Dechambenoit, Ph. D. dissertation – Université Louis Pasteur, **2008**

bis-amidinium bis-tosylate salt that can be easily exchanged by chloride anions *via* a Dowex ion exchange column. BADbenz-2H⁺ can be easily deprotonated and then acidified again with appropriate acid, BAD22-2H⁺ and 23-2H⁺ have to be handled in anhydrous conditions [Scheme 1a]. Deprotonation is carried on in sodium methanolate and anhydrous methanol followed by solid extraction *via* Soxhlet apparatus [Scheme 1] with yield varying from 86% for BAD22 to 60% for BAD23 and around 70% for BADbenz. This method presents the advantage to lead directly to the bis-amidinium cations of BAD22 and BAD23 that, over long period, are instable as free base and show the tendency to hydrolyze, tendency shown by other amidines like the case of 2,2'-bi-2-imidazolinel⁴¹.



Scheme 1. General synthetic steps for cyclic bis-amidine and bisamidinium cation.

Another synthetic way for BAD22 and BADbenz was inspired from the method described by Simonsen, Lever *et al.*⁴² Condensation of two equivalent of diamine on one equivalent of dicyano derivatives (1,4-dicyanobenzene for BADbenz or succinonitrile for BAD22) in the presence of catalytic amount of P₂S₅ will lead to the formation of the desired compounds with yields of around 70% [Scheme 1b].

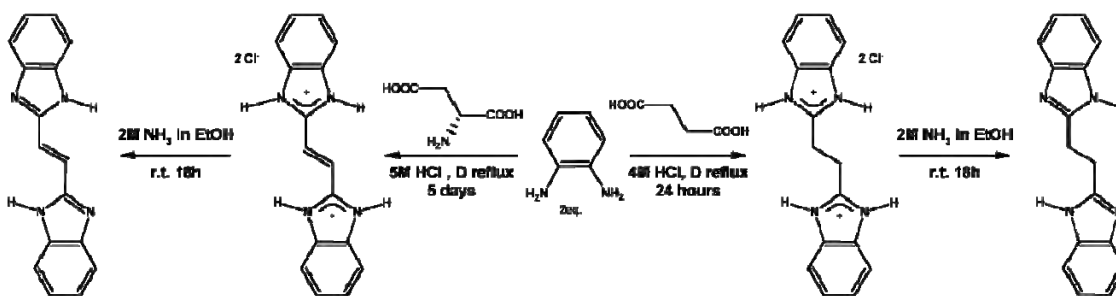
The same procedure has been employed also for BAD23 but in this case formation of polymeric by-products is important. Purification is quite difficult and after

⁴¹ J. C. Wang, J. E. Bauman Jr., *Inorg. Chem.*, **1965**, 1613-1615

⁴² A. B. P. Lever, B. S. Ramaswamy, S. H. Simonsen, L. K. Thompson, *Canadian J. Chem.*, **1970**, 48, 3076-3088

optimisation of the work-up we obtained a maximum yield of 30%. A recent upgrading of the synthetic condition have been published by Ostrowska *et al.*⁴³.

Concerning the molecules of BAD22benz and BAD2d2benz, the synthetic strategy was formerly developed in the group⁴⁴. The synthesis is based on condensation of carboxylic acid and has been developed starting from reaction conditions by Phillips *et al.*⁴⁵.



Scheme 2. Synthetic conditions for BAD22benz and BAD2d2benz.

The tecton BAD22benz has been synthesized by condensation of 1,2-diaminobenzene and succinic acid in acidic medium, the synthesis of BAD2d2benz is a modification of the reaction of Cescon and Day⁴⁶ in which this compound was obtained as side product. Two equivalents of 1,2-diaminobenzene and one equivalent of D-1-aspartic acid are condensed in acidic conditions to obtain the hydrochloride BAD2d2benz-2H⁺. Once isolated, the hydrochloride salt is purified by crystallization and the free base is obtained after stirring in alcoholic ammonia solution [Scheme 2].

For a deeper treatment of these molecules and their synthesis, we will refer to the previous Ph.D. works on this subject⁴⁰ and, for any further characterization, we can refer to the references therein⁴⁷, the synthetic procedure will be reported only for significant improvements.

⁴³ M. Machaj, M. Pach, A. Wołek, A. Zabrzeńska, K. Ostrowska, J. Kalinowska-Tłuścik, B. Oleksyn, *Monatshefte für Chemie*, **2007**, *138*, 1273-1277 ; b) D. Długosz, M. Pach, A. Zabrzeńska, M. Zegar, B. Oleksyn, J. Kalinowska-Tłuścik, K. Ostrowska, *Monatsh Chem.*, **2008**, *139*, 543-548

⁴⁴ Wojciech Jaunky, Ph. D. dissertation – Université Louis Pasteur, **2001**

⁴⁵ a) M. A. Phillips, *J. Chem. Soc.*, **1928**, 2393-2399 ; *J. Chem. Soc.*, **1931**, 1143-1153 ; b) R. L. Shriner, R. W. Upson, *J. Am. Chem. Soc.*, **1941**, *63*, 2277-2278 ; c) L. K. Thompson, B. S. Ramaswamy, E. A. Seymour, *Can. J. Chem.*, **1977**, *55*, 878-888

⁴⁶ L. A. Cescon, A. R. Day, *J. Org. Chem.*, **1962**, *27*, 581-586

⁴⁷ **BAD22**: A. B. P. Lever, B. S. Ramaswamy, S. H. Simonsen, L. K. Thompson, *Canadian J. Chem.*, **1970**, *48*, 3076-3088 ; **BAD23**: a) M. Machaj, M. Pach, A. Wołek, A. Zabrzeńska, K. Ostrowska, J. Kalinowska-Tłuścik, B. Oleksyn, *Monatshefte für Chemie*, **2007**, *138*, 1273-1277 , b) M. W. Hosseini, G. Brand, P. Schaeffer, R. Ruppert, A. De Cian, J. Fischer, *Tetrahedron Lett.*, **1996**, *37*, 1405-1408; **BADbenz3**: O. Felix, M. W. Hosseini, A. De Cian, J. Fischer, *New J. Chem.*, **1997**, *21*, 285-288 ; **BADbenz2**: a) V. Mirkhani, M. Moghadam, S. Tangestaninejad, H. Kargar, *Tetrahedron Lett.*, **2006**, *47*,

II.3.2 Component B: General considerations about amidinium/carboxylate recognition events

The hydrogen bond interaction carboxylate-amidinium could be considered in two ways, as already introduced in § II.1, *i.e.*, using a cyclic bisamidinium as tecton **A**, as discussed in the previous section § II.3.1, and a carboxylate as tecton **B**, or the other way round *i.e.*, using dicarboxylate as tecton **A** and an acyclic amidinium as tecton **B** (see figure 13).

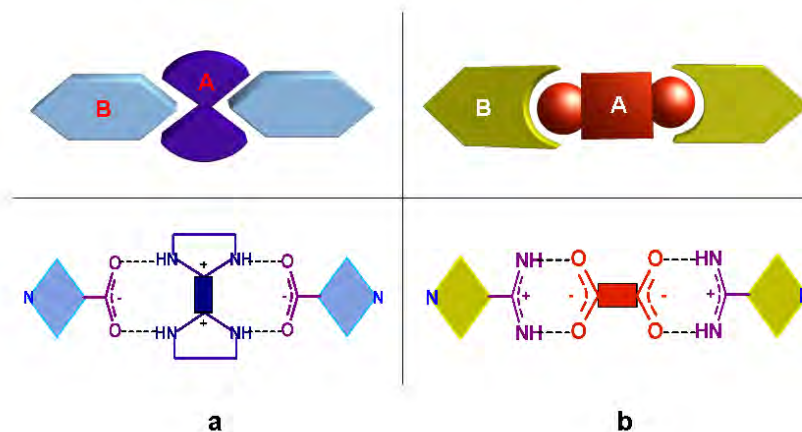


Figure 13. Schematic chart of the possible H bond interaction between tectons A and B when (a) tecton A is a cyclic bisamidinium (BAD) and tecton B is a ligand bearing carboxylate moiety or (b) tecton A is a dicarboxylate and tecton B is ligand bearing an acyclic amidinium.

Both ways have been considered and for this purpose we synthesized both ligands (tecton B) bearing carboxylic acids (see following § II.3.3) and bearing amidines (see following § II.3.4). It is anyway necessary to state precisely that these two H-bonding interaction make use of different recognition pattern as shown in figure 13.

Following Etter's graph set (described in § I.4.1.2), the motif between BAD-carboxylate (Fig. 13a) is of type $R^2_2(9)$ while the motif between carboxylate-amidinium (Fig. 13b) is of type $R^2_2(8)$. Earlier studies demonstrated that recognition between carboxylate and cyclic bisamidinium occurs when there is a d_{N-N} distance (see figure 12) of around 5Å between amidinium moieties which is the case for BAD22 and BAD23 that present a d_{N-N} distance of 5.12Å and 5.00Å respectively.

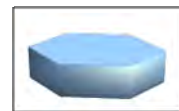
The complementarity between carboxylate and acyclic amidinium has been already studied by Nocera *et al.*⁴⁸ that demonstrated the formation of the hydrogen bond *via* studies in solution, and also, many studies have been performed in our

2129-2132 ; b) G. Levesque, J.-C. Gressir, M. Proust, *Synthesis*, **1981**, 12, 963-965; **BAD22benz**: C. J. Matthews, V. Broughton, G. Berardinelli, X. Melich, G. Brand, A. C. Willis, A. F. Williams, *New J. Chem.*, **2003**, 27, 354-358 ; **BAD2d 2benz**: K. C. Tsou, D. J. Rabiger, B. Sobel, *J. Med. Chem.*, **1969**, 12, 818-822

⁴⁸ a) J. P. Kirby, J. A. Roberts, D. G. Nocera; *J. Am. Chem. Soc.*, **1997**, 119, 9230-9236; b) J. A. Roberts, J. P. Kirby, D. G. Nocera; *J. Am. Chem. Soc.*, **1995**, 117, 8051-8052

Laboratory⁴⁹. Also other considerations such as the difference in pK_a (ΔpK_a between amidine and carboxylic acid is ≈ 10) are quite favourable for a strong-moderate hydrogen bonding as we can predict using the pK_a sliding rule presented in the Introduction (§I 4.1.2).

II.3.3 Component B: Carboxylates bearing ligands, H-bond acceptor



II.3.3.1 Description of the tectons

The ligands were chosen for the recognition with bisamidinium and are bi-functional bipyridine and phenanthroline-like N-donor ligands, favouring N-coordination towards metals by chelating effect, and bearing two carboxylates moieties on the same position of the heterocyclic ring to ensure the $[N^+ \cdots H \cdots O^-]$ recognition pattern.

This was explored using symmetrical and bi-functional ligands such as: 2,2'-bipyridine-3,3'-dicarboxylic acid, 2,2'-bipyridine-4,4'-dicarboxylic acid, 2,2'-bipyridine-6,6'-dicarboxylic acid, 4-(acetic acid)-4'-methyl-2,2'-bipyridine, 2,2'-biquinoline-4,4'-dicarboxylic acid, 1,10-phenanthroline-2,9-dicarboxylic acid and 1,10-phenanthroline-4,7-dicarboxylic acid as presented in figure 14.

Through this study, several parameters will be taken into account: i) the rigidity of the ligands, ii) the relative position of the carboxylates/amidinium substituent on the pyridine ring, iii) the symmetry of the molecule (comparison between symmetric and asymmetric ligands), iv) the presence of one or two donor sites, v) the steric hindrance. The ligands 2,2'-bipyridine-6,6'-dicarboxylic acid and 1,10-phenanthroline-2,9-dicarboxylic acid will be discussed in chapter 3.

⁴⁹ a) Olivier Felix, Ph. D. dissertation – Université Louis Pasteur, **1999** ; b) O. Felix, M. W. Hosseini, A. De Cian, J. Fischer, *New J. Chem.*, **1997**, *21*, 285-288

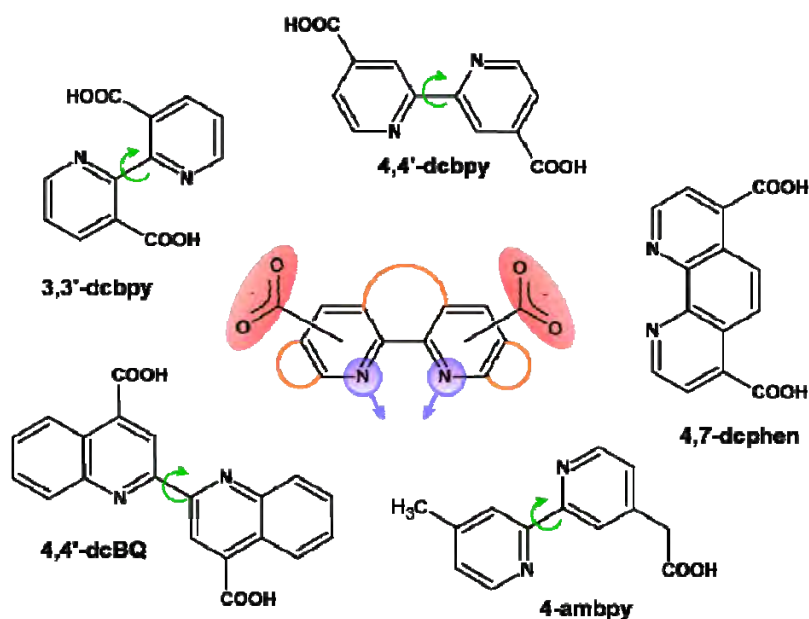


Figure 14. *N,N*-donor coordination ligands towards metals used as hydrogen bonding acceptors.

II.3.3.2 Synthesis of the tectons

The three ligands 4,4'-dicarboxy-2,2'-bipyridine [4,4'-dcbpy], 4,7-dicarboxy-1,10-phenanthroline [4,7-dcphen] and 4-acetoxy-4'-methyl-2,2'-bipyridine [4-ambpy] have been obtained following procedures described in the literature consisting in the oxidation of methyl derivatives. The ligands 3,3'-dicarboxy-2,2'-bipyridine [3,3'-dcbpy] and 4,4'-dicarboxy-2,2'-biquinoline [4,4'-dcBQ], being commercially available, have been purchased*.

Regarding the synthesis of 4,4'-dcbpy, two oxidizing methods are proposed in the literature, one based on potassium permanganate⁵⁰ and the other one on chromium (VI) oxide in aqueous sulphuric acid⁵¹. Both methods have been tested but we found that the second one offers the best yield and reproducibility (scheme 3a).

The 4,7-dicarboxy-1,10-phenanthroline was synthesized following the method proposed by Chandler, Deady and Reiss⁵² (scheme 3b); the first oxidation step is almost quantitative while the second step is responsible for low yield (40%).

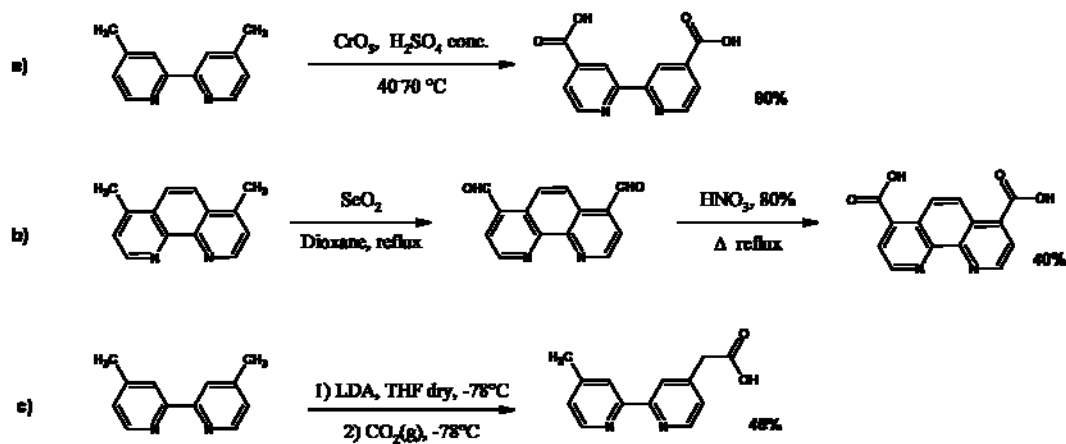
*Also the ligand 4,4'-dicarboxy-2,2'-bipyridine is now commercially available.

⁵⁰ a) G. Sprintschnik, H. W. Sprintschnik, P. P. Kirsch, D. G. Whitten, *J. Am. Chem. Soc.*, **1977**, 4947-4954 ; b) H. Xia, Y. Zhu, D. Lu, M. Li, C. Zhang, B. Yang, Y. Ma, *J. Phys. Chem. B*, **2006**, *110*, 18718-18723

⁵¹ O. Schwarz, D. van Loyen, S. Jockusch, N. J. Turro, H. Dürr, *J. Photochem. Photobio. A: Chemistry*, **2000**, *132*, 91-98

⁵² a) C. J. Chandler, L. W. Deady, J. A. Reiss, *J. Heterocyclic Chem.*, **1981**, *18*, 599-601 ; b) P. Kus, G. Knerr, L. Czuchajowski, *J. Heterocyclic Chem.*, **1991**, *28*, 7-11 ; c) M. Yanagida, L. P. Singh, K. Sayama, K. Hara, R. Katoh, A. Islam, H. Sugihara, H. Arakawa, M. K. Nazeeruddin, M. Grätzel, *J.*

The synthesis of the asymmetric bipyridine (4-ambpy) was achieved *via* a modified procedure by Della Ciana *et al.*⁵³ (scheme 3c) with a simplified work-up and a yield of 45%.



Scheme 3. Synthesis scheme of a) 2,2'-bipyridine-4,4'-dicarboxylic acid, b) 4-acetoxy-4'-methyl-2,2'-bipyridine and c) 1,10-phenanthroline-4,7-dicarboxylic acid.

II.3.3.3 Characterization of the tectons

All the ligands were fully characterized by NMR, IR spectroscopy, MS spectrometry, elemental analysis and melting point and suited the literature data.

Regarding to the XRD data, only the structure of 4,4'-dcbpy figures on the CSD database, so we tried also to obtain the crystal structure of the ligands and we were able to characterize 4,7-dicarboxy-1,10-phenanthroline which crystallizes in two different polymorphs (see § 1.4.2.2). The ligand is in the zwitterionic form ($^-\text{OOC-NH}^+$) in both polymorphs, (α and β phases – see structures I and II in the Annexes), and forms three dimensional hydrogen bonded networks with no solvent molecules included into the lattice.

Polymorph α crystallises into a monoclinic P2(1)/c space group; each carboxylate moiety bridges two or three other molecules *via* (O \cdots HO) and (NH \cdots O) hydrogen bond (see figure 15a) with distances $2.78 < d_{\text{N-O}} < 3.06$ Å and $d_{\text{O-O}} = 2.51$ Å.

Each phenanthroline molecule binds six other molecules, four in the same plane and other two below and above the plane leading to an overall 3D H-bonded packing (see figure 15b).

Chem. Soc., Dalton Trans., **2000**, 2817-2822 ; d) K. Hara, H. Sugihara, L. P. Singh, A. Islam, R. Katoh, M. Yanagida, S. Murata, H. Arakawa, *J. Photochem. Photobiol. A: Chemistry*, **2001**, 145, 117-122

⁵³ L. Della Ciana, I. Hamachi, T. J. Mejer, *J. Org. Chem.*, **1989**, 54, 1731-1735

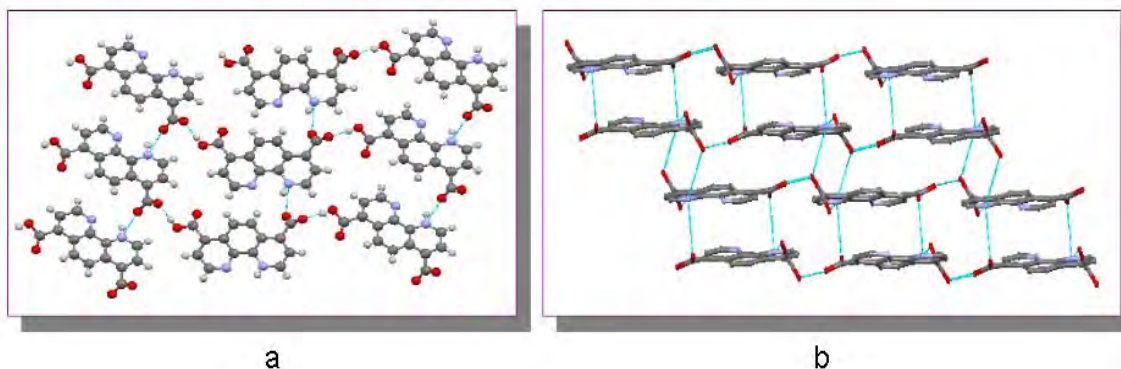


Figure 15. Hydrogen bonded 3D network for the α polymorph of 4,7-dcphen; (a) along x axis (plane yz) showing in particular the hydrogen bond pattern and (b) along the y axis (plane xz).

Polymorph β is more complex and crystallises into a chiral orthorhombic space group $P2(1)2(1)2(1)$ (see also § II.5.2.2). In this packing, each ligand is surrounded by four other ligands (Fig. 16a) through hydrogen bonded, two *via* O··H-O bonds and two *via* NH··O bonds with, in this case, $d_{N-O} = 2.72 \text{ \AA}$ and $d_{O-O} = 2.44 \text{ \AA}$, leading to an overall 3D H-bonded system (figure 16b). Two interpenetrated networks of this kind generate the final 3D structure, as shown in figure 16c.

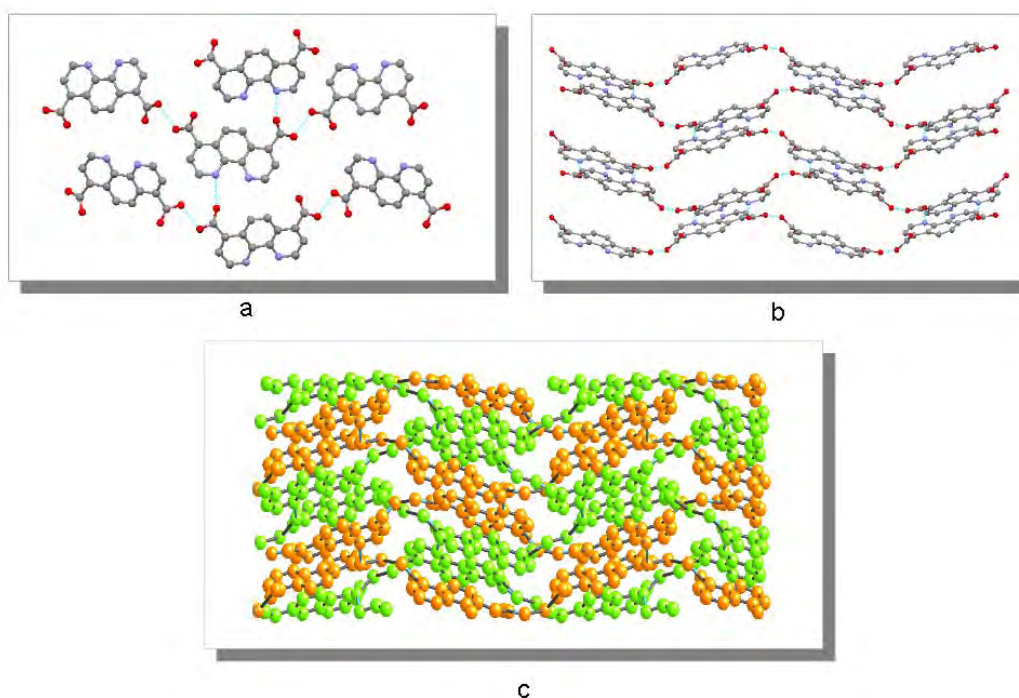


Figure 16. β Polymorphous of 4,7-dcphen: (a) the hydrogen bond pattern leading to a 3D network (shown in b) and both interpenetrated networks (c).

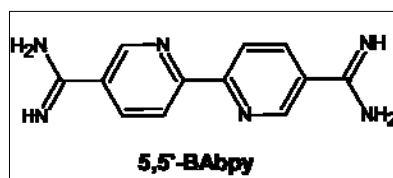
II.3.4 Component B: Amidine bearing ligands, H-bond donor



Because we were interested in this inverted approach, putting an amidinium H-bond donor directly on the ligand (becoming cationic when protonated), a new symmetrical ligand has been designed and synthesised bearing two amidine moieties located in position 5,5'- of the aromatic rings: 5,5'-bisamidine-2,2'-bipyridine (shown in the figure below).

II.3.4.1 Synthesis of the tecton

Different synthetic approach to graft simple amidine functions have been explored since Pinner's method⁵⁴, especially referring to the work of Oxley, Short, Partridge⁵⁵ and more recently from carboxylic acid⁵⁶, thioamides and zinc ammoniate⁵⁷.



The most used synthetic methods arise from nitriles *via* imidates⁵⁸ or in presence of aluminium amides⁵⁹. The ligand has been synthesised following the Garigipati method^{59d} to obtain 5,5'-bisamidine-2,2'-bipyridine as free base and the Schaefer method⁵⁸ to obtain the corresponding hydrochloride salt according to the literature⁶⁰ [Scheme 4].

5,5'-Dibromo-2,2'-bipyridine has been made starting from 2,5-dibromopyridine *via* oxidative addition in a Pd-catalyzed Stille-type coupling reaction. Reaction was first

⁵⁴ A. Pinner, F. Klein, *Ber. Dtsch. Chem. Ges.*, **1877**, *10*, 1889-1893

⁵⁵ a) P. Oxley, W. F. Short, *J. Chem. Soc.*, **1946**, 147-150 ; b) P. Oxley, M. W. Partridge, Robson, W. F. Short, *J. Chem. Soc.*, **1946**, 763-771 ; c) M. W. Partridge, W. F. Short, *J. Chem. Soc.*, **1947**, 390-394 ; d) R. P. Hullin, J. Miller, W. F. Short, *J. Chem. Soc.*, **1947**, 394-396 ; e) P. Oxley, M. W. Partridge, W. F. Short, *J. Chem. Soc.*, **1947**, 1110-1116 ; f) P. Oxley, M. W. Partridge, W. F. Short, *J. Chem. Soc.*, **1948**, 303-309 ; g) P. Oxley, W. F. Short, *J. Chem. Soc.*, **1948**, 1514-1527

⁵⁶ V. B. Piskov, V. P. Kasperovich, L. M. Yakovleva; *Chem. Hetero. Compounds*, **1976**, 917-923

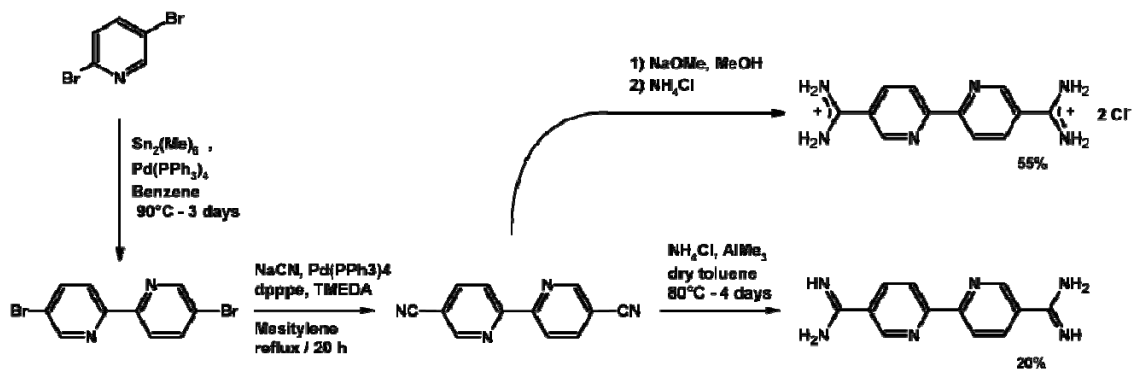
⁵⁷ a) J. Sychała, *Catalysis Letters*, **2006**, *109*, 55-60 ; b) J. Sychała, *Spectroscopy*, **2006**, *20*, 169-176; c) J. Sychała, *Tetrahedron*, **2000**, *56*, 7981-7986

⁵⁸ a) F. C. Schaefer, G. A. Peters; *J. Org. Chem.*, **1961**, *26*, 412-417 ; b) F. C. Schaefer, A. P. Krapcho; *J. Org. Chem.*; **1962**, 1255-1258

⁵⁹ a) A. Basha, M. Lipton, S. M. Weinreb, *Tetrahedron Lett.*, **1977**, *18*, 4171 ; b) G. Neef, U. Eder, G. Sauer, *J. Org. Chem.*, **1981**, *46*, 2824-2826 ; c) J. I. Levin, E. Turos, S. M. Weinreb, *Synth. Comm.*, **1982**, *12*, 989-993 ; d) R. S. Garigipati, *Tetrahedron Lett.*, **1990**, *31*, 1969-1972 ; e) P. A. Gale, *Tetrahedron Lett.*, **1998**, *39*, 38-73-3876

⁶⁰ J. A. Roberts, J. P. Kirby, D. G. Nocera; *J. Am. Chem. Soc.*, **1995**, *117*, 8051-8052

carried out using Michl conditions⁶¹ with tetrakis-triphenylphosphinePd(0) and hexabutyliditin. However the reaction gave poor yields, for that reason, we changed hexabutyliditin with the more reactive hexamethylditin, following the method proposed by Chambron and others⁶², affording the desired compound with a yield of 50%.



Scheme 4. Synthetic way for the obtention of 5,5'-bisamidine-2,2'-bipyridine.

Owing to the conversion of the halogenated precursor to the corresponding nitrile compound, we obtained 5,5'-dicyano-2,2'-bipyridine in good yield according to the literature⁶³. The conversion to bis-amidinium was carried out following a modified Schaefer⁵⁰ procedure in two steps, first *via* alkoxide-catalyzed addition of alcohols to imidate that is converted in a second time by reaction with ammonium hydrochloride with a overall yield of 55%. We obtained directly the bis-amidine from aluminium amide *via* a modified Garigapati reaction with a yield of 20%.

II.3.4.2 Characterization of the tecton

The product has been characterized by NMR, MS, IR (see experimental part). The 5,5'-BAbpy hydrochloride is insoluble in the common solvent, except DMSO, the free base is slightly soluble in alcohols and shows a slight shift toward low field compared to the proton signals of the starting dicyano compound [Fig. 17].

The tectons has been then employed in combination with different dicarboxylic acid, according to the strategy stated in § II.3.2, to test first of all the ligand-carboxylate (**A+B**) tendency to aggregate in the solid state, unfortunately at this moment it hasn't been possible to obtain any single crystal suitable for XRD diffraction.

⁶¹ a) P. F. H. Schwab, F. Fleischer, J. Michl; *J. Org. Chem.*, **2002**, 67, 443-449 ; b) S.-J. Liu, Q. Zhao, R.-F. Chen, Y. Deng, Q.-L. Fan, F.-Y. Li, L.-H. Wang, C.-H. Huang, W. Huang; *Chem. Eur. J.*, **2006**, 12, 4351-4361

⁶² J. I. Bruce, J.-C. Chambron, P. Kölle, J.-P. Sauvage; *J. Chem. Soc., Perkin Trans. 1*, **2002**, 1226-1231

⁶³ J. M. Veauthier, C. N. Carlson, G. E. Collis, J. L. Kiplinger, K. D. John; *Synthesis*, **2005**, 16, 2683-2686

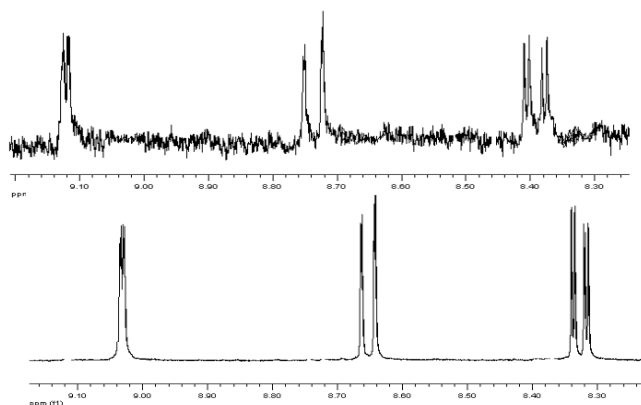


Figure 17. Compared NMR spectra (300MHz) of 5,5'-bisamidine-2,2'-bipyridine (above) and 5,5'-dicyano-2,2'-bipyridine (below) in deuterated MeOH.

II.3.5 Component C: Metal core



Finally, we have to describe the last used tecton: a simple transition metal cation, which is chosen for two characteristics: the structural aspect *i.e.*, the preferred geometry around the metal ion and the affinity for the nitrogen atom rather than the oxygen atom.

Transition metals with octahedral (O_h) and tetrahedral (T_d) geometries, admitting a coordination sphere fulfilled by three bipyridine ligands, should favour the formation of three dimensional networks, while metals with square planar (D_{4h}) geometry should favour the formation of two dimensional networks as stated in the introduction.

Regarding the affinity between ligand and acceptor ion: basing on the Hard-Soft Acid-Base (HSAB) prevision rules by Pearson, which state that '*hard (Lewis) acids prefer to bind to hard (Lewis) bases*' and vice versa '*soft (Lewis) acids prefer to bind to soft (Lewis) bases*'⁶⁴, soft or borderline cations should prefer to bind with the nitrogen of pyridine ring of tecton B, that's considered as borderline ligand, compared with the oxygen of the carboxylic acid.

Following this classification combined with geometric requirements, the most adapted cations are the first row transition divalent metals Mn(II), Fe(II), Co(II), Ni(II), Cu(II), Zn(II) and the *p*-block Sn(II), Pb(II) that prefer octahedral geometry. Monovalent tetrahedral metals like Cu(I) and Ag(I) and divalent square planar metals Pd(II) and

⁶⁴ a) R.G.Pearson, *J.Am.Chem.Soc.*, **1963**, 85, 3533-3543, b) R.G.Pearson, *Science*, **1966**, 151, 172-177 ; c) R.G.Pearson, *Chemical Hardness*, Wiley-VCH, **1997**

Pt(II) that belongs to the soft Pearson class, will also be used. No hard trivalent transition metals will be used.

II.4 Synthesis of transition metallatectons



The envisaged hierarchical strategy for the formation of three components solid state systems leads us to generate and characterize discrete metallatectons (**B+C**), bearing carboxylate moieties as H-bond acceptor, prior to the combination with H-bond donors. For this purpose, we have prepared a series of tetra- tris-, bis- homoleptic and mono- substituted metallatectons. These coordination complexes bear the previously described ligands. These complexes have been obtained using chelating ligands ([3,3'-dcbpy] [4,4'-dcbpy] [4,4'-dcBQ] [4-ambpy] and [4,7-dcphen]) presented in section §II.3.3 [Fig. 14]. Tecton **B** [4-ambpy] will be presented here, though it presents only one H bond acceptor site. In a second step, these metallatectons will be used to form solid state H bonded networks *via* combination with bis-amidinium cations.

II.4.1 Mono-substituted metallatectons $M^{\text{II}}LX_2$

II.4.1.1 General description

Square planar metallic complexes based on Pd(II) and Pt(II) offer the possibility to generate a large variety of metallatectons that, when combined with H bond donor, like bisamidinium cations, could lead to different topologies of mono dimensional networks (the zigzag chain, the crenellated chain or the closed square), as shown in figure 18. Metallatectons composed of [4-ambpy] should lead, in principle, to isolated dimeric units.

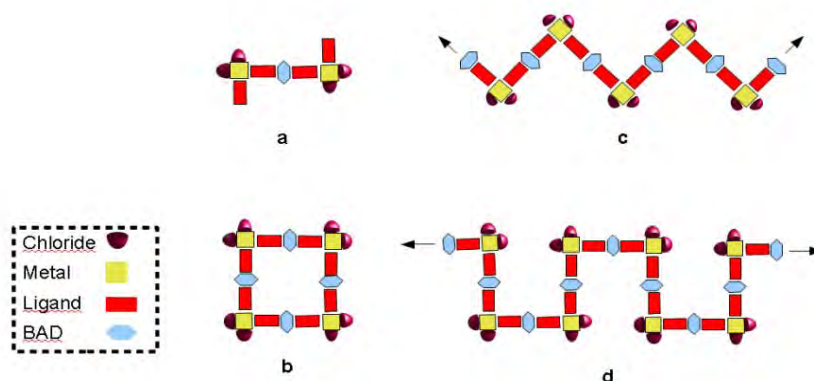


Figure 18. Combination ($A+B+C$) of a monosubstituted metallatectons bearing two carboxylates at the periphery and a linear 4 H-bond donor like Bisamidinium (BAD) leading to a) a dimeric unit, b) a closed tetrameric unit, c) a zigzag 1D network, d) a 1D crenellated chain.

II.4.1.2 Literature outcome

Before the description of the results, we need to have a look on what is described in the literature concerning monosubstituted square planar complexes derived from [3,3'-dcbpy]⁶⁵, [4,4'-dcbpy]⁶⁶, [4,4'-dcBQ]⁶⁷, [4,7-dcphen]⁶⁸, and [4-ambpy]⁶⁹ (Table 2).

⁶⁵ **Pd(II)**: Gao, E.-J.; Liu, X.; Liu, Q.-T.; *Wuji Huaxue Xuebao*, **2002**, *18*, 442-446; **Pt(II)**: a) Yoo, J.; Do, Y.; *Dalton Trans.*, **2009**, *25*, 4978-4986 ; b) Geary, E. A. M.; McCall, K. L.; Turner, A.; Murray, P. R.; McInnes, E. J. L.; Jack, L. A.; Yellowlees, L. J.; Robertson, N., *Dalton Trans.*; **2008**, *28*, 3701-3708 ; c) Senguel, A.; *Turk. J. Chem.*, **2004**, *28*, 703-713; **Mn(II)**: a) Chen, X.-L.; Yao, Y.-J.; Hu, H.-M.; Chen, S.-H.; Fu, F.; Han, Z.-X.; Qin, T.; Yang, M.-L.; Xue, G.-L.; *Inorg. Chim. Acta*, **2009**, *362*, 2686-2697 ; b) Zhang, H. T.; Shao, T.; Wang, H. Q.; You, X. Z., *Acta Cryst., Sect. E: Struct. Rep. Online*, **2003**, *E59*, m342-m344; **Fe(II)**: a) Kwak, O. K.; Min, K. S.; Kim, B. G.; *Inorg. Chim. Acta*, **2007**, *360*, 1678-1683; **Co(II)**: a) Chen, Q.-L.; Chen, J.-Z.; Wang, X.-W.; Zhang, Y.-H.; *Zeit. Natur. B: J. Chem. Sci.*, **2009**, *64*, 335-338 ; b) Zhang, X.-M.; Wu, H.-S.; Chen, X.-M., *Eur. J. Inorg. Chem.*, **2003**, *16*, 2959-2964; **Ni(II)**: a) Zhang, C.-Z.; Mao, H.-Y.; Wang, J.; Zhang, H.-Y.; Tao, J.-C.; *Inorg. Chim. Acta*, **2007**, *360*, 448-454 ; b) Zhang, H. T.; Shao, T.; Wang, H. Q.; You, X. Z.; *Acta Cryst., Sect. C: Cryst. Struct. Commun.*, **2003**, *C59*, m259-m261; **Cu(II)**: a) Wu, J.; *Cryst. Res. Tech.*, **2009**, *44*, 453-456 ; b) Wang, L.-G.; *Acta Cryst., Sect. E: Struct. Rep. Online*, **2007**, *E63*, m3155, m3155/1-m3155/5 ; c) Zhao, B. Z.; Hao, X. R.; Han, Z. G.; Fu, Q.; Chen, Y. G.; *Acta Cryst., Sect. C: Cryst. Struct. Commun.*, **2005**, *C61*, m48-m50; d) Goddard, R.; Hemalatha, B.; Rajasekharan, M. V.; *Acta Cryst., Sect. C: Cryst. Struct. Commun.*, **1990**, *C46*, 33-5 ; **Zn(II)**: a) Lu, L.; Wang, J.; Zhao, B. Z.; Zeng, F. C.; *Acta Cryst., Sect. E: Struct. Rep. Online*, **2007**, *E63*, m2857, Sm2857/1-Sm2857/5 ; **Cd(II)**: Chen, X.-L.; Yao, Y.-J.; Hu, H.-M.; Chen, S.-H.; Fu, F.; Han, Z.-X.; Qin, T.; Yang, M.-L.; Xue, G.-L.; *Inorg. Chim. Acta*, **2009**, *362*, 2686-2697 ; **Ru(II)**: a) Bratsos, I.; Jedner, S.; Bergamo, A.; Sava, G.; Gianferrara, T.; Zangrando, E.; Alessio, E.; *J. Inorg. Biochem.*, **2008**, *102*, 1120-1133 ; b) Shan, B.-Z.; Zhao, Q.; Goswami, N.; Eichhorn, D. M.; Rillema, D. P.; *Coord. Chem. Rev.*, **2001**, *211*, 117-144; **Ag(I)**: a) Chen, X.-L.; Yao, Y.-J.; Hu, H.-M.; Chen, S.-H.; Fu, F.; *J. Coord. Chem.*, **2009**, *62*, 2147-2154 ; b) Guo, H.-Y.; Chen, C.-X.; Wei, Y.-G.; Jin, X.-L.; Fang, C.; Wang, P.; *Chinese J. Chem.*, **2004**, *22*, 816-821

⁶⁶ **Pd(II)**: a) Meyer, S.; Saborowski, S.; Schaefer, B.; *ChemPhysChem*, **2006**, *7*, 572-574 ; b) ten Brink, G.-J.; Arends, I. W. C. E.; Hoogenraad, M.; Verspui, G.; Sheldon, R. A., *Adv. Synth. Catalysis*, **2003**, *345*, 497-505 ; **Pt(II)**: a) Geary, E. A. M.; McCall, K. L.; Turner, A.; Murray, P. R.; McInnes, E. J. L.; Jack, L. A.; Yellowlees, L. J.; Robertson, N., *Dalton Trans.*, **2008**, *28*, 3701-3708 ; b) Du, P.; Schneider, J.; Li, F.; Zhao, W.; Patel, U.; Castellano, F. N.; Eisenberg, R.; *J. Am. Chem. Soc.*, **2008**, *130*, 5056-5058 ; c) Zhang, J.; Du, P.; Schneider, J.; Jarosz, P.; Eisenberg, R.; *J. Am. Chem. Soc.*, **2007**, *129*, 7726-7727; **Mn(II)**: a) Tynan, E.; Jensen, P.; Kruger, P. E.; Lees, A. C.; *Chem. Commun.*, **2004**, *7*, 776-777 ; b) Schareina, T.; Schick, C.; Kempe, R.; *Zeit. Anorg. Allg. Chem.*, **2001**, *627*, 131-133 ; **Fe(II)**: a) Finn, Robert C.; Zubieta, Jon; *Solid State Science*, **2002**, *4*, 83-86 ; **Co(II)**: a) Yoshida, Y.; Tanaka, H.; Saito, G.; Ouahab, L.; Yoshida, H.; Sato, N.; *Inorg. Chem.*, **2009**, *48*, 9989-9991; b) Tynan, E.; Jensen, P.; Kelly, N. R.; Kruger, P. E.; Lees, A. C.; Moubaraki, B.; Murray, K. S.; *Dalton Trans.*, **2004**, *21*, 3440-3447; **Ni(II)**: a) Bancu, L.; Badea, N.; Nita, R.; Meghea, A.; *Mol. Cryst. Liquid Crystals*, **2008**, *486*, 230-238 ; **Cu(II), Zn(II)**: a) Kelly, N. R.; Goetz, S.; Batten, S. R.; Kruger, P. E., *CrystEngComm*, **2008**, *10*, 68-78; b) Tynan, E.; Jensen, P.; Lees, A. C.; Moubaraki, B.; Murray, K. S.; Kruger, P. E.; *CrystEngComm*, **2005**, *7*, 90-95; **Cd(II)**: Liu, Y.-H.; Lu, Y.-L.; Wu, H.-C.; Wang, J.-C.; Lu, K.-L.; *Inorg. Chem.*, **2002**, *41*, 2592-2597; **Ru(II)**: a) Sun, Y.; Machala, M. L.; Castellano, F. N.; *Inorg. Chim. Acta*, **2009**, *363*, 83-287; b) Snaith, H. J.; Zakeeruddin, S. M.; Schmidt-Mende, L.; Klein, C.; Gratzel, M.; *Angew. Chem. Int. Ed.*, **2005**, *44*, 6413-6417

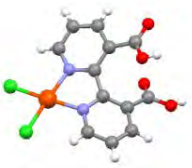
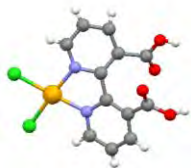
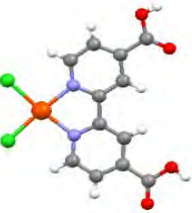
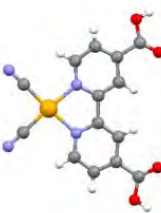
	Pd(II)	Pt(II)	Others
[3,3'-dcbpy]	 Pd(3,3'-dcbpy)Cl ₂ *2 DMSO (XRD see ref.70 ⁷⁰)	 Pt(3,3'-dcbpy)Cl ₂ *2 DMF (XRD see ref.71 ⁷¹) (scheme 5)	Mn(II), Fe(II), Co(II), Ni(II), Cu(II), Zn(II), Cd(II), Ru(II), Ag(I), Re(I), Rh(III), Tb(III), Eu(III)
[4,4'-dcbpy]	 Pd(4,4'-dcbpy)Cl ₂ *DMSO*DMF (XRD this work) (scheme 5)	 Pt(4,4'-dcbpy)(CN) ₂ *3 H ₂ O (XRD see ref.72 ⁷²)	Mn(II), Fe(II), Co(II), Ni(II), Cu(II), Zn(II), Cd(II), Ru(II), Cu(I), Ag(I), Rh(III), Ir(III)
[4,4'-dcBQ]	Pd(4,4'-dcBQ) ²⁺ (ref.67)	NO reference	Cu(II), Zn(II), Pb(II), Ru(II), Ir(III), Os(II)
[4,7-dcphen]	Pd(4,7-dcphen)Cl ₂ – (scheme 5)	Pt(4,7-dcphen) ²⁺ (ref.68)	Cu(II), Ru(II)
[4-ambpy]	Pd(4-ambpy)Cl ₂ – (scheme 5)	NO reference	Ru(II)

Table 2. Sum-up of existing monosubstituted metallatectons derived from **B**, pink colored boxes indicates the metallatectons synthesized in this work.

In table 2 are presented the already existing complexes together with those obtained in this work (in pink) and also their corresponding X ray crystal structure.

⁶⁷ **Pd(II)**: Buffin, B. P.; Belitz, N. L.; Verbeke, S. L., *J. Mol. Catalysis A: Chem.*, **2008**, 284, 149-154 ; **Cu(II)**: Doner L. W.; Irwin P. L.; *Anal. Biochem.*, **1992**, 202, 50-53 ; **Zn(II)**: Xie, J.; *Zeit. Anorg. Allg. Chem.*, **2009**, 635, 384-388; **Pb(II)**: Gregorowicz, Z.; Piwowarska, B.; Buhl, F.; *Roczniki Chemii*, **1967**, 41, 2151-2156; **Ru(II)**: a) Staniszewski, A.; Ardo, S.; Sun, Y.; Castellano, F. N.; Meyer, G. J.; *J. Am. Chem. Soc.*, **2008**, 130, 11586-11587; b) Hoertz, P. G.; Staniszewski, A.; Marton, A.; Higgins, G. T.; Incarvito, C. D.; Rheingold, A. L.; Meyer, G. J.; *J. Am. Chem. Soc.*; **2006**, 128, 8234-8245

⁶⁸ **Pt(II)**: a) Islam, A., Sugihara, H.; Hara, K.; Singh, L. P.; Katoh, R.; Yanagida, M.; Takahashi, Y.; Murata, S.; Arakawa, H.; Fujihashi, G.; *Inorg. Chem.*, **2001**, 40, 5371-5380; **Ru(II)**: a) Hara, K.; Sugihara, H.; Singh, L. P.; Islam, A.; Katoh, R.; Yanagida, M.; Sayama, K.; Murata, S.; Arakawa, H.; *J. Photochem. Photobio., A: Chem.*, **2001**, 145, 117-122

⁶⁹ **Ru(II)**: a) Geneste, F.; Moinet, C.; *New J. Chem.*, **2004**, 28, 722-726; b) Kim, B. H.; Lee, D. N.; Park, H. J.; Min, J. H.; Jun, Y. M.; Park, S. J.; Lee, W.-Y.; *Talanta*, **2004**, 62, 595-602

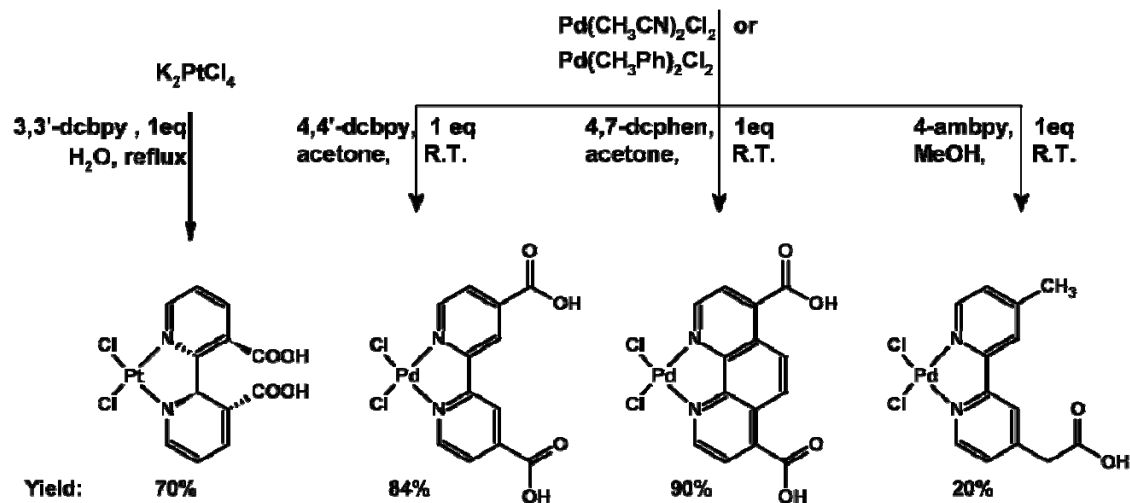
⁷⁰ Liu, X.; Gao, E.-J.; Cheng, M.-C.; Sun, Y.-G.; *Jiegou Huaxue*, **2006**, 25, 477-480

⁷¹ Yoo, J.; Kim, J.-H.; Sohn, Y. S.; Do, Y.; *Inorg. Chim. Acta*, **1997**, 263, 53-60

⁷² Kato, M.; Kishi, S.; Wakamatsu, Y.; Sugi, Y.; Osamura, Y.; Koshiyama, T.; Hasegawa, M.; *Chem. Lett.*, **2005**, 34, 1368-1369

II.4.1.3 Obtained results

We managed to obtain monosubstituted complex with [3,3'-dcbpy], [4,4'-dcbpy], [4,7-dcphen], [4-ampy]. Synthesis was done following the literature in the case of already known complexes, the new complexes were obtained from adapted literature procedures.



Scheme 5. Synthesis of the monosubstituted carboxylic acid metallatectons derived from [3,3'-dcbpy], [4,4'-dcbpy], [4,7-dcphen] and [4-ampy].

All the complexes were fully characterized by NMR, IR spectroscopy, MS spectrometry and elemental analysis (see experimental section).

The new complex Pd(4,4'-dcbpy)Cl₂ has been also characterized by X-ray diffraction (see structure XIV in the Annexes). The palladium complex is planar and in the crystal lattice each carboxylate binds a molecule of DMSO or DMF [Fig. 19a], two molecules are linked through the solvent and a short contact ($d_{C-Cl} = 3.44 \text{ \AA}$) between a chloride atom and the carbon of the carboxylic acid moiety, as shown in figure 19b.

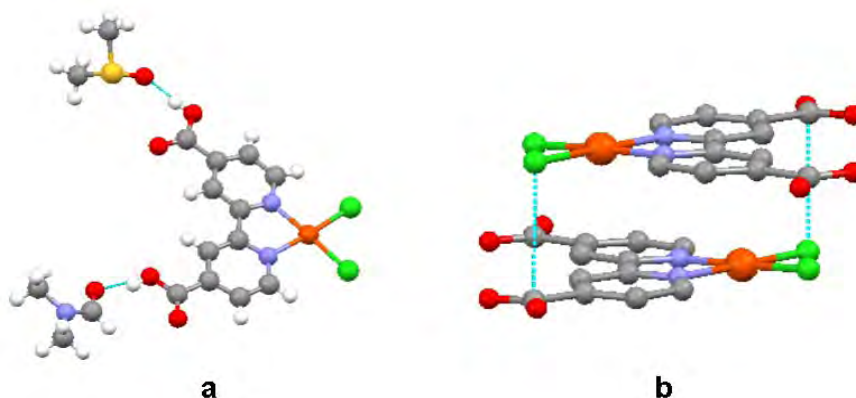


Figure 19. The complex [Pd(4,7-dcbpy)Cl₂]*DMSO*DMF (a) and the particular short range contact C-Cl.

II.4.2 Di-substituted tectons $M^{II}L_2X_2$

II.4.2.1 General description

Square planar metallatectons bearing four recognition sites for hydrogen bond when combined with bond donor like biamidinium cations could lead to bi-dimensional networks whereas tetrahedral metallatectons should lead to three-dimensional diamondoid networks as illustrated in figure 20. If the disubstituted metallatectons possessed only two recognition sites we would return to the case of 1D networks.

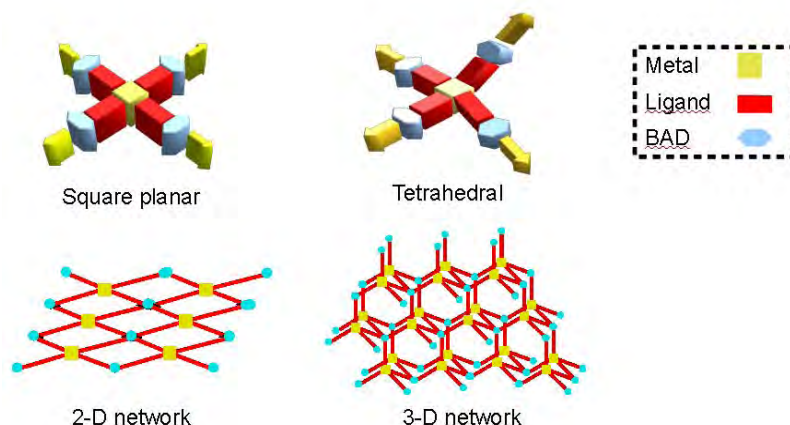


Figure 20. Combination (A+B+C) of a disubstituted metallatectons bearing two carboxylates at its periphery and a linear 4-H bond donor like Bisamidinium (BAD) leading to 2D grid and to diamondoid 3D networks.

II.4.2.2 Literature outcome

In table 3 are shown the already existing complexes derived from [3,3'-dcbpy]⁷³, [4,4'-dcbpy]⁷⁴, [4,4'-dcBQ]⁷⁵, [4,7-dcphen]⁷⁶ together with those obtained in this work (in pink) and also the corresponding X ray crystal structure.

⁷³ **M(II):** a) Dawid, U.; Pruchnik, F. P.; Starosta, R.; *Dalton Trans.*, **2009**, 17, 3348-3353; b) Kilic, A.; Durap, F.; Aydemir, M.; Baysal, A.; Tas, E.; *J. Organomet. Chem.*, **2008**, 693, 2835-2842; c) Xie, P.-H.; Hou, Y.-J.; Wei, T.-X.; Zhang, B.-W.; Cao, Y.; Huang, C.-H.; *Inorg. Chim. Acta*, **2000**, 308, 73-79; d) Tennakone, K.; Senadeera, G. K. R.; De Silva, D. B. R. A.; Kottegoda, I. R. M.; *Appl. Phys. Lett.*, **2000**, 77, 2367-2369; e) Heimer, T. A.; Heilweil, E. J.; Bignozzi, C. A.; Meyer, G. J.; *J. Phys. Chem. A*, **2000**, 104, 4256-4262; f) Hou, Y.-j.; Xie, P.; Zhang, B.; Cao, Y.; Xiao, X.; Wang, W.; *Inorg. Chem.*, **1999**, 38, 6320-6322; **Fe(II)** Ferrere, S.; *Inorg. Chim. Acta*; **2002**, 329, 79-92

⁷⁴ **Cu(I):** a) Constable, E. C.; Redondo, A. H.; Housecroft, C. E.; Neuburger, M.; Schaffner, S.; *Dalton Trans.*, **2009**, 33, 6634-6644; b) Psychogios, N.; Regnouf-de-Vains, J.-B.; Stoeckli-Evans, H. M.; *Eur. J. Inorg. Chem.*, **2004**, 12, 2514-2523; **Fe(II)/Ru(II)/Os(II):** a) Bomben, P. G.; Robson, K. C. D.; Sedach, P. A.; Berlinguette, C. P.; *Inorg. Chem.*, **2009**, 48, 9631-9643; b) Kim, D.; Lee, K.; Roy, P.; Birajdar, B. I.; Spiecker, E.; Schmuki, P.; *Angew. Chem. Int. Ed.*, **2009**, 48, 9326-9329; c) Cicillini, S. A.; Prazias, A. C. L.; Tedesco, A. C.; Serra, O. A.; Santana da Silva, R.; *Polyhedron*, **2009**, 28, 2766-2770; d) Eskelinen, E.; Luukkanen, S.; Haukka, M.; Ahlgren, M.; Pakkanen, T. A.; *Dalton*, **2000**, 16, 2745-2752; e) Bessho, T.; Yoneda, E.; Yum, J.-H.; Guglielmi, M.; Tavernelli, I.; Imai, H.; Rothlisberger, U.; Nazeeruddin, M.

K.; Gratzel, M.; *J. Am. Chem. Soc.*, **2009**, *131*, 5930-5934; f) Rawling, T.; Austin, C.; Buchholz, F.; Colbran, S. B.; McDonagh, A. M.; *Inorg. Chem.*, **2009**, *48*, 3215-3227; g) E. Coronado, J. R. Galamascaros, C. Marti-Gastaldo, E. Palomares, J. R. Durrant, R. Vilar, M. Gratzel, Md. K. Nazeeruddin; *J. Am. Chem. Soc.*, **2005**, *127*, 12351-12-357; h) Xu, Y.; Eilers, G.; Borgstroem, M.; Pan, J.; Abrahamsson, M.; Magnuson, A.; Lomoth, R.; Bergquist, J.; Polivka, T.; Sun, L.; *Chem.-Eur. J.*, **2005**, *11*, 7305-7314; i) T. Fujihara, A. Kobajashi, M. Iwai, A. Nagasawa; *Acta Cryst, Sect. E: Struct. Rep. Online*, **2004**, *60*, m1172-m1174; j) Kleverlaan, C. J.; Indelli, M. T.; Bignozzi, C. A.; Pavanin, L.; Scandola, F.; Hasselman, G. M.; Meyer, G. J.; *J. Am. Chem. Soc.*, **2000**, *122*, 2840-2849; k) E. Eskelinen, S. Luukkanen, M. Maukka, M. Ahlgren, T. A. Pakkanen; *J. Chem. Soc., Dalton Trans.*, **2000**, 2745-2750; l) Sauve, G.; Cass, M. E.; Coia, G.; Doig, S. J.; Lauermann, I.; Pomykal, K. E.; Lewis, N. S.; *J. Phys. Chem. B*, **2000**, *104*, 6821-6836; m) Kirsch, A. K.; Schaper, A.; Huesmann, H.; Rampi, M. A.; Moebius, D.; Jovin, T. M.; *Langmuir*, **1998**, *14*, 3895-3900; n) Heimer, T.A.; Bignozzi, C. A.; Meyer, G. J.; *J. Phys. Chem.*, **1993**, *97*, 11987-94; **Eu(III), Gd(III)**: Guillaumont, D.; Bazin, H.; Benech, J.-M.; Boyer, M.; Mathis, G.; *ChemPhysChem*, **2007**, *8*, 480-488

⁷⁵ **Cu(I)**: a) Djoko, K. Y.; Xiao, Z.; Huffman, D. L.; Wedd, A. G.; *Inorg. Chem.*, **2007**, *46*, 4560-4568; b) Schultz, D.; Nitschke, J. R.; *PNAS*, **2005**, *102*, 11191-11195; c) Bucci, R.; Carunchio, V.; Magri, A. D.; Magri, A. L.; *Annali di Chimica*, **1994**, *84*, 509-20; d) Braun, R. D.; Wiechelman, K. J.; Gallo, A. A.; *Analyt. Chim. Acta*, **1989**, *221*, 223-38 ; **Ru(II)**: a) Yanagida, M.; Miyamoto, K.; Sayama, K.; Kasuga, K.; Kurashige, M.; Abe, Y.; Sugihara, H.; *J. Phys. Chem. C*, **2007**, *111*, 201-209; b) Hoertz, P. G.; Staniszewski, A.; Marton, A.; Higgins, G. T.; Incarvito, C. D.; Rheingold, A. L.; Meyer, G. J.; *J. Am. Chem. Soc.*, **2006**, *128*, 8234-8245; c) Islam, A.; Sugihara, H.; Singh, L. P.; Hara, K.; Katoh, R.; Nagawa, Y.; Yanagida, M.; Takahashi, Y.; Murata, S.; Arakawa, H.; *Inorg. Chim. Acta*, **2001**, *322*, 7-16

⁷⁶ **Ag(I)**: C. Carpanese, S. Ferlay, N. Kyritsakas, M. Henry, M. W. Hosseini; *Chem. Comm.*, **2009**, 6786-6788; **Ru(II)**: a) Sugihara, H.; Sano, S.; Yamaguchi, T.; Yanagida, M.; Sato, T.; Abe, Y.; Nagao, Y.; Arakawa, H.; *J. Photochem. Photobiol., A: Chem.*, **2004**, *166*, 81-90; b) Hara, K.; Horiuchi, H.; Katoh, R.; Singh, L. P.; Sugihara, H.; Sayama, K.; Murata, S.; Tachiya, M.; Arakawa, H.; *J. Phys. Chem. B*, **2002**, *106*, 374-379; c) Islam, A.; Sugihara, H.; Hara, K.; Singh, L. P.; Katoh, R.; Yanagida, M.; Takahashi, Y.; Murata, S.; Arakawa, H.; *J. Photochem. Photobiol., A: Chem.*, **2001**, *145*, 135-141; d) Hara, K.; Sugihara, H.; Singh, L. P.; Islam, A.; Katoh, R.; Yanagida, M.; Sayama, K.; Murata, S.; Arakawa, H.; *J. Photochem. Photobiol., A: Chem.*, **2001**, *145*, 117-122; e) Hara, K.; Sugihara, H.; Tachibana, Y.; Islam, A.; Yanagida, M.; Sayama, K.; Arakawa, H.; Fujihashi, G.; Horiguchi, T.; Kinoshita, T.; *Langmuir*, **2001**, *17*, 5992-5999; f) Yanagida, M.; Singh, L. P.; Sayama, K.; Hara, K.; Katoh, R.; Islam, A.; Sugihara, H.; Arakawa, H.; Nazeeruddin, M. K.; Gratzel, M.; *Dalton*, **2000**, *16*, 2817-2822; g) Schwarz, O.; van Loyen, D.; Jockusch, S.; Turro, N. J.; Durr, H.; *J. Photochem. Photobiol., A: Chem.*, **2000**, *132*, 91-98; h) Sugihara, H.; Singh, L. P.; Sayama, K.; Arakawa, H.; Nazeeruddin, Md. K.; Gratzel, M.; *Chemistry Letters*, **1998**, *10*, 1005-1006


	Cu(I)	Ag(I)	Pd(II)	Pt(II)	Other s
[3,3'-dcbpy]	No reference	No reference	No reference	No reference	Fe(II), Co(II), Ru(II),
[4,4'-dcbpy]	Cu(4,4'-dcbpy) ³⁻ (ref.75)	Ag(4,4'-dcbpy) ₂ (scheme 6)	Pd(4,4'-dcbpy) ₂ Cl ₂ (scheme 6)	Pt(4,4'-dcbpy) ₂ Cl ₂ (scheme 6)	Fe(II), Ru(II), Os(II), Rh(III), Eu(III), Gd(III)
[4,4'-dcBQ]	Cu(4,4'-dcBQ) ³⁻ (ref.76)	No reference	No reference	No reference	Ru(II)
[4,7- dcphen]	No reference	 Ag(4,4'-dcphen) ₂ *DMSO (XRD this work) (scheme 6)	No reference	No reference	Ru(II)
[4-ambpy]	No reference	No reference	No reference	No reference	None

Table 3. Sum-up of existing disubstituted metallatectons derived from **B**, pink colored boxes indicates the metallatectons synthesized in this work.

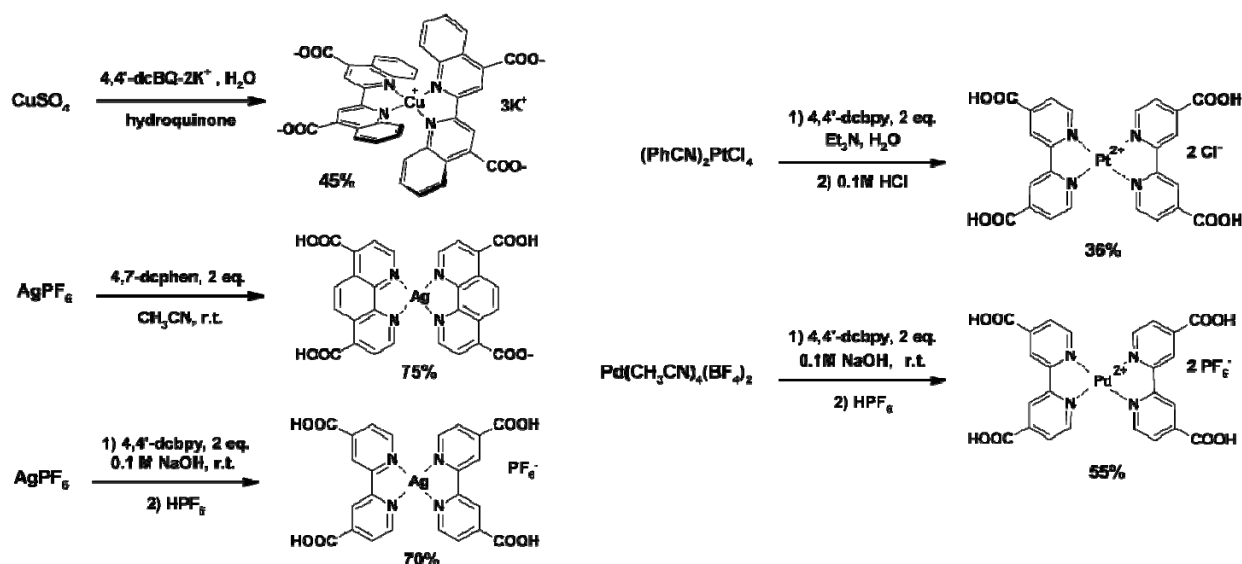
To the best of our knowledge, no bi-substituted homoleptic complexes with carboxylate bipyridine or phenanthroline of Ag(I), Pd(II) and Pt(II) are known. To the best of our knowledge again, no disubstituted homoleptic complexes with 3,3'-dcbpy or 4,7-dcphen and 4-ambpy using tetrahedral or square planar metals are known.

II.4.2.3 Obtained results

The synthesis of the target complexes with 4,4'-dcBQ, 4,4'-dcbpy and 4,7-dcphen is summarized in scheme 6. The synthetic protocol for [4,4'-dcBQ] copper(I) complex was developed from an electrochemical investigation⁷⁷, reducing Cu(II) to Cu(I), stabilized by the bisquinoline ligand. Pd(II) complex was synthesised from Pd(II)(acetonitrile)₂(BF₄)₂ in water, and Pt(II) complex from bis(benzonitrile)Pt(II) dichloride in water (see Experimental part).

The synthesis of [Ag(4,7-dcphen)₂] was performed at room temperature, in acetonitrile from the ligand and AgPF₆ salt with almost quantitative yields and [Ag(4,4'-dcbpy)₂] could be obtained using ethanol as solvent. All the complexes were fully characterized via NMR, MS, microanalysis, IR and UV (see Experimental section).

⁷⁷ R. D. Gallo, K. J. Wiechelmann, A. A. Gallo; *Anal. Chim. Acta*; **1989**, 221, 223-238



Scheme 6. Synthesis of the disubstituted tetrahedral and square planar complexes derived from [4,4'-dcBQ], [4,4'-dcbpy] and [4,7-dcphen].

Single crystals of $[\text{Ag}(4,7\text{-dcphen})_2]$ were obtained, revealing a compound of formula: $[\text{Ag}(4,7\text{-dcphen})_2]^+\text{DMSO}$ (see structure XV in the Annexes). The geometry around the silver center is not square planar but *pseudo* tetrahedral with NAgN_{cis} angle equal to 70° and dihedral angle equal to 131° between the planes formed by the two ligands, as illustrated in figure 21a. This geometry is analogous to what was found in compound $[\text{Ag}(\text{phendio})_2]\text{ClO}_4$ (phendio: 1,10-phenanthroline-5,6-dione).⁷⁸ The isolated complex is neutral and one of the four carboxylates located at the periphery is deprotonated to neutralise the positive charge on the metal center. In the crystalline state, $\text{Ag}(4,7\text{-dcphen})_2$ forms a 1-D chain [Fig. 21b] *via* hydrogen bonding between carboxylate-carboxylic acid ($\text{C}-\text{O}^- \cdots \text{H}-\text{O}$) with $d_{\text{O}\cdots\text{O}} = 2.51 \text{ \AA}$ and the chains are packed *via* π -stacking ($d_{\pi-\pi} \approx 3.6 \text{ \AA}$) and weak interactions through DMSO molecules.

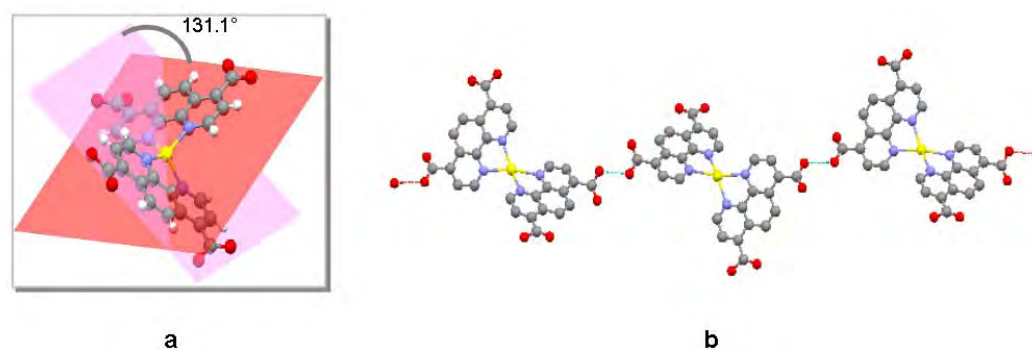


Figure 21. Crystal structure of the isolated $\text{Ag}(4,7\text{-dcphen})_2$ complex.

⁷⁸ M. McCann, B. Coyle, S. McKay, P. McCormack, K. Kavanagh, M. Devereux, V. McKee, P. Kinsella, R. O'Connor, M. Clynes; *Biometals*, **2004**, *17*, 635-645

II.4.3 Tri-substituted tectons

II.4.3.1 General description

Octahedral metals are suitable for tri-substitution by bidentate ligands. They are bearing six or three binding sites for hydrogen bonding that, when combined with H bond donor, could lead to tri-dimensional cubic networks as illustrated in figure 21.

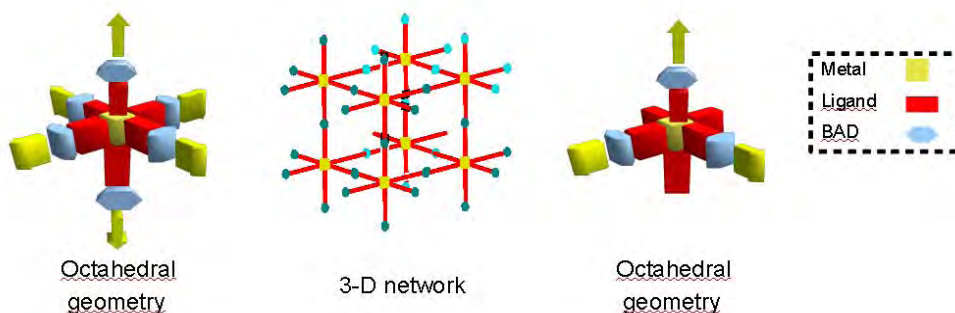


Figure 22. Combination ($A+B+C$) of a trisubstituted octahedral metallatectons bearing two (left) or one (right) carboxylate at the periphery and a linear H bond donor like bisamidinium (BAD) leading to 3D cubic networks.

II.4.3.2 Literature outcome

Table 4 represent the already existing complexes together with those obtained in this work (in pink) concerning trisubstituted octahedral complexes derived from [3,3'-dcbpy]⁷⁹, [4,4'-dcbpy]⁸⁰, [4,4'-dcBQ], [4,7-dcphen]⁸¹, and [4-ambpy]; as summarized in

⁷⁹ **Ru(II):** a) Gillard, R. D.; Hill, R. E. E.; *J. Chem. Soc., Dalton Trans.: Inorg. Chem.*, **1974**, *11*, 1217-36; b) Gillard, R. D.; Hill, R. E. E.; Maskill, R.; *J. Chem. Soc.A: Inorg., Phys., Theor.*, **1970**, *5*, 707-10

⁸⁰ **Fe(II):** a) Elliott, C. M.; Caramori, S.; Bignozzi, C. A.; *Langmuir*, **2005**, *21*, 3022-3027; b) Liao, K. H.; Waldeck, D. H.; *J. Phys. Chem.*, **1995**, *99*, 4569-76; c) Ferrere, S.; *Inorg. Chim. Acta*; **2002**, *329*, 79-92; **Os(II):** a) Sauve, G.; Cass, M. E.; Doig, S. J.; Lauermaun, I.; Pomykal, K.; Lewis, N. S.; *J. Phys. Chem. B*, **2000**, *104*, 3488-3491; b) Liao, K. H.; Waldeck, D. H. ; *J. Physical Chem.*, **1995**, *99*, 4569-76; c) Zakeeruddin, S. M.; Fraser, D. M.; Nazeeruddin, M. K.; Graetzel, M.; *J. Electroanalytical Chem.*, **1992**, *337*, 253-83; **Ru(II):** a) Muldoon, J.; Ashcroft, A. E.; Wilson, A. J.; *Chem.-A Eur. J.*, **2010**, *16*, 100-103; b) Sun, Y.; Machala, M. L.; Castellano, F. N.; *Inorg. Chim. Acta*, **2009**, *363*, 283-287; c) Schwalbe, M.; Schaefer, B.; Goerls, H.; Rau, S.; Tschierlei, S.; Schmitt, M.; Popp, J.; Vaughan, G.; Henry, W.; Vos, J. G.; *Eur. J. Inorg. Chem.*, **2008**, *21*, 3310-3319; d) Zhou, M.; Robertson, G. P.; Roovers, J.; *Inorg. Chem.*, **2005**, *44*, 8317-8325; e) Bae, E.; Choi, W.; *Environ. Sci. Tech.*, **2003**, *37*, 147-152; f) Schwarz, O.; van Luyen, D.; Jockusch, S.; Turro, N. J.; Durr, H.; *J. Photochem. Photob., A: Chem.*, **2000**, *132*, 91-98; g) E. Eskelinen, S. Luukkanen, M. Maukka, M. Ahlgren, T. A. Pakkanen; *J. Chem. Soc., Dalton Trans.*, **2000**, 2745-2750; **Co(III):** a) Matthews, C. J.; Elsegood, M. R. J.; Bernardinelli, G.; Clegg, W.; Williams, A. F.; *Dalton Trans.*, **2004**, *3*, 492-497; b) Uddin, Md. J.; Yoshimura, A.; Ohno, T.; *Bullet. Chem. Soc. Japan*, **1999**, *72*, 989-996 ; **Eu(III)/Tb(III):** a) Masuda, Y.; Wada, S.; Nakamura, T.; Matsumura-Inoue, T.; *J. Alloys Comp.*, **2006**, *408-412*, 1017-1021; b) Calefi, P. S.; Ribeiro, A. O.; Pires, A. M.; Serra, O. A.; *J. Alloys Comp.*, **2002**, *344*, 285-288

Table 4 only tri-substituted complexes with Fe(II), Ru(II) and Os(II) or lanthanides are known till now.

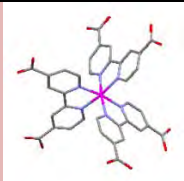
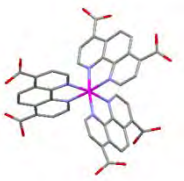
	Ru(II)	Fe(II)	Others
[3,3'-dcbpy]	Ru(3,3'-dcbpy) ²⁺ (ref.79)	No reference	No reference
[4,4'-dcbpy]	 Ru(4,4'-dcbpy) ₃ ⁸² (ref.82) (XRD this work) (scheme 7)	Fe(3,3'-dcbpy) ²⁺ (ref.80)	Os(II), Ir(III), Co(III), Eu(III), Tb(III)
[4,4'-dcBQ]	[Ru(4,4'-dcBQ) ₃ Cl ₂] (scheme 7)	No reference	No reference
[4,7-dcphen]	 Ru(4,7-dcphen) ₃ *2(H ₂ O) (ref.81) (XRD this work) (scheme 7)	No reference	No reference
[4-ambpy]	No reference	Fe(4-ambpy) ₃ (SO ₄) (scheme 7)	No reference

Table 4. Sum-up of existing trisubstituted metallatectons derived from **B**, pink colored boxes indicates the metallatectons synthesized in this work.

II.4.3.3 Obtained results

The obtained compounds are presented in scheme 7. The tris-homoleptic complex [Fe(4-ambpy)₃](SO₄) was synthesized following a modified Schilt⁸³ procedure and characterized by NMR, MS and IR (see experimental section).

The trisubstituted complex of Ru (II) with 4,4'-dicarboxy bipyridine was synthesised according to the classical procedure⁸⁴ as its chloride salt that was

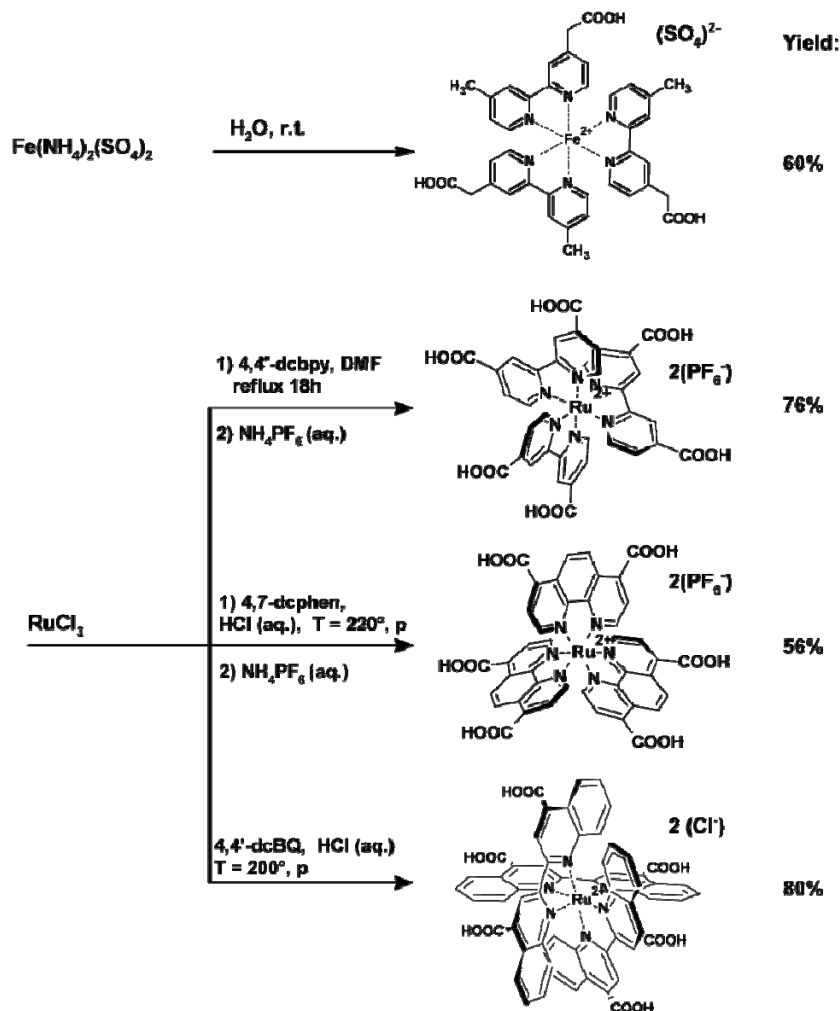
⁸¹ **Ru(II)**: Schwarz, O.; van Loyen, D.; Jockusch, S.; Turro, N. J.; Durr, H.; *J. Photochem. Photob., A: Chem.*, **2000**, *132*, 91-98

⁸² a) Schwalbe, M.; Schaefer, B.; Goerls, H.; Rau, S.; Tschierlei, S.; Schmitt, M.; Popp, J.; Vaughan, G.; Henry, W.; Vos, J. G.; *Eur. J. Inorg. Chem.*, **2008**, *21*, 3310-3319; b) Eskelinen, E.; Luukkanen, S.; Haukka, M.; Ahlgren, M.; Pakkanen, T. A.; *Dalton*, **2000**, *16*, 2745-2752

⁸³ a) A. A. Schilt, *J. Am. Chem. Soc.*, **1960**, *82*, 3000-3005 ; b) S. Ferrere, B. A. Gregg; *J. Am. Chem. Soc.*, **1998**, *120*, 843-844

⁸⁴ M. Zhou, G. P. Robertson, J. Roovers; *Inorg. Chem.*, **2005**, *44*, 8317-8325E.

afterward converted into hexafluorophosphate derivate in order to improve the poor solubility, the correlate single crystal was instead obtained through hydrothermal synthesis following the literature⁸⁵. The 4,7-dicarboxy phenanthroline and 4,4'-dicarboxy bisquinoline analogues were synthesized *via* hydrothermal synthesis.



Scheme 7. Synthesis of tri-substituted octahedral metallatectons derived from, [4,4'-dcbpy], [4,4'-dcBQ], [4,7-dcphen], and [4-ambpy].

[Ru(4,4'-dcBQ)₃]Cl₂ was characterised by NMR, MS, IR, UV and elemental analysis; [Ru(4,4'-dcbpy)₃] and [Ru(4,7-dcphen)₃], as shown in figure 23, were also characterised by XRD on single crystal.

The compound of formula [Ru(4,4'-dcbpy)₃]*1.5(H₂O) is a *pseudo* polymorph of the corresponding structure published by Pakkanen *et al.* (ref.85) which differs by the number of solvent molecules in the crystal lattice (see structure XII in the Annexes). Each octahedral Ru complex binds, through (COO...HOOC) H-bonding, six others

⁸⁵ Eskelinen, S. Luukkanen, M. Haukka, M. Ahlgrén, T. A. Pakkanen; *J. Chem. Soc., Dalton Trans.*, **2000**, 2745-2752

molecules ($2.48 < d_{O-O} < 2.51 \text{ \AA}$) forming a four-fold interpenetrated 3-D hydrogen bonded network [Fig. 23a].

For the other ligand, a compound of formula $[\text{Ru}(4,7\text{-dcphen})_3] \cdot 2(\text{H}_2\text{O})$ is obtained (see structure XIII in the Annexes), forming a single 3-D network through carboxylates H-bonding ($2.44 < d_{O-O} < 2.98 \text{ \AA}$). This is due to the fact that, in this case, each Ru complex binds seven other molecules and the final network has no enough space for interpenetration [Fig.23b].

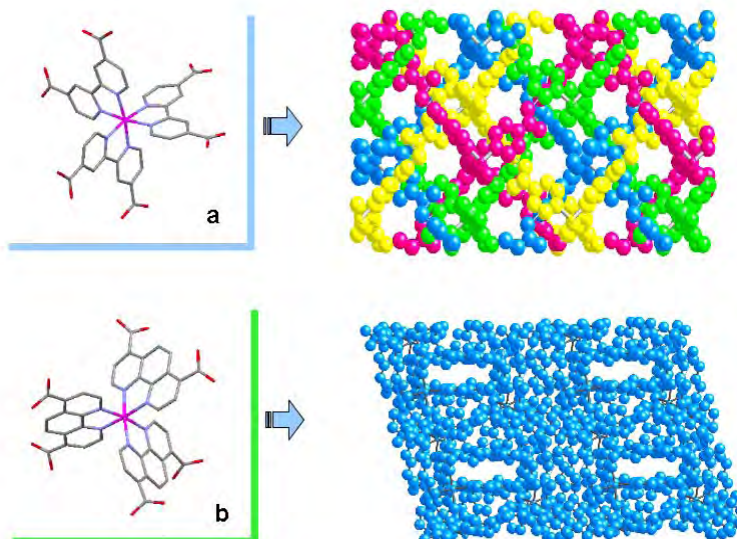


Figure 23. XRD structures of trisubstituted complexes of a) $[\text{Ru}(4,4'\text{-dcbpy})_3] \cdot 1.5(\text{H}_2\text{O})$ and b) $[\text{Ru}(4,7\text{-dcphen})_3] \cdot 2(\text{H}_2\text{O})$.

II.4.4 Tetra-substituted tectons

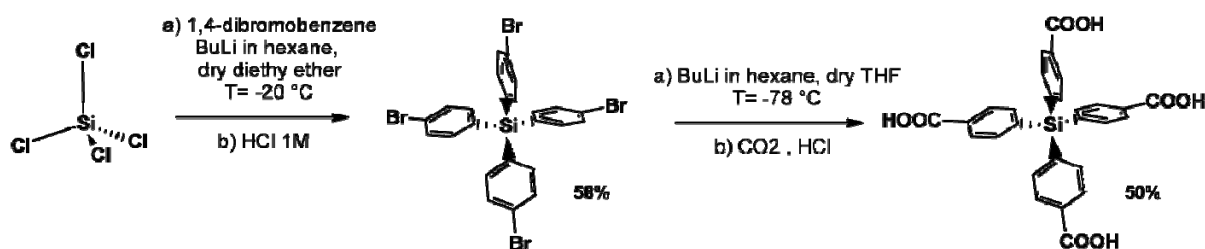
Parallel to the study of tectons B, N-donor bidentate ligands, we extended the study to a tetra-substituted metallatecton, bearing one carboxylate group at the periphery, using, this time, a monodentate N-donor tecton and a central silicon atom. Silicon-based connecting units are generally synthetically more readily accessible compared with their carbon analogous and join the properties of the semi-metallic silicon core.

This tecton (scheme 8) may behave as a tetrahedral metallatecton, being able to form diamandoid 3D networks (see figure 20) when combined with H bond donors, as in the case of adamantane-1,3,5,7-tetracarboxylic acid^{86,87} or tetrakis(*p*-

⁸⁶ O. Ermer; *J. Am. Chem. Soc.*, **1988**, *110*, 3747-3754

⁸⁷ S. Ferlay, S. Koenig, M. W. Hosseini, J. Pansanel, A. De Cian, N. Kyritsakas; *Chem. Comm.*; **2002**, 218-219

boronicphenyl)silane⁸⁸. We synthesised and characterized (see Experimental section) a tetrahedral tetrakis(4-carboxyphenyl)silane⁸⁹, using the synthetic pathway⁹⁰ presented in scheme 8.



Scheme 8. Synthesis of tetrahedral tetrakis(4-carboxyphenyl)silane.

II.4.5 Metallatectons as building blocks for H-bonded coordination networks: some conclusions

Several new association of metal and tectons (**B+C**) has led to a series of new metallatectons that may act as building blocks for the formation of H-bonded networks when combined with H bond donors.

Unfortunately, following the two steps approach described in figure 1, attempts to obtain single crystals of deprotonated metallatectons combined with amidinium cations were not successful for all the metal complexes that have been synthesised. In most cases, in fact, we recovered amorphous powder precipitates; in case of [Ag(4,7-dcphen)₂] complex the yellow crystalline precipitate has been identified with the complex itself and for [Cu(4,4'-dcBQ)₂]K₃ the formed purple crystals rapidly lost their crystallinity getting amorphous once drawn out of the solvent. For that reason, the hierarchical approach for building three components H bonded networks was no longer pursued.

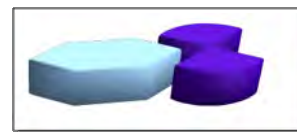
We will now focus on 'one pot' synthesis, but a preliminary study of the purely organic (**A+B**) combination will be first undertaken.

⁸⁸ a) J. H. Fournier, T. Maris, J. D. Wuest, W. Z. Guo, E. Galoppini; *J. Am. Chem. Soc.*; **2003**, *125*, 1002-1006 ; b) H. M. El-Kaderi, J. R. Hunt, J. L. Mendoza-Cortes, A. P. Cote, R. E. Taylor, M. O'Keeffe, O. M. Yaghi; *Science*, **2007**, *316*, 268-272

⁸⁹ a) J.B. Lampert, Y. Zhao, C. L. Stern; *J. Phys. Org. Chem.*; **1997**, *10*, 229-232 ; b) J. B. Lambert, Z. Q. Liu, C. Q. Liu; *Organometallics*, **2008**, *27*, 1464-1469

⁹⁰ a) J.-H. Fournier, X. Wang, J. D. Wuest; *Can. J. Chem.*; **2003**, *81*, 376-380 ; b) R. P. Davies, R. J. Less, P. D. Lickiss, K. Robertson, A. J. P. White; *Inorganic Chemistry*, **2008**, *47*, 9958-9964

II.5 Formation of two components assemblies



In this part we intend to study the ability of tectons **B** to form H bonds with bisamidinium cations (tectons **A**), in the solid state. This work has been essential i) to perform a screening concerning the tendency of the different ligand-amidine (**A+B**) combination to aggregate in the crystalline form, ii) to preliminary optimize crystallisation conditions and iii) to collect data to compare with the H-bond nodes in the crystal structure of the three components metallic assembly (**A+B+C**).

II.5.1 Choice and description of the nodes - Choice of bisamidinium tectons

As stated in section § II.3.2.1, the recognition in dihapto mode of H bond, between cyclic bisamidinium cations and carboxylate groups, occurs when the distance between N-N atoms in the cations are almost equal to 5Å. For that reason we restricted our study to the dications presented in figure 24.

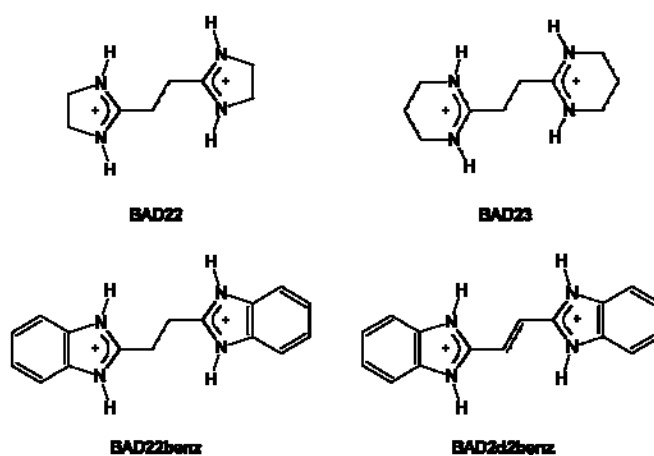


Figure 24. Bisamidinium cations used as tectons in the network formation..

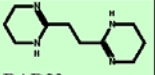
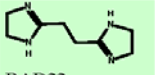
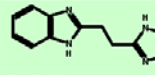
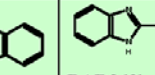
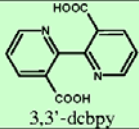
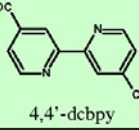
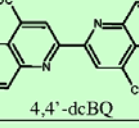
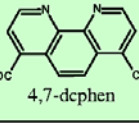
The chosen tectons [Fig. 24] are based on a C2 (**S**) spacer between amidine moieties both as single bond (BAD22, BAD23 and BAD22benz) and as double bond (BAD2d2benz). The vinyl bridge in BAD2d2benz can be considered as a shortening of the d_{N-N} distance and confers an increased rigidity to the structure as well.

All these tectons are strong bases in the un-protonated amidine form and in the presence of proton donor compounds like carboxylic acids, they undergo acid-base reaction (proton transfer). The base character is related to the electronic delocalization of double bond between the two nitrogen atoms where one is formally an amine and the other is of the imine type. As already said, the difference in pK_a between amidine

and carboxylic acid is ($\Delta pK_a \approx 10$) big enough to favour the proton transfer from acid to base⁹¹. In order to obtain single crystals of H bonded assemblies, we can chose to synthesize the free base of **A** to form in situ the acid-base adduct or *vice versa* we can use the amidinium cation and mix it in the crystallization medium with the carboxylate anion.

II.5.2 Formed Organic H-bonded networks

The combination of the amidinium cations (tecton **A**), with different ligands (tecton **B**) is presented in Table 5.

	 BAD23	 BAD22	 BAD22benz	 BAD2d2benz
 3,3'-dcbpy	☹️	☹️	☹️	☹️
 4,4'-dcbpy	☹️	👍	☹️	☹️
 4,4'-dcBQ	👍	☹️	☹️	☹️
 4,7-dcphen	👍	☹️	☹️	☹️

Diagonal notes in Table 5:
 - Between 4,4'-dcbpy and BAD23: BAD23 hydrolyzed
 - Between 4,7-dcphen and BAD22: BAD22 hydrolyzed

Table 5. Summary of the organic network obtained upon combination of the used bis-amidines (tectons **A**) with dicarboxylic acids (tectons **B**).

As we can see in table 5, we were able to obtain suitable single crystals for X-ray diffraction only with BAD23 and in one case with BAD22, for the other combinations the quality of the crystals was not good enough for XRD analysis; on the contrary, no crystals at all could be obtained with BAD22benz and BAD2d2benz but only amorphous powders, this motivated our decision not to use further on these tectons for the building of three components systems.

The structures were obtained using a tecton **A**/tecton **B** ratio of 1:1 for slow diffusion of a DMSO solution of the ligand into a CHCl_3 solution of BAD for 4,4'-dcbpy and 4,7-dcphen or *via* slow evaporation of a water-ethanol solution in the case of 4,4'-dcBQ (see Annexes). We also had to face the problem of hydrolysis of BAD23 and BAD22 (tecton **A**) that occurs during crystallisation process, leading to 1,3-

⁹¹ a) S.-O. Shan, D. Herschlag; *Proc. Natl. Acad. Sci. USA*, **1996**, 93, 14474-14479 ; b) S. L. Johnson, K. A. Rumon; *J. Phys. Chem.*, **1965**, 69, 74-86

diaminopropane and 1,2-diaminoethane respectively. The corresponding structures obtained with tectons **B** will not be shown here.

As we already pointed out, directional $^+N-H\cdots O^-$ charge assisted hydrogen bonds would lead, in principle, to a dihapto recognition mode between carboxylate and BAD22 or BAD23, and to a 1-D system in the crystalline state with a 1:1 stoichiometry. In the following section we will give a structural description of the obtained organic networks.

II.5.2.1 1D-network obtained upon combination of BAD23 with [4,4'-dcBQ]

The obtention of the network formed upon combination of BAD23 and [4,4'-dcBQ] is particularly reproducible: the same crystal structure was obtained using different crystallization conditions. The acid and the base in their neutral form were mixed in aqueous-ethanolic solution and left evaporate to obtain colourless crystals of a compound with general formula $[(C_{20}H_{10}N_2O_4)(C_{10}H_{20}N_4)] \cdot 3(H_2O)$ or $[(4,4'\text{-dcBQ})(\text{BAD23})] \cdot 3(H_2O)$ (see structure VI in the Annexes).

In the crystalline form, tectons **A** and **B** are fully protonated and deprotonated respectively (see table 6 for C-O distances), and the compounds present two different mono-dimensional chains connected by three water molecules. For the recognition pattern, in one case, a μ -bis(monohapto) H bond mode is observed (chain 1 – figure 25) leading to a zig-zag chain and in the second case, a μ -bis(dihapto) recognition mode is observed (chain 2 – figure 25), forming another zig-zag chain with a different orientation, both chains present a tilt angle of 83.4° [Fig. 25]. In this case, the recognition pattern between **A** and **B** is *a priori* not predictable.

Considering the hydrogen bonding distances d_{N-O} , they vary between 2.76 and 2.86 Å and particularly are 2.81 and 2.86 Å for chain 2 (see table 6) and 2.76 Å for chain 1.

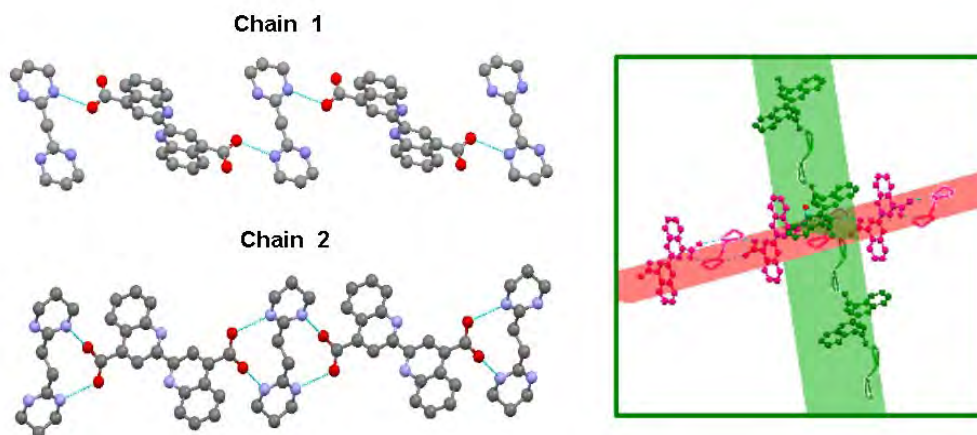


Figure 25. Both H bond modes adopted in BAD23[4,4'-dcBQ]. In Chain 1, a μ -bismonohapto H bond mode and in Chain 2, a μ -bisdihapto H bond mode.

	Chain 1 (bis-monohapto)	Chain 2 (bis-dihapto)
d(N-O)	2.76 Å - 2.76 Å	2.86 Å - 2.81 Å / 2.86 Å - 2.81 Å
d(NH-O)	1.88 Å - 1.88 Å	2.00 Å - 1.94 Å / 2.00 Å - 1.94 Å
d(C-O)	1.26 Å - 1.21 Å	1.26 Å - 1.25 Å

Table 6. : Selected distances in $BAD23*[4,4'-dcBQ]$

Each one of these two mono-dimensional chains uses one of the three water molecules located in the crystal structure to form a bidimensional sheet (different coloured in the figure 26); these alternating sheets are connected through the third of the three water molecules (red labelled in the figure 26) in the whole crystal packing.

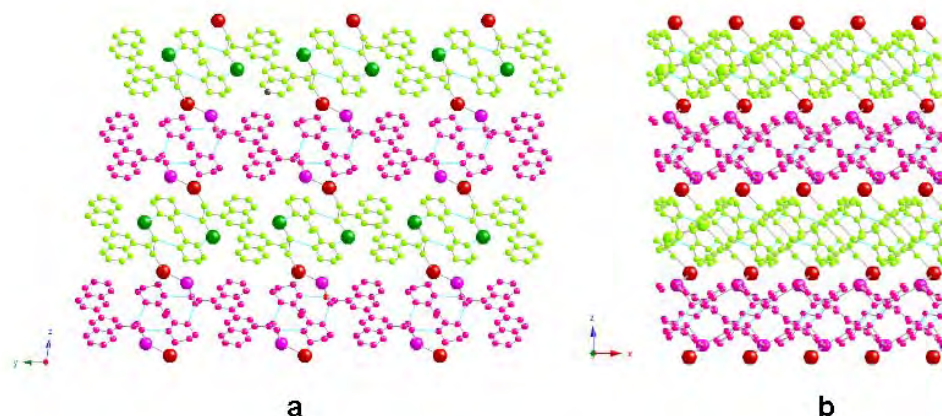


Figure 26. View of the stacking of the plane connected by water molecules along x axis (a) and along y axis (b) in $BAD23*[4,4'-dcBQ]$. The three water molecules are underlined by different colours: green the one connecting Chain1 in Sheet1; violet the one connecting Chain2 in Sheet2 and red the one connecting two planes.

II.5.2.2 1D-network obtained upon combination of $BAD23$ with [4,7-dcphen]

The network is formed by combining in a 1:1 tecton **A**/tecton **B** ratio a DMSO solution of the acid 4,7-dicarboxy-1,10-phenanthroline and base $BAD23$. Colourless crystals of a compound with general formula $[(BAD23)*(4,7-dcphen)]*2(CHCl_3)$ or were obtained (see structure V in the Annexes).

In the crystal, tectons **A** and **B** are fully protonated and deprotonated respectively and the obtained network is monodimensional, the chains being connected by $CHCl_3$ solvent molecules. The H bond donor tectons **A** adopts a unique μ -bis(dihapto) H bond mode, leading to the expected one dimensionnal system, with d_{N-O} distances involved in H bond varying between 2.76 and 2.66 Å. [Fig. 27a].

The network belongs to a chiral space group $P2(1)2(1)2(1)$ as the network formed by the ligand alone (see § II.3.2.4); considering that the network is formed by molecules without stereogenic centre, the crystal chirality likely comes from the conformation of the ligand 4,7-dcphen in the solid state. If we look closer at the ligand,

we can notice a slight torsion of the carboxylate moiety [Fig. 27b] around the C-C axis that confers chirality to the molecule and, as consequence, to the network.

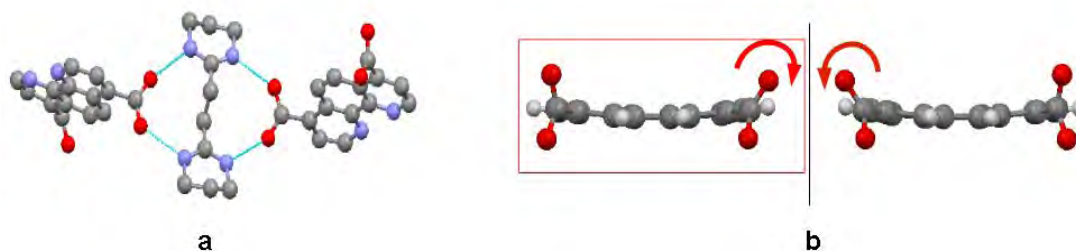


Figure 27. a) The bis-dihapto hydrogen bonding recognition mode in the mono-dimensional network for $[(BAD23)*(4,7-dcphen) [(BAD23)*(4,7-dcphen)]*2(CHCl_3)]$, b) the rotation of the COO^- that confers chirality to the network.

Finally, the packing is composed of parallel single chains sliding along an axis of rototranslation in alternation (red and yellow in figure 28), each chain is surrounded by chloroform molecules that fill the empty space in between the chains affording the whole close packing.

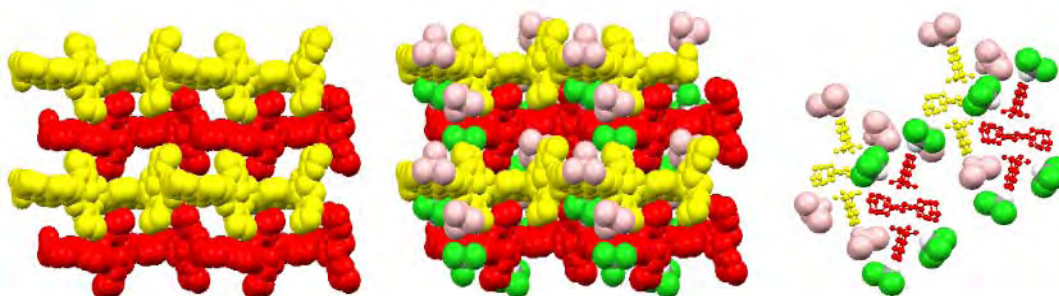


Figure 28. For $[(BAD23)*(4,7-dcphen)]$, representations of the packing of the mono-dimensional network, along x axis (left, center) and, on the right, particular view of the position of the water molecules (viewed from the z axis).

In this particular case, the recognition pattern between **A** and **B** has respected the prediction.

II.5.2.3 2D-network obtained upon combination of Bad22 with [4,4'-dcbpy]

After many attempts, we were able to crystallize suitable single crystals based on tectons 4,4'-dcbpy (tecton **B**) and BAD22 (tecton **A**). The crystal was obtained by mixing a DMSO solution of the acid form of 4,4'-dcbpy and a $CHCl_3$ solution of the basic form of BAD22 using a **A**:**B** ratio of 1:1, leading to a compound of general formula $[(4,4'-dcbpy)(BAD22)]*2(H_2O)$ (see structure IX in the Annexes).

In the network, tectons **A** and **B** are fully protonated and deprotonated respectively and the bis-amidinium cation adopts a bis-monohapto H bond mode to

form linear single chains with both d_{N-O} distances of 2.75 Å.

The chains are connected by the two water molecules to form bi-dimensional sheets, but the layers are connected only through π -stacking ($d_{C-C} \approx 3.6$ Å) between the superimposed chains and through weak hydrogen bonds among water molecules ($d_{O-O} > 3.3$ Å) [Fig. 29].

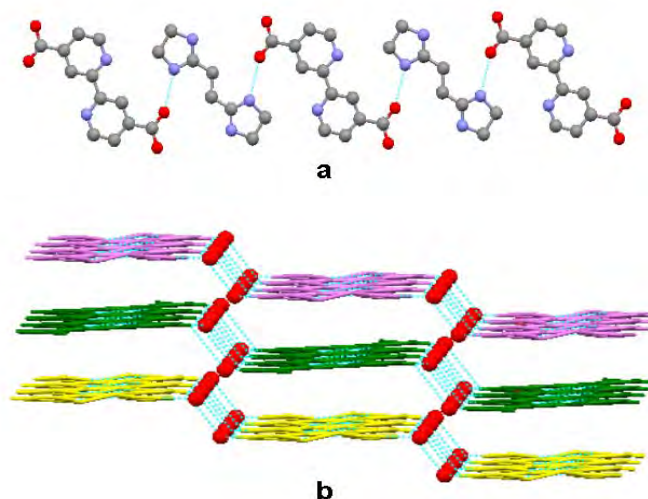


Figure 29. a) Bis-monohapto H bond mode in $[(4,4'\text{-dcbpy})(\text{BAD22})]*2(\text{H}_2\text{O})$; b) Stacking of the planes and connection between the chains via water molecule, view along $[110]$.

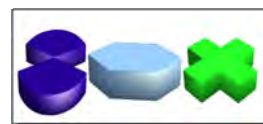
The recognition pattern between **A** and **B** is, in this case, not predictable; in the network, tecton **A** is not connected in the bis-dihapto coordination mode, which is probably due to metric constraints imposed by the five members ring of the amidine moiety.

1.5.2.4 General conclusion concerning the (A+B) formation

Crystallisation of bipyridine, phenanthroline and bisquinoline dicarboxylic acid (tectons **B**) with cyclic bis-amidines (tecton **A**) revealed to be difficult and not to lead systematically to the same H bond recognition pattern. Crystallisation conditions were depending on the solubilisation of the di-acid and the choice of solvent is limited both for bis-amidines and for diacids, in fact, carboxylic acids are soluble only in DMSO and DMF as well BAD22benz and BAD2d2benz. In addition, BAD22 and BAD23 are soluble in CHCl_3 and CH_2Cl_2 but they hydrolyze very easily in alcohols and water. Using the correspondent salts of carboxylates and bis-amidinium makes solubility more efficient but this couldn't help to get monocrySTALLINE materials.

All the obtained structure from tectons **A** and tectons **B** have a 1:1 stoichiometric ratio and form 1-D chains or 2-D sheets due to the connectivity imposed by H bond mode. The hydrogen bonding modes adopted in preference are the bis-dihapto, as in the case of $[\text{BAD23}*4,7\text{-dcphe}]$, the bis-monohapto, as for $[\text{BAD22}*4,4'\text{-dcbpy}]$, or both as for $[\text{BAD23}*4,4'\text{-dcBQ}]$ and the predictability of the chosen interaction is not

easy. Although the obtention of single crystals revealed to be not so easy (most times we recovered amorphous powders), the networks formed by BAD22 and BAD23 filled our expectation for the purpose to obtain hybrid networks with the adding of metal as second assembling node (tecton **C**) and thus we continued the project.



II.6 Hybrid organic/inorganic networks

II.6.1 Network conception

Finally, after all the preliminary studies concerning the combinations of the three tectons **A**, **B** and **C**, we were able to examine the combination of the tectons for the formation of coordination / H-bonded metallic networks using the one-pot strategy.

This approach may be regarded as a combinatorial approach involving a set of three families of starting tectons **A+B+C**, mixed together. If we consider our initial five tectons **B** and four bisamidinium tectons **A**, with the possibility offered by the metal of the periodic table (early transition metals), we can see that the total combination is huge. For that reason, we restricted our study to 3 Tectons **B** (H bond acceptor), that have been implied in the formations of organic H bonded network with two bisamidinium tectons **A** (see conclusion § 1.5.2.4), so that our study is "limited" to 3x2xM possible combinations, as shown in Table 7.

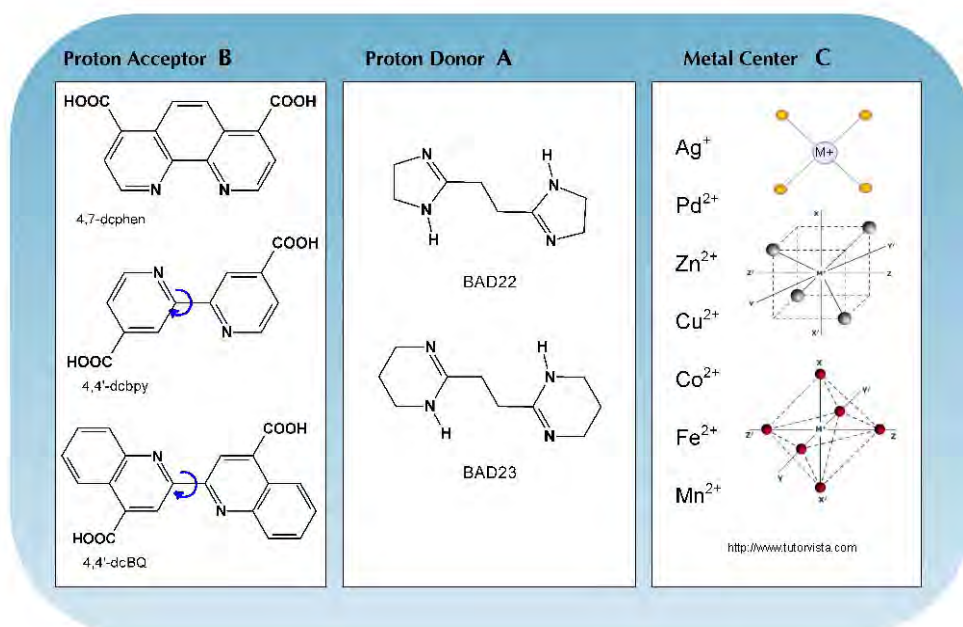


Table 7. The three components (**B**, **A** and **C**) used to build hybrid organic-inorganic networks, using one-pot method.

Many attempts have been made to test the different combinations of the tectons, varying the reagent concentration and the solvents when possible. Among all the attempts, two examples that will be discussed below demonstrate the practicability of the approach. Other structures for which one of the tectons is missing or hydrolyzed won't be discussed here (see Annexes for crystal structure details).

II.6.2 2-D networks with BAD23, 4,7-dcphen and Ag(I)

According to our expectation and following the strategy previously illustrated, a system composed of four components, a dicationic and a dianionic tecton, a metal cation and his counter anion led to the formation of a 2-D H bonded network⁹².

II.6.2.1 Structural analysis

The combination of an AgXF_6 salt ($X = \text{P, As, Sb}$) (**C**), BAD23 (tecton **A**) and [4,7-dcphen] (tecton **B**) afforded a series of three isomorphous crystals, that were analysed using X ray diffraction on single crystal and revealed the following general formula $\{[\text{Ag}(\text{C}_{14}\text{H}_6\text{N}_2\text{O}_4)_2][\text{C}_{10}\text{H}_{20}\text{N}_4]_2\} \text{XF}_6 \cdot 2\text{MeOH}$ ($X = \text{P, As, Sb}$) (see structures XIX, XX and XXI in the Annexes). Yellow colourful, needle shaped crystals were obtained after some weeks from slow evaporation of aqueous-ethanolic solution of AgXF_6^- ($X = \text{P, As, Sb}$) salt [Fig. 30]. Other silver salts with different counter ions were also tested, but it was not possible to obtain single crystals suitable for XRD analysis.

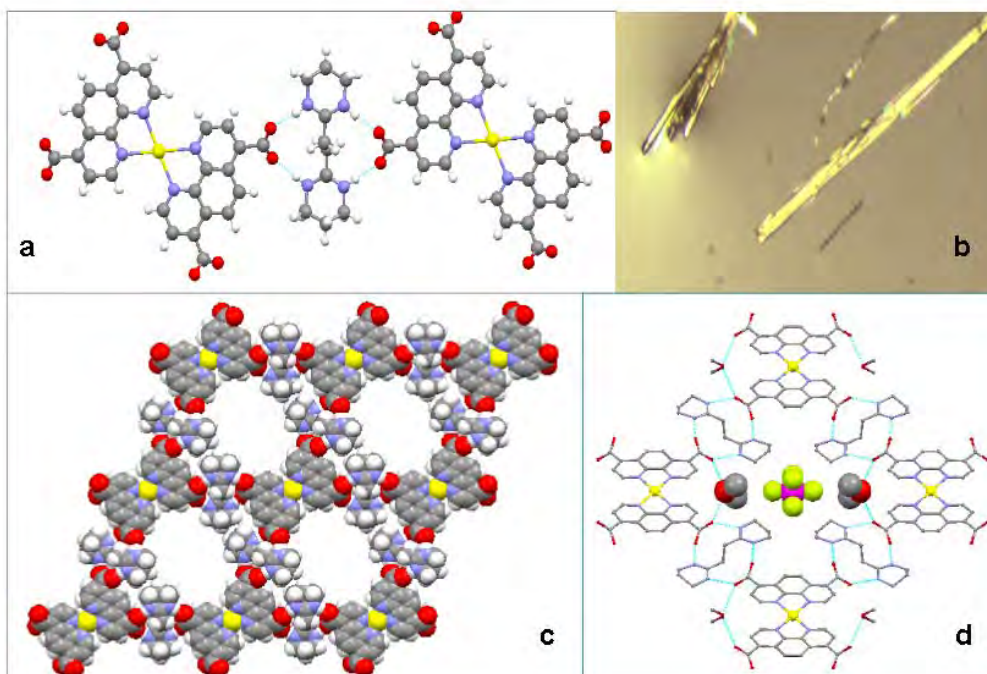


Figure 30. For network $\{[\text{Ag}(\text{C}_{14}\text{H}_6\text{N}_2\text{O}_4)_2][\text{C}_{10}\text{H}_{20}\text{N}_4]_2\} \text{XF}_6 \cdot 2\text{MeOH}$ ($X = \text{P, As, Sb}$) a) Details of hydrogen bonding mode; b) picture of the needle shaped crystal, c) 2-D network arrangement

⁹² C. Carpanese, S. Ferlay, N. Kyritsakas, M. Henry, M. W. Hosseini; *Chem. Comm.*, **2009**, 6786-6788

(solvents and anions molecules are omitted for clarity); d) enlargement of the network cavity with the relative position of anion and MeOH molecules.

The network is composed of [BAD23-2H]²⁺ as dicationic hydrogen bond donor and of [4,7-dcphen]²⁻ as hydrogen bond acceptor that constitute the H-bonding assembling node, the coordination assembling node is assured between the chelating N-donor site of phenanthroline and a silver cation (Ag⁺) with a square planar geometry. The three networks, formed using the three different silver salts, are isostructural and crystallise in the space group monoclinic C2/m; besides they form 2-D cationic grids and the charge neutralisation of the assembly is guaranteed by the rather weakly coordinating XF₆⁻ anion (X= P, As, Sb). Remarkably the lattice is completed by two molecules of methanol and not ethanol, as we could expect, but this fact is reasonably explainable considering the 1% methanol impurity inside the used solvent.

	d(N-O)	d(NH-O)	d(C-O)	d(Ag-N)	N ⁺ AgN ⁻ _{cis}
SbF₆⁻	2.74 Å 2.75 Å	1.88 Å 1.87 Å	1.21 Å 1.25 Å	2.36 Å 2.36 Å	69.6° 110.3°
AsF₆⁻	2.74 Å 2.75 Å	1.88 Å 1.87 Å	1.23 Å 1.25 Å	2.36 Å 2.36 Å	69.8° 110.7°
PF₆⁻	2.79 Å 2.75 Å	1.92 Å 1.87 Å	1.23 Å 1.24 Å	2.38 Å 2.38 Å	70.0° 109.9°

Table 8. Distances and angles for the three {[Ag(C₁₄H₆N₂O₄)₂][C₁₀H₂₀N₄]₂} XF₆ *2MeOH (X= P, As, Sb) isostructural networks.

The silver cation is, in this case, well adapted for self-assembling with chelating phenanthroline. With respect to the isolated metallatecton (see § II.4.2), the coordination geometry around disubstituted Ag(I) changes from square planar to tetrahedral. The connection between metallatecton and tecton B is ensured by a bis(dihapto) H bond mode, leading thus to a cationic 2D layer composed of rhombohedral motives, with distances and angles shown in table 8.

Concerning the packing of the layers, they don't superimpose and are slightly shifted with respect to the others. The stacking of the planes is due to several contributions: i) hydrogen bonding between carboxylates and hydroxyl groups of methanol ($d_{O-O} \approx 2.8$ Å), ii) columbic interactions between the positive charged complex and the negative charged anion, iii) π - π stacking of the phenanthroline rings in a face-to-face shifted manner ($d_{\pi-\pi} = 3.8$ Å) (see § I.1.2.3). This packing leads to channels that are filled with the anions and two MeOH solvent molecules that was found to be disordered over two positions with an occupancy of 50%. The solvent molecules fill two side positions into the cavities, like they occupy two lateral rooms, while the bigger central chamber is filled by the bulky hexafluorometallate anions [Fig. 31].

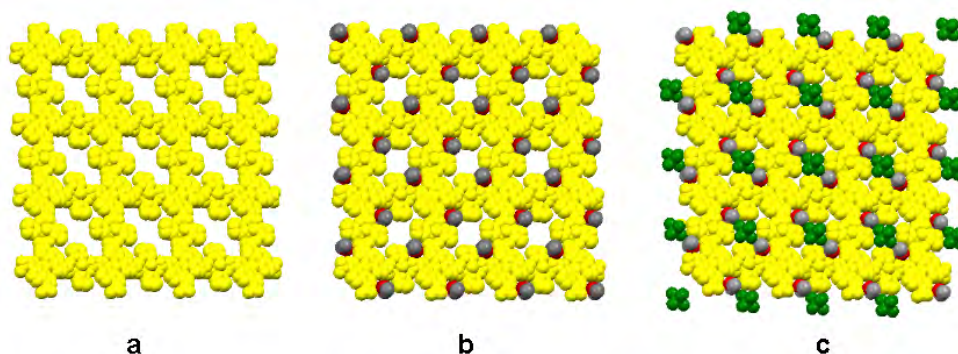


Figure 31. Filling of the cavities in $\{[Ag(C_{14}H_6N_2O_4)_2][C_{10}H_{20}N_4]_2\} XF_6 \cdot 2MeOH$ ($X = P, As, Sb$). a) the coordination-hydrogen bonding network; b) solvent molecule ($MeOH$) filling the side cavities; c) anion (XF_6^-) molecules filling the central holes.

The shifting of the plane creates a "chain of anions" not perpendicular to the plane but crossing transversally the layers as you can see in figure 32 with d_{F-F} distance between the apical fluorine of 3.31 Å.

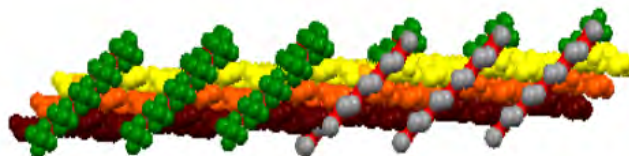


Figure 32. Alignment of the XF_6^- and solvent molecules through the shifted cationic planes along y axis for $\{[Ag(C_{14}H_6N_2O_4)_2][C_{10}H_{20}N_4]_2\} XF_6 \cdot 2MeOH$ ($X = P, As, Sb$).

From the analysis of the cell parameters and channels volume, we can see that the planes adapt their spacing to the size of the anions, as seen in table 9.

	Cell parameters	Volume (\AA^3)	Cavity diameter (\AA)
SbF₆⁻	a = 21.8809(18) Å $\alpha = 90^\circ$ b = 23.0194(18) Å $\beta = 98.574(4)^\circ$ c = 5.3675(5) Å $\gamma = 90^\circ$	2673.3(4) \AA^3	10.26Å – 9.43Å
AsF₆⁻	a = 21.538(2) Å $\alpha = 90^\circ$ b = 23.019(2) Å $\beta = 98.638(5)^\circ$ c = 5.3934(5) Å $\gamma = 90^\circ$	2643.7(4) \AA^3	10.21Å – 9.20Å
PF₆⁻	a = 21.4159(17) Å $\alpha = 90^\circ$ b = 23.109(3) Å $\beta = 99.117(6)^\circ$ c = 5.4593(6) Å $\gamma = 90^\circ$	2667.7(5) \AA^3	10.15Å - 9.10Å

Table 9. Cell parameters, lattice volume and diameter of the inner cavities are compared for the three networks $\{[Ag(C_{14}H_6N_2O_4)_2][C_{10}H_{20}N_4]_2\} XF_6 \cdot 2MeOH$ ($X = P, As, Sb$).

In order to better understand the network assembly, we compared the formed assembling nodes in the bi-dimensional network with the isolated nodes *i.e.*, the isolated metallatecton between 4,7-dcphen and silver (§ II.4.2.3) and the organic hydrogen bonding network between 4,7-dcphen and BAD23 (§ II.5.2.2).

We could observe that, for the metallatecton, the geometry around the metal is tetrahedral with $\text{NAgN}_{\text{cis}} \approx 70^\circ$ and a dihedral angle of 28° (§ II.4.2.3), but, in the network, the geometry has been forced to be square planar with $\text{NAgN}_{\text{cis}} \approx 70^\circ$ and $\text{NAgN}_{\text{trans}} \approx 180^\circ$ (see figure 33).

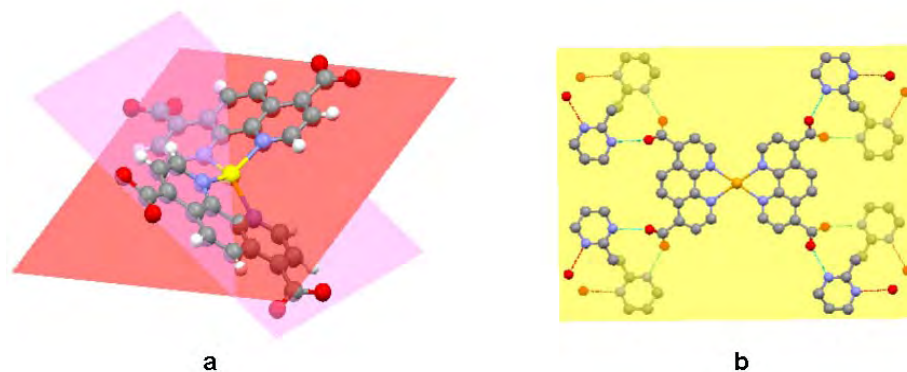


Figure 33. a) The distorted tetrahedral geometry for the isolated $\text{Ag}(4,7\text{-dcphen})_2$ metallatecton and b) the square planar geometry in the lattice of $\{[\text{Ag}(\text{C}_{14}\text{H}_6\text{N}_2\text{O}_4)_2][\text{C}_{10}\text{H}_{20}\text{N}_4]_2\} \text{XF}_6 \cdot 2\text{MeOH}$ ($X = \text{P}, \text{As}, \text{Sb}$).

Finally we can reconstruct and schematize the three components network formation as the assembly of organic single chains, based on hydrogen bonding through a bis-dihapto recognition mode, interconnected by metallic nodes, based on coordination bonding, keeping the square planar geometry, as shown in figure 34.

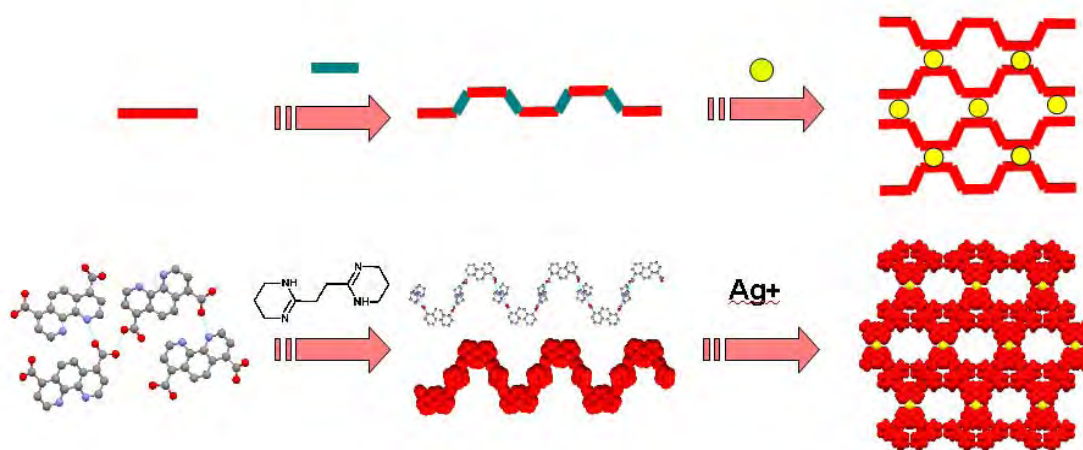


Figure 34. Schematic representation of the network supposed assembly for $\{[\text{Ag}(\text{C}_{14}\text{H}_6\text{N}_2\text{O}_4)_2][\text{C}_{10}\text{H}_{20}\text{N}_4]_2\} \text{XF}_6 \cdot 2\text{MeOH}$ ($X = \text{P}, \text{As}, \text{Sb}$).

II.6.2.2 XRPD and thermal studies

Though the crystals were very difficult to obtain after several weeks of evaporation at room temperature, the final compound was stable both in the crystallisation medium and in air which allowed us to perform X-ray diffraction on the

microcrystalline powder and verify that, for the three isostructural networks, the crystals form a single phase [see figure 35 a, b and c].

Thermogravimetric analysis measurements confirm the stability of the compound over a quite large temperature range with incoming decomposition from 225°C. In the case of AgSbF_6 derivative we can see that the first slope matches well with the lost in weight corresponding to the lost of two methanol molecules [Fig. 35d] but for PF_6 it corresponds only to 1.4 molecules. Unfortunately was not possible to repeat the measurements in the case of AgAsF_6 and AgPF_6 because of the small quantity of recovered crystals.

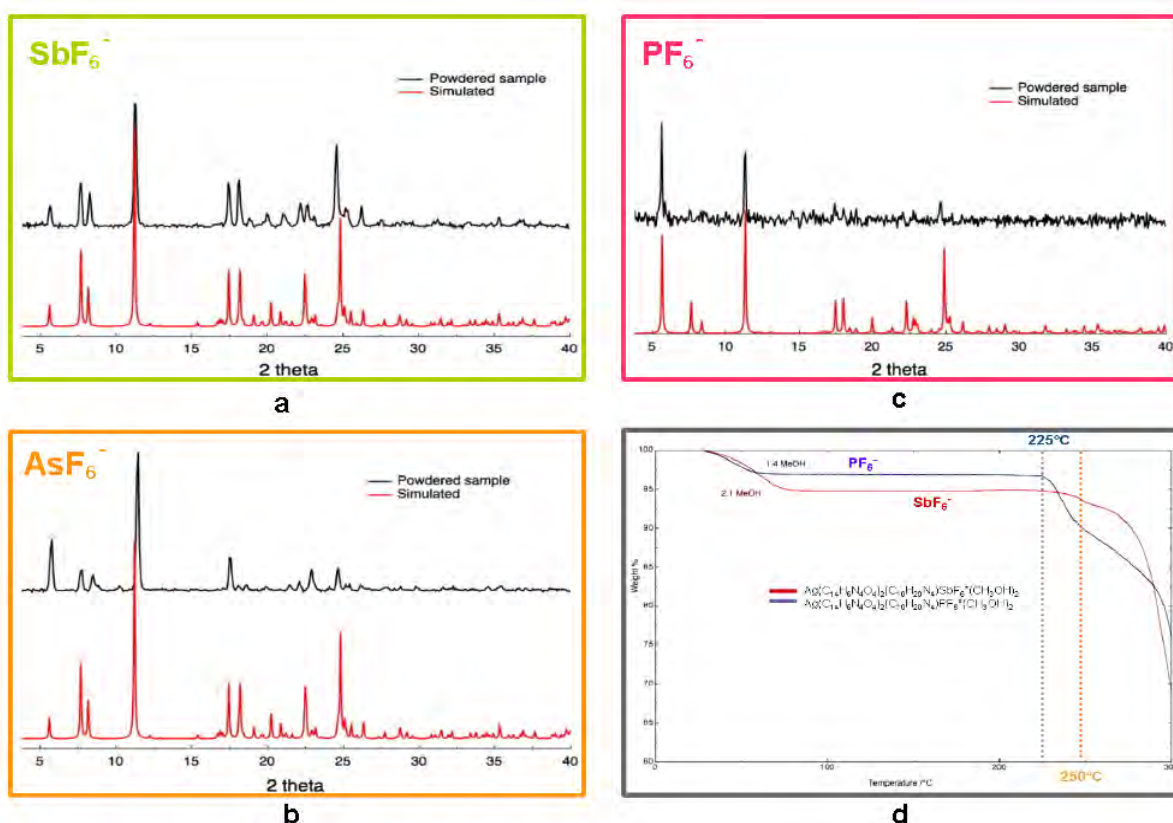


Figure 35. PXRD patterns are compared with simulated patterns from crystallographic data for $[\text{Ag}(\text{C}_{14}\text{H}_6\text{N}_2\text{O}_4)_2][\text{C}_{10}\text{H}_{20}\text{N}_4]_2 \text{SbF}_6 \cdot 2\text{MeOH}$ (a), $[\text{Ag}(\text{C}_{14}\text{H}_6\text{N}_2\text{O}_4)_2][\text{C}_{10}\text{H}_{20}\text{N}_4]_2 \text{AsF}_6 \cdot 2\text{MeOH}$ (b) and $[\text{Ag}(\text{C}_{14}\text{H}_6\text{N}_2\text{O}_4)_2][\text{C}_{10}\text{H}_{20}\text{N}_4]_2 \text{PF}_6 \cdot 2\text{MeOH}$ (c). TGA measurements for SbF_6 and PF_6 (d).

Another example of a three-component system is given here below with the same **A** and **B** tectons, using copper (II) as tecton **C**.

II.6.3 3-D network with BAD23, 4,7-dcphen and Cu(II)

In the same crystallisation conditions as described above, *i.e.*, using a neutral aqueous solution of 4,7-dcphen and BAD23 and an ethanolic solution of $\text{Cu}(\text{CF}_3\text{SO}_3)$, after evaporation over some months, we were able to obtain green crystals suitable for XRD analysis that is a new example of a three-component system.

II.6.3.1 Structural analysis

The compound of general formula $\{[\text{Cu}(\text{C}_{14}\text{H}_6\text{N}_2\text{O}_4)_2][\text{C}_{10}\text{H}_{20}\text{N}_4]\} \cdot 2\text{H}_2\text{O}$ is composed of a disubstituted complex hydrogen bonded to the bisamidinium (tecton **A/B** ratio 2:1); there are also two molecules of water in each unit cell (see structure XXII in the Annexes).

The copper atoms present a pseudo octahedral coordination sphere [Fig. 36b], they are surrounded by four nitrogens belonging to N-donor phenanthroline and two oxygens, coming from two deprotonated carboxylate anions, belonging to the neighbouring tectons. Each copper atom bears four carboxylates, four C-O bonds are occupied in hydrogen bonding with bis-amidinium, in the already observed bis dihapto mode [Fig. 36a], and two are occupied in Cu-O bonds with the near molecules. Owing to the use of different donating atoms from the neighbouring ligands, copper complexes form an infinite chain through carboxylate-copper coordination (see figure 37).

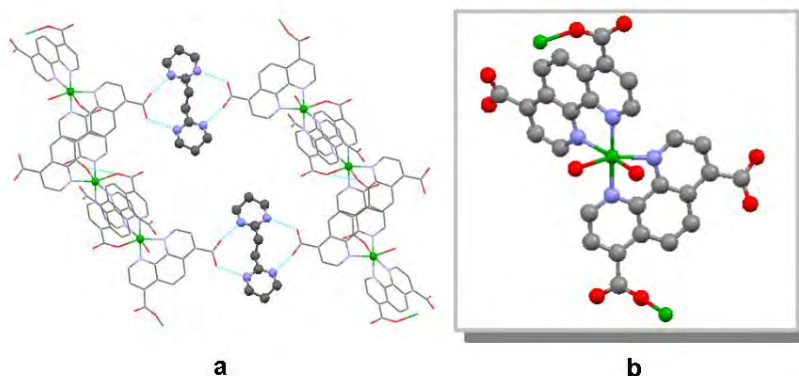
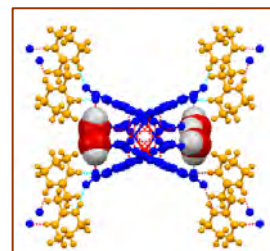


Figure 36. a) Bis-dihapto coordination mode between $[\text{BAD23-2H}]^{2+}$ $[\text{4,7-dcphen}]^{2-}$; b) coordination geometry around $\text{Cu}(\text{II})$ metal cation for $\{[\text{Cu}(\text{C}_{14}\text{H}_6\text{N}_2\text{O}_4)_2][\text{C}_{10}\text{H}_{20}\text{N}_4]\} \cdot 2\text{H}_2\text{O}$.

The bonding distances Cu-N and Cu-O are $1.97 < d_{\text{Cu-N}} < 2.15 \text{ \AA}$ and $d_{\text{Cu-O}} = 2.28 \text{ \AA}$, $\text{N}\hat{\text{C}}\text{uN}_{\text{cis}}$ angle is equal to 9.2° with a torsional angle of 95.2° between the two chelating ligands, $\text{O}\hat{\text{C}}\text{uO}_{\text{cis}}$ angle is 78.2° and the chain is strengthened by π -stacking between phenanthroline rings ($\approx 3.5 \text{ \AA}$).

All the carboxylates on both ligands are deprotonated with the typical $d_{\text{C-O}}$ distances of $1.24\text{--}1.25 \text{ \AA}$; two of them, as already told, are occupied in the coordination sphere of the metal and two participate to the recognition pattern between carboxylate and amidinium [Fig. 36a] with bonding distances $d_{\text{N-O}}$ between 2.76 and 2.84 \AA and $d_{\text{NH-O}}$ between 1.90 and 1.97 \AA . The last two carboxylates are binding two water molecules in a side position along the chain, as we can see in the side picture, these water molecules do not interfere with the lattice packing.



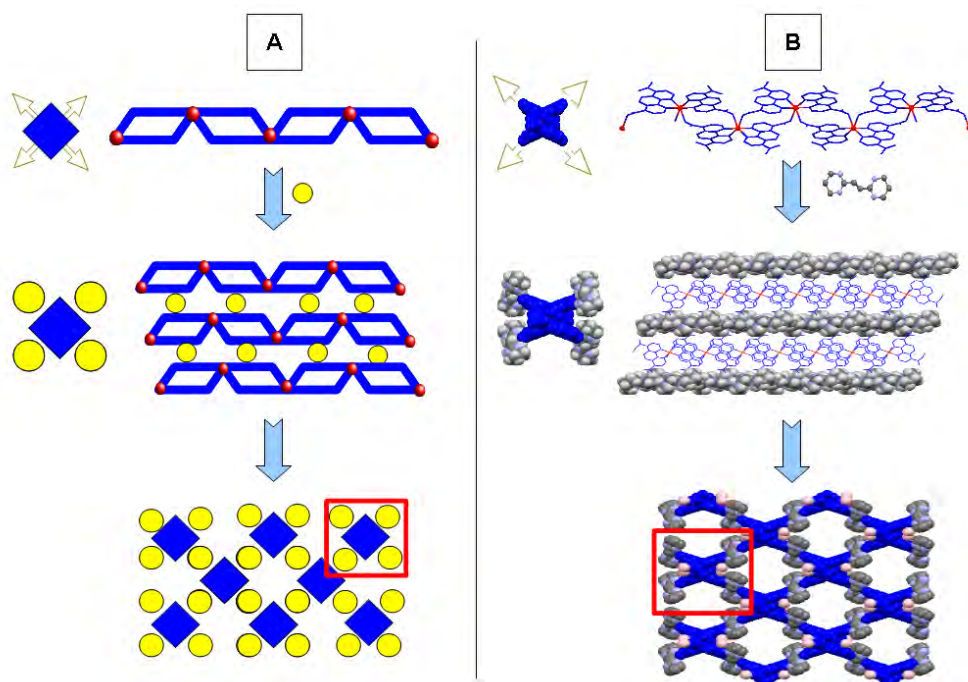


Figure 37. Schematic (A) and real (B) views of the 3-D H bonded coordination network for $\{[\text{Cu}(\text{C}_{14}\text{H}_6\text{N}_2\text{O}_4)_2][\text{C}_{10}\text{H}_{20}\text{N}_4]\} \cdot 2\text{H}_2\text{O}$ and its building blocks.

The mono-dimensional copper chains (blue in figure 37) are connected through four hydrogen bonded bis-amidinium (represented by yellow circles in figure 37A), leading to an overall 3 D system. The network is three-fold interpenetrated (see § I.3.2.4) and this guarantee the closest packing lattice with the filling of the free space, as shown in figure 38.

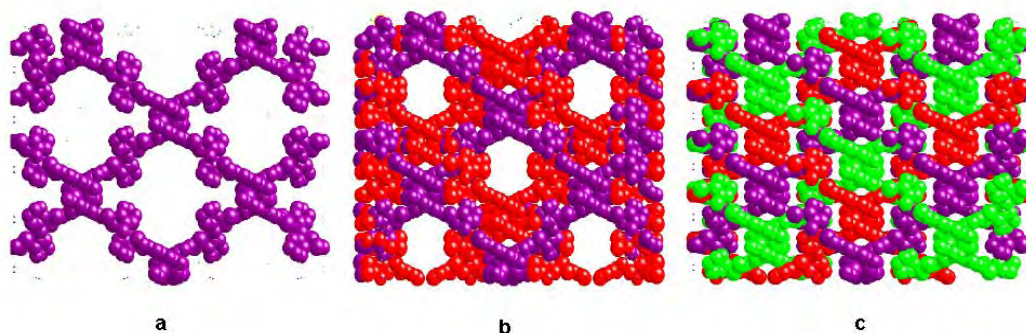


Figure 38. View of the three interpenetrating 3-d networks along z axis for $\{[\text{Cu}(\text{C}_{14}\text{H}_6\text{N}_2\text{O}_4)_2][\text{C}_{10}\text{H}_{20}\text{N}_4]\} \cdot 2\text{H}_2\text{O}$.

Due to the very small quantity of obtained crystals, and to the very long crystallisation time (> 4 months), it was not possible to characterize further the formed network.

II.6.4 Conclusions on the presented three components hybrid networks

Unfortunately we could recover suitable single crystals only for the two systems $[\text{Ag}(\text{C}_{14}\text{H}_6\text{N}_2\text{O}_4)_2][\text{C}_{10}\text{H}_{20}\text{N}_4]_2(\text{XF}_6) \cdot 2\text{MeOH}$ ($\text{X} = \text{P}, \text{As}, \text{Sb}$) and $\{[\text{Cu}(\text{C}_{14}\text{H}_6\text{N}_2\text{O}_4)_2][\text{C}_{10}\text{H}_{20}\text{N}_4]\} \cdot 2\text{H}_2\text{O}$, for the other **A+B+C** systems we obtained mostly amorphous powders and in some cases colloidal precipitates but the study of these precipitates is made difficult by the simultaneous presence of multiple phases. The difficulty of the work was generally increased by the great hydrolysis affinity of tectons **B**.

For both these two systems the H-bonding interaction mode adopted by the carboxylate with the bis-amidinium has been the bis-dihapto as expected. It is also interesting to notice that both obtained networks involve ligand 4,7-dcphen, this could be explained by the rigid, preorganized structure of the three aromatic rings that also favour packing through π -stacking, the ligand 4,4'-dcbpy has only two rings and the freedom degree along the C-C bond could disfavour the packing, concerning the 4,4'-dcBQ ligands, it is probably too bulky for optimal packing.

The copper network confirms the hypothesis that one of the main constraint for the formation of networks based on three-substituted octahedral metallatectons of the first row transition metal series $\text{M}(\text{II})$ (where $\text{M} = \text{Mn}, \text{Fe}, \text{Co}, \text{Ni}, \text{Cu}, \text{Zn}$) is the competition between oxygen and nitrogen for the formation of bond with the metal center.

II.7 General conclusions

In this work, we have developed and applied two different approaches to obtain hybrid organic-inorganic networks based on self-complementarity between bis-amidinium tectons (tecton **A**) and a carboxylate bearing N donor ligand (tecton **B**) and coordination bonds with metal **C**. Using the so called 'hierachical approach', we synthesised different metallatectons but the second step, the growth of single crystals with bis-amidinium tectons revealed to be highly difficult. Nevertheless, it was an opportunity to build a library of new mono-, di- and tri-substituted complexes based on transition metals and N donor ligands bearing one or two carboxylate groups at their periphery.

The second-used method, which is called the "one pot approach", has been more effective and allowed us to find good experimental conditions to overcome solubility problems and to obtain single crystals to perform a solid state study. We were here able to characterize 4 new H-bonded coordination networks, belonging to two distinguished families, demonstrating the possibility of using a three component system leading to hybrid networks. The long crystallisation time together with the scarce quantity of recovered crystals make difficult to use this synthetic approach for developing and studying the functional properties of these networks as was the initial purpose of this project.

Chapter III

Hybrid Networks based on Carboxylates Complexes

III.1 Coordination abilities of the used tectons

The incoming chapter concerns the employment of 2,9-dicarboxy-1,10-phenanthroline and 6,6'-dicarboxy-2,2'-bipyridine as tectons for the construction of coordination and hydrogen bonded networks. With respect to the tectons introduced in chapter II, these two tectons offer different and peculiar coordination ability. For that reason, they are described separately here. Both ligands, depicted in figure 1, differ from the ligands described in §II.3.3 for the position of the carboxylic groups on the pyridyl ring. The substitution in *ortho*-position opens the way for the participation of the carboxylate moiety to the binding of metal centres in conjunction with N atoms.

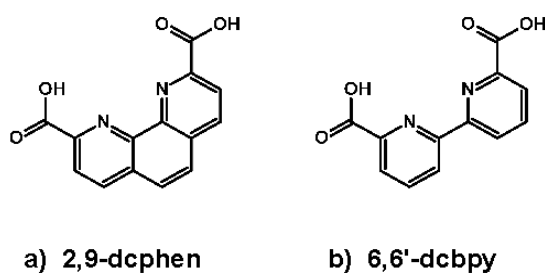


Figure 1. The ligands a) 2,9-dicarboxy-1,10-phenanthroline [2,9-dcphen] and b) 6,6'-dicarboxy-2,2'-bipyridine [6,6'-dcbpy] used as tectons for coordination complexes and networks building.

Compared to [6,6'-dcbpy], the phenanthroline based ligand [2,9-dcphen], owing to the loss of the rotational freedom, is more rigid and furthermore shows a greater propensity to form π - π interactions. For 2,9-dcphen, the comparative study by Melton, VanDerveer and Hancock¹ concerning the binding constants ($\log K_1$) with a variety of metal ions, shows enhanced thermodynamic stability compared to similar ligands without the reinforcing aromatic scaffold.

The multiple coordination ability of both ligands is depicted in figure 2. The versatility of the coordination ability of the carboxylate group suggests also that, even when engaged in binding metal centres, the carboxylate group remains capable of interacting with other molecules, for example, through hydrogen bonding.

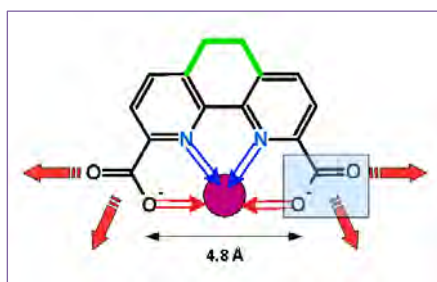


Figure 2. Coordination abilities of ligands 6,6'-dcbpy and 2,9-dcphen towards metallic ions.

¹ D. L. Melton, D. G. VanDerveer, R. D. Hancock, *Inorg. Chem.*, **2006**, 45, 9306-9314

III.2 Literature background

The interest in compounds bearing O-alkoxy/N-donor (COOR/N-bpy) ligands arises from different domains and many complexes have been prepared with different metals. Such ligands are used for the binding of oxophilic metals such as lanthanides for biomedical purposes², or for complexation of heavy metals (Pb, Cd, and Hg) for water and soil remediation. Alkoxy-carbonyl ruthenium complexes have been prepared for photo-electrochemical application³ or as anti tumor mimics⁴. When coupled with alkaline or alkaline-earth metal cations (Rb, Cs, Ca, Ba), these ligands are intended for transportation in biological systems. These general applications concern all the ligands having the same carbon skeleton of 6,6'-dcbpy and 2,9-dcphen, among them the most used ones are the ester alkoxy-carbonyl (COOR) derivatives exhibiting higher solubility. The examples that will be detailed herein are more strictly related to the carboxylic acid derivatives.

III.2.1. Coordination complexes and networks based on 6,6'-dcbpy

To the best of our knowledge, the only known metal complexes based on 6,6'-dcbpy for which the structure was obtained by X-ray diffraction methods on single crystal are those containing lanthanides Eu(III), Tb(III) and Gd(III) cations showing luminescent properties⁵. Ru(II/IV)⁶ and Cd(II)⁷ complexes have been studied as Gd(III) mimics for application in magnetic resonance imaging. In table 1 are gathered the known structures of metal complexes between 6,6'-dcbpy and metal ions collected from the CSD data bank. Although all complexes lead to the formation of coordination networks, only the coordination sphere around the metal is illustrated. The metal complexes based on Cd(II) and Tb(III) form molecular networks utilizing the multi-faceted coordination mode of carboxylate, as introduced in §III.1.

In order to present a complete view of the available crystallographic data, we also show structures of the tetra-substituted ligand 4,4',6,6'-tetracarboxy-2,2'-bipyridine [H₄-tcbpy]⁸ and 4,4'-dimethylcarboxy-6,6'-dicarboxy-2,2'-bipyridine [Me₂-tcbpy].⁹

² Blake, R. C., II; Li, X.; Yu, H.; Blake, D. A.; *Biochem.*, **2007**, *46*, 1573-1586

³ T.-J. J. Kinnunen, M. Haukka, T. A. Pakkanen; *J. Organomet. Chem.*, **2002**, *654*, 8-15

⁴ P. I. Anderberg, M. M. Harding, I. J. Luck, P. Turner; *Inorg. Chem.*, **2002**, *41*, 1365-1371

⁵ a) J. C. G. Bünzli, L. J. Charbonnière, R. F. Ziessel; *J. Chem. Soc., Dalton Trans.*, **2000**, 1917-1923; b) V.-M. Mikkala, M. Kwiatkowski, J. Kankare, H. Takalo; *Helvetica Chim. Acta*, **1993**, *76*, 893-898

⁶ a) P. Homanen, M. Haukka, M. Ahlgren, T. A. Pakkanen; *Inorg. Chem.*, **1997**, *36*, 3794-3797; b) L. Duan, A. Fischer, Y. Xu, L. Sun; *J. Am. Chem. Soc.*, **2009**, *131*, 10397-10399

⁷ J. C. Knight, A. J. Amoroso, P. G. Edwards, L.-L. Ooi; *Acta Cryst.* **2006**, *E62*, m3306-m3308

⁸ N. R. Kelly, S. Goetz, S. R. Batten, P. E. Kruger, *CrystEngComm*, **2008**, *10*, 1018-1026

⁹ N. R. Kelly, S. Goetz, S. R. Batten, P. E. Kruger, *CrystEngComm*, **2008**, *10*, 68-78

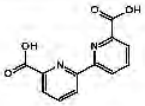

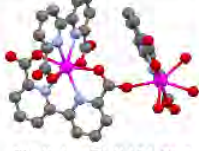
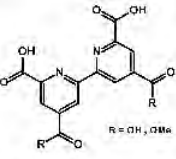
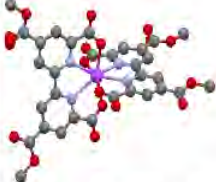

	Cd(II)	Tb(III)	Yb(III), Gd(III), Sm(III)	Ba(II)
 <p>6,6'-dcbpy</p>	 <p>$\{[\text{Cd}(\text{L})(\text{H}_2\text{O})_2]_n \cdot 2(\text{H}_2\text{O})\}$</p>	 <p>$[\text{Tb}(\text{L})_2-\mu-\text{Tb}(\text{L})(\text{H}_2\text{O})_3]_n \cdot 2(\text{H}_2\text{O}) \cdot 2(\text{MeOH})$</p>		
 <p>R=OH, [H_4-tcbpy] R=OMe, [Me_2-tcbpy]</p>			 <p>$\{[\text{Ln}(\text{Me}_2\text{-tcbpy})_2]_n \cdot (\text{H}_2\text{O})_n \cdot \text{MeOH} \cdot \text{H}_2\text{O}\}$ n=1,2</p>	 <p>$[\text{Ba}_2-\mu-\text{Tb}(\text{H}_4\text{-tcbpy})(\text{H}_2\text{O})_2]$</p>

Table 1. Gallery of different complexes obtained with 6,6'-dcbpy and Cd (II) (ref.7), Tb (III) (ref. 5a), Me₂-tcbpy with lanthanides and Ba (II) (ref.9) (for clarity only the metal coordination sphere is depicted).

In all cases, the ligand is tetradentate and coordinates as [N,N-O,O], the completion of the coordination sphere depends on the metal. The lanthanides Yb(III), Gd(III), Sm(III) are usually octa-coordinated by two ligands, instead, the structure based on Tb(III) presents a dimer in which one Tb atom is octa-coordinated, surrounded by two ligands, and the second only hepta-coordinated surrounded by one ligand and three water molecules; the final network is H-bonded through interstitial solvent molecules.

With Cd(II) and Ba(II) coordination networks are formed. Cd(II) is hepta-coordinated, the coordination sphere is composed of the [N,N-O,O] set offered by the ligand and completed by two water molecules and one oxygen from a neighbouring carboxylate group. Finally, Ba(II) presents an octa-coordinated sphere and is surrounded by one ligand and four other oxygen atoms belonging to the neighbour carboxylate units.

For 2,9-dcphen, the same search and comparison are presented here below for discrete metal complexes and networks.

III.2.2 Coordination complexes and networks based on 2,9-dcphen

The coordination with 2,9-dcphen is richer than with 6,6'-dcbpy. The ligand 2,9-dcphen has been explored for complexation of lanthanides^{1,10}, particularly europium and terbium for their luminescent properties, and also uranium.¹¹ Furthermore, 2,9-dcphen was used for the binding of the first row transition metals such as Cr(III)¹², Fe(II/III)¹³, Co(II)¹⁴, Ni(II)¹⁵, Cu(II)¹⁶ and alkaline-earth Mg(II)¹⁷ and Ba(II)¹⁸ metal cations. With all these metals, polymeric species based on coordination and/or hydrogen bond were obtained displaying a large variety of coordination geometry, although with some recurrence, around the metal. In the following, we will report on some representative examples and we will point out the coordination arrangement around the metals proving the versatility of the ligand coordination ability.

III.2.2.1 Networks based on metal + ligand

In table 2 are illustrated some examples of coordination complexes containing 2,9-dicarboxy-1,10-phenanthroline for which XRD structures are available (for corresponding references see the paragraph above).

¹⁰ a) Harbuzaru, B. V.; Corma, A.; Rey, F.; Jorda, J. L.; Ananias, D.; Carlos, L. D.; Rocha, J.; *Angew. Chem., Int. Ed.*, **2009**, *48*, 6476-6479, S6476/1-S6476/9 ; b) Fan, L.-L.; Li, C.-J.; Meng, Z.-S.; Tong, M.-L.; *Eur. J. Inorg. Chem.*, **2008**, *25*, 3905-3909 ; c) Coates, J.; Gay, E.; Sammes, P. G.; *Dyes and Pigments*, **1997**, *34*, 195-205 ; d) P. G. Sammes G. Yahioğlu, G. Yearwood, *J. Chem. Soc., Chem. Commun*, **1992**, 1282-1283 ; e) Templeton, E., F. Gudgin, Pollak, A., *J. Luminesc.*, **1989**, *43*, 195-205 ; f) Evangelista, R. A.; Pollak, A., *Eur. Pat. Appl.*, **1986**, EP 171978 A1 19860219

¹¹ Dean, N. E.; Hancock, R. D.; Cahill, C. L.; Frisch, M.; *Inorg. Chem.*, **2008**, *47*, 2000-2010 ; b) Blake, R. C., II; Li, X.; Yu, H.; Blake, D. A., *Biochem.*, **2007**, *46*, 1573-1586 ; c) Blake, R. C., II; Pavlov, A. R.; Khosraviani, M.; Ensley, H. E.; Kiefer, G. E.; Yu, H.; Li, X.; Blake, D. A.; *Bioconjugate Chem.*, **2004**, *15*, 1125-1136

¹² A. Moghimi, R. Alizadeh, M. C. Aragoni, V. Lippolis, H. Aghabozorg, P. Norouzi, F. Isaia, S. Sheshmani, *Z. Anorg. Allg. Chem.*, **2005**, *631*, 1941-1946

¹³ a) N. J. Williams, N. E. Dean, D. G. VanDerveer, R. C. Luckay, R. D. Hancock; *Inorg. Chem.*, **2009**, *48*, 7853-7863; b) E. Koenig, G. Ritter, K. Madeja; *J. Inorg. Nuclear Chem.*, **1981**, *43*, 2273-2280

¹⁴ a) A. Moghimi, R. Alizadeh, A. Shokrollahi, H. Aghabozorg, M. Shamsipur, A. Shokravi; *Inorg. Chem.*, **2003**, *42*, 1616-1624 ; b) S. Sheshmani, H. Aghabozorg, F. M. Panah, R. Alizadeh, G. Kickelbick, B. Nakhjavan, A. Moghimi, F. Ramezanipour, H. R. Aghabozorg, *Z. Anorg. Allg. Chem.*, **2006**, *632*, 469-474

¹⁵ Y.-B. Xie, J.-R. Li, X.-H. Bu, *J. Mol. Struct.*, **2005**, *741*, 249-253

¹⁶ A. Moghimi, R. Alizadeh, H. Aghabozorg, A. Shokravi, M. C. Aragoni, F. Demartin, F. Isaia, V. Lippolis, A. Harrison, A. Shokrollahi, M. Shamsipur; *J. Mol. Struct.*, **2005**, *750*, 166-173

¹⁷ K.-M. Park, I. Yoon, J. Seo, Y. H. Lee, S. S. Lee; *Acta Crystallogr. Sect. E*, **2001**, *57*, m154-m156

¹⁸ a) C. J. Chandler, R. W. Gable, J. M. Gulbis, M. F. Mackoy, *Aus. J. Chem.*, **1988**, *41*, 799-805 ; b) C. J. Chandler, L. W. Deady, J. A. Reiss, *Aus. J. Chem.*, **1988**, *41*, 1051-1061

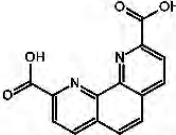
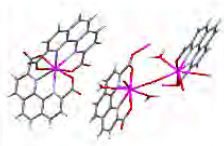
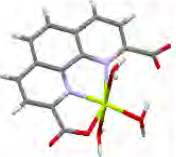
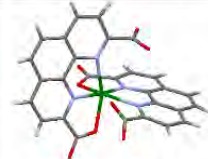
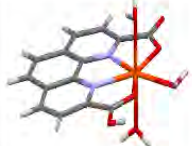
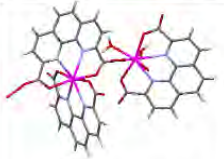

	Eu(III)	Ni(II)	Co(II),Cu(II),Cr(III)	Fe(III)
 2,9-dcphen	 $[Eu_3(L)_2(OH)(H_2O)_4] \cdot 2(H_2O)$	 $[Ni(L)(H_2O)_3] \cdot (H_2O)$	 $\{[B_2]^{2+}[Cu/Co/Cr(L)_2]^{2-}\}_n \cdot n(H_2O)$ $\{[B]^{+}[Cr(L)_2]^{+}\} \cdot 5(H_2O)$	 $[Fe(L-H_{1/2})(H_2O)_3]^{1.5+}$
	Eu(III), Tb(III)		Cu(II)	
	 $[Eu_3(L)_3(H_2O)_2] \cdot 3(H_2O)$		 $[Cu(L)_2(H_2O)_2] \cdot 2(H_2O)$	

Table 2. Gallery of different complexes obtained with 2,9-dcphen and various metals. Eu (above - ref. 10a), Eu/Tb (below - ref. 10b), Ni (ref. 15), Co (ref. 14), Cr (ref. 12), Cu (above - ref.16), Cu (below - ref. 10b) and Fe (ref. 13a).

Eu and Tb are (as in the case of 6,6'-dcbpy) octa-coordinated with a dodecahedral geometry. In all cases, the ligand behaves as tetradentate [N,N-O,O] set, the metal coordinates two ligands or one ligand plus two water molecules plus two carboxylates from the neighbouring molecules. This mixed coordination is forced by the oxidation state of the metal (+3) to form, on the whole, neutral dimeric complexes.

The nickel is smaller and prefers an octahedral coordination geometry, its coordination sphere includes one ligand [N,N-O] and three H₂O molecules. The case of iron (III) is more complicated since the complex is cationic; the metal is hepta-coordinated with almost regular pentagonal bipyramid geometry, the ligand is tetradentate [N,N-O,O], one carboxylate is completely deprotonated and the second one shares his proton with the neighbouring molecule; a perchlorate anion balances the charge. The coordination sphere is completed by water molecules.

The geometry assumed by Co (II), Cu (II) and Cr (III) (Table 2, upper case) is octahedral, it is interesting to know the presence of a base (B) as H bond acceptor in the network. The ligand behaves as tridentate [N,N-O] unit, both carboxylate groups are deprotonated, leading to an anionic complex. In table 2 (bottom), a second geometry assumed by the copper (II) in the absence of base is presented. In this case, the complex forms a neutral dimer and copper (II) is penta-coordinated with a trigonal bipyramid geometry completed as usual by water molecules.

All these complexes behave as building blocks and form hybrid molecular networks. The crystal structure of the networks based on cobalt, copper and chromium are particularly adapted to our purposes, being of the same type as the three

components networks presented in §II.2.3.2, and deserve a deeper analysis reported hereafter.

III.2.2.2 Networks based on metal + ligand + base

Moghimi and co-workers (ref. 12, 14, 16) described H-bonded networks involving the already presented ligands and additional bases (B). The networks have been constructed from a three components system: metal, ligand (2,9-dcphen) and base such as guanidine (GH) or diaminopyridine (pyda). We will examine in particular the system based on Co(II) and guanidinium, as H-bond donor, that leads to a H-bonded network of formula: $[\text{Co}(\text{L})_2](\text{GH})_2 \cdot 4(\text{H}_2\text{O})$ (ref. 14b).

Each bi-substituted, octahedral complex (already described in the previous §) is surrounded by five guanidinium cations [Fig. 3a] connecting the network *via* both mono- and di-hapto type hydrogen bonding (see figure 3b). The unit cell is constituted basically of two cobalt complexes and the crystal lattice is formed by the repetition of this 'dimeric' entity connected *via* H-bonds through the lattice water molecules, as shown in figure 3c.

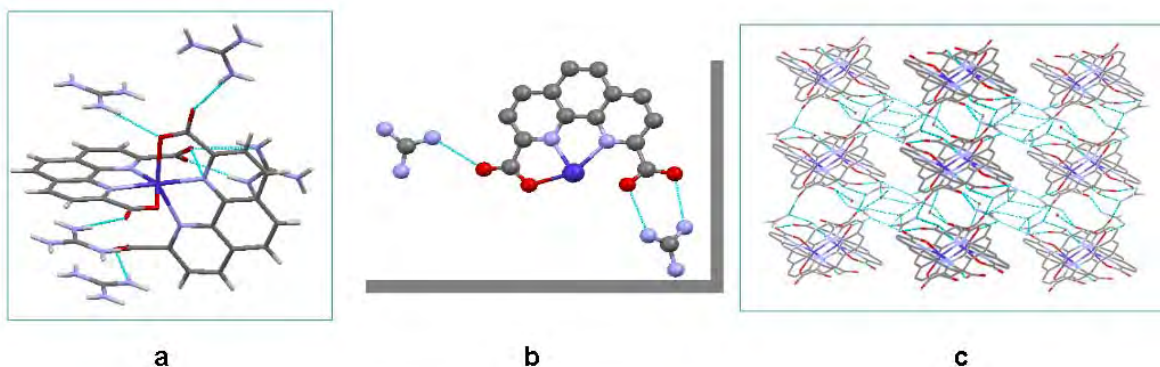


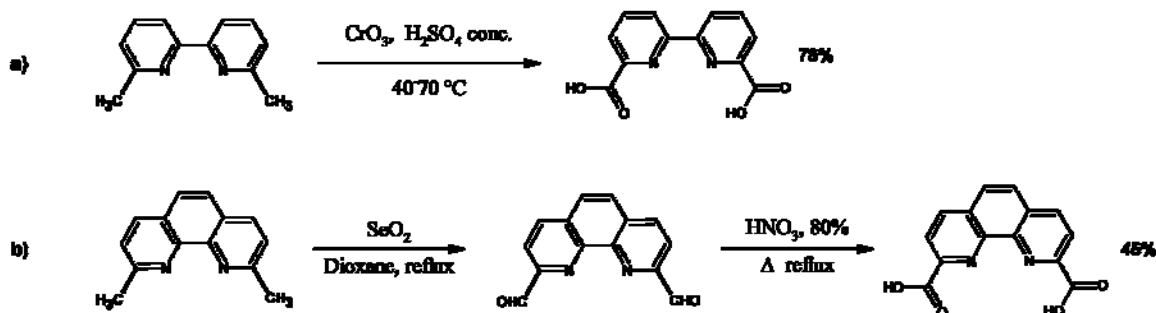
Figure 3. Crystal structure of $[\text{Co}(\text{L})_2](\text{GH})_2 \cdot 4(\text{H}_2\text{O})$. a) Coordination sphere of the complex surrounded by five GH molecules. b) Particular of the coordination and hydrogen bond pattern and (c) the whole crystal packing.

In this chapter we will investigate the coordination abilities of both ligands towards transition metals in particular Cu(I) and (II) and Zn(II), that can adopt tetrahedral, but also octahedral or pyramidal square based geometry. Finally, the assemblies formed with Ag(I), well known for its coordination versatility, will be presented.

III.3 Used tectons for coordination complexes and networks formation

III.3.1 Ligand synthesis

Both ligands 2,9-dicarboxy-1,10-phenanthroline [2,9-dcphen] and 6,6'-dicarboxy-1,10-bipyridine [6,6'-dcbpy] were synthesized according to literature procedures presented below.



Scheme 1. Synthetic route for the synthesis of 6,6'-dcbpy (a) and 2,9-dcphen (b).

The synthesis of 6,6'-dcbpy was carried out following the classical oxidation with CrO_3 in concentrated sulphuric acid that, among all the methods proposed in literature¹⁹, seemed to be the most appropriate one in term of yield.

The synthesis of 2,9-dcphen was carried out following the procedure reported by Chandler, Deady and Reiss²⁰, requiring two oxidation steps: first with SeO_2 to obtain the diformyl derivate and then with concentrated nitric acid.

III.3.2 Structural characterization

The targeted ligands were fully characterized by conventional methods (see Experimental part), confirming the literature results, and by X-ray diffraction on single crystal (see Annexes).

For 2,9-dcphen, the di-acid was dissolved in water in presence of organic bases triethylamine or tributylamine; suitable single crystals for X-ray diffraction were obtained both in the case of the hydrated form and as tributylamine and water adducts.

Here will be described the crystal structure of general formula $[(2,9\text{-dcphen})_2] \cdot 5(\text{H}_2\text{O})$ [Structure XXVIII in the Annexes]. As shown in figure 4a, the compound forms a dimer *via* direct hydrogen bonding between two carboxylic acid groups ($d_{\text{O} \cdots \text{O}} = 2.52 \text{ \AA}$) of two neighbouring 2,9-dcphen molecules while all other

¹⁹ a) J. C. G. Bünzli, L. J. Charbonnière, R. F. Ziessel ; *J. Chem. Soc., Dalton Trans.*, **2000**, 1917-1923 ; b) V.-M. Mukkala, M. Kwiatkowski, J. Kanakare, H. Takalo, *Helv. Chim. Acta*, **1993**, 76, 893-899 , c) E. Buhleier, W. Wehner, F. Vögtle, *Chem. Ber.*, **1978**, 111, 200-204

²⁰ C. J. Chandler, L. W. Deady, J. A. Reiss, *J. Heterocyclic Chem.*, **1981**, 18, 599-601

intermolecular hydrogen bonding connections are mediated by water molecules. The [COO/COOH] moiety presents the typical distances for carboxylates $1.24 \leq d_{C-O} \leq 1.27$ Å. Hydrogen bonding distances between 2,9-dcphen and the connected water molecules range between 3.03-2.96 Å for d_{N-O} and between 2.84 and 2.68 Å for d_{O-O} .

Figure 4 illustrates two views of the crystal packing showing an alternation of organic and water layers (see figure 4c) with the stacking ($d_{\pi-\pi} = 3.5-3.7$ Å) in head-to-tail fashion of consecutive phenanthroline units (figure 4b, along the z axis).

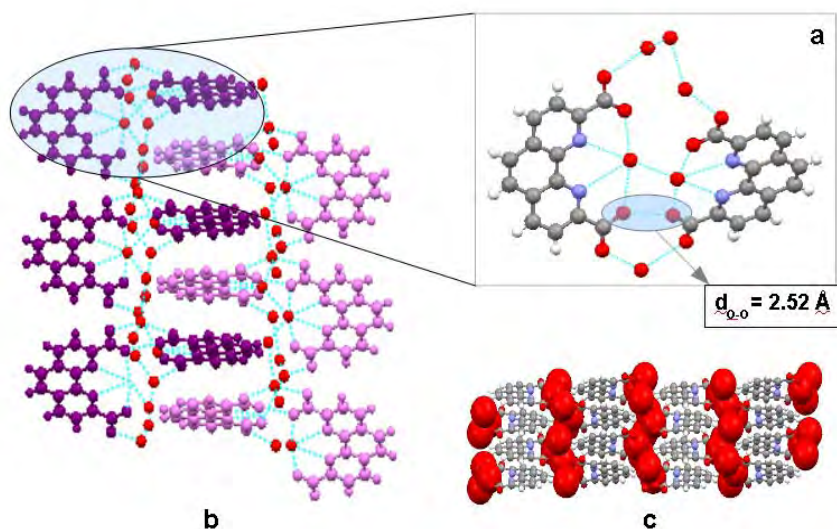


Figure 4. For $[(2,9\text{-dcphen})_2] \cdot 5(\text{H}_2\text{O})$: a) dimeric unit of 2,9-dcphen formed via direct hydrogen bonding between carboxylate, b) π - π stacking interactions along z axis, c) crystal packing view along z axis.

For 6,6'-dcbpy, instead, the crystal structure was obtained upon cooling to room temperature followed by slow evaporation of a hot, saturated DMSO solution of the ligand. The colourless single crystals suitable for X-ray diffraction have the general formula $[(6,6'\text{-dcbpy})_2] \cdot 2(\text{DMSO})$ [Structure XXIX in the Annexes] and the crystal structure is illustrated in figure 5.

As we can see in figure 5b and 5c, the molecules are packed in a way to form linear arrays, the latter are connected *via* (CH...O) hydrogen bonds between the aromatic protons of bipyridine and the oxygen atoms belonging to the solvent or to the carboxylic acid moieties ($d_{\text{CH-O}} = 2.60\text{-}2.38$ Å) (Fig. 5a). Hydrogen bonding also occurs between carboxylic acid groups and dimethylsulfoxide solvent molecules ($d_{O-O} = 2.59\text{-}2.54$ Å; $d_{\text{OH-O}} = 1.75$ Å).

The molecular arrays are stacked to form tilted planes with distances of 4.5 Å implying π -stacking interaction (Fig. 5d). However, the packing is mainly driven by short contacts with DMSO molecules which ensure contacts both within each layer and between them.

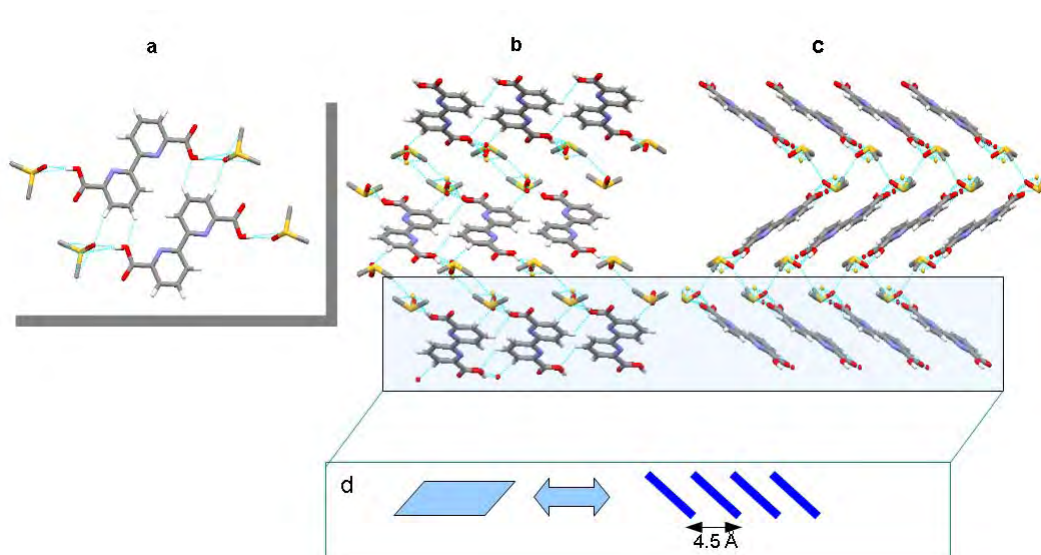


Figure 5. Crystal packing for $\{[(6,6'\text{-dcbpy})_2] \cdot 2(\text{DMSO})\}$: a) hydrogen bonding pattern between ligand and DMSO; b) packing view along the y axis and c) along x axis. In d: schematic representation of the 1D array formed by the bipyridine molecule (trapezium) and the derived plane with π -stacking distance.

III.4 Hybrid Networks based on Carboxylates Complexes

III.4.1 Context

As pointed out in section § III.1, many different combinations may be explored using these two ligands and metals centres possessing different characteristics such as lanthanides, alkaline, alkaline-earth, transition metal, etc. Both [6,6'-dcbpy] and [2,9-dcphen] ligands exhibit preferences for hard, borderline and soft metals. Taking into account distance criteria (4.8 Å between the two O atoms of the two carboxylate moieties, Fig. 2) both ligands may accommodate large cations. Our choice was restricted to three: Zn (II), Cu (I/II) and Ag (I) cations which are borderline-soft metals forming more labile species and offering more flexible coordination sphere. Furthermore, to the best of our knowledge, the complexation of Zn and Ag cations by ligands [6,6'-dcbpy] and [2,9-dcphen] has not been explored to date at the solid state.

Because our interest in the generation of hybrid hydrogen bonded networks composed of organic tectons, metal cations and alkaline anionic species, as pointed out in the section III.2.2.2, many crystallisation attempts were performed both in the presence and in the absence of a base. Different organic bases such as BAD23 (see Chapter II), triethylamine, tributylamine and methylamine were tested. The presence of the base is generally required for the solubilisation of the organic tecton in a aqueous medium.

III. 4.1.1 Network summary

Mixing, under self-assembly conditions (see Annexe A), the ligand and the metal (Zn(II), Cu(I or II) and Ag(I)) salts, different hybrid hydrogen bond/coordination networks, illustrated in table 3, were obtained. Therein, we present the structural analysis of these architectures.

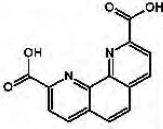

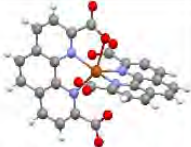


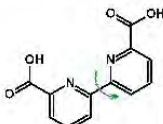


	Zn(II)		Cu(II)		Ag(I)
 2,9-dcphen	 $[Zn(2,9-dcphen)(H_2O)_3] \cdot 2 H_2O$	 $[Zn(2,9-dcphen)_2] \cdot MeOH \cdot H_2O$	 $[Cu(2,9-dcphen)(H_2O)_3] \cdot H_2O$	 $[Ag(2,9-dcphen)_6] \cdot HPF_6$	
 6,6'-dcbpy	 $[Zn(6,6'-dcbpy)(H_2O)_2]$	 $\{[Zn(6,6'-dcbpy)_2](Et_3N)_4\} [6,6'-dcbpy] \cdot MeOH \cdot 11 H_2O$			

Table 3. Summary of networks obtained upon combining Zn(II), Cu(II), Ag(I) metal salts with either [6,6'-dcbpy] or [2,9-dcphen].

III.4.2 Structural Analysis

III.4.2.1 Hybrid networks based on zinc(II)

For both combinations of 2,9-dcphen and 6,6'-dcbpy with zinc salts were obtained single crystals suitable for X ray diffraction with formula $[Zn(6,6'-dcbpy)(H_2O)_2]$ [Structure XXXII in the Annexes] and $\{[Zn(2,9-dcphen)(H_2O)_3] \cdot 2(H_2O)\}$ [Structure XXX in the Annexes]. In both cases the crystals were obtained *via* slow diffusion of a methanol solution of $Zn(SiF_6)_2$ in a water-alcoholic solution of the ligand dissolved in presence of a base, usually triethylamine, with M/L ratio of 1:1. The zinc salt $Zn(SiF_6)_2$ has been chosen because it has been successfully used in the group. Isostructural crystals with both ligands were also obtained starting from $Zn(BF_4)_2$. However, in this case, the crystal quality appeared to be rather poor indicating an influence of the counter ion on the crystallization process.

In figure 6 are compared the coordination geometry around the zinc cation complexed by each ligands. Unexpectedly, the resulting complexes exhibit different geometries. In both cases, the ligand behaves as a tetradentate unit offering the [N,N-O,O] set with two O atoms belonging to the carboxylate units and two N atoms of the bipyridine ring. The coordination sphere around the metal centre is completed by two or three water molecules.

In the case of $[\text{Zn}(6,6'\text{-dcbpy})(\text{H}_2\text{O})_2]$, the Zn cation assumes a distorted octahedral geometry, the water molecules are not perpendicular to the plane sketched by the ligand but bent ($\theta = 129.4^\circ$) (see figure 6a). For $[\text{Zn}(2,9\text{-dcphen})(\text{H}_2\text{O})_3]$, the geometry is a regular pentagonal bipyramid and Zn is hepta-coordinated with three water molecules, one in the plane of the pyramid and the other two at the vertexes ($\theta = 176.9^\circ$) (see figure 6b).

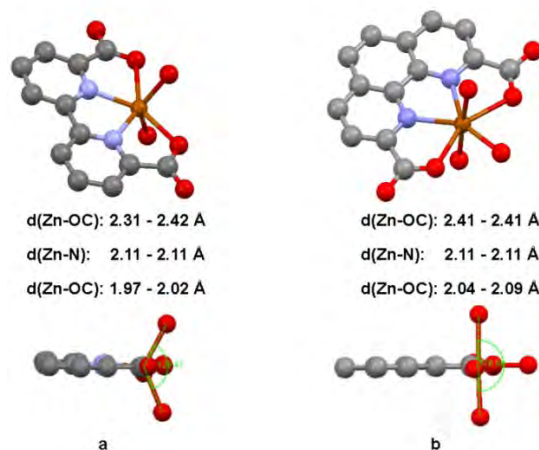


Figure 6. Coordination sphere around Zn(II) for (a) $[\text{Zn}(6,6'\text{-dcbpy})(\text{H}_2\text{O})_2]$ and (b) $[\text{Zn}(2,9\text{-dcphen})(\text{H}_2\text{O})_3]$.

Both metal complexes act as building units to form hydrogen bonded networks. Concerning $[\text{Zn}(6,6'\text{-dcbpy})(\text{H}_2\text{O})_2]$, it forms a two dimensional network *via* hydrogen bonding between water molecules bound to the metal and carboxylate units of the ligand. The C-O distances, in the 1.25-1.26 Å range, are typical for carboxylate implying the anionic nature of the ligand. Zn-O and Zn-N distances are given in figure 6.

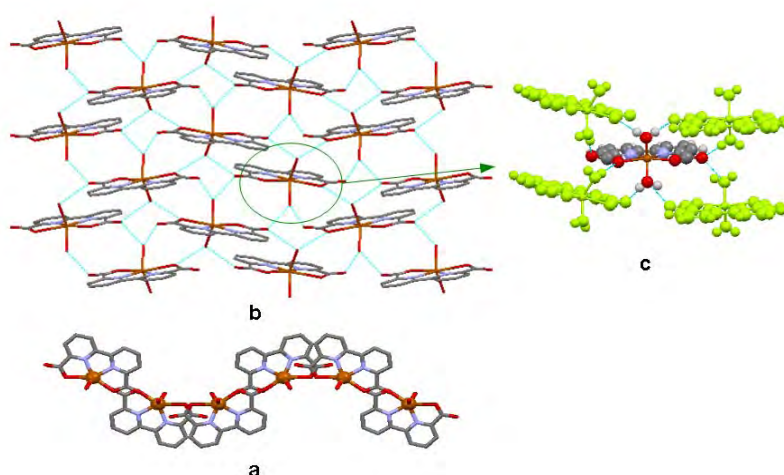


Figure 7. a) 2-D network formed by $[\text{Zn}(6,6'\text{-dcbpy})(\text{H}_2\text{O})_2]$, b) bi-dimensional sheet viewed along the x axis and c) hydrogen bonding motif.

Each complex is bound to four other molecules *via* hydrogen bonds through carboxylate-water interconnections (OC-O...H-OH) [Fig. 7c]. This connectivity leads to

a corrugated two dimensional sheet (see figure 7a (along z axis) and figure 7b (along the x axis)). The purity of the crystalline phase could not be checked by XRPD.

$\{[\text{Zn}(2,9\text{-dcphen})(\text{H}_2\text{O})_3]*2(\text{H}_2\text{O})\}$ crystallises with two water molecules and forms a 1-D network. Mono-dimensional chains are formed *via* hydrogen bonding between carboxylates ($d_{\text{C-O}} = 1.25 \text{ \AA}$) and water molecules located within the coordination sphere of the metal [Fig. 8a and b]; each chain is connected to the one below and the one above *via* hydrogen bonding with two water molecules located within the crystal lattice (shown in blue in Fig. 8c in order to distinguish from water molecules bound to the metal centre) leading to the formation of a 2-D sheet [Fig. 8c], O-O distances are in the 2.79-2.84 \AA range. There is also π -stacking between aromatic rings with interaromatic distance of 3.56 \AA .

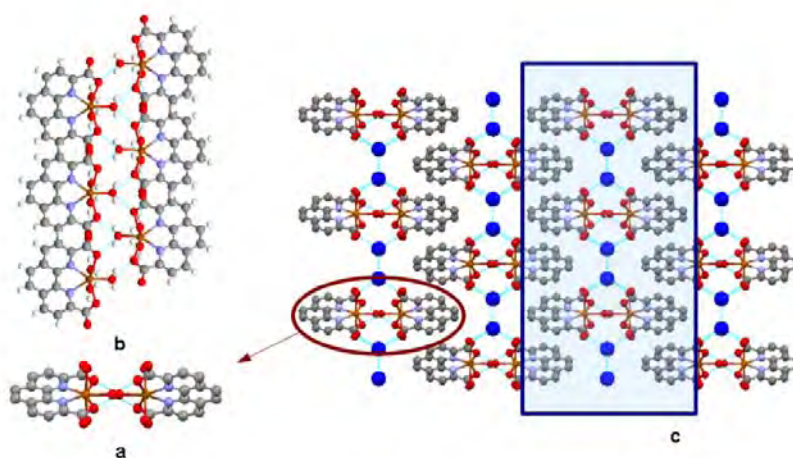


Figure 8. 3-D packing for $\{[\text{Zn}(2,9\text{-dcphen})(\text{H}_2\text{O})_3]*2(\text{H}_2\text{O})\}$. a) 1-D hydrogen bonded single chain (a) view along the x axis and (b) along the y axis. c) In the square is focused the interconnection between chains through water molecules.

Focusing on the 1-D chain, it appears that each complex binds four other molecules as well as four water molecules located in the second coordination sphere of the metal [Fig.9a]. Interactions between two carboxylate units $[\text{CO}\cdots\text{OC}]$ and between one carboxylate and one water located within the coordination sphere of Zn cation $[\text{CO}\cdots\text{HO}]$ are highlighted in figure 9b.

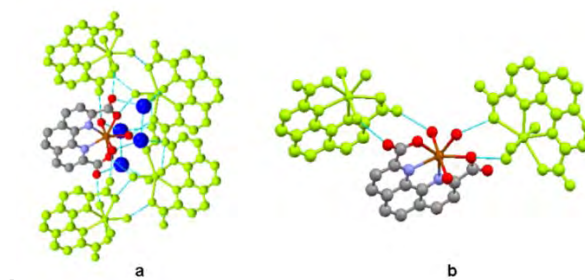


Figure 9. For $\{[\text{Zn}(2,9\text{-dcphen})(\text{H}_2\text{O})_3]*2(\text{H}_2\text{O})\}$: a) the complex surrounded by four other molecules and four lattice solvent molecules (in blue) and, in (b), a portion of the structure showing the H-bonding pattern.

The fit between the PXRD profile of the crystalline powder with the simulated one (from XRD data) [Fig. 10] demonstrates that the crystalline material is monophasic. The TGA analysis in the 30-130 °C range shows a weight loss between 30-70 °C corresponding to 3.5 water molecules. PXRD measurements on the TGA sample (green line in figure 10) shows the loss of crystallinity and appearance of a second phase, probably corresponding to the reorganized dehydrated material.

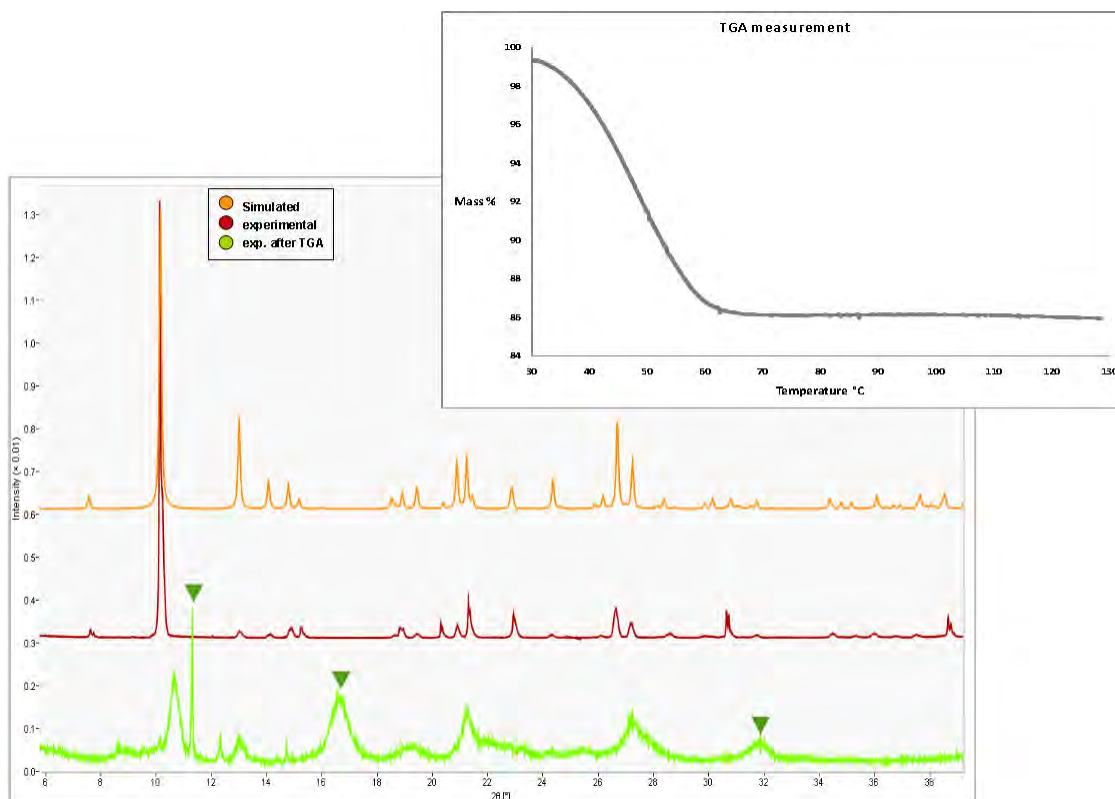


Figure 10. PXRD and TGA measurement for $\{[Zn(2,9\text{-dcphen})(H_2O)_3]*2(H_2O)\}$.

Using slow diffusion of a methanol solution of $Zn(SiF_6)_2$ into a water-alcoholic solution of ligand 6,6'-dcbpy dissolved in presence of triethylamine as base with a M/L ratio of 1:2, single crystals of general formula $\{[Zn(6,6'\text{-dcbpy})_2(Et_3N)_4][6,6'\text{-dcbpy}]\}_2*MeOH*(H_2O)_{11}$ were obtained (see structure XXXIII in the Annexes).

As it can be seen on figure 11a, the zinc atom is octa-coordinated and each ligand is tetradentate [N,N-O,O] as for the monosubstituted complex, the Zn-X distances are: 2.37; 2.37; 2.45; 2.50 Å for Zn-O and 2.14; 2.15; 2.18 and 2.18 Å for Zn-N.

Each ZnL_2 molecule is surrounded by four triethylamine molecules with which it interacts through [N...HO] hydrogen bonds thus leading to the dicationic species $[Zn(6,6'\text{-dcbpy})_2(Et_3N)_4]^{2+}$. Although, the position of protons can not be precisely determined, the C-O distance, in the range of 1.23 to 1.27 Å, is in between the one usually observed for carboxylate and carboxylic acid groups. This implies that protons are located on triethylamine as triethylammonium cations $(Et_3NH)^+$ and shared with anionic carboxylates. The N-O distances are 2.72, 2.73, 2.74 and 2.77 Å [Fig. 11b].

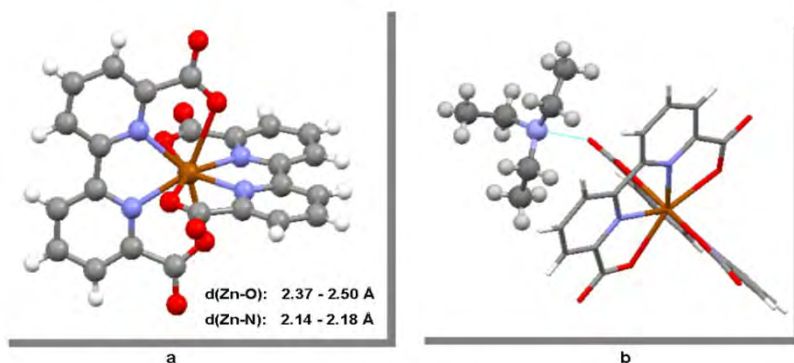


Figure 11. a) Coordination geometry around Zn and b) hydrogen bonding between the ligand and triethylamine in $\{[\text{Zn}(6,6'\text{-dcbpy})_2(\text{Et}_3\text{N})_4][6,6'\text{-dcbpy}]\}_2 \cdot \text{MeOH} \cdot 11(\text{H}_2\text{O})$.

The crystal packing is ensured by alternate 2-D layers formed by the cationic unit $[\text{Zn}(6,6'\text{-dcbpy})_2(\text{Et}_3\text{N})_4]^{2+}$ and the counterion $[6,6'\text{-dcbpy}]^{2-}$ (see figure 11a and b). Layers are interconnected by hydrogen bonds *via* solvent molecules, one methanol (grey in figure 12c) and eleven water molecules (red in figure 12c).

TGA experiment up to 400 °C, not presented here, shows a continuous decrease of weight corresponding to more than half of the total weight. This may be attributed to the loss of methanol, water and triethylamine.

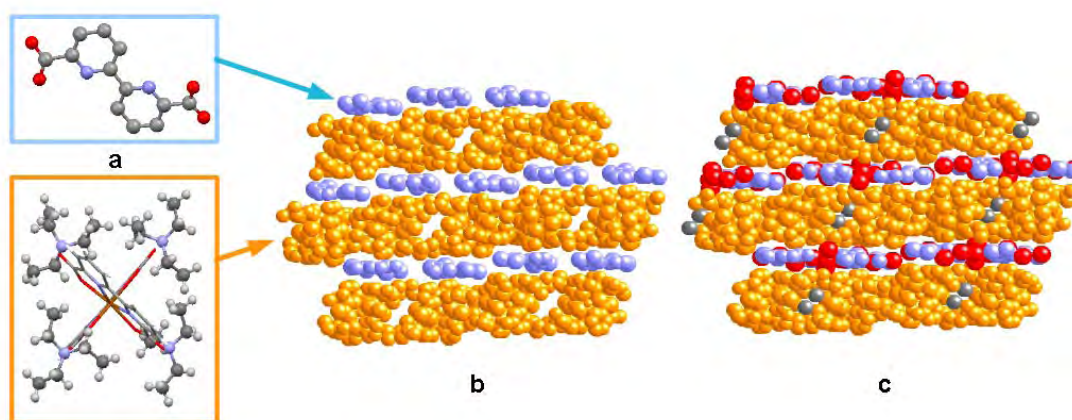


Figure 12. Crystal packing for $\{[\text{Zn}(6,6'\text{-dcbpy})_2(\text{Et}_3\text{N})_4][6,6'\text{-dcbpy}]\}_2 \cdot \text{MeOH} \cdot 11(\text{H}_2\text{O})$ view along the *x* axis showing a) and b) the alternation of cations $[\text{Zn}(6,6'\text{-dcbpy})_2(\text{Et}_3\text{N})_4]^{2+}$ and anions $[6,6'\text{-dcbpy}]^{2-}$ and c) the localisation of solvent molecules.

The complex $[\text{Zn}(2,9\text{-dcphen})_2] \cdot \text{MeOH} \cdot \text{H}_2\text{O}$ has been instead prepared upon slow diffusion of a methanol solution of ZnSiF_6 into a DMF solution of 2,9-dcphen (see structure XXXI in the Annexes).

In contrast with the previous structures, Zn cation is pentacoordinated adopting a distorted trigonal bipyramid geometry. Its coordination sphere is composed of one phenanthroline molecule acting as a [N,N] bidentate ligand and the other behaving as a [N,N-O] tridentate site. The Zn-X and Zn-O distances are 2.02; 2.07; 2.09; 2.19 Å and

2.30; 2.59; 2.78; 2.84 Å respectively (see figure 13a). The latter indicate a rather loose Zn-O bond.

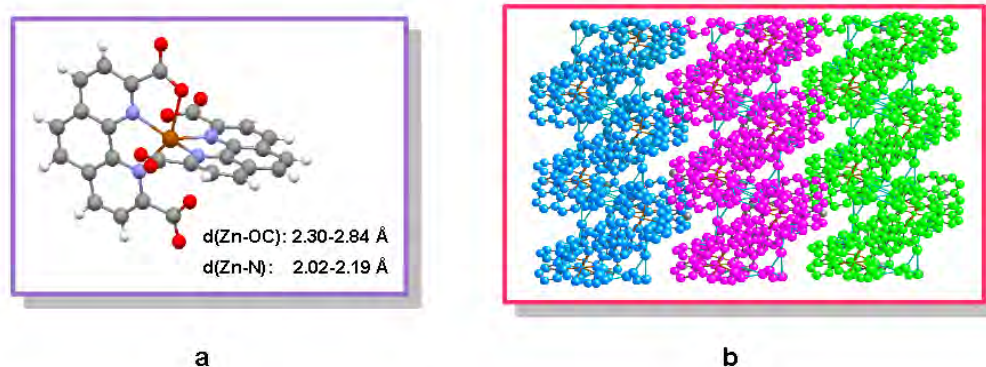


Figure 13. a) Coordination geometry around Zn and b) crystal packing view perpendicular the plane [0.1.1] for $[Zn(2,9-dcphen)_2] \cdot MeOH \cdot H_2O$.

The quality of the crystal data was not good enough to properly estimate the position of hydrogen atoms, however, one may suppose they are shared among the four $[COO^-]$ groups. The C-O distance varies between 1.18 and 1.28 Å. $[Zn(2,9-dcphen)_2]$ complexes form a wavy sheet through hydrogen bonds occurring between carboxylate and carboxylic acid moieties $[COO \cdots HOOC]$ with O-O distances (d_{O-O}) in the 2.43-2.45 Å range. Consecutive planes, interconnected by methanol and water molecules, are shown in figure 13b using different colours. Owing to the rather small quantity of the compound prepared, unfortunately, it was not possible to check the purity of the phase by PXRD.

Although in the case of zinc, both complexes formed with 6,6'-dcbpy and 2,9-dcphen could be structurally studied in the crystalline phase, in the case of copper and silver, only structures with 2,9-dcphen could be investigated. These structures are commented here after.

III.4.2.2 Hybrid network based on Copper(II)

Starting from a mixture of the copper salt $[Cu(I)(CH_3CN)_4]PF_6$, the ligand 2,9-dcphen and triethylamine as base, green crystals of general formula $\{[Cu(II)(2,9-dcphen)(H_2O)]_2 \cdot 2(H_2O)\}$ were obtained and analysed using X ray diffraction on single crystal. In this case, no base was found in the crystal lattice. Furthermore, due to air oxidation of copper resulting from the crystallisation conditions (evaporation at room temperature, see structure XXXIV in the Annexes), Cu(II) was found to be the metallic partner.

In the crystal, the complex forms a dimeric unit, each copper is penta-coordinated with a square pyramid geometry. 2,9-dcphen acts as a tri-dentate [N,N-O] ligand and the coordination sphere around Cu(II) is completed by one oxygen atom of the

carboxylate moiety coordinated to the neighbouring copper complex and one oxygen atom belonging to a water molecule occupying the apical position [Fig. 10a].

The C-O distances of the carboxylate groups range from 1.28 to 1.22 Å implying that one of the two units shows a more enhanced double bond character. The pyramid type geometry adopted by the metal centre is deformed with a Cu-O apical distance of 2.17 Å (see figure 14) and Cu-X distances within 1.90-2.15 Å range. The XCuY angles are different ($\text{NCuN} = 79.5^\circ$, $\text{OCuO} = 99^\circ$ and $\text{NCuO} = 78^\circ$ and 101°). The square base of both pyramids is distorted and the apical positions for both complexes are tilted by an angle in the 96.7° - 99.6° range [Fig. 14a].

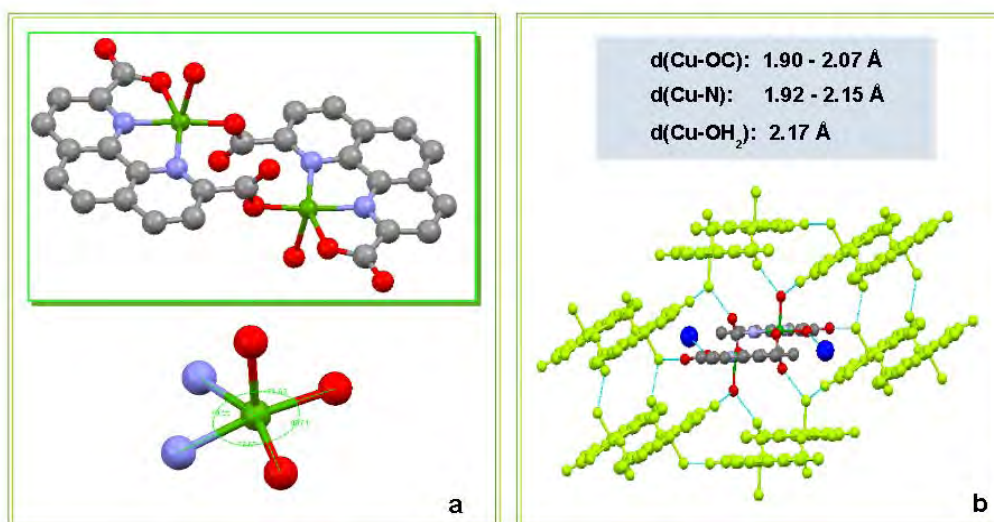


Figure 14. In $\{[\text{Cu}(\text{II})(2,9\text{-dcphe}n)(\text{H}_2\text{O})]_2 \cdot 2(\text{H}_2\text{O})\}$: (a) geometry around copper (II) metal cores and b) interconnection of dimers by hydrogen bonding.

In the crystal, each dimer is connected *via* hydrogen bonds to six other molecules (coloured in green in figure 14b) with $[\text{O}\cdots\text{O}]$ and $[\text{OH}\cdots\text{O}]$ distances in the 2.72-2.77 Å and 1.88-2.00 Å range respectively. The interconnection of dimers leads to the formation of a two dimensional network with a crenellated profile as shown in figure 15a and b. The wavy sheets are intersected and interact through stacking interactions between phenanthroline rings with an average distance of ca 3.65 Å (Figure 15c).

The crystal also contains two lattice water molecules (O atoms in blue on figure 14b in order to be distinguished from carboxylate O atoms). It is worth noting that water molecules are hydrogen bonded within the second coordination sphere of the complex [$d_{\text{O}\cdots\text{O}} = 3.00 \text{ \AA}$; $d_{\text{OH}\cdots\text{O}} = 2.80 \text{ \AA}$] and are not involved in the connectivity pattern of the network. These second sphere water molecules are rather located inside the deformed channels of the network, the channels exhibit a radius around 6.4-6.6 Å.

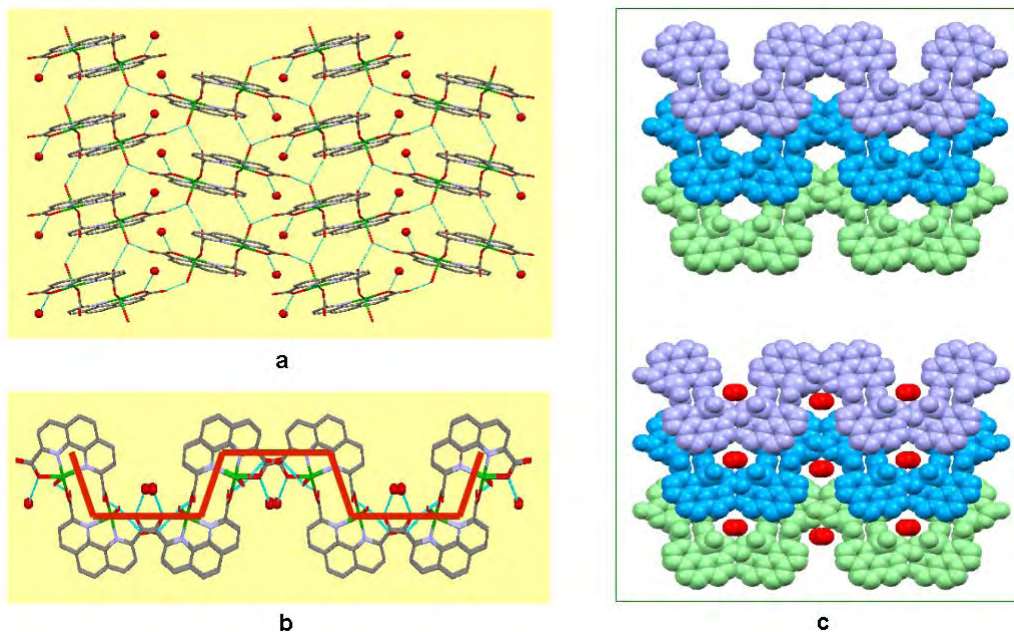


Figure 15. Different views of the network formed by dimeric units of $\{[Cu(II)(2,9-dcphen)(H_2O)]_2 \cdot 2(H_2O)\}$ are shown: a) the 2D sheet along the x axis and b) the profile of the sheet along the z axis, c) the stacking of consecutive planes and the water molecules (in red) filling the cavities.

Comparing the space group $P2_1/c$ and the lattice parameters of this structure with the copper dimer presented in section § III.2.2.1 (ref. 10b), it appears that both structures $\{[Cu(II)(2,9-dcphen)(H_2O)]_2 \cdot 2(H_2O)\}$ are completely isomorphous and the only difference resides in the way the crystal was generated. Indeed, whereas here, the crystalline material was obtained starting from $[Cu(I)(CH_3CN)_4PF_6]$ salt upon air oxidation of Cu(I) into Cu(II) under water/ CH_3CN diffusion and in the presence of the base Et_3N , in the published case, crystals were formed by *in situ* oxidation of 2,9-dimethyl-1,10-phenanthroline with $Cu(NO_3)_2$ copper salt under acid (HNO_3) solvothermal conditions.

Comparison of PXRD profiles, the one simulated from single crystal data and the observed one from crystalline powder (yellow and green lines in figure 15), shows only a partial fit. In particular the experimental profile shows a decreased crystallinity and the presence of a second phase (green triangles) that, in a first hypothesis, could be attributed to a partially dehydrated compound.

TGA measurement between $30^\circ C$ and $130^\circ C$ shows a weight loss between $80-110^\circ C$ corresponding to ~ 2.5 water molecules. PXRD performed on the sample after TGA measurement (green line in figure 16) shows a further loss in crystallinity and a change of the profile. Indeed, the peaks (labelled in green) probably corresponding to the dehydrated phase increase while the peaks (labelled in violet) corresponding to the original hydrated phase decrease. Further measurements have to be done to confirm this hypothesis.

The TGA study seems to demonstrate the ability of this compound to lose the two water molecules trapped inside the crystal lattice. The next step will be the study of the resorption ability of the compound toward the same or different solvent.

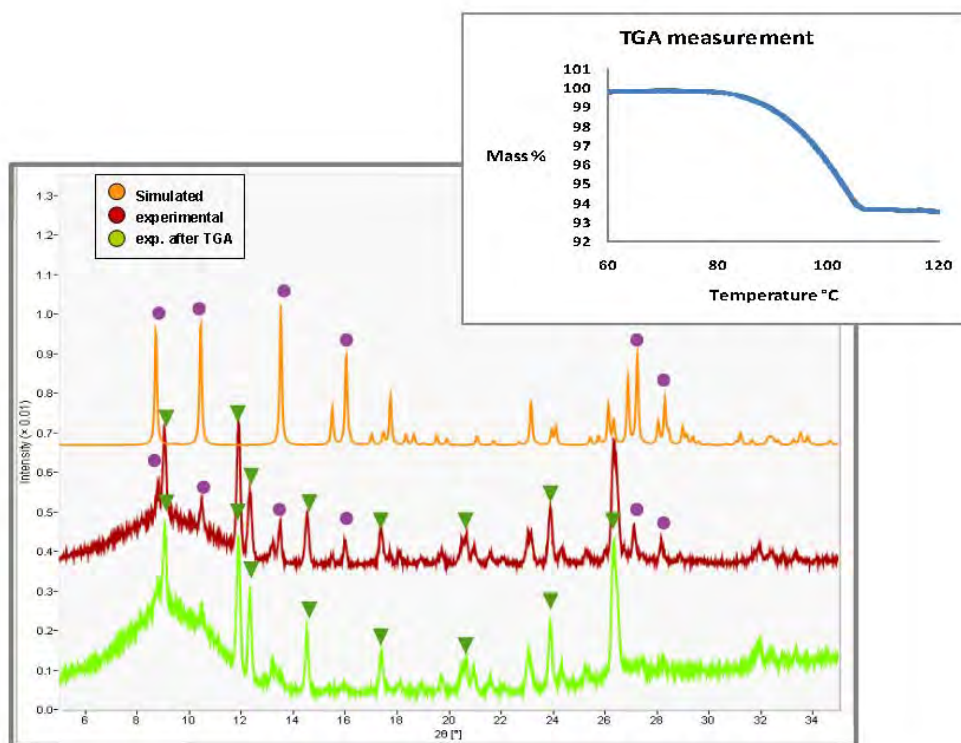


Figure 16. TGA measurement and PXRD comparison for $\{[Cu(II)(2,9-dcphen)(H_2O)]_2 \cdot 2(H_2O)\}$; the peaks belonging to the two phases are labelled with violet dots (hydrated phase) and green triangles.

III.4.2.3 Coordination network based on Silver(I)

Both ligands 6,6'-dcbpy and 2,9-dcphen were combined with different silver salts AgX ($X = BF_4^-, SbF_6^-, AsF_6^-, PF_6^-, CH_3SO_3^-$). A network with molecular formula $\{[Ag(2,9-dcphen-H)]_8(HPF_6)\}$ [structure XXXV in the Annexes] was obtained after slow diffusion of an ethanol solution of $AgPF_6$ in a water solution of 2,9-dcphen and BAD23 (following the approach developed in section §II). The disordered solvent molecules in the structure have been squeezed to have a better resolution and structural refinement.

The same off-white crystals were obtained also for the $AgAsF_6$, however, the quality of crystals was lower than the one with $AgPF_6$.

The compound of formula $\{[Ag(2,9-dcphen-H)]_8(HPF_6)\}$ is a mono-dimensional coordination network presenting a rare case of Ag-Ag infinite interaction which may be regarded as a cationic silver wire [Fig. 17b]. Each silver atom is hexa-coordinated, 2,9-dcphen behaves as a tetra-dentate (η^4) [N-N-O-O] ligand and bridges three silver atoms (μ^3). Thus, the coordination sphere around each Ag cation is composed of the [N,N-O-O-Ag-Ag] set. Whereas the two nitrogen atoms are given by phenanthroline

ligand, the two oxygen atoms belong to the neighbouring ligands [Fig. 17a]. The geometry around the metal centre is a severely distorted octahedral with distances for the trans Ag atoms within the 2.90-3.27 Å range. These distances are considerably longer than the Ag-N or Ag-O ones which are in the 2.37-2.54 Å and 2.35-2.44 Å ranges respectively.

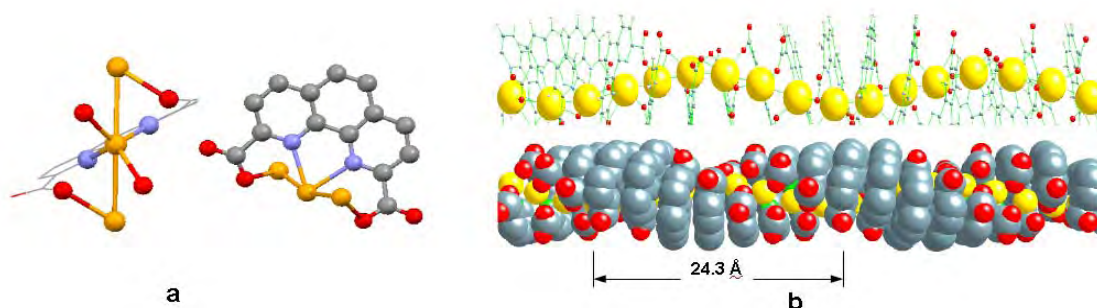


Figure 17. Coordination network $\{[Ag(2,9-dcphen-H)]_8(HPF_6)\}$ a) zoom on the coordination sphere around silver atoms, b) view of the 1D helical chain with the silver wire inner scaffold.

Concerning the carboxylate units, the overall charge balance and the number of proton present suggest that the ligand is in its mono-anionic [2,9-dcphen-H]⁻ form. For all the ligands, the C-O distances are in the range of 1.22 to 1.29 Å (which is in accordance with the distance for carboxylate group) except for one where the C-O distances are 1.17 Å and 1.42 Å, which is in accordance with the distances for carboxylic acid. The 1-D architecture is helicoidal and cationic in nature and the charge neutralisation is ensured by (PF₆⁻) anions occupying free space between helical chains (see figure 18b).

Concerning the Ag-Ag distances ranging from 2.90 to 3.27 Å, they are within the 2.80-4.22 Å interval reported in the literature.²¹ Interestingly, the observed Ag-Ag distance falls within the range observed for Ag-Ag separation in the metallic state (2.89 Å) and the sum of van der Waals radii (3.44 Å).

As stated above, the geometry of the 1-D network is not linear but helicoidal with 8 silver atoms in the unit cell and a pitch of 24.3 Å. The arrangement of the phenanthroline units around the metal wire is shifted probably due to stacking interactions [$d_{\pi-\pi} = 3.5-3.7$ Å]. Each single helix is chiral but the overall crystal is a racemate (space group P-1) since both helices with opposite handedness are present (see figure 18b). The packing of helices generates roomy cavities between single chain

²¹a) X.-F. Zheng, L.-G. Zhu; *CrystGrowthDes*, **2009**, 9, 4407-4414; b) J. A. Frey, C. R. Samanam, J.-L. Montchamp, A. F. Richards; *Eur. J. Inorg. Chem.*; **2008**, 463-470; c) K. Cheng, H.-L. Zhu, Y.-G. Li; *Z. Anorg. Allg. Chem.*, **2006**, 632, 2326-2330; d) F.-T. Xie, H.-Y. Bie, L.-M. Duan, G.-H. Li, X. Zhang, J.-Q. Xu; *J. Solid State Chem.*, **2005**, 178, 2858-2866; e) Q.-M. Wang, T. C. W. Mak; *Inorg. Chem.*, **2003**, 42, 1637-1643; f) A. J. Blake, N. R. Champness, P. Hubberstey, W.-S. Li, M. A. Withersby, M. Schröder; *Coord. Chem. Rev.*, **1999**, 183, 117-138

behaving as cylinders. Channels thus formed are filled with anions and solvent molecules that have been squeezed during the refinement process.

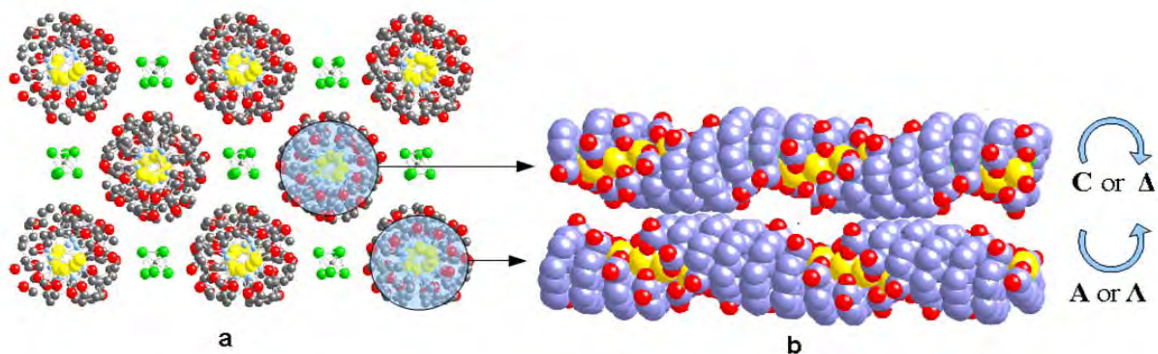


Figure 18. For coordination network $\{[Ag(2,9-dcphen-H)]_8(HPF_6)\}$: a) the crystal lattice formed by stacking of the parallel infinite chains viewed \perp to the plane $[1,1,1]$ and (b) neighbouring chains having opposite chirality. Solvent molecules and the PF_6 anions (green) are housed inside channels.

The experiment was repeated many times with the same conditions or varying the concentration and the base (triethylamine, tributylamine, methylamine) but unfortunately up till now we could not reproduce this structure. The potentiality of this structure as molecular nanowire for the transport of electrons or protons is quite evident and will be developed in the future.

III.5 Conclusions

The exploration of different connectivity of analogous ligands 6,6'-dcbpy and 2,9-dcphen afforded interesting complexes and networks. The particularity of the employed ligands resides in the simultaneous presence of carboxylate and N-donor chelating units. Owing to the *ortho* positioning of the carboxylates moieties with respect to the chelating units on the aromatic rings, both types of heteroatoms may participate in the binding of the same metal centre. This was not the case for the series of ligands presented in chapter II, and for that reason they have been discussed in a separated chapter.

Although a three component (metal+ligand+base) system could be obtained, unfortunately this was restricted to $\{[Zn(6,6'-dcbpy)_2(Et_3N)_4][6,6'-dcbpy]\}_2 \cdot (MeOH) \cdot 11(H_2O)$ structure between zinc cation and 6,6'-dcbpy ligand. In the other cases, only two components (metal+ligands) networks were discovered with Zn(II), Cu(II) and Ag(I).

The silver helical cationic wire obtained may be of interest for the generation of metallic silver wires exhibiting peculiar charge transport through the Ag-Ag bond for

possible application in the field of nanodevices²². However, the preparative procedure must be improved and further tuned.

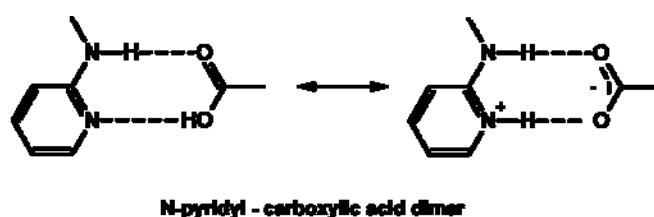
²²a) Eisele, D. M.; Berlepsch, H.; Bottcher, C.; Stevenson, K. J.; Vanden Bout, D. A.; Kirstein, S.; Rabe, J. P.; *J. Am. Chem. Soc.*, **2010**, *132*, 2104-2105 ; b) Tan, X.; Yang, G., *J. Phys. Chem. C*, **2009**, *113*, 19926-19929 ; c) Streb, C.; Tsunashima, R.; MacLaren, D. A.; McGlone, T.; Akutagawa, T.; Nakamura, T.; Scandurra, A.; Pignataro, B.; Gadegaard, N.; Cronin, L., *Angew. Chem. Int. Ed.*, **2009**, *48*, 6490-6493, S6490/1-S6490/13 ; d) Lu Wei; N. K.-M.; Che Chi-Ming, *Chem. Asian J.*, **2009**, *4*, 830-4 ; e) Fages, F.; Wytko, J. A.; Weiss, J.; *Comptes Rendus Chimie*, **2008**, *11*, 1241-1253 ; f) Nakanishi, T.; *Hyomen*, **2008**, *46*, 105-115 ; g) Morikawa M.-A.; Yoshihara M.; Endo T.; Kimizuka N.; *J. Am. Chem. Soc.*, **2005**, *127*, 1358-9 ; h) Schenning, A. P. H. J.; Meijer, E. W.; *Chem. Commun.*; **2005**, *26*, 3245-3258 ; i) Grevin, B.; Rannou, P.; *Nature Materials*, **2004**, *3*, 503-504 ; j) Akutagawa, T.; Nakamura, T.; *Springer Series in Chemical Physics*, **2003**, *70*, 123-147

Chapter IV

Networks and Complexes based on Polyamides Ligands

IV.1 Aim of the work

As already stated in the introduction (§ I), the aim of this work is the investigation and the development of supramolecular architectures based on both hydrogen and coordination bonds. In order to control the formation of extended assemblies, a strategy based on stable and reliable hydrogen bonding motives as recognition patterns was pursued. Along this line, in this final chapter, we shall focus on hydrogen bonding interactions occurring between carboxylic acid and N-pyridyl amine (Scheme 1). This hydrogen bonding pattern was demonstrated to be rather strong with one of the highest occurrence probability ($P_m = 82\%$, CSD survey conducted by Allen and co-workers¹) (see § I.5.2.2).



Scheme 1. Recognition pattern between carboxylic acid and N-pyridyl amine.

Based on these observations, we have designed a new series of tectons. The latter, presented in the following section, were combined with H bond acceptors such as carboxylic acids and transition d-metal cations.

IV.2 Design of ligands and networks conception

IV.2.1 Ligand design

As schematically presented in scheme 2, the designed ligands are symmetrical. They are based on a "core" (zone1) [Fig. 1a] derived from N-aromatic rings capable of binding metal cations (for analogy see section §II.3.3). Different cores such as bipyridine, biquinoline and naphthyridine backbones were used. As transition metals adopting the tetrahedral coordination geometry, Cu(I) appeared particularly appropriate for this purpose, as demonstrated by Hamilton *et al*² (see section §IV.2.2.2), for steric reason related to the size of the ligand. However, other metals, in particular with an octahedral coordination geometry, could also be considered.

¹ F. H. Allen, W. D. S. Motherwell, P. R. Raithby, G. P. Shields, R. Taylor; *New J. Chem.*, **1999**, 23, 25-34

² a) M. S. Goodman, A. D. Hamilton, J. Weiss; *Tetrahedron Lett.*, **1994**, 35, 8943-8946 ; b) M. S. Goodman, A. D. Hamilton, J. Weiss; *J. Am. Chem. Soc.*, **1995**, 117, 8447-8455

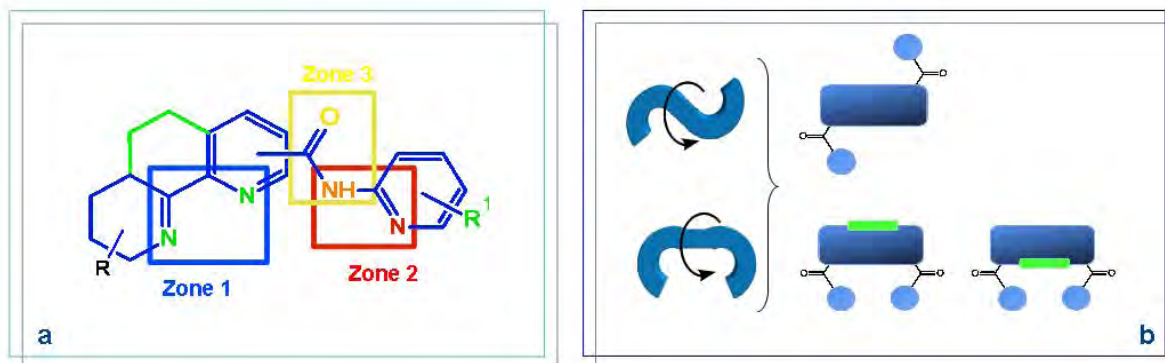


Figure 1. a) Schematic representation of ligands possessing three types of interacting zones and b) schematic representation of the possible conformations of the symmetrical ligands (back-to-face) and (face-to-face).

To the above mentioned rigid backbone, N-pyridyl polycarboxamide type “arms” (zone 2 and 3) have been appended, leading to a overall flexible ligand [Fig. 1a]. Due to the rotational freedom of the arms (on the same side (*face-to-face*) or on the opposite side (*back-to-face*)) and of the two linked aromatic moieties, in the case of bipyridine and biquinoline based ligands, several isomers may be formed (Fig. 1b).

The N-pyridyl amide (zone 2, red) has been chosen as a reliable recognition site for the carboxylic group (see section §IV.1). Interestingly, the viability of the H-bond interaction motif in solution has also been demonstrated.³ The carboxamide group (zone 3, yellow) has been introduced for his propensity to interact with anions. Indeed, several investigations have underlined their ability to bind H_2PO_4^- , F^- , Cl^- and benzoate anions.⁴

IV.2.2 Networks conception

On the basis of the shape and connectivity patterns of the ligand through coordination and/or H bonding, several possibilities for network formation may be envisaged as shown in figure 2.

³ a) F. Garcia-Tellado, S. Goswami, S.-K. Chang, S. J. Geib, A. D. Hamilton; *J. Am. Chem. Soc.*, **1990**, *112*, 7393-7394 ; b) F. Garcia-Tellado, S. J. Geib, S. Goswami, A. D. Hamilton; *J. Am. Chem. Soc.*, **1991**, *113*, 9265-9269 ; c) J. Yang, E. Fan, S. J. Geib, A. D. Hamilton; *J. Am. Chem. Soc.*, **1993**, *115*, 5314-5315 ; d) S. J. Geib, C. Vicent, E. Fan, A. D. Hamilton; *Angew. Chem. Int. Ed.*; **1993**, *32*, 119-121 ; e) B. König, O. Möller, P. Bubenitschek; *J. Org. Chem.*, **1995**, *60*, 4291-4293

⁴ a) M. H. Keefe, K. D. Benkstein, J. T. Hupp; *Coord. Chem. Rev.*, **2000**, *205*, 201-208; b) P. A. Gale, S. Camiolo, G. J. Tizzard, C. P. Chapman, M. E. Light, S. J. Coles, M. B. Hursthouse; *J. Org. Chem.*, **2001**, *66*, 7849-7853 ; c) Z. Yin, Z. Li, A. Yu, J. He, J.-P. Cheng; *Tetrahedron Lett.*, **2004**, *45*, 6803-6806

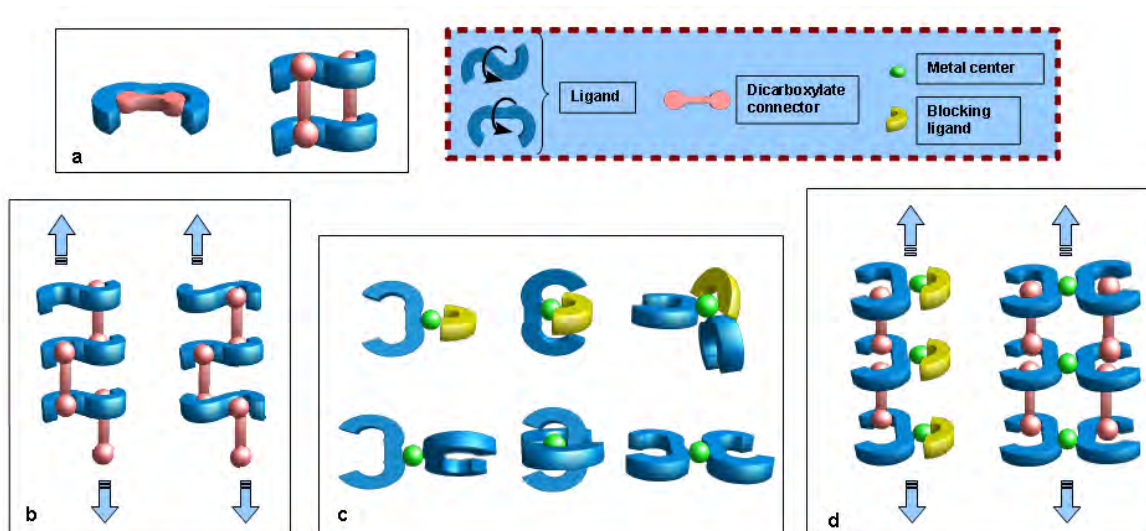


Figure 2. Possible organisation in the solid state of the carboxamido-pyridyl ligands and dicarboxylic acid derivatives forming: a) inclusion compounds or tetramers; b) purely organic hydrogen bonded single chains; c) metallic complexes; d) hybrid coordination / H-bonding network involving also different type of metal centers.

We shall refer to figure 2 to describe how, in our intention, it might be possible to build different molecular networks with increasing complexity or discrete species. In order to explore these possibilities, first of all, ligands were structurally characterized. In a second step, the prepared ligands were combined either with dicarboxylic acids or with metal cations. Finally, simultaneous combinations of ligands with both carboxylic units and metal cations will be explored.

IV.2.2.1 Combination with dicarboxylic units as H bond acceptors

By design, the use of these ligands bearing two symmetrical connecting sites in combination with divergently oriented dicarboxylic units could lead to infinite architectures [Fig. 2c] although, one can not exclude the formation of tetrameric assemblies [Fig. 2a right]. As mentioned above, for ligands possessing rotational freedom around the link between the two aromatic moieties, the hydrogen bonding sites (N-pyridyl amide, red zone 2 and carboxamide group, yellow zone 3 in figure 1a) may be oriented towards the same side (face-to-face) or the opposite sides (back-to-face), whereas the face-to-face rotamer may lead to the formation of discrete inclusion complexes (Fig. 2a left), for the other back-to-face isomer, one may expect the formation of mono-dimensional chains with linear, zigzag, crenulated or helical geometry (see section §I.3.2.2). Furthermore, the ligands may be either *syn*-parallel or *anti*-parallel oriented leading thus to two different arrangements (Fig. 2b).

IV.2.2.2 Combination with transition metal ions

Owing to the presence of chelating units, in principle, the prepared neutral ligands must form complexes with almost all transition metal cations possessing all possible geometries.

However, for the face-to-face isomer when pointing to the same side as N,N-coordinating site [Fig. 1b], the formation of complexes of the ML_2 type with square planar geometry around the metal cannot occur for steric reasons (see figure 2c). Examples of homoleptic $Cu(I)^2$ complexes for which the metal centre adopts the tetrahedral coordination geometry and heteroleptic $Ru(II)^5$ complexes displaying luminescence properties have been reported.

IV.2.2.3 Combination with transitions metal ions and dicarboxylic acids as H bond acceptors

In the case of simultaneous contributions of H- and coordination bonding, among many other possibilities, one may expect the formation of one dimensional hybrid networks solely based on H bonding. Two simple and representative examples are shown on figure 2d. The simplest case (Fig. 2d-left) consists in a 1-D H-bonded network appended with heteroleptic metal complexes bearing an auxiliary ligand. Although on figure 2d the geometry around the metal is square planar (Fig. 2d left), the same type of architecture may be formed with metal centres adopting the tetrahedral coordination geometry. The second architecture (Fig. 2d-right) consists in the interconnection of consecutive 1-D H-bonded networks by metal cations adopting the square planar geometry only. The final aim of this part was to obtain these architectures. Towards that, a series of intermediate steps have been explored.

IV.2.3 Project

After the synthesis and characterisation of the targeted ligands, they were combined with aromatic or aliphatic dicarboxylic acid derivatives of different size and various transition metal (first row: Cr, Mn, Fe, Co, Ni, Cu, Zn, Ag; second row: Pd, Pt, Ag, Cd and third row: Au, Pt, Hg). As counter ion, non-coordinating BF_4^- , coordinating NO_3^- and Cl^- and organic acac or hfac derivatives have been used.

The information collected through these preliminary studies were expected to help with the design and prediction for the final hybrid architectures based on both H- and coordination bonding processes.

In the next section, a literature survey is illustrated through few selected examples dealing with the recognition patterns envisaged, and will be followed by the report of our results and comments on them.

⁵ M. H. Keefe, K. D. Bekstein, J. T. Hupp; *Coord. Chem. Rev.*, **2000**, 205, 201-228

IV.3 Literature examples

The literature examples are mainly related to purely organic systems (§ IV.3.1), however, when associated with transition metals, some interesting results have been obtained in the field of luminescent sensors (§ IV.3.2)⁶.

IV.3.1. Purely organic systems with pyridine carboxamide and carboxylic acids

The pyridine carboxamide moiety has been often studied as a prototype of molecular recognition by hydrogen bonding of carbohydrates⁶ and in the formation of anticancer agent as G-quartet ligands.⁷ In material chemistry, this motif has been exploited for the self-assembly of organic liquid-crystalline polymers as described below (Fig. 3)⁸.

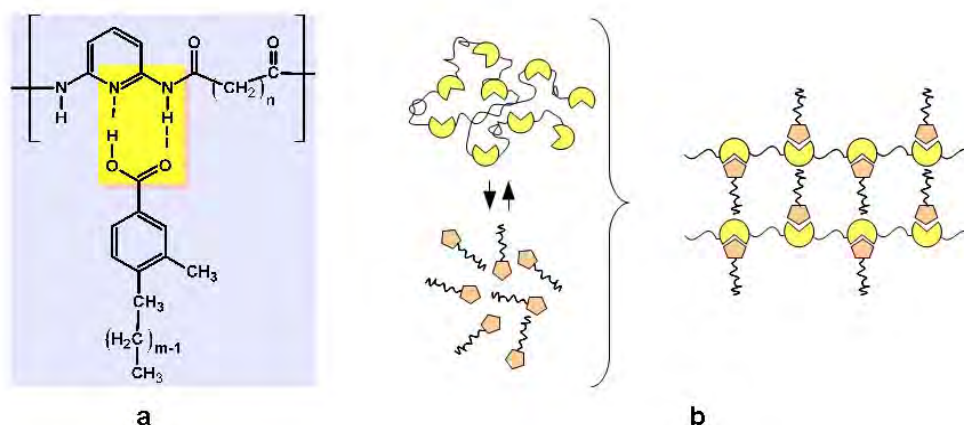


Figure 3. Supramolecular H bonded polyamides associated with carboxylic acids forming liquid-crystals; a) recognition pattern between the different units and b) proposed liquid-crystalline structure from XRD pattern of the mesogenic phases (ref.8).

The formation of hydrogen bonds between carboxylic acids and (methylpyridyl)aryl amides is also documented in the design of synthetic receptors for carboxylic acids. Indeed, Hamilton⁹ has shown that, by increasing the length of the

⁶ a) M. Mazik, H. Bandmann, W. Sicking; *Angew. Chem. Int. Ed.*; **2000**, 39, 551-554; b) M. Mazik, W. Sicking; *Chem. Eur. J.*, **2001**, 7, 664-670

⁷ Nucleic acid filaments rich in guanine are able to form structures with four filaments known as G-quadruplex. These structures are linked through hydrogen bonding among the guanine and stabilized by a monovalent cation.

a) G. Pennarun, C. Granotier, L. R. Gauthier, D. Gaomez, F. Hoffschir, E. Mandine, J.-F. Riou, J.-L. Mergny, P. Mailliet, F. D. Boussin; *Oncogene*, **2005**, 24, 2917-2928 ; b) A. De Cian, E. DeLemos, J.-L. Mergny, M.-P. Teulade-Fichou, D. Monchard; *J. Am. Chem. Soc.*, **2007**, 129, 1856-1857

⁸ T. Kato, O. Ihata, S. Ujiie, M. Tokita, J. Watanabe; *Macromolecules*, **1998**, 31, 3551-3555

⁹ a) F. Garcia-Tellado, S. J. Geib, S. Goswami, A. D. Hamilton; *J. Am. Chem. Soc.*, **1991**, 113, 9265-9269 ; b) S. J. Geib, C. Vicent, E. Fan, A. D. Hamilton; *Angew. Chem. Int. Ed.*; **1993**, 32, 119-121

dicarboxylic acid beyond the optimum, the formation of helical structures, as illustrated in figure 4a, is observed. Helical ribbons are formed by oligopyridinecarboxamides mediated by metal coordination¹⁰ or through direct H bond folding. The conjugation of the aromatic rings with the amide moiety and intramolecular hydrogen bonding stabilizes a conformer in which the N-pyridyl amine moiety points to the same side of the molecule favouring thus the folding of the oligomers as demonstrated by Huc *et al* (Fig 4b).¹¹

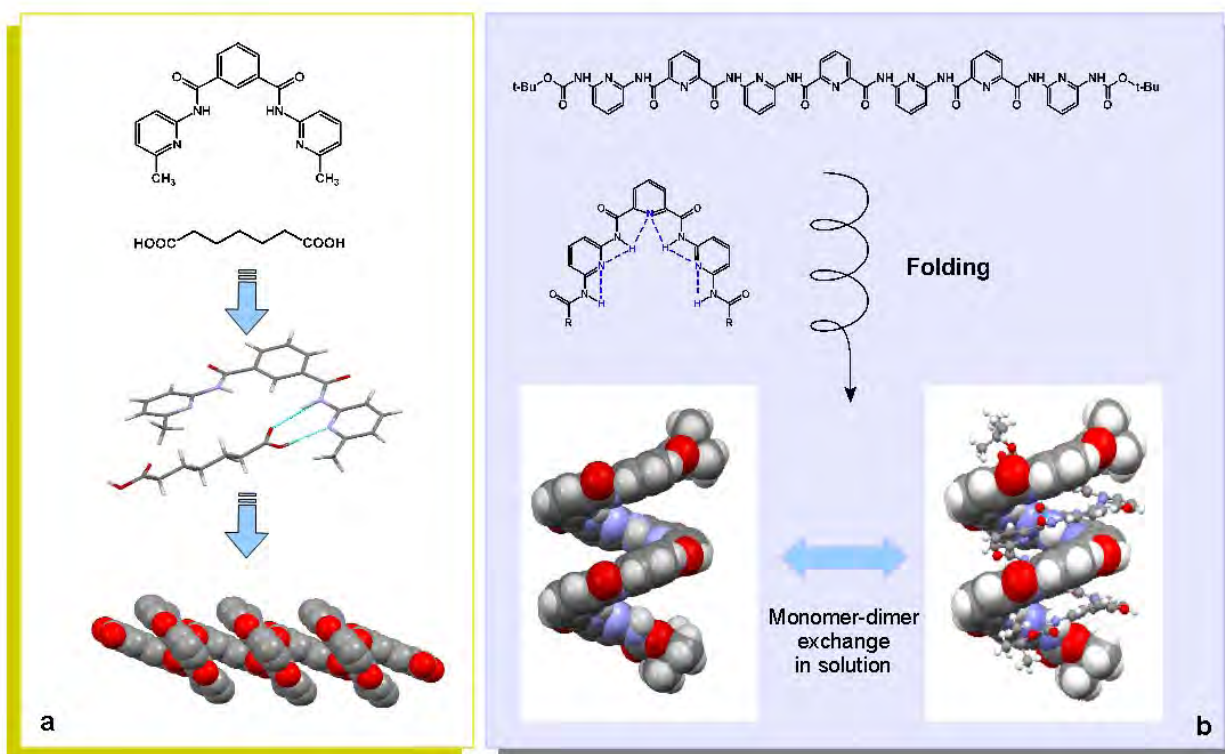


Figure 4. a) H-bonded helical supramolecular structure formed between heptandioic acid and a benzene derivative of (6'-methylpyridyl)amide (ref. 9b); b) H-bonded helical supramolecular structure derived from the direct folding of a poly(-2-pyridine)carboxamide oligomer (ref. 11c).

IV.3.2. Systems involving transition metals

Transition metals have been rarely combined with this type of hydrogen bonding system. As examples, host ruthenium complexes as luminescent anions receptors have been chosen. These complexes contain functional groups next to the binding sites for signalling and sensing of target guest species (Cl⁻, H₂PO₄⁻ and carboxylates

¹⁰ F. Stomeo, C. Lincheneau, J. P. Leonard, J. E. O'Brien, R. D. Peacock, C. P. McCoy, T. Gunnlaugsson; *J. Am. Org. Chem.*, **2009**, *131*, 9636-9637

¹¹ a) C. Bao, Q. Gan, B. Kauffmann, H. Jiang, I. Huc; *Chem. Eur. J.*, **2009**, *15*, 11530-11536 ; b) J. Garric, J.-M. Léger, I. Huc; *Angew. Chem. Int. Ed.*; **2005**, *44*, 1954-1958 ; c) V. Berl, I. Huc, R. G. Khoury, M. J. Krishe, J.-M. Lehn, *Nature*, **2000**, *407*, 20-723

such as benzoate).¹² In figure 5 are depicted two examples. The first one (Fig. 5a), reported by Beer *et al*¹³, shows a specific receptor for organic phosphate derivatives and the second one (Fig. 5b), due to Watanabe *et al*¹⁴, represents a receptor for chloride or acetate anions.

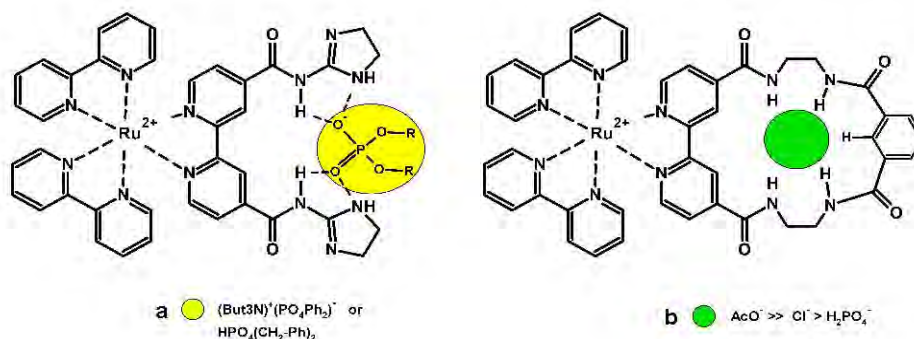


Figure 5. Anion receptor molecules based on hydrogen bonding bearing the $Ru(bpy)_3^{2+}$ moiety as a light collecting antenna for luminescent sensing of a) phosphodiester (ref. 13) and b) acetate and chloride (ref. 14).

IV.4 Target polyamides ligands

The general scheme of the targeted ligands was presented in section § IV.2.1. So far, we have focused on symmetrical naphthyridine, bipyridine and biquinoline backbones illustrated in figure 6; as appended group, the *ortho*-methyl pyridyl was chosen because 2-amino-6-methylpyridine is commercially available and furthermore the presence of the methyl group enhances the solubility of the ligand.

With respect to the N,N- coordination donor site, two different positions, mainly *ortho*-position for [2,7-mpanaphthy] and [6,6'-mpabpy] or *para*-position for [4,4'-mpaBQ] have been explored.

¹² a) I. Dumazet, P. D. Beer; *Tetrahedron Lett.*, **1999**, 40, 785-788 ; b) P.D. Beer; *Acc. Chem. Res.*, **1998**, 31, 71-80 ; c) P. D. Beer, S. W. Dent; *Chem Commun.*, **1998**, 825-828

¹³ P. D. Beer, F. Szemes, V. Balzani, C. M. Sala, M. G. B. Drew, S. W. Dent, M. Maestri; *J. Am. Chem. Soc.*, **1997**, 119, 11864-11875

¹⁴ S. Watanabe, O. Onogawa, Y. Komatsu, K. Yoshida, *J. Am. Chem. Soc.*, **1998**, 120, 229-230

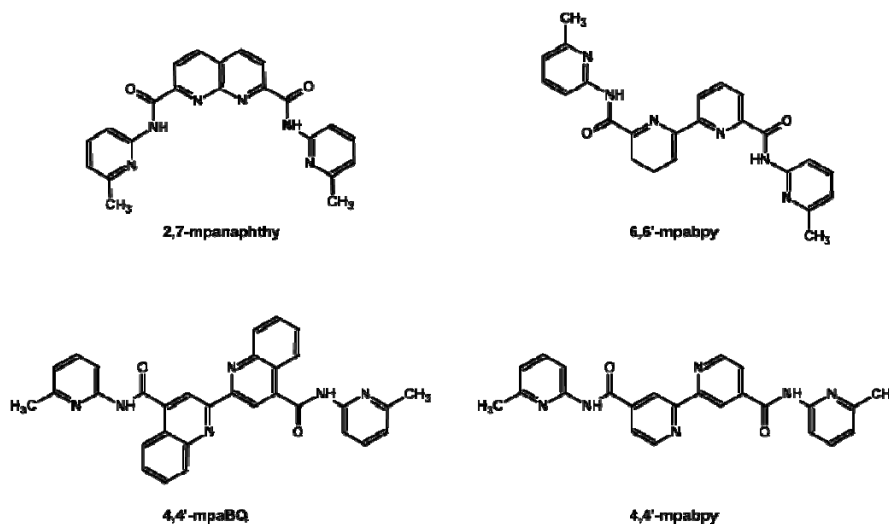


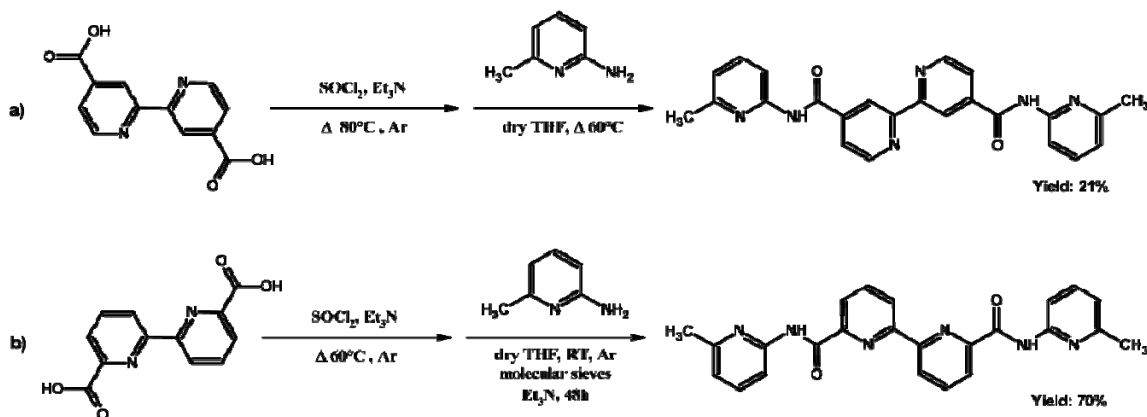
Figure 6. Targeted ligands.

IV.4.1 Ligands synthesis

The most common and general method for the preparation of substituted amides is the condensation of primary and secondary amines with acyl chlorides.

IV.4.1.1 [4,4'-mpabpy] and [6,6'-mpabpy]

The synthesis of 4,4'-Bis-[N-(6-methylpyridin-2-yl)carbamoyl]-2,2'-bipyridine ([4,4'-mpabpy]) and 6,6'-Bis-[N-(6-methylpyridin-2-yl)carbamoyl]-2,2'-bipyridine ([6,6'-mpabpy]) has been achieved using the classical Schotten-Baumann reaction [Scheme 2]. However, the reaction conditions have been modified. Indeed, replacing dichloromethane, in which no condensation was observed, by dry THF, we obtained [4,4'-mpabpy] in 21% yield and [6,6'-mpabpy] in 70% yield. The starting dicarboxylic acids were synthesized by oxidation of the di-methyl derivatives as already described in section § II.3.3.2 for [4,4'-dcbpy] and in section § III.3.1 for [6,6'-dcbpy].

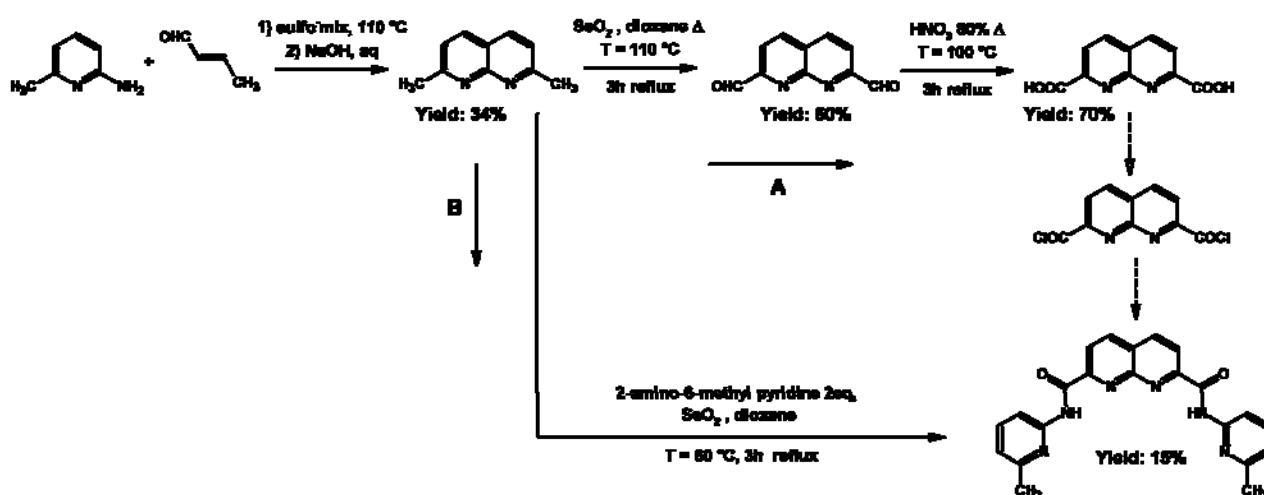


Scheme 2. Synthetic strategy for the preparation of [4,4'-mpabpy] (a) and [6,6'-mpabpy] (b).

IV.4.1.2 [2,7-mpanaphthy]

The synthesis of 2,7-Bis-[N-(6-methylpyridin-2-yl)carbamoyl]-1,8-naphthyridine ([2,7-mpanaphthy]) has required the preparation of 2,7-dicarboxy-1,8-naphthyridine.¹⁵ The latter was prepared starting from 2-amino-6-methylpyridine, crotonaldehyde and sulfo-mix, using the Skraup reaction condition affording the 2,7-dimethyl-1,8-naphthyridine¹⁶ which was first oxidized by SeO₂ into 2,7-dicarboxylaldehyde and then into 2,7-dicarboxylic acid using concentrated nitric acid. The subsequent steps leading to the desired pyridin-carbamoyl derivate were the formation of the acyl chloride and the acylation of the primary amine. Overall, the multistep strategy consisting in five stages is highlighted in scheme 3A.

Interestingly, a slight change in the oxidation conditions allowed to obtain directly [2,7-mpanaphthy] in 15% yield [Scheme 3B].



Scheme 3. The preparation of [2,7-mpanaphthy] following the a five-step strategy (A) and following the shortened two-steps pattern (B).

IV.4.1.3 [4,4'-mpaBQ]

For the synthesis of [4,4'-mpaBQ], starting from the commercially available 4,4'-dicarboxy-2,2'-biquinoline, different methods for the *in situ* activation of the carboxylic acid were explored.

Since the classical use of carbonyldiimidazole (CDI) as coupling agent was found to be too mild, a mixed phosphoric anhydride derivative¹⁷ under the Niu¹⁸ conditions

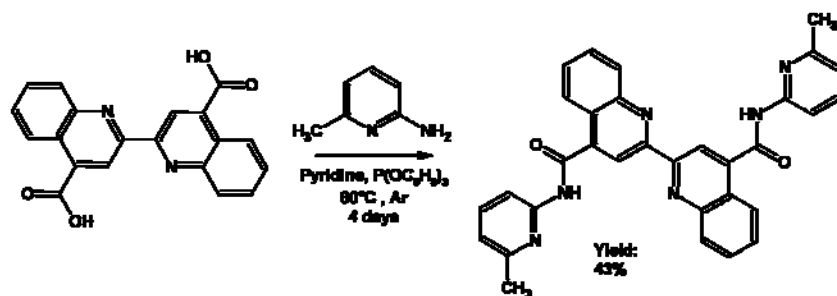
¹⁵ a) C. J. Chandler, L. W. Deady, J. A. Reiss, V. Tzimos; *J. Heterocycl. Chem.*, **1982**, 1017-1019 ; b) C. J. Fahrni, A. Pfaltz; *Helv. Chim. Acta*, **1998**, *81*, 491-506

¹⁶ M. A. Gavanagh, V. M. Cappo, C. J. Alexander, M. L. Good; *Inorg. Chem.*, **1976**, *15*, 2615-2621

¹⁷ T. Shioru, S. Hamada; *Chem. Pharm. Bull.*, **1974**, *22*, 849-852

¹⁸ Y.-Y. Niu, Y.-L. Song, J. Wu, H. Hou, Y. Zhu, X. Wang; *Inorg. Chem. Commun.*, **2004**, *7*, 471-474

using triphenyl phosphite, was employed to obtain [4,4'-mpaBQ] in one step following [Scheme 4].



Scheme 4. Short synthesis of [4,4'-mpaBQ].

All ligands were characterized by NMR, MS, IR, elemental analysis and melting point (see Experimental part); for the four ligands, their crystal structures (shown bellow) were also obtained by X-ray diffraction on single crystal.

IV.5 Structural study of the four ligands

This structural study is divided into three parts: 1) the solid state characterisation of ligands (§IV.5); 2) the formation, in the solid state, of hydrogen bonded networks between ligands and different dicarboxylic acids (§IV.6) and 3) the crystallisation of ligands with *d*-metal cations (§IV.7). Through these investigations, our aim was to gather information on ligand conformation, their ability to form hydrogen bonds with targeted recognition motif, their ability to bind metal cations and, finally, to study their spatial arrangement.

IV.5.1. Ligand 2,7-Bis-[N-(6-methylpyridin-2-yl) carbamoyl]-1,8-naphthyridine - [2,7-mpanaphthy]

The 1,8-naphthyridine-*bis*-amide ligand has been crystallised in two "pseudo-polymorphs". The first one was obtained upon slow diffusion of a methanol solution of the metal salt into a chloroform solution of the ligand. The obtained compound [(2,7-mpanaphthy)*2(H₂O)] includes two water molecules in the crystal lattice (see structure XXXVII in the Annexes). The second pseudo-polymorph, [(2,7-mpanaphthy)*DMSO], crystallised upon cooling a saturated DMSO solution (see structure XXXVIII in the Annexes).

For both crystals, the ligand presents the same metrics that will not be described here in details, however, the different packing of both compounds are presented separately. In both cases, owing to the rigid nature of naphthyridine backbone, the conformation of the amide groups, with the carbonyl pointing out and the four nitrogen looking towards the interior, leads to a pocket shaped ligand that contains the solvent molecules as shown in figure 7.

In [(2,7-mpanaphthy)*2(H₂O)] both water molecules are hydrogen bonded to the nitrogen of the pyridine ring [$d_{\text{N-O}} = 2.89 \text{ \AA}$; $d_{\text{NH-O}} = 2.02 \text{ \AA}$]; there are also hydrogen bonds between oxygen atoms [$d_{\text{O-O}} = 2.76 \text{ \AA}$] as shown in figure 7a, while no hydrogen bond links DMSO with the ligand [Fig. 7b]. In both structures, the 2,7-mpanaphthy ligand is not totally flat but tilted with respect to methylpyridyl moiety with an angle of 7.6° for [(2,7-mpanaphthy)*2(H₂O)] and 6.5° for [(2,7-mpanaphthy)*DMSO] (see figure 6d). Accordingly, some distances depicted in figure 7c are shorter in [(2,7-mpanaphthy)*DMSO] than in [(2,7-mpanaphthy)*2(H₂O)]: $d(\text{N}_{\text{py}}-\text{N}_{\text{py}}) = 7.18 \text{ \AA}$ vs 7.43 \AA and $d(\text{Me}-\text{Me}) = 5.61 \text{ \AA}$ vs 6.40 \AA .

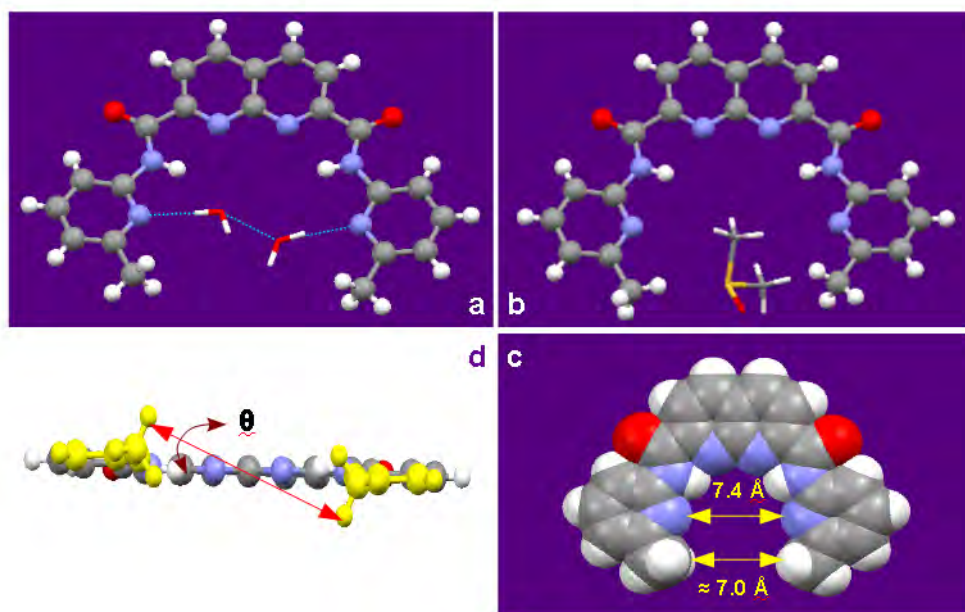


Figure 7. Location of the solvent molecules inside the pocket formed by the ligand for (a) [(2,7-mpanaphthy)*2(H₂O)] and (b) for [(2,7-mpanaphthy)*DMSO]. The molecule is not totally flat with a torsion angle around the amide bond (c) and (d).

Concerning the packing, in [(2,7-mpanaphthy)*DMSO], the ligands form alternate arrays pointing towards opposite directions, the connection within the arrays is ensured by short interactions through solvent molecules, with mainly C-H...O type interactions ($d_{\text{C-O}} = 3.18\text{-}3.56 \text{ \AA}$; $d_{\text{CH-O}} = 2.42\text{-}2.68 \text{ \AA}$). These arrays are extended over planes that are connected *via* DMSO-ligand interactions.

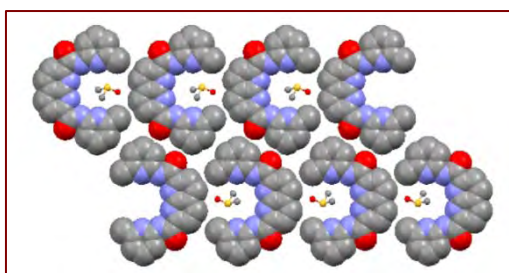


Figure 8. Packing of [(2,7-mpanaphthy)*DMSO] molecules forming alternated arrays.

The crystal packing is dominated by π - π -stacking between the planes with a distances of ca 3.54 Å and short contact mainly between the S=O group of DMSO and the C-H of the methyl group on 2,7-mpanaphthy or between the carbonyl group (C=O) on 2,7-mpanaphthy and the methyl (C-H) of DMSO.

The packing is completely different for [(2,7-mpanaphthy)*2(H₂O)]. Two different arrays (blue and fuchsia in figure 9) are formed through H bonds with water molecules, in a face-to-face arrangement and connected into a 1-D tubular chain through water molecules (see figure 9b and c). The tubular channels filled with solvent are packed along the z axis.

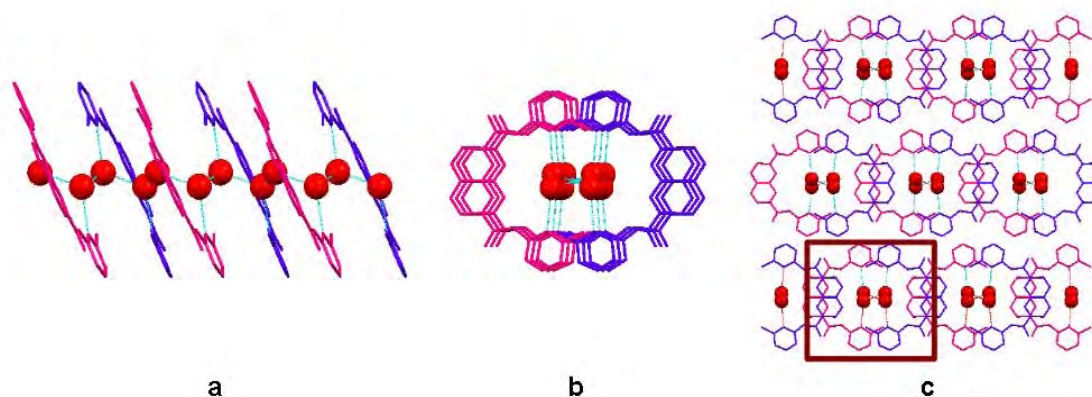


Figure 9. Crystal packing of [(2,7-mpanaphthy)*2(H₂O)]; (a) a single chain viewed along the y axis and (b) along the z axis; (c) 3-D packing view along the z axis.

IV.5.2 Ligand 4,4'-Bis-[N-(6-methylpyridin-2-yl) carbamoyl]-2,2'-bipyridine - [4,4'-mpabpy]

Contrary to the naphthyridine derivative, the ligand 4,4'-mpabpy crystallises without solvent molecules into a 2-D hydrogen bonded network (see structure XXXIX in the Annexes).

The main connecting motif is the intermolecular hydrogen bond (C=O...H-N) between the carbonyl groups and the amidic group of two neighbouring molecules (see figure 10a), so that each ligand (blue in figure 10b) is surrounded by four other ligand molecules (grey in figure 10b). A second non-covalent interaction, a distorted and loose π - π -stacking (distance of ca 3.8 Å) (Fig. 10b), arises between pyridine rings and contributes to the formation of the 2D network. Each individual molecule is twisted around the amide bond by 23.5°.

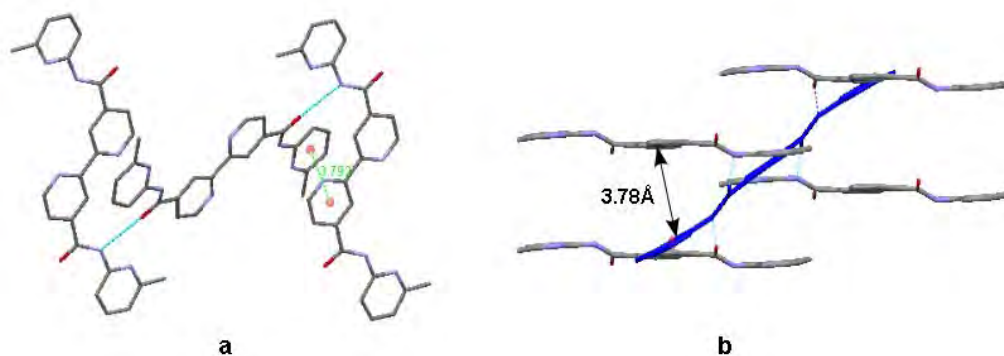


Figure 10. (a) The intermolecular ($C=O\cdots H-N$) hydrogen bond motif and (b) the π -stacking interactions for [4,4'-mpadcbpy].

This intermolecular cross-links lead to bi-dimensional sheets in which molecules are disposed in a fish bone type arrangement (shown in figure 11 along the x, y and z axis). This type of packing results from the overlap of the methyl pyridyl arms maximising the π - π -stacking interactions. The leaning planes are stacked in an anti-parallel mode, one on the top of the other, as shown in the lateral view in figure 11c.

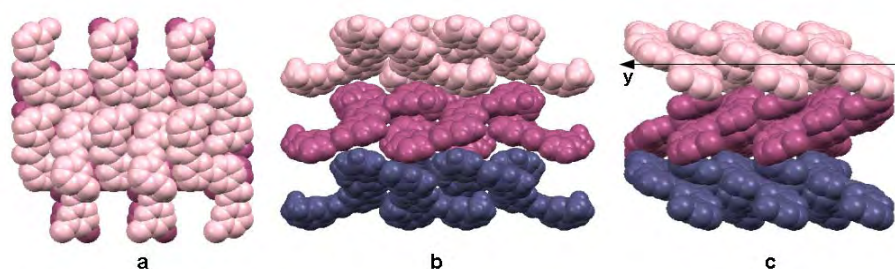


Figure 11. The 2-D planes formed by 4,4'-mpabpy along the three axis x (a), y (b) and z (c) axis.

IV.5.3 Ligand 6,6'-Bis-[N-(6-methylpyridin-2-yl)carbamoyl]-2,2'-bipyridine - [6,6'-mpabpy]

The ligand 6,6'-mpabpy crystallises from DMSO/EtOH mixture with four molecule of water leading to a compound of formula [(6,6'-mpabpy) \cdot 4(H₂O)] (see structure XL in the Annexes).

Figure 12a shows that the water molecules connect the ligands through hydrogen bonds [$d_{N-O} = 2.80 \text{ \AA}$; $d_{O-O} = 1.11 \text{ \AA}$ and 2.83 \AA] forming 1D single chains. In marked contrast with [4,4'-mpabpy], not direct intermolecular hydrogen bonds through the amide moieties are present.

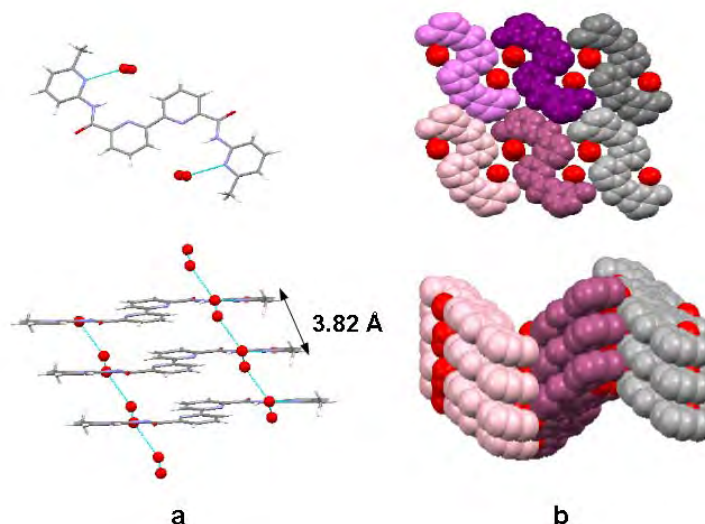


Figure 12. *a) The ligand 4,4'-mpabpy is hydrogen bonded to 4 water molecules (top view along the y axis) and single chains are formed by stacking of ligand molecules connected through water molecules (bottom view along c axis); b) the packing of [4,4'-mpabpy]*4(H₂O) showing the waved planes.*

The formation of the network is dominated by weak interactions between (C=O...H-C) and (C...H-C), and the molecules are disposed diagonally contributing to the network's waving shape as shown in figure 12b. π -stacking between pyridine rings is quite loose with distances of ca 3.8 Å and the ligand molecule is almost flat, meaning that the four conjugated rings lay on the same plane, with only a small torsional angle of ca 5° around the amide bond. In figure 12b, on top, are visible the channels formed by the crystal packing and filled with the solvent.

IV.5.4 Ligand 4,4'-Bis-[N-(6-methylpyridin-2-yl)carbamoyl]-2,2'-biquinoline - [4,4'-mpaBQ]

The biquinoline derivative is insoluble in all the common solvents included DMSO and DMF. However, it may be dissolved in chloroform upon addition of trifluoroacetic acid (TFA) which causes a colour change from colourless to bright yellow. The crystallisation occurs at 6 < pH < 7 as [4,4'-mpaBQ]*2(CF₃COOH)*(CHCl₃) with a Ligand/TFA ratio of 1:2 (Fig. 13a) (see structure XLI in the Annexes).

As we can see on figure 13b, the torsional angle of the amide moiety with respect to the plane of the biquinoline backbone is important ($\theta = 40.5^\circ$) and both amide moieties are twisted towards opposite directions. This conformation creates an empty space for binding two carboxylic acid (TFA) molecules through the expected hydrogen bond motif (NH...O-C). In figure 13a, one may see that the proton is localized on the pyridine ring forming a CAHB (NH⁺...⁻O-C) between a pyridinium cation and a carboxylate anion with N-O distances of 2.65 and 2.76 Å and NH-O distances of 1.77 and 1.88 Å.

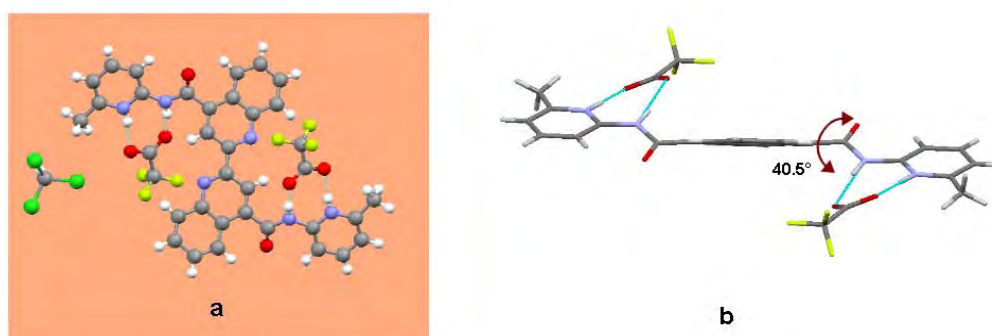


Figure 13. Hydrogen bonding between amide and carboxylate in $[4,4'$ -mpaBQ] $\cdot 2(\text{CF}_3\text{COOH})\cdot(\text{CHCl}_3)$ (a), the large torsion angle allowing the hydrogen bonding below and above the plane (b).

The ligands are stacked through π -stacking (the shortest $d_{\pi-\pi}$ is 3.69 Å) and the packing leads to the formation of channels (Fig. 14a) in all three directions (in figure 14 viewed along the y axis) that are filled with TFA (green) and CHCl_3 (yellow) molecules [Fig. 14b].

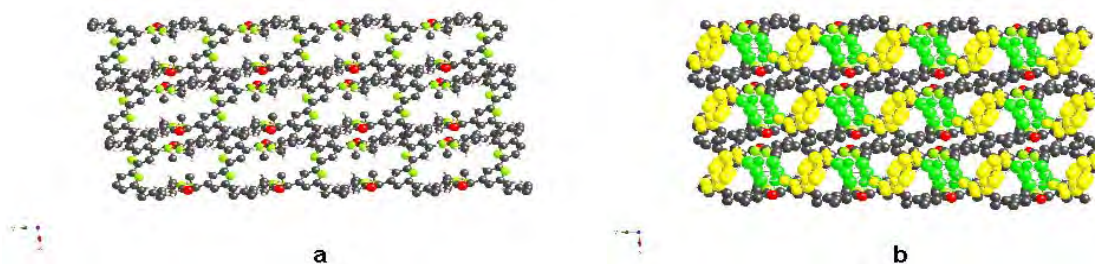
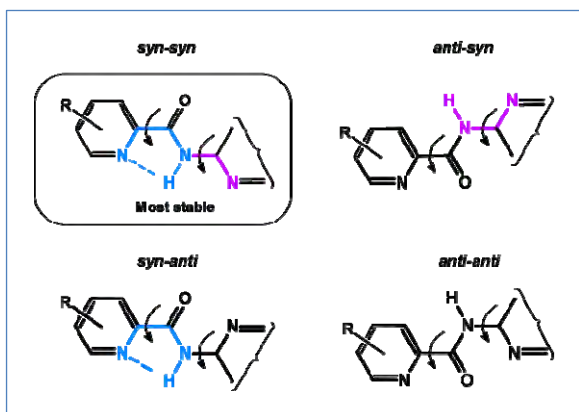


Figure 14. (a) View of the crystal packing for $[4,4'$ -mpaBQ] $\cdot 2(\text{CF}_3\text{COOH})\cdot(\text{CHCl}_3)$ without solvents and (b) filled with TFA (green) and chloroform (yellow) molecules in the $[010]$ plane.

IV.5.5 Some conclusions

The structure of the four targeted ligands have been determined in the solid state leading to the following features. Ligands with the bipyridine and biquinoline skeleton, owing to the rotation around the C-C bond connecting the aromatic rings, are centrosymmetric. In the case of [2,7-mphanaphthy], owing to the rigid nature of the backbone, the convergent disposition of the appended substituents leads to the formation of pockets capable of lodging small solvent molecules (DMSO and water).

For all the obtained structures, the amide carbonyl group (C=O) points towards the opposite direction (outside sphere) with respect to the N-pyridine site (inside sphere) so that, generally, the three nitrogen atoms prefer to be located on the same side of the molecule (syn-syn conformer, as shown in scheme 5), which is favourable for H-bonding (see § IV.3, figure 4).



Scheme 5. The *syn-syn* disposition revealed the most stable conformer among the possible conformers of pyridylamide arm.

This feature together with the more or less pronounced torsion angle around the amide-bipyridine moiety, leads to the opposite disposition of the methyl group

of the two pyridine extremities with respect to the coplanar bipyridine/biquinoline/naphthyridine planes. This disposition can lead to chiral 1D H-bonded chains when the ligand is engaged with dicarboxylic acids. The last example obtained with $[4,4'$ -mpaBQ] $\cdot 2(\text{TFA})$ tends to confirm our expectation; indeed, adding an acid to the compound induces a colour change from colourless (free ligand) to bright yellow (ligand + TFA).

IV.6 Structural study of the ligands with dicarboxylic acids

As explained in section §IV.2, ligands were combined with divergent dicarboxylic acids. The ligands $[2,7\text{-mpanaphthy}]$, $[4,4'\text{-mpabpy}]$, $[6,6'\text{-mpabpy}]$, previously described, have been mixed in crystallisation tubes at room temperature with several different dicarboxylic acids depicted in figure 15.

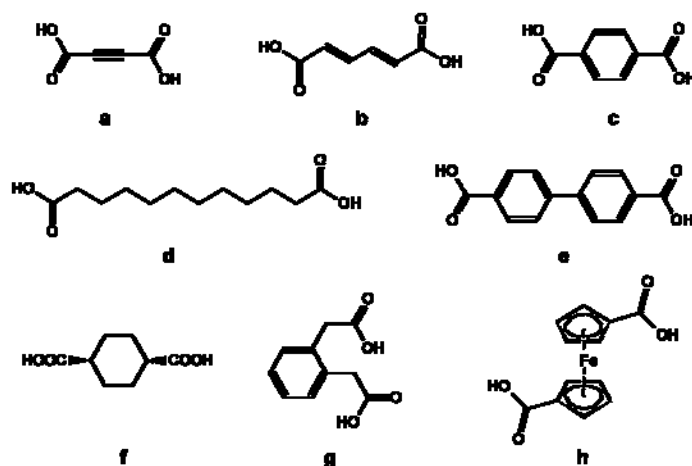


Figure 15. Tested dicarboxylic acid for the formation of H bonded networks with polyamide ligands: a) acetylene dicarboxylic acid, b) *trans, trans*-1,3-butadiene-1,4-dicarboxylic acid, c) terephthalic acid, d) dodecanedioic acid, e) biphenyl-4,4'-dicarboxylic acid, f) cyclohexane-*trans*-1,4-dicarboxylic acid, g) 2,2'-benzene-1,2-diyl diacetic acid, h) ferrocene dicarboxylic acid.

Among the four ligands tested, only in one case *i.e.*, the combination of [4,4'-mpabpy] with ferrocene dicarboxylic acid [Ferroxdc], we were able to obtain single crystals suitable for XRD analysis. The structure is described below. For combinations of diacids with [6,6'-mpabpy], the latter shows a marked tendency to crystallise alone. For the other two ligands [2,7-mpanaphthy] and [4,4'-mpaBQ], attempts to obtain crystals were unsuccessful. Owing to its very low solubility in most common solvents, ligand [4,4'-mpaBQ] was not tested.

IV.6.1 [4,4'-mpabpy] and Ferrocenedicarboxylic acid

A hydrogen bonded 1D network of formula $[\text{Fe}(\text{C}_6\text{H}_5\text{O}_2)_2][\text{C}_{24}\text{H}_{20}\text{N}_6\text{O}_2]$ or $[(\text{Ferroxdc})_2(4,4'\text{-mpabpy})_2]$ was obtained upon slow diffusion of a chloroform solution of the ligand into an *iso*-propanol solution of the dicarboxylic acid (see Annexe A). In the crystal, the two components are in 1:1 ratio and no solvent molecules are present in the lattice (see structure XLIII in the Annexes).

Within the chains, the connectivity is characterised by an alternating sequence of ligand and metallocene, as shown in figure 16b. There are two connecting nodes between the carboxylic acid and the ligand, (i) the expected N-pyridyl amide-carboxylic acid double H-bond recognition motif (see § IV.1), (ii) a single H-bond recognition mode between the second carboxylic acid and the nitrogen of one bipyridine ring [Fig. 16a]. The distances for both bonds are the following: $d_{\text{N}\cdots\text{O}} = 2.68, 2.79$ and 2.85 \AA and $d_{\text{NH}\cdots\text{O}} = 1.85, 1.99$ and 2.01 \AA .

There is no proton transfer between carboxylic acid and pyridine (hydrogen are omitted for clarity on the figure); the torsion angle between the two carboxylic acid on the ferrocene is of 78.1° .

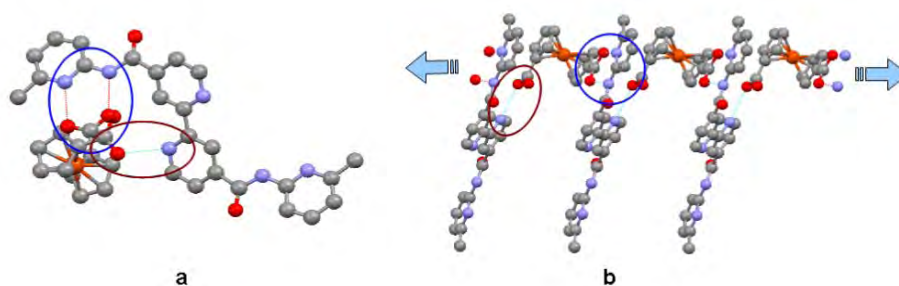


Figure 16. For $\{[4,4'\text{-mpabpy}]_2[\text{Ferroxdc}]_2\}$: a) both hydrogen bonding motives highlighted in red and blue circles and b) the formed H-bonded 1D chain.

The crystal packing (monoclinic, $P2(1)/n$) leads to the double hydrogen bonded 1D chains disposed along the x axis (green and orange in the figure 17a), each double chain is surrounded by other six mono dimensional chains in a hexagonal packing mode and constitutes one of the edge of the interlaced hexagonal cells as schematized in figure 17b.

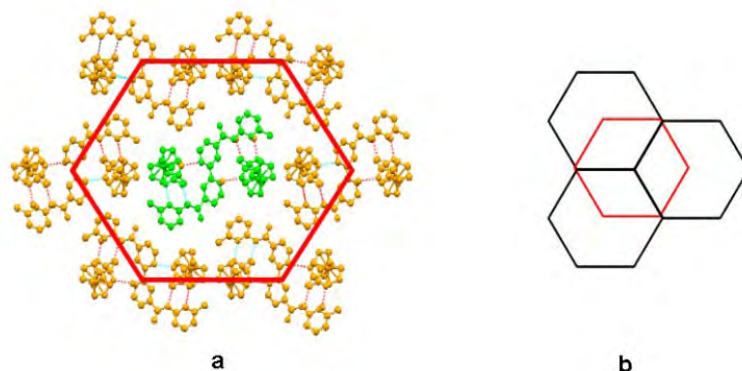


Figure 17. Crystal packing of $[2,7\text{-mphanaphthyl}]_2[\text{Ferroxdc}]_2$ double chains along the a axis (a) and schematic representation of the topological hexagonal disposition of the chains in the crystal (b).

When looking closer to the double chains, we can see that the main central motif [Fig. 18a] is based on two single chains embedded one into the other [Fig. 18b], the embedding is ensured by π - π stacking of the perfectly superimposed ligand rings with $d_{\pi-\pi} = 3.97$ and 4.07 Å.

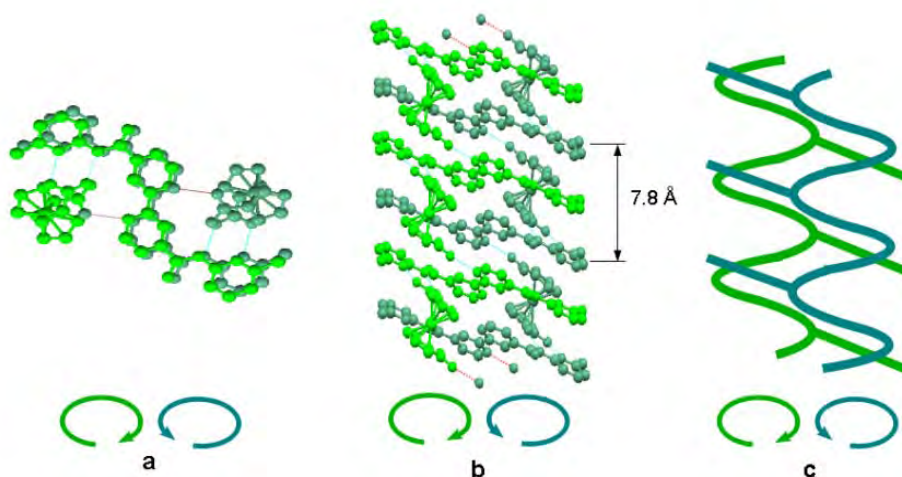


Figure 18. View of an isolated double 1D chain (a) along the x axis and (b) along the y axis, (c) embedding of two different helical chains through the pyridine 'tail'.

Each double chain is formed by the interlacing of two helical single chain of opposed chirality (P and M) with a pitch of 7.8 Å [Fig. 18b], the fourth pyridine ring is not involved in the hydrogen bonding pattern and behaves as a "tail", a simplified illustration of the chains interpenetration is proposed in figure 18c, the overall crystal lattice, being a racemate, is, of course, achiral.

This unique example of crystal structure between polyamides ligands and dicarboxylic acids shows the tendency of these types of ligands to form helical chains as already seen in the literature (see section § IV.2.1).

The third step now is to study the binding behaviour of these ligands towards metal cations.

IV.7 Structural study of the ligands with transition metals

In parallel to the crystallisation of hydrogen bonded structures, we have studied also the formation of metallic complexes under crystallisation conditions at room temperature. Three ligands [2,7-mpanaphthy], [4,4'-mpabpy] and [6,6'-mpabpy] have been combined with transition metal cations (Mn, Fe, Co, Ni, Cu, Zn, Ag, Pd and Pt).

Whereas metal complexation by [4,4'-mpabpy] and [6,6'-mpabpy] should lead to the formation of five member chelating rings, for [2,7-mpanaphthy], in principle, only four member chelating rings or binuclear complexes are expected.¹⁹

Appropriate crystallisation conditions were found to be difficult and suitable single crystals for XRD studies were obtained only in three cases using combinations of Cu(II), Mn(II) and Pt(II) with [2,7-mpanaphthy] and [4,4'-mpabpy] ligands.

IV.7.1 [2,7-mpanaphthy] and Cu(II)

The first structure concerns the combination of [2,7-mpanaphthy] and $\text{Cu}(\text{CF}_3\text{SO}_3)_2$. Crystals were obtained upon slow diffusion of an ethanol solution of the metal salt into a THF solution of the ligand. The ligand undergoes a spontaneous metal assisted hydrolysis of one of the two amide moieties leading to a non symmetrical di-substituted {2-[N-(6-methylpyridin-2-yl)carbamoil]-7-carboxy-1,8-naphthyridine} ([2-mono(mpanaphthy)]) ligand. A copper complex of general formula $\{[\text{Cu}(\text{II})(2\text{-mono(mpanaphthy)})_2(\text{H}_2\text{O})](\text{CF}_3\text{SO}_3)_2\}$ is formed without the presence of solvent molecules in the lattice (see structure XLII in the Annexes).

Copper is pentacoordinated and surrounded by the [N,N-O,O,O] set with a square based pyramid geometry, the five coordinated atoms are two N of the naphthyridine rings, two O belonging to the carboxylic acid moieties and one O atom of a water molecule occupying the apical position [Fig. 19a]. The complex is also characterised by four hydrogen bonds connecting the two ligands through the carboxylate unit and three nitrogen atoms with N-O distances of 3.35, 2.85, 2.61 Å. The methyl group of the pyridyl ring exhibits a torsion angle of ca 10°. It is noteworthy to point out that ligands are in the zwitterionic form with a proton transfer from the carboxylic acid to the methylpyridine ring ($\text{COOH} \leftrightarrow \text{COO}^-$ and $\text{PyN} \leftrightarrow \text{PyNH}^+$). The

¹⁹ a) A. Biffis, L. Conte, C. Tubaro, M. Basato, L.A. Aronica, A. Cuzzola, A. M. Caporusso; *J. Organomet. Chem.*, **2010**, 695, 792-798 ; b) Y. Chen, J.-S. Chen, X. Gan, W.-F. Fu; *Inorg. Chim. Acta*, **2009**, 362, 2492-2498

cationic charge on the compound is balanced by the presence of two $(\text{CF}_3\text{SO}_3)^-$ anions, as shown in figure 19b. The latter are also connected to the rest of the complex *via* H bonding.

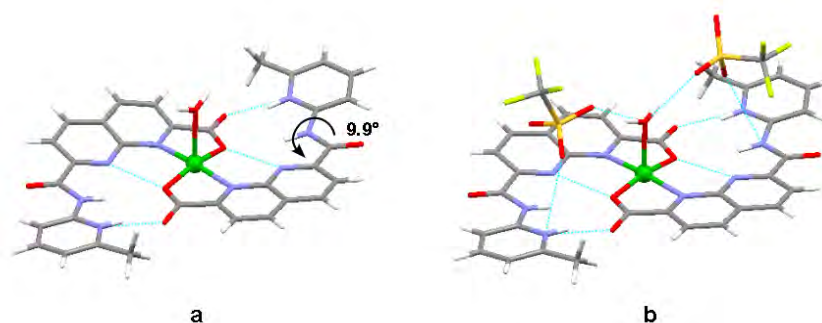


Figure 19. Di-substituted complex of $\{[\text{Cu}(\text{II})(2\text{-mono}(\text{mpanaphthy}))_2(\text{H}_2\text{O})](\text{CF}_3\text{SO}_3)_2\}$. a) Charge assisted hydrogen bonds between ligands and torsion around amide and b) second coordination sphere occupied by CF_3SO_3^- counterions.

The whole packing results from the formation of sandwiched units between two of these complexes (figure 20 left). This peculiar disposition probably maximizes the π - π stacking between the ligands (distance of ca 3.8 Å) [Fig. 19a]. The crystal packing is tight along the y and z axis. However, along the x axis, channels filled with the triflate counterions are formed [Fig. 20b].

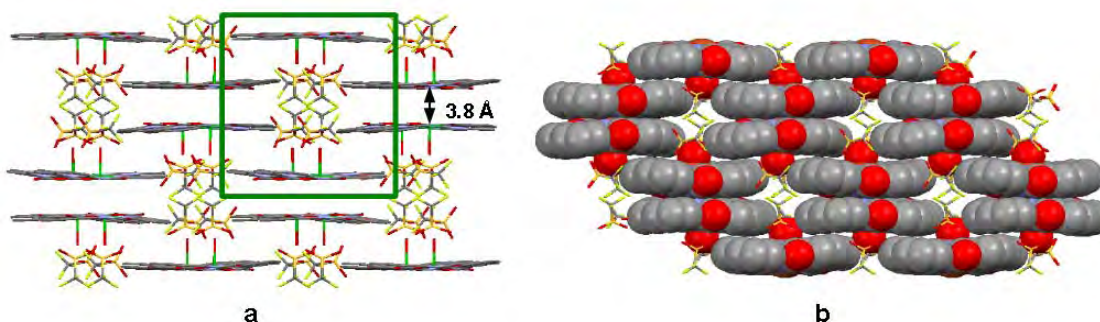


Figure 20. Crystal packing of $\{[\text{Cu}(\text{II})(2\text{-mono}(\text{mpanaphthy}))_2(\text{H}_2\text{O})](\text{CF}_3\text{SO}_3)_2\}$ complexes view along the x axis; a) in the green frame, single sandwich unit and b) filling of channels with CF_3SO_3^- in the spacefilling model.

IV.7.2 [4,4'-mpabpy] and Mn(II)

By slow diffusion of an alcoholic solution of manganese salt $\text{Mn}(\text{hfac})_2$ into a CHCl_3 solution of the ligand [4,4'-mpabpy] with a stoichiometric ratio of 2:1, crystals of sufficient quality and with formula $\{[\text{Mn}(\text{II})(\text{hfac})_2(\text{H}_2\text{O})_2] \subset \text{Mn}(\text{II})(4,4'\text{-mpabpy})(\text{hfac})_2\}_2$ were obtained (see structure XLIV in the Annexes).

The compound is formed by cocrystallisation of two Mn complexes, due to the used 2:1 metal/ligand stoichiometry. The mono-substituted complex and the $\text{Mn}(\text{hfac})_2$ salt are present in the crystal lattice forming a dimeric cage complex $[\text{Mn}(\text{II})(4,4'$ -

mpabpy)(hfac)₂] containing one [Mn(II)(hfac)₂(H₂O)₂] molecule (see figure 21c). All the species are neutral and interconnected *via* hydrogen bonds.

As we can see in figure 21a and b, there is a change of the geometry around the manganese centre when compared to the original Mn(hfac)₂ salt. In the latter the metal adopts the octahedral coordination geometry with two water molecules occupying the apical positions and the hexafluoroacetylacetonate anions in the square base of the pyramid [Fig.21b]. In the case of [Mn(II)(4,4'-mpabpy)(hfac)₂] complex, the [4,4'-mpabpy] ligand replaces the two water molecules, changing the geometry to trigonal prismatic [Fig. 21a].

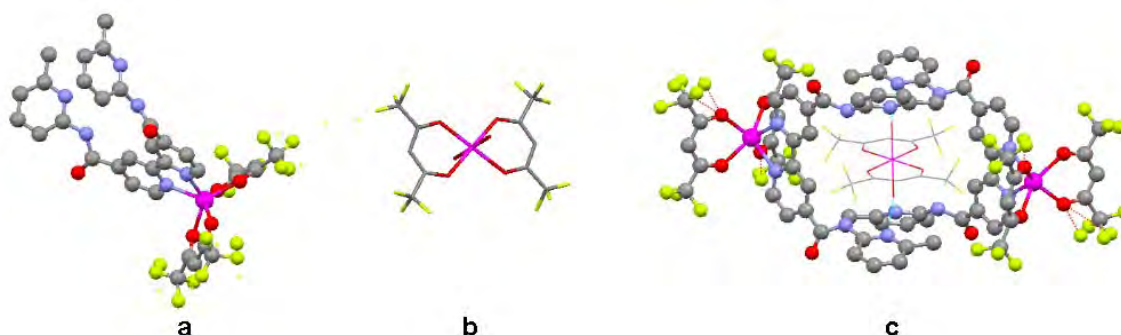


Figure 21. a) [Mn(II)(4,4'-mpabpy)(hfac)₂] complex; b) [Mn(II)(hfac)₂(H₂O)₂] guest molecule and c) inclusion trimer {[Mn(II)(hfac)₂(H₂O)₂] ⊂ Mn(II)(4,4'-mpabpy)(hfac)₂]₂}.

Two molecules of [Mn(II)(4,4'-mpabpy)(hfac)₂] encapsulate one molecule of the [Mn(II)(hfac)₂(H₂O)₂] salt through hydrogen bonding between the oxygen atom of the apical water molecules and the nitrogen of the methylpyridine rings with O-N distances (*d*_{O-N}) of 2.68- 2.71 Å, forming thus a dimeric cage. The torsional angle around the amide bond is, in this case, rather substantial (63.8° and 73.0°), this torsion directs the N-pyridyl amide moieties towards the inner cavity leading to four convergent binding sites able to form the inclusion complex. The whole packing is composed of stacks with short distances between trimeric aggregates (see figure 22).

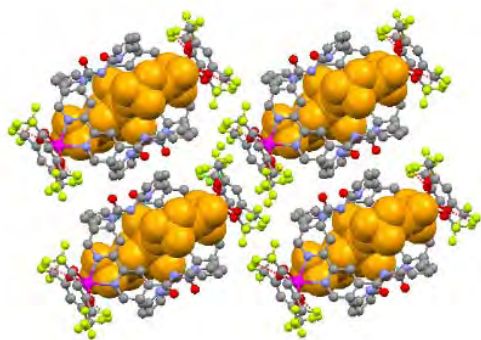


Figure 22. Crystal packing of the inclusion trimeric units for {[Mn(II)(hfac)₂(H₂O)₂] ⊂ Mn(II)(4,4'-mpabpy)(hfac)₂]₂}

IV.7.3 [4,4'-mpabpy] and Pt(II)

The last crystals (formula $[\text{Pt(II)}(4,4'\text{-mpabpy})\text{Cl}_2]\cdot(\text{C}_3\text{H}_6\text{O})$) were obtained upon slow diffusion followed by evaporation of an acetonitrile solution of the platinum complex $[\text{Pt}(\text{benzonnitrile})_2\text{Cl}_2]$ into a solution of the ligand [4,4'-mpabpy] in acetone (see structure XLV in the Annexes).

The platinum complex is formed, as expected, through substitution of both benzonitrile ligands by the chelating [4,4'-mpabpy] units, the two chloride anions, occupying the other two coordination positions, act as blocking ligands. The coordination geometry around the metal is square planar [Fig. 23a], typical of the Pt(II) complexes, with distances: $d_{\text{Pt-N}} = 2.01 \text{ \AA}$ and $d_{\text{Pt-Cl}} = 2.29 \text{ \AA}$. The configuration of the ligand is interesting since three out of four pyridine rings are coplanar and the fourth one twisted with an angle $> 30^\circ$ leading to a 'bow' shape complex (see figure 23b).

Within the arm that lays on the same molecular plane, the carbonyl is pointing outside and the two amino-pyridine nitrogen atoms are oriented towards the acetone molecule hosted inside the cavity formed by the ligand. This arrangement allows the binding of the solvent molecule (acetone) through $[\text{C-O}\cdots\text{H-N}]$ hydrogen bonding ($d_{\text{NH-O}} = 2.20 \text{ \AA}$ and $d_{\text{N-O}} = 3.05 \text{ \AA}$). The other arm is too far to form a second hydrogen bond with acetone and prefers twisting in order to form connections with other surrounding molecules.

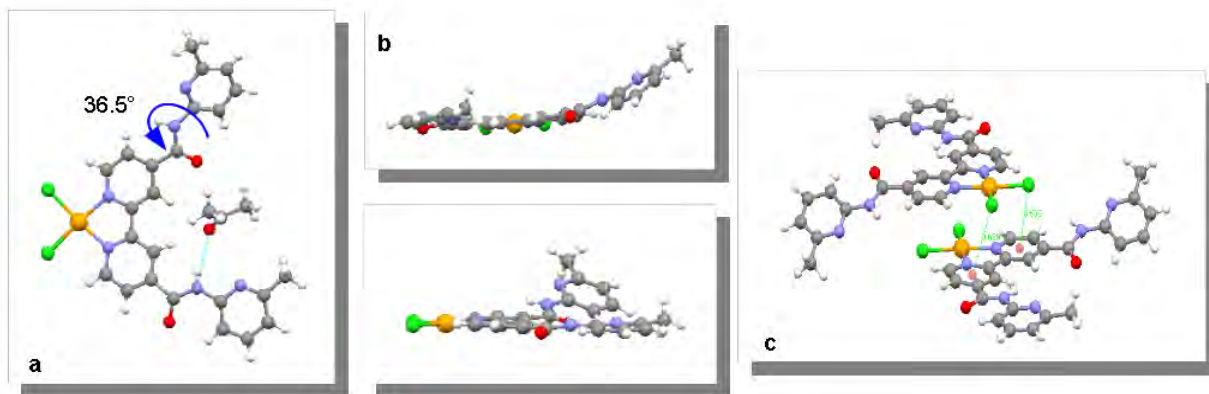


Figure 23. a) Coordination sphere for $[\text{Pt(II)}(4,4'\text{-mpabpy})\text{Cl}_2]\cdot(\text{C}_3\text{H}_6\text{O})$, b) lateral view showing the bow shape adopted by the complex and c) disposition of two consecutive complexes.

The overall network is tridimensional and the crystal packing, illustrated in figure 24, results from different type of short intermolecular contacts, which are mainly of the $[\text{N}\cdots\text{HC}]$ and $[\text{CO}\cdots\text{HC}]$ hydrogen bonding type between the amide group and the benzene C-H with distances: $d_{\text{N-C}} = 3.44\text{-}3.23 \text{ \AA}$, $d_{\text{N-HC}} = 2.62\text{-}2.66 \text{ \AA}$, $d_{\text{O-C}} = 3.31 \text{ \AA}$, $d_{\text{O-HC}} = 2.38 \text{ \AA}$.

Remarkably, no π - π interactions are found. However, weak Cl... π interactions²⁰, with $d_{\text{Cl}-\pi} = 3.53$ - 3.66 Å are observed [Fig. 23c].

Molecules form zig-zag planes which are stacked one on the top of the other (see figure 24b and d). Molecules are interconnected in all three directions *via* loose hydrogen bonds. Acetone molecules fill the empty spaces as illustrated in figure 24c.

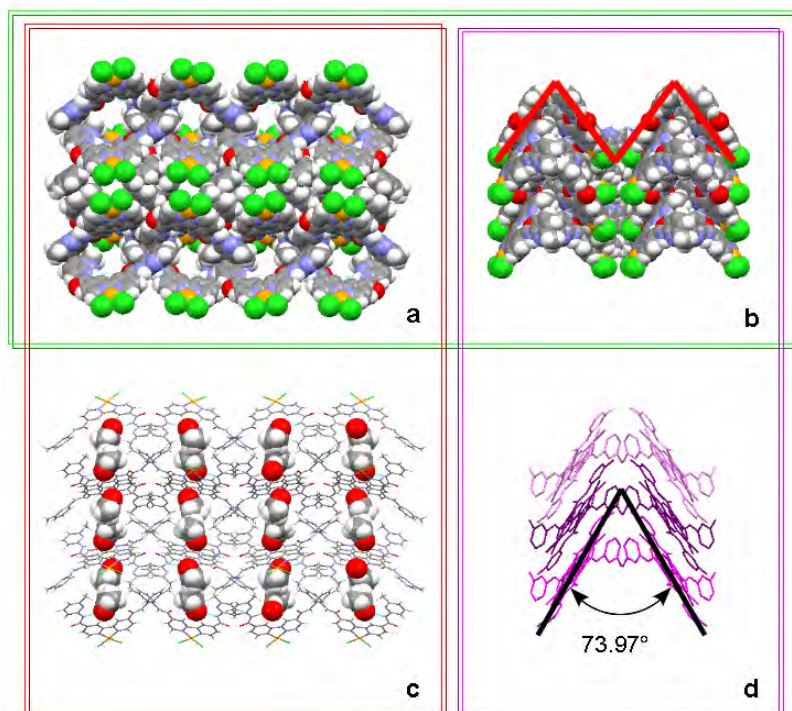


Figure 24. Crystal packing of $[Pt(II)(4,4'\text{-mpabpy})Cl_2] \cdot (C_3H_6O)$ complex view along the x axis (a) and along the z axis (b); c) crystal packing comprising acetone molecules and d) the angle formed between molecules.

The manganese and platinum complexes with the ligand [4,4'-mpabpy] confirm our hypothesis that it is possible to use the ligand as chelating complex towards metal cations and, at the same time, exploit the N-pyridyl amide ability to form hydrogen bonds. However, the prediction of such assemblies is rather difficult and remains challenging.

IV.8 Conclusions

This preliminary study on N-pyridyl carboxamide ligands appended with bipyridine type moieties gave interesting results that require further investigations. As expected, the crystal structure of $[(4,4'\text{-mpaBQ}) \cdot (CF_3COOH)]$ (§ IV.5.1.4) showed the targeted hydrogen bonding pattern between carboxylate (COO^-) anion and the N-

²⁰ M. Mascal, A. Armstrong, M. D. Bartberger; *J. Am Chem. Soc.*, **2002**, *124*, 6274-6276; b) T. Dorn, C. Janiak, K. Abu-Shandi; *CrystEngComm*, **2005**, *7*, 633-641

pyridinium (HN-C-NH)⁺ cation. Furthermore, the crystal structure of [4,4'-mpabpy]₂[Ferroxdc]₂ (§ IV.5.2.1) showed, in addition to the H-bonding motif, the formation of an helical architecture. Dealing with metal complexes, the few obtained results account for the fact that the naphthyridyne appended with two side arms are not the best ligands for hosting metal centres for steric reasons. Conversely the bipyridine based ligand exhibits the expected behaviour.

Since the collected crystal data on both the hydrogen bonding with dicarboxylates and the complex formation with transition metal, is still unfinished, no tests have been done yet to obtain hybrid networks.

The results obtained are nevertheless encouraging and should lead to further new hybrid architectures. However, this requires the development of adapted crystallisation procedures.

Chapter V

General conclusions and perspectives

V.1 General conclusions and perspectives

During this work, using the basic concepts of molecular tectonics, we were interested in the rational design of molecular assemblies. The aim of the undertaken investigations was to develop three-component systems based on H-bond donor, H-bond acceptor tectons and metal centres or complexes. In order to achieve a better predictive capability, we tried to better understand the different envisaged connectivity patterns.

This ambitious project was based (Chapter II & III) on the use of a recognition motif between a carboxylate (RCOO^-), as H-bond acceptor, and a cyclic bisamidinium cation ($\text{C-NH}^+\text{-C}$) as H-bond donor. These recognition patterns have been previously developed in the group for building purely organic networks [Fig. 1a]. A second recognition motif between N-pyridyl carboxamide ($(\text{C}=\text{O})\text{NH-Py}$) and carboxylic acid [Fig. 1b] was also developed (Chapter IV).

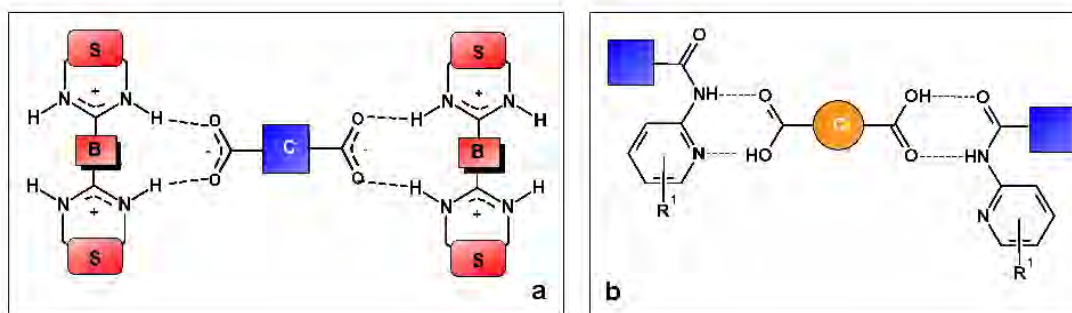


Figure 1. a) Carboxylate-bisamidinium and b) N-pyridyl carboxamide-carboxylic acid H bond recognition motives for building molecular networks.

V.1.1 Hybrid networks based on carboxylates ligands and bisamidinium cations (Chapter II and III)

In the first part, we used the so-called "one pot approach" to obtain hybrid organic-inorganic networks based on complementarity between bis-amidinium tectons (BAD22 and BAD23) and carboxylate derivatives bearing a N-donor ligand (4,4'-dcbpy, 4,4'-dcBQ, 4,7-dcphen, etc.). This strategy is based on the simultaneous use of H bonding and coordination events with transition metals. We were able to determine experimental conditions to overcome solubility problems and to demonstrate that the carboxylate-bisamidinium recognition motif leading to purely organic systems may be extended to hybrid metal containing architectures. Two three-component systems based on Ag (I) and Cu (II) cations [Fig.2] have been obtained. The obtained crystals exhibit a rather good stability over the time both in the solvents and when exposed to air. However, these achievements showed two important drawbacks which are the intrinsic instability of the bisamidinium cation towards hydrolysis and the long period

required for the crystallization process. In order to overcome this difficulty, we have to develop new crystallization processes.

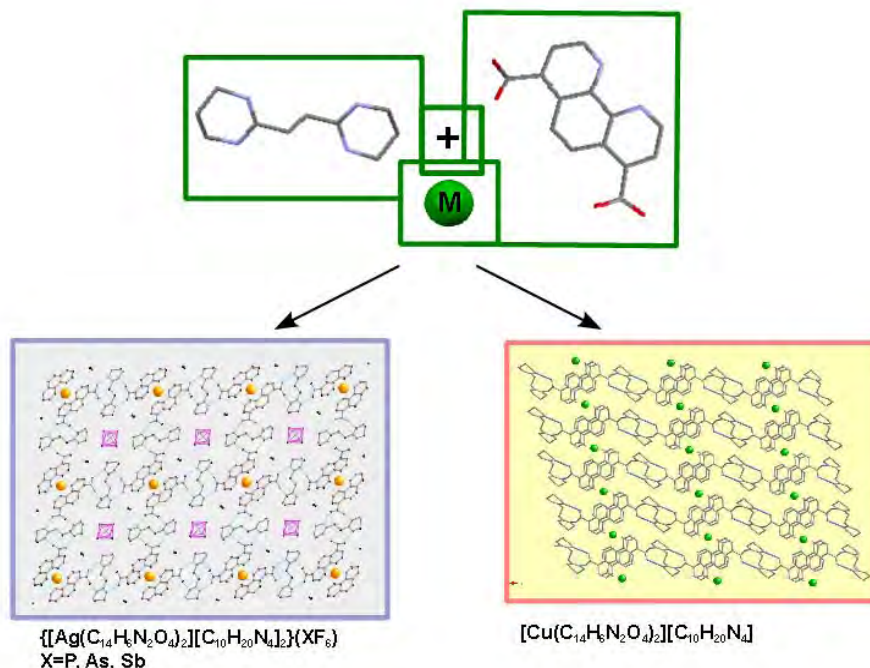


Figure 2. Hybrid three-components systems based on BAD23, 4,7-dcphen, Ag (I) or Cu (II): (left) $\text{Ag}(\text{C}_{14}\text{H}_6\text{N}_2\text{O}_4)_2[\text{C}_{10}\text{H}_{20}\text{N}_4]_2 (\text{XF}_6)$ ($\text{X}=\text{P, As, Sb}$) 2-D networks and (right) $[\text{Cu}(\text{C}_{14}\text{H}_6\text{N}_2\text{O}_4)_2][\text{C}_{10}\text{H}_{20}\text{N}_4]$ 3-D network.

Beside these results, obtained by a one-pot approach, we also used a stepwise approach which was based on the initial synthesis of different metallatectons bearing carboxylate ligands as building blocks followed by the formation of hybrid networks in the presence of bis-amidinium tectons as a subsequent step.

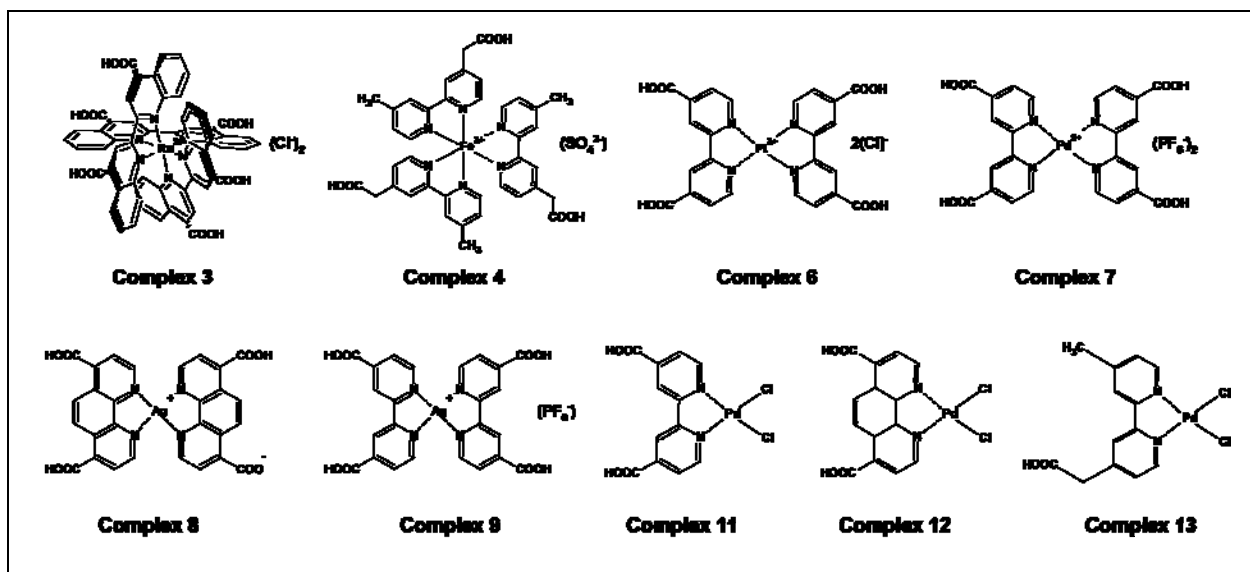


Figure 3. Gallery of the new complexes synthesized and presented in chapter II.

This strategy required the synthesis of new complexes [Fig. 3] based on transition metals and N-donor ligands bearing one or two carboxylate groups at their periphery. The low solubility of both ligands and final complexes, required the development of adapted procedures for the synthesis and the purification of each compound (see Experimental part). Although many attempts have been made, unfortunately, no crystalline materials were obtained using this strategy.

New directions have been explored which require further development in the future: i) the H-bond donor (amidinium moiety) may be combined with the N donor ligand¹ (see § II.3.2) and the H-bond acceptor (carboxylate) located on the connector, this strategy needs to be deeply investigated; ii) the use of another H-bond acceptor based on more stable bisamidinium cations, such as BADbenz2/BADbenz3², which were previously shown in the group to be stable towards hydrolysis.

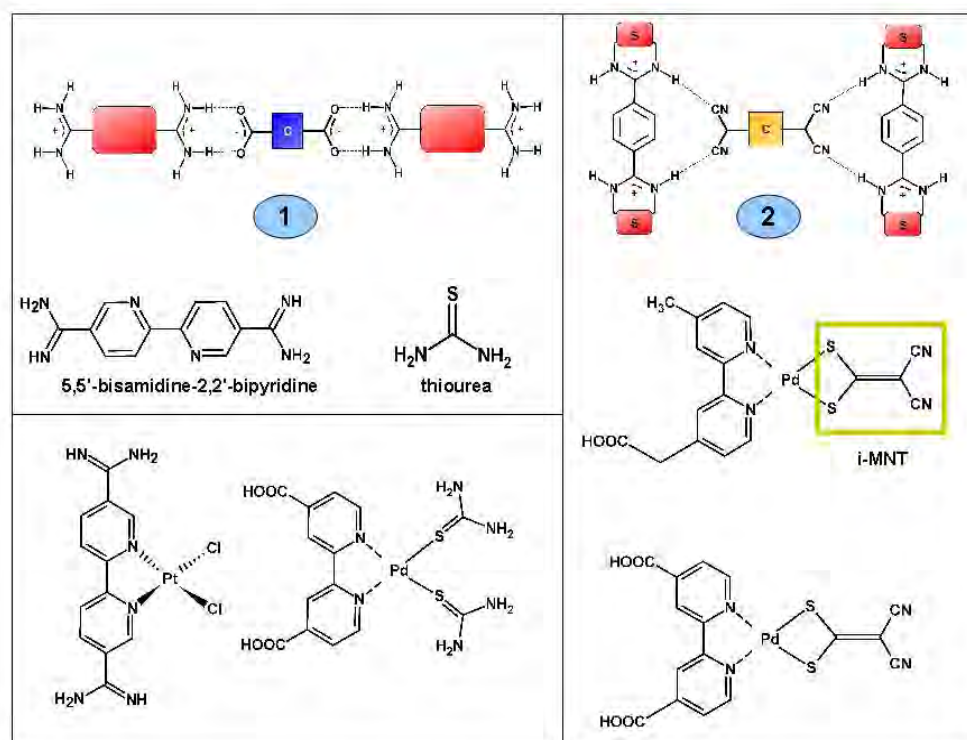


Figure 4. New perspectives: in **1**, the use of a new *N,N*-donor ligands bearing amidinium moieties and, in **2**, the use of the recognition motif between nitrile H-bond acceptor groups and cyclic benzo-bisamidinium H-bond donor group.

Along these lines, we intended to prepare heteroleptic Pd(NN)(SS)-type complexes for which NN is a bipyridine and SS is the chelating dithiolate ligand, 1,1-dicyano-3,2-ethylenedithiolate (i-MNT) or two thioureas, [Fig. 4-1]. The new complexes

¹ J. P. Kirby, J. A. Roberts, D. G. Nocera, *J. Am. Chem. Soc.*; **1997**, *119*, 9230-9236

² P. Dechambenoit, S. Ferlay, N. Kyritsakas, M. W. Hosseini, *J. Am. Chem. Soc.*, **2008**, *130*, 17106–17113

bear different binding sites that can be of interest for simultaneous recognition of carboxylate anions by amidinium or cyclic benzo-bisamidinium cations (see figure 4-2).

In the second part (Chapter III), using the ligands 6,6'-dcbpy and 2,9-dcphen, that present a different connectivity pattern towards metal action, new compounds have been prepared. The interesting feature associated with the new ligands results from the fact that the carboxylate unit, being localized close to the chelating moiety, may participate in the binding of metal cations. This was not the case for ligands presented in chapter II. Unfortunately, we were not able to obtain three components H bonded systems, however, we generated and characterized new coordination networks using Zn (II) or Ag (I).

The coordination network involving Ag (I) seems rather interesting and should be further fully exploited [Fig. 5a]. To better understand the behavior and formation of this structure, it seems necessary to undertake an accurate study of crystallization conditions over a range of pH. Besides, using a ligand with more condensed aromatic rings, as those one proposed in figure 5b, it might be possible to favor, through π -stacking, the formation of helical chains associating the electron transport properties of π -conjugated polycyclic aromatic hydrocarbons³ such as chrysene, perylene or dibenzo-perylene. Very interesting is also the possibility to assemble this kind of structures through template assisted synthesis: forming, for example, molecular nanorods within silica nanotubes⁴ or, using a biological scaffold, assembling chromophoric helical stacks within protein nanotubes⁵.

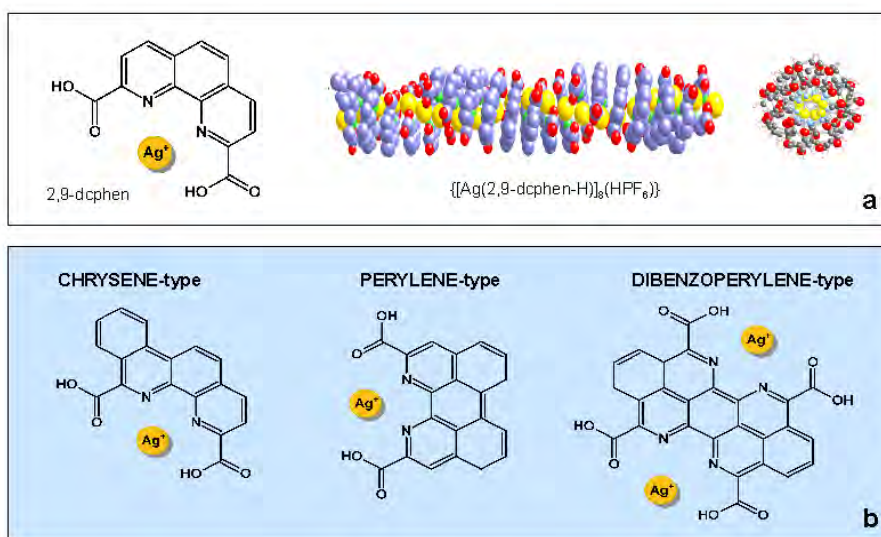


Figure 5. a) Formation of the striking $\{[Ag(2,9-dcphen-H)]_8(HPF_6)\}$ helical 1-D network, b) possible evolution of the heteroaromatic ligand in order to obtain 1-D silver chains.

³ X. Li, A. Staykov, K. Yoshizawa; *J. Phys. Chem. C*, **2010**, *114*, 9997-10003

⁴ R. O. Al-Kaysi, R. J. Dillon, L. Zhu, C. J. Bardeen; *J. Colloid Interface Sci.*, **2008**, *327*, 102-107

⁵ A. de la Escosura, P. G. A. Janssen, A. P. H. J. Schenning, R. J. M. Nolte, J. J. L. M. Cornelissen; *Angew. Chem. Int. Ed.*, **2010**, *49*, DOI: 10.1002/anie.201001702

V.1.2 Hybrid networks based on polyamide ligands (Chapter IV)

This study on the formation and the coordination of N-pyridyl carboxamide substituted bipyridine-like ligands gave some interesting preliminary results encouraging to further pursue the project. Whereas the crystal structure of $[(4,4'\text{-mpaBQ})^*(\text{CF}_3\text{COOH})]$ (§ IV.5.1.4) shows hydrogen bonding motif between the carboxylate (COO^-) anion and the N-pyridinium (HN-C-NH^+) cation, the crystal structure of $[4,4'\text{-mpabpy}]_2[\text{Ferroxdc}]_2$ (§ IV.5.2.1) not only confirms the robustness of the recognition pattern but in addition shows the possibility of forming a helical chain.

The project presents also other interesting possibilities of extension such as:

- (i) the reduction of the carbonyl group [fig. 6A];
- (ii) the use of a rigid phenanthroline backbone instead of the bipyridine one;
- (iii) the functionalization of the pyridyl ring with, for example, an amine moiety [Fig. 6C].

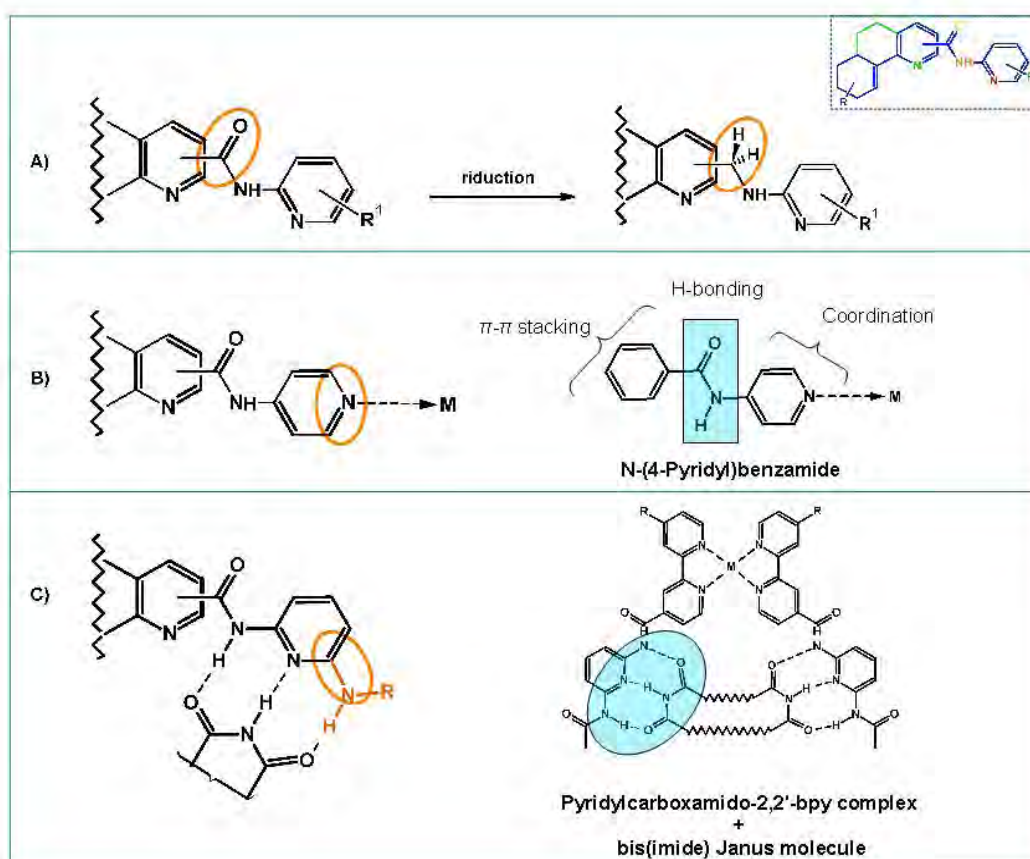


Figure 6. Perspectives of further development of the work. A) Reduction of the carbonyl group, B) changing the nitrogen position on the pyridyl moiety will generate a divergent coordination site as for the networks based on NPBA (ref.4); C) adding a third H-bonding site to strengthen and make the binding more selective, as for the bi(imide) Janus compounds (ref.5).

As demonstrated in the case of the ligand 4,4'-mpabpy, the use of the N-pyridyl carboxamide makes the amidic C=O eligible for intervening in the hydrogen bonding

network; the reduction of the carbonyl function to N-pyridyl amine moiety could reasonably avoid this interference and favor the formation of the desired recognition pattern.

We can also change the position of the nitrogen on the pyridyl fragment [Fig. 6B], this will add a second divergent binding site for the coordination event. This approach has been used by Stang *et al.*⁶ using N-(4-pyridyl)benzamide (NPBA) for building supramolecular networks based on coordination bonds, H-bonding and π - π stacking interactions.

Another possibility may be the increase of the number of hydrogen bonds within the recognition pattern, thus shifting from a 'two-point recognition' motif to a 'three-point recognition' motif (see figure 6C). This could be achieved by changing the methyl substituent in 6'- position on the pyridyl substituent with, for example, an amine group. The self-recognition illustrated in the figure 6C (blue circle) between the DAD (Donor-Acceptor-Donor) profile of a 2',6'-bis(amino)pyridine and a bi(imide) is recognized as one of the most probable (see § IV I.1). This approach has been used for example by Huc, Lehn *et al.*⁷ in the Dynamic Combinatorial Chemistry approach.

⁶ J. C. Noveron, M. S. Lah, R. E. Del Sesto, A. M. Arif, J. S. Miller, P. J. Stang; *J. Am. Chem. Soc.*, **2002**, *124*, 6613-6625

⁷ I. Huc, M. J. Krishe, D. P. Funeriu, J.-M. Lehn; *Eur. J. Inorg. Chem.*, **1999**, 1415-1420

Chapter VI

Experimental Section

VI.1 Generalities

Chemicals

3,3'-Dicarboxy-2,2'-bipyridine, 4,4'-Dimethyl-2,2'-bipyridine, 6,6'-Dimethyl-2,2'-bipyridine, 2,9-Dimethyl-1,10-phenanthroline, 4,7-dimethyl-1,10-phenanthroline were purchased from SigmaAldrich.

The synthesis of 4,4'-Dicarboxy-2,2'-bipyridine, 6,6'-Dicarboxy-2,2'-bipyridine, 4,7-Dicarboxy-1,10-phenanthroline, 2,9-Dicarboxy-1,10-phenanthroline, 4-Carboxymethyl-4'-methyl-2,2'-bipyridine and Tetrakis(4-carboxyphenyl)silane was achieved by adapting reported literature procedures.

Solvents

Analytical solvents

Acetone ACS reagent (Sigma-Aldrich)
Acetonitrile ACS reagent (Sigma-Aldrich)
Chloroform stabilized ISO reagent (Sigma-Aldrich)
Dichloromethane 99.9% (Fluka)
N,N-Dimethylformamide 99.8% (Fluka)
Dimethylsulfoxide 99.5% (Riedel de Haën)
1,4-Dioxane purum for analysis (Sds)
Methanol – RS for HPLC (Carlo Erba)
Ethanol Absolute - RPE ACS reagent (Carlo Erba)
Isopropyl alcohol RPE Acs reagent (Carlo Erba)
1-Butanol R.P. Normapur AR (Prolabo)
Water chromasolv plus for HPLC (SigmaAldrich)
Tetrahydrofurane 99.9% p.a. stabilized (SigmaAldrich)
Triethylamine min 99% (Riedel-de Haën)
Benzene ACS reagent (Riedel-de Haën)

Technical solvents

Ethyl acetate (SDS-99.8%)
Acetone (Carlo Erba-99.8%)
Chloroform RE (Carlo Erba-99%)
Dichloromethane (SDS-99.95%)
Cyclohexane (SDS-99.8%)
Methanol (Carlo Erba-99.9%)
Ethanol (Carlo Erba-96.2%)
Diethyl ether (SDS-99.7%)

Toluene RE (Carlo Erba->99%)
n-Pentane synthesis grade (Sds-99%)
Petroleum ether 35°-60° RE (Carlo Erba)

Dry solvents

THF was distilled over sodium prior to use
Dichloromethane was distilled over P₂O₅ prior to use

Acids & Bases

Sulfuric acid 95-97% (Sigma Aldrich)
Nitric acid fuming 100% Gr for analysis (Merck)
Hydrochloric acid 37% ACS reagent (SigmaAldrich)
Hydrochloric acid 0.1 mol Fixanal (Fluka) was used to prepare 0.1M HCl solution
Potassium hydroxide 0.1 mol Fixanal (Riedel-de Haën) was used to prepare 0.1M KOH solution
Sodium hydroxide 0.1 mol Fixanal (Riedel-de Haën) was used to prepare 0.1M NaOH solution

Chromatographic supports

Silica gel 60 (0.063-0.200 mm) - Merck 7734
Aluminium oxide 90 active neutral (0.063-0.200 mm) - Merck 1077
TLC aluminium sheets silica gel 60 F₂₅₄ - Merck 5554
Aluminium oxide pre-coated plastic sheets 0.2 mm Polygram Alox N/UV₂₅₄ – Macherey-Nagel
Sephadex G-15, 40-120 µm bead size (Sigma-Aldrich)
Lipophilic Sephadex LH20, 25-100 µm bead size (Sigma-Aldrich)

Analysis and instrumentation

a) ¹H- and ¹³C-NMR spectra were recorded at room temperature if not mentioned otherwise on Bruker AV300 (300 MHz), Bruker AV 400 (400 MHz) and Bruker DRX-500 (500 MHz) spectrometers by the NMR service of the Institut de Chimie of the University of Strasbourg. The NMR spectra were referenced to the residual peak of the used deuterated solvent.

The chemical shifts of the proton signals are given in ppm followed by the multiplicity of the signal (s: singlet, d: doublet, t: triplet, dd: doublet of doublets, q: quadruplet, m: multiplet) in brackets, the coupling constants are given in hertz.

b) Mass spectra were recorded by the Mass Spectrometry service of the Institut de Chimie of the University of Strasbourg. ESI-MS were obtained on a microTOF LC spectrometer (Bruker Daltonics), MALDI spectra were obtained on TOF/TOF Autoflex II spectrometer (Bruker Daltonics).

c) Elemental analysis were performed by the Microanalysis service of the Institut de Chimie of the University of Strasbourg; compounds containing Ru were analysed by the Service Central D'Analyse of CNRS in Solaize (France).

d) Melting points were obtained on a Büchi 510 melting point apparatus in a capillary tube.

e) FT-IR spectra were recorded on a Shimadzu FTIR-8400S spectrometer as KBr pellets or as powders with the ATR detector, as specified. The following abbreviations are used to characterise the observed bands: w (weak), m (middle), s (strong), b (broad).

f) UV-visible spectra were measured on a Perkin Elmer Uvikon XL spectrometer. Wavelengths are given in nm and extinction coefficients (ϵ) are presented in $\text{L}\cdot\text{mol}^{-1}\cdot\text{cm}^{-1}$.

g) X-ray analyses were performed on a Bruker APEX8 CCD Diffractometer equipped with a liquid N_2 Oxford Cryosystem device at 173(2) K, using graphite-monochromated $\text{Mo-K}\alpha$ ($\lambda = 0.71073 \text{ \AA}$) radiation.

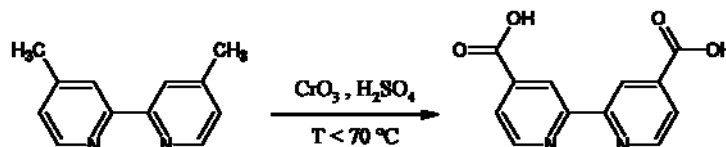
h) Powder diffraction studies (PXRD) diagrams were collected on a Bruker D8 diffractometer using monochromatic $\text{Cu-K}\alpha$ ($\lambda = 1.54056 \text{ \AA}$) radiation with a scanning range between 3 and 40° and using a scan rate of 0.2°/min.

i) Thermal Gravimetric analyses were performed on a Perkin Elmer Pyris TGA6 machine. All measurements were carried out under nitrogen flow (20 mL/min) and a heating rate of 2°C/min.

VI.2 Synthesis of ligands

Ligand 1

2,2'-Bipyridine-4,4'-dicarboxylic acid - [4,4'-dcbpy]¹



Experimental:

4,4'-Dimethyl-2,2'-bipyridine (commercially available) (5 g; 27 mmol) was added at once to 100 ml of 95 % H₂SO₄ keeping the temperature at 20 °C. The colourless solution was stirred at r.t. for 15 minutes and then CrO₃ (13.5 g, 135 mmol) was added carefully in small portions while cooling in a ice-water bath. The brown-yellow solution was stirred while keeping the temperature lower than 70 °C until the colour turned to green. The green solution was poured in a minimum amount of ice and was left to precipitate at 4°C overnight. The product was recrystallized from hot water and methanol. Yield: 94%

Characterization:

Molecular Formula: C₁₂H₈N₂O₄ **Molecular Weight:** 244.20

Deprotonated form:

¹H-NMR [D₂O/Et₃N, 300MHz, 25°C, δ(ppm)]: 8.58 (d, broad, 2H, 6,6'-H), 8.21 (s, 2H, 3,3'-H), 7.68 (d broad, 2H, 5,5'-H)

¹³C-NMR [D₂O/Et₃N, 300MHz, 25°C, δ(ppm)]: 172.7 (COO), 155.6, 149.6 (CH), 146.3, 123.3 (CH), 121.1 (CH)

Protonated form:

¹H-NMR [DMSO, 300MHz, 25°C, δ(ppm)]: 8.91 (dd, J_{5,6}=4.9 Hz, J_{3,6}=0.8 Hz, 2H, 6,6'-H), 8.84 (dd, J_{6,3}=0.8 Hz, J_{5,3}=1.6 Hz, 2H, 3,3'-H), 7.90 (dd, J_{6,5}=4.9 Hz, J_{3,5}=1.6 Hz, 2H, 5,5'-H)

¹³C-NMR [DMSO, 300MHz, 25°C, δ(ppm)]: 166.5 (COO), 155.9, 151.0 (CH), 140.2, 123.9 (CH), 120.0 (CH)

MS (ESI -): m/z 243.1 [M-H]⁻, 487.1 [2M-H]⁻

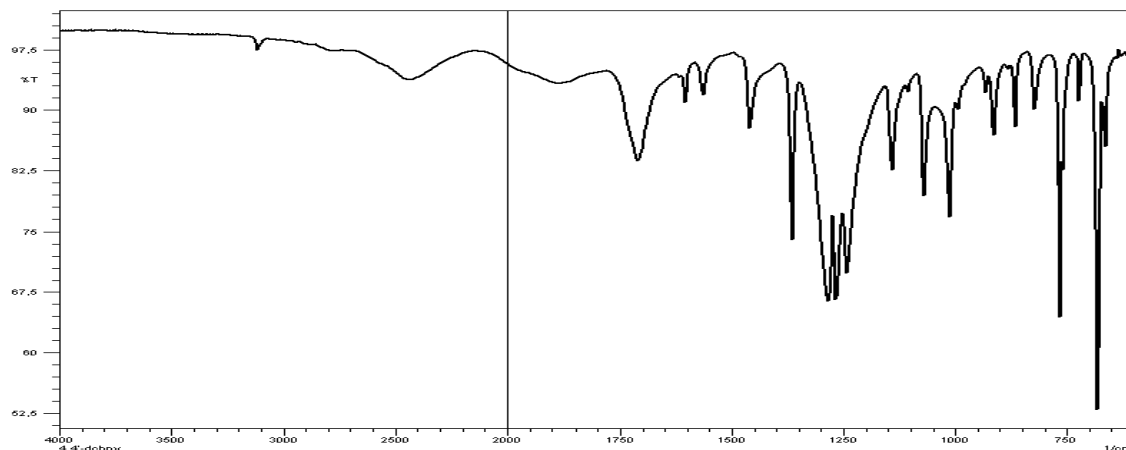
¹ O. Schwarz, D. van Loyen, S. Jockusch, N. J. Turro, H. Dürr; *J. Photochem. Photobiol. A: Chemistry*; **2000**, *132*, 91-98

mp (°C): >300 °C

Elemental analysis: Found: C, 56.69; N, 10.71; H, 4.47.

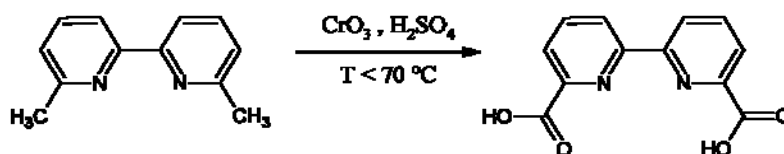
Calc. for $C_{12}H_8N_2O_4 \cdot CH_3OH$: C, 56.52; N, 10.14; H, 4.37.

IR (ATR): 3114, 2440, 1710 s (ν C=O), 1604, 1563, 1461 m, 1364 s, 1287 s, 1266 s, 1242 s (ν C-O), 1142 m, 1071 m, 1014 m, 766 m, 681 m cm^{-1}



Ligand 2

2,2'-Bipyridine-6,6'-dicarboxylic acid - [6,6'-dcbpy]^{2,3}



Synthesis:

Commercially available 6,6'-Dimethyl-2,2'-bipyridine (1 g; 5.4 mmol) was added slowly to a 30 ml solution of 95% H_2SO_4 in an ice-water bath. The mixture was stirred at r.t. for 30 minutes before CrO_3 (2.6 g; 27 mmol) was added carefully in small portions in a ice-water bath. The mixture was stirred while keeping the temperature lower than 70 °C for 30 minutes and was further stirred overnight at r.t. When the colour of the solution had turned from brown to dark-green, the reaction mixture was poured into ice and was left to precipitate in the fridge overnight. The greenish precipitate was filtered and acetone was added to the mother liquor causing further precipitation. The precipitate was again filtered. This procedure was replicated

² E. Buhleier, W. Wehner, F. Vögtle; *Chem. Ber.*, **1978**, *111*, 200-204

³ V.-M. Mukkala, M. Kwiatkowski, J. Kankare, H. Takalo; *Helvetica Chim. Acta*, **1993**, *76*, 893-899

several times. All recovered precipitates were combined and recrystallized from hot water and washed with acetone to afford a white powder (0.7 g). Yield: 55%

Characterization:

Molecular Formula: $C_{12}H_8N_2O_4$ **Molecular Weight:** 244.20

Deprotonated form:

1H -NMR [D_2O/Et_3N , 300MHz, 25°C, δ (ppm)]: 8.32 (dd, $J_{3,4}=7.8$ Hz, $J_{3,5}=1.1$ Hz, 2H, 3,3'-H), 7.96 (t, $J_{3,4}=J_{3,5}=7.8$ Hz, 2H, 4,4'-H), 7.86 (m, $J_{4,5}=7.7$ Hz, $J_{3,5}=1.1$, 2H, 5,5'-H)

^{13}C -NMR [D_2O/Et_3N , 300MHz, 25°C, δ (ppm)]: 172.8 (COO), 154.9, 153.3, 138.7 (CH), 123.9 (CH), 123.5 (CH)

Protonated form:

1H -NMR [DMSO, 300MHz, 25°C, δ (ppm)]: 8.75 (d, $J_{3,4}=7.2$ Hz, 2H, 3,3'-H), 8.17 (m, $J_{4,3}=7.2$ Hz, $J_{4,5}=7.5$ Hz, 4H, 4,4',5,5'-H)

^{13}C -NMR [DMSO, 300MHz, 25°C, δ (ppm)]: 166.3 (COO), 154.8, 148.4, 139.3 (CH), 125.7 (CH), 124.5 (CH)

XRD – formula $[(C_{12}H_8N_2O_4) \cdot 2(C_2H_6OS)]$, see structures **XXVIII** in 'Annexes - Crystal structures'

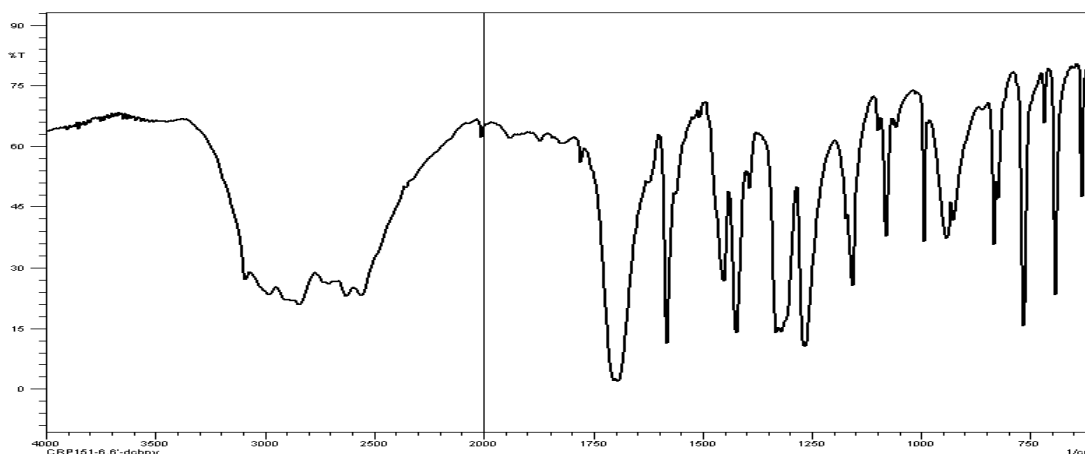
MS (ESI -): m/z 243.0 $[M-H]^-$, 487.1 $[2M-H]^-$

mp (°C): 285-288 °C

Elemental analysis: Found: C, 58.27; N, 11.18; H, 3.48.

Calc. for $C_{12}H_8N_2O_4$: C, 59.02; N, 11.47; H, 3.30.

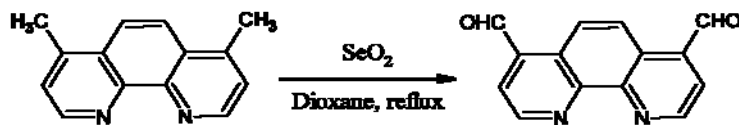
IR (KBr): 2980 broad (ν O-H), 2600 broad, 1693 s (ν C=O), 1582 m, 1452 m, 1423 m, 1330 s (δ C-O), 1266 s (ν C-O), 1157, 1080, 993, 941, 832, 764 m, 692 $m\text{ cm}^{-1}$



Ligand 3

1,10-Phenanthroline-4,7-dicarboxylic acid - [4,7-dcphen]^{1,4}

a) 4,7-Diformyl-1,10-phenanthroline



Synthesis:

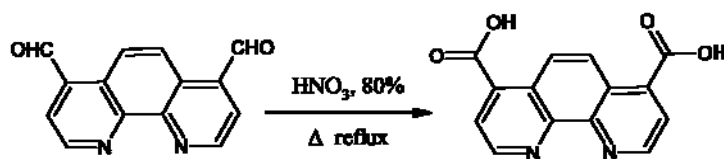
Selenium dioxide (5 g, 45 mmol) was dissolved in 150 ml of 1,4-dioxane/water 4% v/v mixture (6 ml of water in 144 ml of dioxane). 4,7-Dimethyl-1,10-phenanthroline (commercially available) (2 g, 9.2 mmol) was added to the clear solution and the mixture was heated to reflux over 2 h 30. The dark orange suspension was filtered through Celite while hot. Product was separated as yellow powder from the cold filtrate and recrystallized from THF. Yield: 80%.

Characterization:

¹H-NMR [DMSO, 300MHz, 25°C, δ(ppm)]: 10.70 (s, 2H, CHO), 9.47 (d, J_{2,3}=4.3 Hz, 2H, 2,9-H), 9.13 (s, 2H, 5,6-H), 8.28 (d, J_{2,3}=4.3 Hz, 2H, 3,8-H)

¹³C-NMR [DMSO, 300MHz, 25°C, δ(ppm)]: 194.6(COH), 151.7(CH), 150.9, 146.5, 137.2, 126.6(CH), 124.9(CH)

b) 1,10-Phenanthroline-4,7-dicarboxylic acid



Synthesis:

In a flask equipped with a condenser, 80% HNO₃ (30 ml) was added dropwise over 30 minutes to 4,7-diformyl-1,10-phenanthroline (1.6g, 5.9 mmol) cooled to 0 °C in an ice-water bath. The orange solution was first heated at 70°C for 3h, then allowed to cool to room temperature. The

⁴ M. Yanagida, L. P. Singh, K. Sayama, K. Hara, R. Katoh, A. Islam, H. Sugihara, H. Arakawa, M. K. Nazeeruddin, M. Grätzel; *J. Chem. Soc., Dalton Trans.*, **2000**, 2817-2822

mixture was poured into ice-water and left to precipitate at 4°C overnight. The product was separated from the green solution by filtration and recrystallized from methanol. Yield: 90%

Characterization:

Molecular Formula: $C_{14}H_8N_2O_4$ **Molecular Weight:** 268.22

Deprotonated form:

1H -NMR [D_2O/Et_3N , 300MHz, 25°C, δ (ppm)]: 8.91 (d, $J_{2,3}=4.6$ Hz, 2H, 2,9-H), 8.05 (s, 2H, 5,6-H), 7.60 (d, $J_{3,2}=4.6$ Hz, 2H, 3,8-H)

^{13}C -NMR [D_2O/Et_3N , 300MHz, 25°C, δ (ppm)]: 174.0 (COO), 149.3 (CH), 146.2, 144.3, 124.0 (CH), 123.6, 119.6 (CH)

Protonated form:

1H -NMR [DMSO, 300MHz, 25°C, δ (ppm)]: 9.25/9.35 (d, $J_{2,3}=4.9$ Hz, 2H, 2,9-H), 8.76/8.86 (s, 2H, 5,6-H), 8.15/8.35 (d, $J_{3,2}=4.9$ Hz, 2H, 3,8-H) (shift is due to the concentration)

^{13}C -NMR [DMSO, 300MHz, 25°C, δ (ppm)]: 167.9 (COO), 150.6 (CH), 146.4, 137.0, 125.3 (CH), 124.1 (CH)

XRD – formula [$C_{14}H_8N_2O_4$], see structures **I** and **II** in ‘Annexes - Crystal structures’

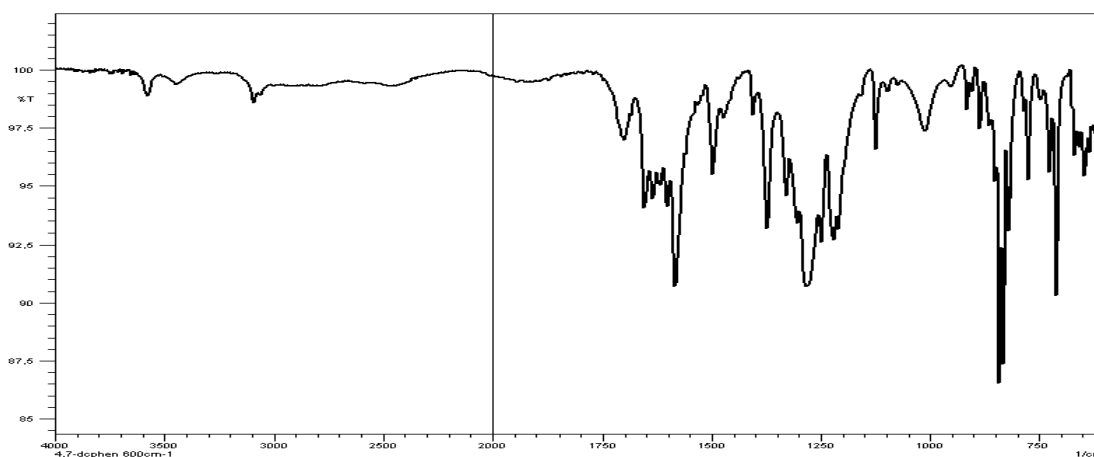
MS (ESI +): m/z 269.0 [$M+H$]⁺

mp (°C): >300 °C

Elemental analysis: Found: C, 61.99; N, 10.64; H, 3.24.

Calc. for $C_{14}H_8N_2O_4$: C, 62.69; N, 10.44; H, 3.00.

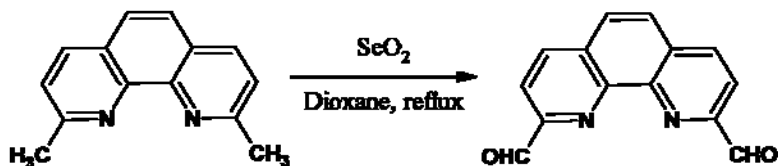
IR (ATR) : 3439, 3113, 2782 (ν O-H broad), 2452, 1887, 1722 (ν C=O, s), 1604, 1563, 1461, 1366, 1287 (ν C-O, s), 1142, 1071, 1014, 766s, 681 cm^{-1}



Ligand 4

1,10-Phenanthroline-2,9-dicarboxylic acid - [2,9-dcphen]^{4,5}

a) 2,9-Diformyl-1,10-phenanthroline



Synthesis:

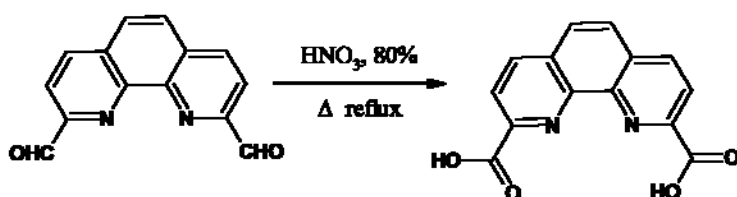
Selenium dioxide (12.5 g; 112 mmol) was dissolved in 1,4-dioxane/water 3% v/v mixture (10 ml of water in 300 ml of dioxane). 2,9-Dimethyl-1,10-phenanthroline (Neocuproine, commercially available) (5 g; 23 mmol) was added to the clear solution and the mixture was heated to reflux for 3 h 30.

The dark orange suspension was filtered through Celite while hot and immediately a white/yellow powder separated from the cooled filtrate. The product was filtered and washed with ethanol to obtain 2.68 g of a yellow powder. Yield= 47%

Characterization:

¹H-NMR [DMSO, 300MHz, 25°C, δ(ppm)]: 10.34 (s, 2H, CHO), 8.77 (s, J_{3,4}=8.2 Hz, 2H, 4,7-H), 8.29 (d, J_{3,4}=8.2 Hz, 3,8-H), 8.25 (s, 2H, 5,6-H)

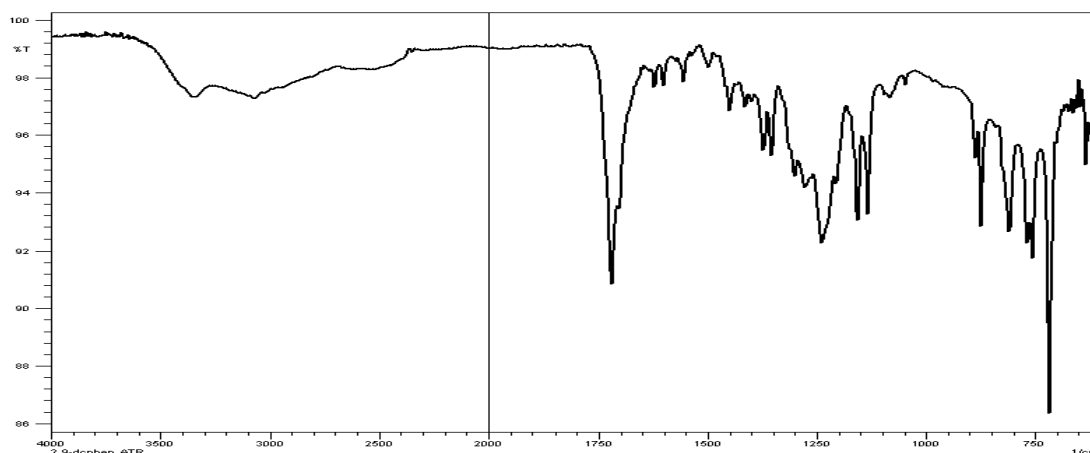
b) 1,10-Phenanthroline-2,9-dicarboxylic acid

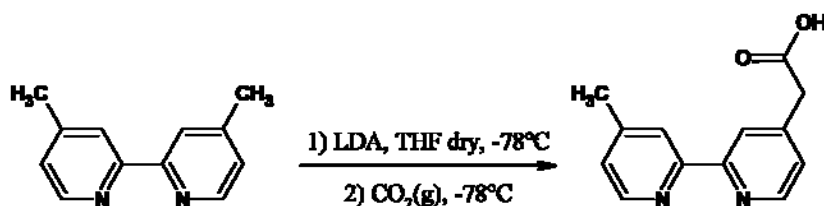


Synthesis:

In a flask equipped with a condenser 80% HNO₃ (30ml) was added dropwise over 30 minutes to 2,9-diformyl-1,10-phenanthroline cooled to 0° C in a ice-water bath. The orange solution was heated to 70 °C for 4 h and then poured into ice-water and placed in the fridge overnight to obtain a fine crystalline precipitate in a quantitative yield (2.9 g). The product was then recrystallized from hot water. Yield: 94%

⁵ C. J. Chandler, L. W. Deady, J. A. Reiss; *J. Hetero. Chem.*, **1981**, *18*, 599-601

Characterization:**Molecular Formula:** $C_{14}H_8N_2O_4$ **Molecular Weight:** 268.22**Deprotonated form:** **1H -NMR [D_2O/Et_3N , 300MHz, 25°C, δ (ppm)]:** 8.15 (d, $J_{3,4}=8.3$ Hz, 2H, 4,7-H), 7.96 (d, $J_{4,3}=8.3$ Hz, 2H, 3,8-H), 7.57 (s, 2H, 5,6-H) **^{13}C -NMR [D_2O/Et_3N , 300MHz, 25°C, δ (ppm)]:** 173.0 (COO), 153.4, 144.1, 137.8 (CH), 129.4, 127.1 (CH), 122.6 (CH)**Protonated form:** **1H -NMR [DMSO, 300MHz, 25°C, δ (ppm)]:** 8.72 (d, $J_{3,4}=8.3$ Hz, 2H, 4,7-H), 8.42 (d, $J_{4,3}=8.3$ Hz, 2H, 3,8-H), 8.17 (s, 2H, 5,6-H) **^{13}C -NMR [DMSO, 300MHz, 25°C, δ (ppm)]:** 166.5 (COO), 148.3, 144.6, 139.0 (CH), 131.0, 128.8 (CH), 124.0 (CH)**XRD** – formula [$(C_{14}H_8N_2O_4) \cdot 2.5(H_2O)$], see structures **XXVII** in ‘Annexes - Crystal structures’**MS (ESI -):** m/z 267.1 $[M-H]^-$, 535.1 $[2M-H]^-$ **mp (°C):** 236-240 °C**Elemental analysis:** Found: C, 55.66; N, 9.52; H, 4.01.Calc. for $C_{14}H_8N_2O_4 \cdot H_2O$: C, 55.26; N, 9.20; H, 3.97.**IR (ATR) :** 3350 broad (ν O-H), 2500 broad, 1721 s (ν C=O), 1383 m, 1273 s (δ C-O), 1233 s (ν C-O), 873, 807, 767, 717 $m\text{ cm}^{-1}$ 

Ligand 5**4-Acetoxy-4'-methyl-2,2'-Bipyridine - [4-ambpy]⁶****Synthesis:**

A solution of 4,4'-Dimethyl-2,2'-bipyridine (4 g; 21 mmol) in dry THF (120 ml) was added under Ar atmosphere *via* cannula to a 2 M solution of LDA in THF (13 ml; 23 mmol) cooled at -78 °C in a acetone/dry-ice bath. The addition was carried on over 20 minutes and the resulting dark solution was stirred at -78°C for another 2h before dry gaseous CO₂ was bubbled through the solution *via* a teflon cannula while keeping temperature at -78°C.

After few minutes, a white precipitate appeared and the mixture was first poured into a beaker with dry ice and then left to return to r.t. and until CO₂ has been completely evaporated. Diethyl ether was added and the precipitate was filtered off and washed several times with diethyl ether and ethyl acetate until no starting product was detected by TLC (CH₂Cl₂/MeOH 9:1).

The yellow solid was dissolved in 400 ml of water, the pH was adjusted to ~7 by a 0.1M HCl solution (40 ml) and the volume of the solution reduced to 40 ml. The white precipitate thus formed was filtrated and washed with the minimum quantity of cold ethanol. Yield: 48%

Characterization:

Molecular Formula: C₁₃H₁₂N₂O₂ **Molecular Weight:** 228.24

Deprotonated form:

¹H-NMR [D₂O/Et₃N, 300MHz, 25°C, δ(ppm)]: 8.48 (dd, J_{6,5}=5.2Hz, 1H, 6-H), 8.39 (d, J_{6',5'}=5.1 Hz, 1H, 6'-H), 7.79 (s, J_{5',3'}=1.7Hz, 1H, 3'-H), 7.75 (s, J_{5,3}=1.6Hz 1H, 3-H), 7.37 (dd, J_{5',6'}=5.1Hz, J_{5',3'}=1.7Hz, 1H, 5'-H), 7.29 (dd, J_{5,6}=5.2Hz, J_{5,3}=1.6 Hz, 1H, 5-H), 3.61 (s, 2H, CH₂), 2.38 (s, 3H, CH₃)

¹³C-NMR [D₂O/Et₃N, 300MHz, 25°C, δ(ppm)]: 178.5 (COO), 155.1, 154.7, 150.3, 148.7(CH), 148.5, 148.4 (CH), 125.2 (CH), 125.0 (CH), 123.9 (CH), 122.9 (CH), 44.1 (CH₂), 20.4 (CH₃)

Protonated form:

⁶ L. Della Ciana, I. Hamachi, T. J. Meyer; *J. Org. Chem.*, **1989**, *54*, 1731-1735

$^1\text{H-NMR}$ [MeOD, 300MHz, 25°C, δ (ppm)]: 8.52 (d, $J_{6,5}=5.0$ Hz, 1H, 6-H), 8.48 (d, $J_{6',5}=5.0$ Hz, 1H, 6'-H), 8.19 (s, 1H, 3-H), 8.07 (s, 1H, 3'-H), 7.40 (dd, $J_{5,6}=5.0$ Hz, 1H, 5-H), 7.28 (dd, $J_{5',6}=5.0$ Hz, 1H, 5'-H), 3.62 (s, 2H, CH₂), 2.46 (s, 3H, CH₃)

$^{13}\text{C-NMR}$ [MeOD, 300MHz, 25°C, δ (ppm)]: 176.2 (COO), 155.6, 155.5, 149.0, 148.9, 148.6 (CH), 148.4 (CH), 124.8 (CH), 124.5 (CH), 122.6 (CH), 122.2 (CH), 44.1 (CH₂), 19.7 (CH₃)

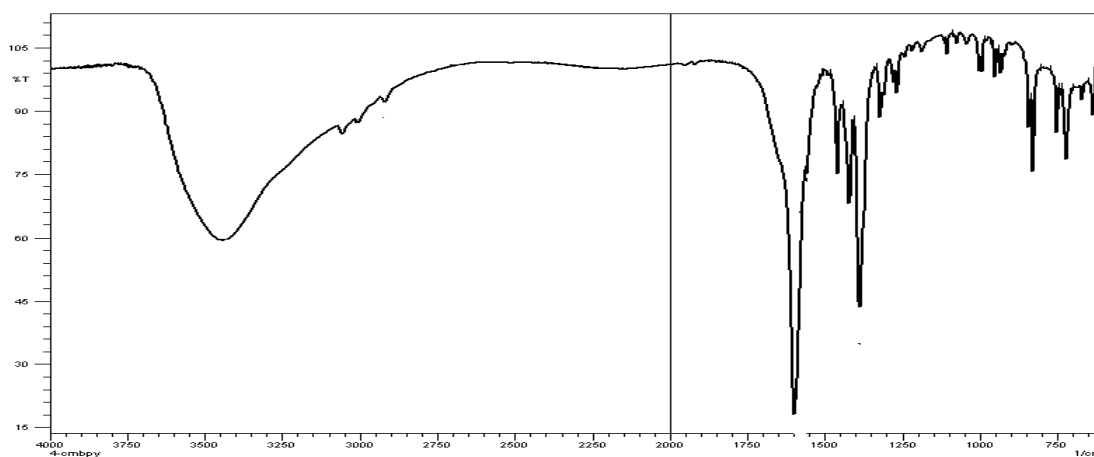
MS (ESI +): m/z 229.1 [M+H]⁺

mp (°C): 198-200 °C

Elemental analysis: Found: C, 64.44; N, 11.36; H, 5.28.

Calc. for C₁₃H₁₂N₂O₂*1/3(HCl): C, 64.97; N, 11.65; H, 5.17.

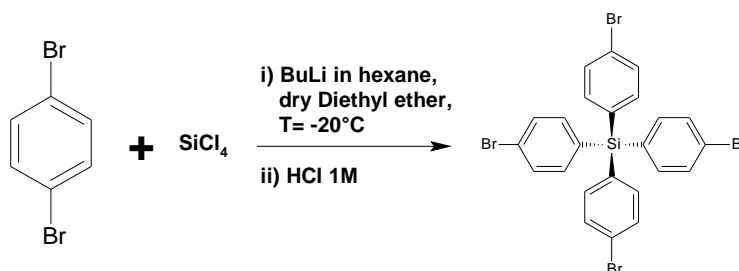
IR (KBr): 3444 (v, OH), 3054, 3003, 2917 (v, CH₃), 1599 (v_a, COO⁻), 1460, 1420, 1388 (v_s, COO⁻), 827, 720 cm⁻¹



Ligand 6

Tetrakis(4-carboxyphenyl)silane⁷

a) Tetrakis(4-bromophenyl)silane



⁷ J.H. Fournier, X. Wang, J.D. Wuest; *Can. J. Chem.*; **2003**, *81*, 376-380

Synthesis:

1,4-Dibromobenzene (commercially available) (23.6 g; 100 mmol) in 250 ml of freshly distilled diethyl ether was stirred for 15 min under Ar atmosphere at -20°C in a acetone/dry ice bath before a solution of 2.5M BuLi in hexane (40 ml; 100 mmol) was added dropwise at -20°C .

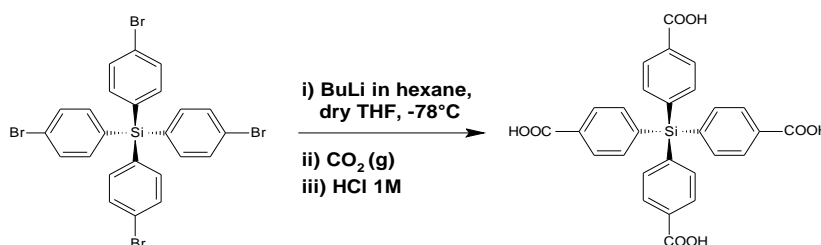
The mixture was kept at r.t. for 15 min before SiCl_4 (2.85 ml; 24.9 mmol) was added dropwise affording a milky suspension. The mixture was stirred at -10°C for 30 min then left to return to r.t. in 1h and stirred at r.t. for another hour.

A solution of 1M HCl (60 ml) was added to quench the reaction and water (200 ml) was added to promote phase separation. The aqueous phase was extracted with diethyl ether (4*100 ml) and the combined organic extracts were dried over MgSO_4 , filtered and evaporated under reduced pressure. The desired product was recrystallized several times from $\text{CH}_2\text{Cl}_2/\text{MeOH}$ mixture to obtain 9.5 g of white powder. Yield= 58%

Characterization:

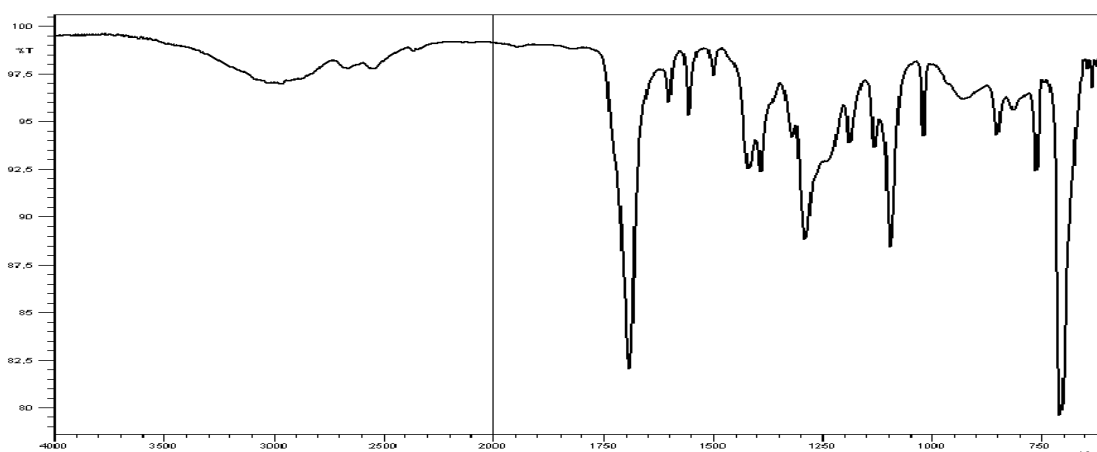
$^1\text{H-NMR}$ [CDCl_3 , 300MHz, 25°C , $\delta(\text{ppm})$]: 7.55 (d, $J_{3,4}=8.4$ Hz, 8H, H-3), 7.35 (d, $J_{3,4}=8.4$ Hz, 8H, H-4)

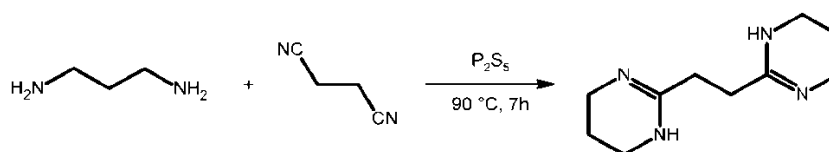
$^{13}\text{C-NMR}$ [CDCl_3 , 300MHz, 25°C , $\delta(\text{ppm})$]: 137.6 (CH), 131.48 (CH), 131.43, 125.4

b) Tetrakis(4-carboxyphenyl)silane**Synthesis:**

A solution of tetrakis(4-bromophenyl)silane (4 g; 6.1 mmol) in dry THF (400 ml) was stirred under Ar atmosphere at -78°C in a acetone/dry ice bath for 20 min before 2.5M BuLi in hexane (20 ml; 30 mmol) was added dropwise. The resulting mixture was kept at -78°C for 1h and then CO_2 was bubbled through the suspension during 3h at -78°C .

The mixture was left to return to r.t. then was acidified with 200 ml of a 1M HCl solution, the solvent was reduced in volume and the aqueous phase was extracted with ethyl acetate (4x100 ml) and the combined organic extracts were washed well with brine, dried over MgSO_4 and evaporated under reduced pressure. The desired product was recrystallized from acetone/petroleum ether to get 1.58 g of white powder. Yield: 50%

Characterization:**Molecular Formula:** C₂₈H₂₀N₆O₈Si **Molecular Weight:** 512.54**Deprotonated form:****¹H-NMR** [D₂O/Et₃N, 300MHz, 25°C, δ(ppm)]: 7.84 (d, 8H, J_{4,3}=8.3Hz, H-3), 7.63 (d, 8H, J_{3,4}=8.3Hz, H-4)**¹³C-NMR** [D₂O/Et₃N, 300MHz, 25°C, δ(ppm)]: 175.0 (COO), 138.1, 136.6, 136.3 (CH), 128.5 (CH)**Protonated form:****¹H-NMR** [Acetone-d₆, 300MHz, 25°C, δ(ppm)]: 8.12 (d, J_{4,3}=4.9 Hz, 8H, 3-H), 7.75 (d, J_{4,3}=4.9 Hz, 8H, 4-H)**¹³C-NMR** [Acetone-d₆, 300MHz, 25°C, δ(ppm)]: 167.25 (COO), 139.2, 137.0 (CH), 133.2, 129.7 (CH)**MS (ESI -):** m/z 511.1 [M-H]⁻**mp (°C):** >300 °C**Elemental analysis:** Found: C, 65.15; H, 4.98.Calc. for C₂₈H₂₀O₈*C₃H₆O: C, 65.25; H, 4.59.**IR (ATR) :** 1691 s (ν C=O), 1600, 1555, 1499, 1417 m, 1319 m, 1289 s (δ C-O), 1266s (ν C-O), 1094 m, 1019, 759, 705 s cm⁻¹

BAD23**1,2-Bis-(1,4,5,6-tetrahydropyrimidin-2-yl)ethane⁸****Synthesis:**

Succinonitrile (13,8 g; 0.17 mmol) and P_2S_5 (~40 mg) were charged into a three necked flask under Ar, 1,3-Diamino propane (24.8 g; 0.33 mmol) was added and the yellow solution was heated at 90°C for 7h until slowdown of gas evolution. Solution turned green then a yellow solid forming a solid lump precipitated.

Toluene (15 ml) was added and the reaction mixture was stirred and the solid was crashed, the solution was filtrated on a frit and filtrate first washed with warm toluene and then with toluene/ $CHCl_3$ (95:5). The solution was evaporated leaving a light yellow powder that was recrystallized from the minimum amount of $CHCl_3$ /toluene mixture. The product is sensitive to aqueous and alcoholic medium and is stored under dry atmosphere to avoid hydrolysis. Obtained 11.5 g of white crystalline product. Yield: 35%

Characterization:

Molecular Formula: $C_{10}H_{18}N_4$ **Molecular Weight:** 194.27

¹H-NMR [$CDCl_3$, 300MHz, 25°C, δ (ppm)]: 3.19 (t, 8H, H-4',4'',6',6''), 2.16 (s, 4H, H-1,2), 1.56 (q, 4H, H-5',5'')

¹³C-NMR [$CDCl_3$, 300MHz, 25°C, δ (ppm)]: 158.8, 41.1 (CH_2), 32.42 (CH_2), 20.3 (CH_2)

HRMS (ESI +): m/z found: 195.160 [$M+H$]⁺ ; calculated for $C_{24}H_{21}N_6O_2$: 195.161 [$M+H$]⁺

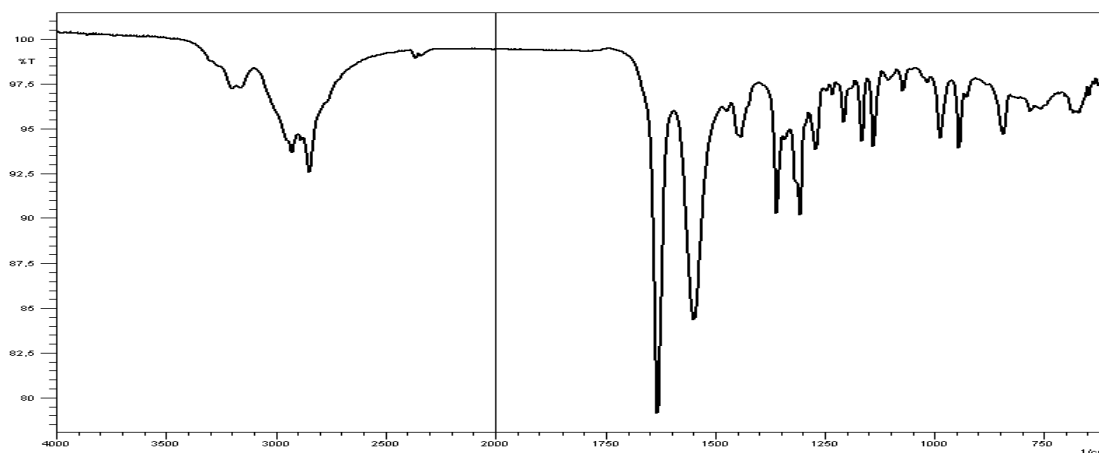
mp (°C): 197-199 °C

Elemental analysis: Found: C, 58.95; N, 27.70; H, 9.18.

Calc. for $C_{10}H_{18}O_4 \cdot 1/2H_2O$: C, 59.06; N, 27.57; H, 9.42.

IR (ATR) : 3200 (m, broad) 2926, 2847 (s, broad), 1632 s, 1548 s, 1359 m, 1306 m, 1166 w, 1139 w, 986 w, 943 w, 842 cm^{-1}

⁸ M. Machaj, M. Pach, A. Wołek, A. Zabrzeńska, K. Ostrowska, J. Kalinowska-Tłuścik, B. Oleksyn; *Monatshefte für Chemie*, **2007**, 138, 1273-1277



Ligand 7

5,5'-Bisamidine-2,2'-bipyridine – [5,5'-BAbpy]

a) 5,5'-Dibromo-2,2'-bipyridine⁹



Synthesis:

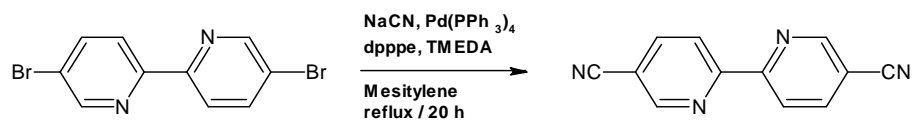
Under Ar atmosphere, 2,5-Dibromopyridine (7.23 g; 30 mmol) and tetrakis(triphenylphosphine)Pd (720 mg; 10% w/w) were mixed in 250 ml benzene to give a yellow solution. Hexamethylditin (5 g; 15 mmol) was added to the solution and the reaction was heated to 90°C for 3 days. After the reaction was cooled down to r.t., diethylether (300 ml) was added and the mixture kept at 4°C overnight causing the formation of a white precipitate. The mother liquor was reduced and precipitation was repeated several times.

Precipitate were combined and purified by chromatographic column on SiO₂ using CHCl₃/cyclohexane 1:1 as eluent to obtain 2.34 g of white powder. Yield: 50% .

Characterization:

¹H-NMR [CDCl₃, 300MHz, 25°C, δ(ppm)]: 8.70 (dd, J_{3,6}=0.7 Hz, J_{4,6}=2.3 Hz, 2H, H-6,6'), 8.28(dd, J_{6,3}=0.7 Hz, J_{4,3}=8.5 Hz, 2H, H-3,3'), 7.93 (dd, J_{6,4}=2.3 Hz, J_{3,4}=8.5 Hz, 2H, H-4,4')

⁹ J. I. Bruce, J.-C. Chambron, P. Kölle, J.-P. Sauvage; *J. Chem. Soc., Perkin Trans. 1*, **2002**, 1226-1231

b) 5,5'-Dicyano-2,2'-bipyridine¹⁰**Synthesis:**

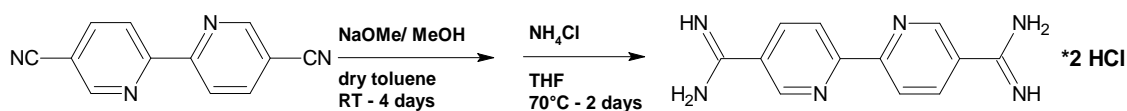
In a two necked flask, 5,5'-Dibromobipyridine (1.53 g; 4.9 mmol), dpppe (540 mg; 1.22 mmol), NaCN (480 mg; 9.8 mmol), Pd(OAc)₂ (140 mg; 0.6 mmol), mesitylene (20 ml) and 0.5 ml of TMEDA were mixed Under Ar atmosphere and the brown suspension thus obtained was stirred for 20 min at r.t. before heating under reflux for 20 h.

The reaction mixture was cooled to r.t. before 20 ml of water (HPLC grade) was added and the suspension was stirred for 30 min and filtered on a frit. The solid was dissolved in 250 ml of CH₂Cl₂ and the insoluble solid was filtered. The aqueous phase was extracted with CH₂Cl₂ (2x15 ml) and the organic phases were combined, dried with MgSO₄ and solvent was removed under vacuum. The solid was washed several times with pentane to remove mesitylene in excess and purified by chromatography on Al₂O₃ (eluent CH₂Cl₂) to obtain 600 mg of a white powder. Yield: 60%

Characterization:

¹H-NMR [CD₂Cl₂, 300MHz, 25°C, δ(ppm)]: 8.96 (dd, J_{3,6}=0.8 Hz, J_{4,6}=2.1 Hz, 2H, H-6,6'), 8.62 (dd, J_{6,3}=0.8 Hz, J_{4,3}=8.3 Hz, 2H, H-3,3'), 8.14 (dd, J_{6,4}=2.1 Hz, J_{3,4}=8.3 Hz, 2H, H-4,4')

¹³C-NMR [CD₂Cl₂, 300MHz, 25°C, δ(ppm)]: 156.9, 152.1 (CH), 140.5 (CH), 121.4 (CH), 116.5, 110.6

c) 5,5'-Bisamidinium-2,2'-bipyridine hydrochloride**Synthesis:**

5,5'-Dicyanobipyridine (135 mg; 0.65 mmol) was stirred in 36 ml of dry toluene under Ar atmosphere to obtain a pale yellow solution. A freshly prepared solution of NaOMe 5.8% in MeOH (0.2 ml; 0.16 mmol) was added and the reaction was heated at 70°C for 2 days, affording a yellow precipitate.

¹⁰ J. M. Veauthier, C. N. Carlson, G. E. Collis, J. L. Kiplinger, K. D. John.; *Synthesis*, **2005**, *16*, 2683-2686

The reaction mixture was evaporated to obtain 190 mg of bis-amidate intermediate as a powder (quantitative yield) which was dissolved in 30 ml of THF. NH_4Cl (80 mg; 1.5 mmol) was added and the mixture was refluxed for 36 h at 70°C .

The solvent was evaporated and the product was suspended in 100 ml of dichlorometane, filtered and washed with MeOH (3x10 ml) and water (3x10 ml) to afford 112 mg of a yellowish powder. Yield: 55%

Characterization:

Molecular Formula: $\text{C}_{12}\text{H}_{14}\text{N}_6\text{Cl}_2$

Molecular Weight: 313.18

$^1\text{H-NMR}$ [DMSO, 300MHz, 25°C , $\delta(\text{ppm})$]: 9.17 (dd, 1H, $J=0.7$ Hz, $J=2.1$ Hz, 2H, H-6,6'), 8.57 (dd, 1H, $J=0.7$ Hz, $J=8.3$ Hz, 2H, H-3,3'), 8.50 (dd, 1H, $J=2.1$ Hz, $J=8.3$ Hz, 2H, H-4,4')

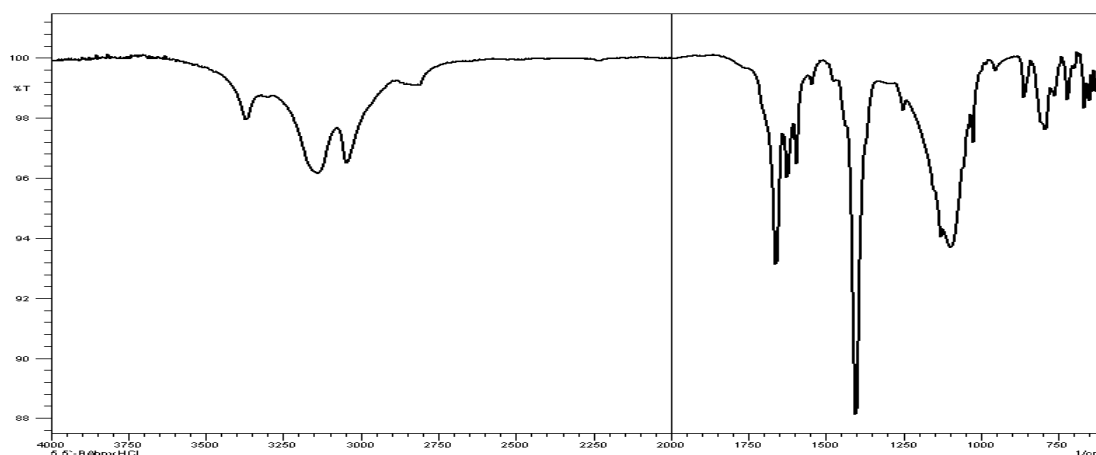
$^{13}\text{C-NMR}$ [DMSO, 300MHz, 25°C , $\delta(\text{ppm})$]: 157.8, 153.0 (CH), 142.1 (CH), 121.8 (CH), 117.4, 110.4

MS (ESI +): m/z 241.06 $[\text{M-H-2Cl}]^+$

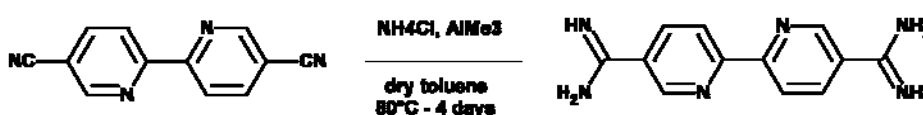
mp ($^\circ\text{C}$): 155-160 $^\circ\text{C}$

Elemental analysis: Many attempts to obtain satisfactory elemental analysis were unsuccessful.

IR (ATR) : 3368 w, 3141 w ($\nu_a \text{N-H}_2$), 3044w, 2830 w, 1659 m ($\nu_a \text{N=C-N}$), 1625, 1595 w, 1402 s, 1088 (s, broad), 1025, 860, 788 m, 719 cm^{-1}



d) 5,5'-Bisamidine-2,2'-bipyridine



Synthesis:

In a water-ice bath and under Ar, a fresh solution of AlClMeNH_2 was prepared by adding dropwise 10 ml (20 mmol) of a 2M AlMe_3 solution in toluene to a suspension of NH_4Cl (1.1 g; 20 mmol) in 50 ml dry toluene at 0°C and stirring for 2h at r.t. until complete gas evolution. In a two-necked flask at 0°C , to a suspension of 450 mg (2.18 mmol) of 5,5'-dicyano-2,2'-bipyridine in 30 ml of dry toluene, 13 ml of AlClMeNH_2 solution (1M in toluene) was transferred carefully over a period of 15 min.

The reaction mixture was allowed to come to r.t. and was then heated at $70\text{--}80^\circ\text{C}$ for 4 days affording a brown mixture. To the latter, 30 ml of ethylacetate was added and the organic phase was washed with water (3x50 ml). The aqueous phase was extracted with CH_2Cl_2 (3x20 ml), diluted 1M HCl was added until pH=2 was reached followed by 1M NaOH solution to reach pH=9. The latter operation caused the precipitation of a yellow solid which was collected.

The crude product was recrystallized several times from MeOH to obtain 110 mg of a pale yellow product. Yield: 21%

Characterization:

Molecular Formula: $\text{C}_{12}\text{H}_{12}\text{N}_6$

Molecular Weight: 240.26

$^1\text{H-NMR}$ [MeOD, 300MHz, 25°C , $\delta(\text{ppm})$]: 9.12 (dd, 1H, $J=0.8$ Hz, $J=2.3$ Hz, 2H, H-6,6'), 8.74 (dd, 1H, $J=0.8$ Hz, $J=8.4$ Hz, 2H, H-3,3'), 8.39 (dd, 1H, $J=2.4$ Hz, $J=8.3$ Hz, 2H, H-4,4')

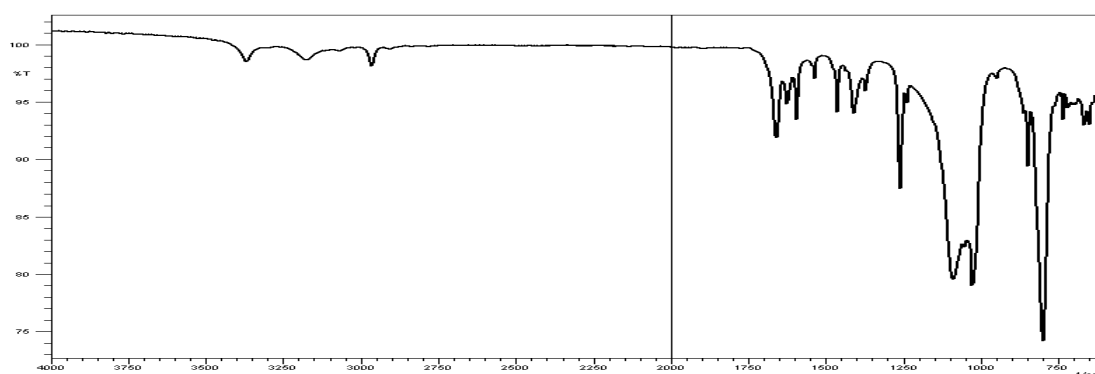
$^{13}\text{C-NMR}$ [MeOD, 300MHz, 25°C , $\delta(\text{ppm})$]: 158.4, 153.5 (CH), 142.3 (CH), 122.78 (CH), 117.6, 112.0

MS (ESI+): m/z 241.06 (100, $\text{M}+\text{H}^+$)

mp ($^\circ\text{C}$): decompose after 250°C

Elemental analysis: Many attempts to obtain satisfactory elemental analysis were unsuccessful.

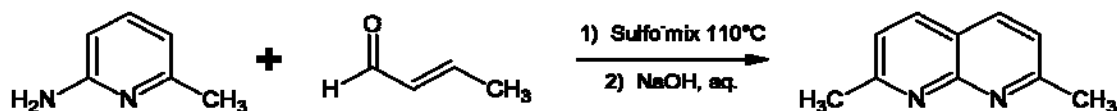
IR (KBr): 3368w, 3176w, 2962, 1659m, 1625, 1593, 1410, 1260m, 1088s, 1053s, 1025, 860, 846, 799s cm^{-1}



Ligand 8

2,7-Bis-[N-(6-methylpyridin-2-yl)]carbamoyl-1,8-naphthyridine - [2,7-mpanaphthy]

a) 2,7-Dimethyl-1,8-naphthyridine ^{11,12,13}



Synthesis:

In a three necked flask, 23 ml of nitrobenzene (27 g; 0.22 mmol) were added to 68 ml of oleum-20% SO₃ cooled in a water-ice bath to maintain the temperature below 20°C. The solution was heated at 65°C overnight. The mixture turned from orange to brown. After 24 h, a sample of the mixture was dissolved in water for testing the formation of sulfo-mix.

Water (50ml) was added to the chilled sulfo-mix at 0°C in a water-ice bath. The mixture was allowed to return to r.t. and 2-amino-6-methyl pyridine (10.8 g; 0.10 mmol) was added under Ar. The brown solution was heated at 110 °C. Separately, crotonaldehyde (28 ml; 0.34 mmol) was heated to the same temperature before it was transferred dropwise *via* double needle cannula over a period of 30 min.

Heating and stirring were maintained at 110°C for 30 min and water was removed by distillation. The black reaction mixture was cooled and neutralized with a saturated NaOH solution (200 ml). This reaction is **very exothermic** and should be carried out carefully.

The solid mud was separated by filtration from the water mother liquor and the two phases were managed separately. The solid phase was extracted with CHCl₃ using a soxlet apparatus and the aqueous phase was extracted into CHCl₃ using a liquid/liquid apparatus.

The organic phase resulting from the solid phase extraction was purified by column chromatography (silica gel, CHCl₃/isopropanol 9:1), whereas, the organic phase resulting from the liquid/liquid extraction was first purified on active carbon then by column chromatography (alumina, CHCl₃/isopropanol 9:1).

Both collected products were combined and further purified by chromatography (silica gel, CHCl₃/isopropanol 9:1) and finally by sublimation (80°C / 0,01mmHg). Yield: 34%

¹¹ M. A. Cavanaugh, V. M. Cappel, C. J. Alexander, M. L. Good; *Inorg. Chem.*; **1976**, *15*, 2615-2621

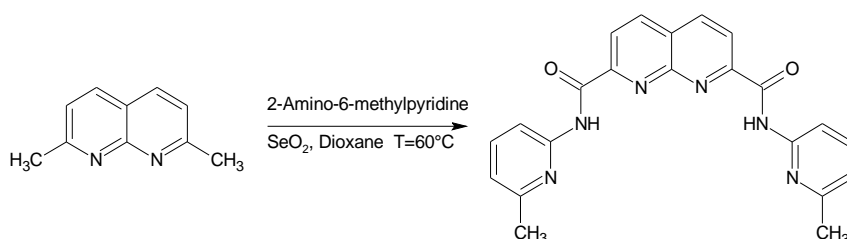
¹² Y. Hamada, I. Takeuchi; *Chem. Pharm. Bull.*; **1971**, *19*, 1857-1860

¹³ W. W. Paudler, T. J. Kress; *J. Heterocycl. Chem.*; **1967**, *4*, 284-289

Characterization:

¹H-NMR [CDCl₃, 300MHz, 25°C, δ(ppm)]: 7.99 (d, 2H, 4,5-H), 7.29 (d, 2H, 3,6-H), 2.77 (s, 6H, CH₃)

¹³C-NMR [CDCl₃, 300MHz, 25°C, δ(ppm)]: 162.61, 155.62, 136.41(CH), 122.05(CH), 118.58, 25.55(CH₃)

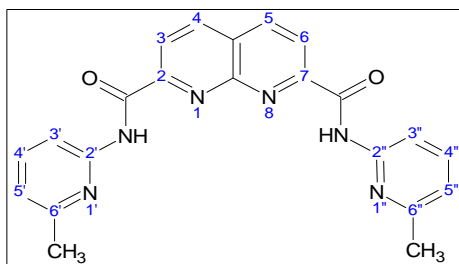
b) 2,7-Bis-[N-(6-methylpyridin-2-yl)carbamoyl]-1,8-naphthyridine**Synthesis:**

To a hot mixture (60°C) of SeO₂ in dioxane (380 ml), 2,7-Dimethyl-1,8-naphthyridine (5 g; 31 mmol) and 2-Amino-6-methylpyridine (6.7 g ; 62 mmol) were added. The obtained orange-red mixture was heated at 60°C for 3 h 30. The black-brown solution was filtrated on celite while hot and the filtrate was evaporated under vacuum to 250 ml; CH₂Cl₂ (250 ml) was added and the organic phase was extracted with water (2x100 ml) and a saturated solution of NaCl (100 ml). The aqueous phase was extracted with CH₂Cl₂ (3x30 ml) and combined organic fractions were dried over Na₂SO₄ and evaporated to dryness. The crude product was purified on a chromatographic column (CH₂Cl₂/isopropanol (95:5) on alumina) affording in 1.8 g of a yellow powder and recrystallized from 60% HNO₃. Yield: 14 %.

Characterization:

Molecular Formula: C₂₂H₁₈N₆O₂

Molecular Weight: 398.41



¹H-NMR [THF, 300MHz, 25°C, δ(ppm)]: 10.39 (s, 2H, NH), 8.57 (d, 2H, J_{3,4}=8.5 Hz, H-3,6), 8.32 (d, 2H, J_{3,4}=8.5 Hz, H-4,5), 8.02 (d, 2H, J_{3',4'}=8,2 Hz, H-3',3''), 7.48 (d, 2H, J_{3',4'}=8,2 Hz, J_{4',5'}=7,5 Hz, H-4,4''), 6.79 (d, 2H, J_{4',5'}=7,5 Hz, H-5',5''), 2.26 (s, 6H, CH₃).

¹³C-NMR [THF, 300MHz, 25°C, δ(ppm)]: 161.4(C=O), 157.4, 153.6, 152.9, 150.5, 139.9(CH), 138.4(CH), 126.3, 120.8(CH), 119.3(CH), 110.2(CH), 23.2(CH₃).

XRD: formula $[(C_{22}H_{18}N_6O_2) \cdot 2(H_2O)]$, see structure **XXXV**, and formula $[(C_{22}H_{18}N_6O_2) \cdot DMSO]$, see structure **XXXVI** in 'Annexes - Crystal structures'

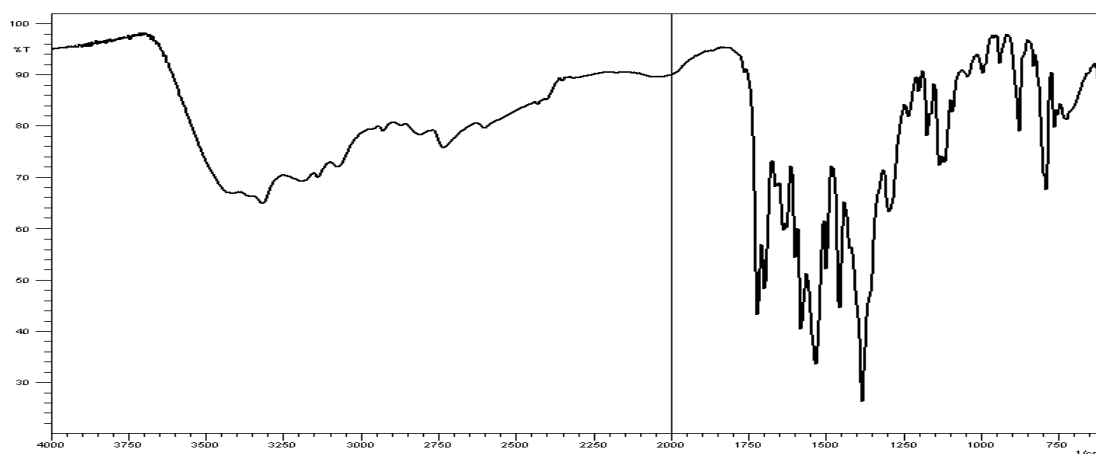
MS (ESI +): m/z 399.15 $[M+H]^+$, 797.29 $[2M+H]^+$

mp (°C): 242-247 °C

Elemental analysis: Found: C, 53.02; N, 18.88; H, 4.56.

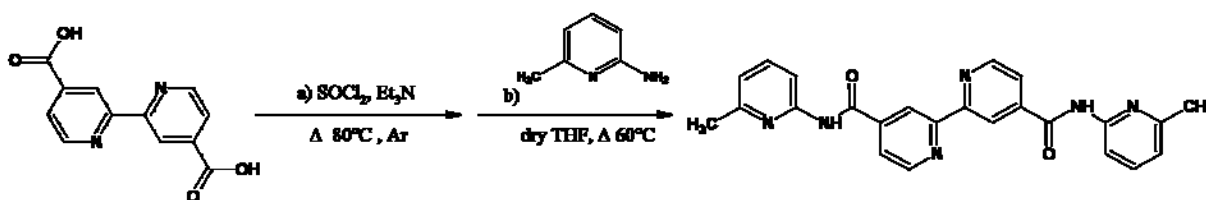
Calc. for $C_{22}H_{18}N_6O_2 \cdot 2H_2O \cdot HNO_3$: C, 53.11; N, 19.70; H, 4.66.

IR (KBr): 3316 (broad), 2731, 1720, 1698, 1579, 1531 s, 1455, 1388 s, 1293, 1132, 875, 786 cm^{-1}



Ligand 9

4,4'-Bis-[N-(6-methylpyridin-2-yl)carbamoyl]-2,2'-bipyridine - [4,4'-mpabpy]



Synthesis:

Under Ar, to a suspension of 4,4'-dicarboxy-2,2'-bipyridine (500 mg, 2.0mmol) in 12 ml of $SOCl_2$ was added 0.1 ml of triethylamine and the yellow solution was refluxed at 80°C overnight.

The reaction mixture was evaporated under vacuum for two days, then the yellow precipitate was handled quickly under Ar to avoid hydrolysis of the acyl-chloride.

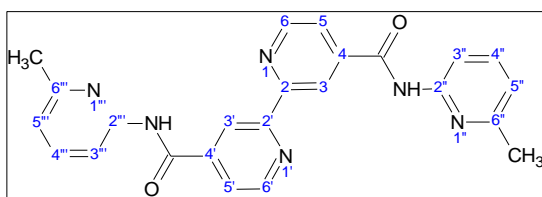
2-Amino-6-methylpyridine (430 mg, 4.0 mmol) in 12 ml of dry THF was added to the crude product and the mixture was refluxed overnight at 60 °C.

The obtained pink solution was quenched with a saturated NaHCO₃ solution (20 ml) and the precipitate was filtered off and washed several times with CHCl₃. The aqueous phase was extracted with CHCl₃ (4x15 ml) and the combined organic phases were dried over Na₂SO₄ and evaporated to obtain a yellow product. The crude product was purified by chromatography on silica gel (petroleum ether/ethyl acetate 1:1) to obtain 180 mg of a white powder. Yield: 21%

Characterization:

Molecular Formula: C₂₄H₂₀N₆O₂

Molecular Weight: 424.45



¹H-NMR [CDCl₃, 300MHz, 25°C, δ(ppm)]: 8.91 (dd, J_{3,5}=1.8Hz, J_{3,6}=0.8Hz, 2H, H-3,3' bpy), 8.88 (dd, J_{6,3}=0.8 Hz, J_{6,5}=5.0Hz, 2H, H-6,6' bpy), 8.83 (s, 2H, NH), 8.20 (d, J_{3'',4''}=8.2 Hz, 2H, H-3'',3'' py), 7.90 (dd, J_{5,3}=1.8 Hz, J_{5,6}=5.0 Hz, 2H, H-5,5' bpy), 7.68 (dd, J_{4'',3''}=8.2 Hz, J_{4'',5''}=7.4 Hz, 2H, H-4'',4'' py), 6.98 (d, J_{5'',4''}=7.4 Hz, 2H, H-5'',5'' py), 2.48 (s, 6H, CH₃)

¹³C-NMR [CDCl₃, 300MHz, 25°C, δ(ppm)]: 163.6(C=O), 157.1, 156.2, 150.4(CH), 150.3, 142.6, 138.9(CH), 122.1(CH), 120.0(CH), 117.7(CH), 111.2(CH), 24.0(CH₃)

MS (ESI +): m/z 425 [M+H]⁺, 855 [2M+Li]⁺

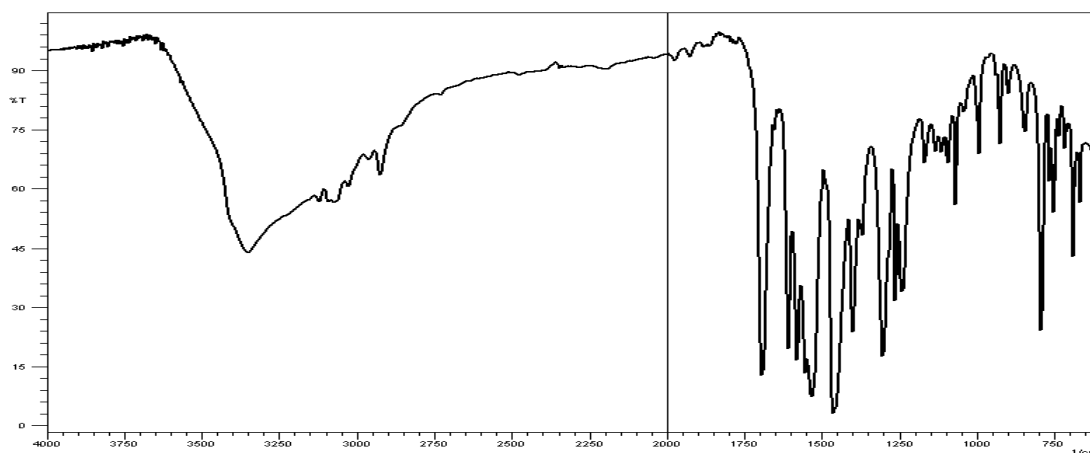
XRD - formula [(C₂₄H₂₀N₆O₂)], see structure **XXXVII** in 'Annexes - Crystal structures'

mp (°C): 245-250 °C

Elemental analysis: Found: C, 63.41; N, 18.01; H, 5.14.

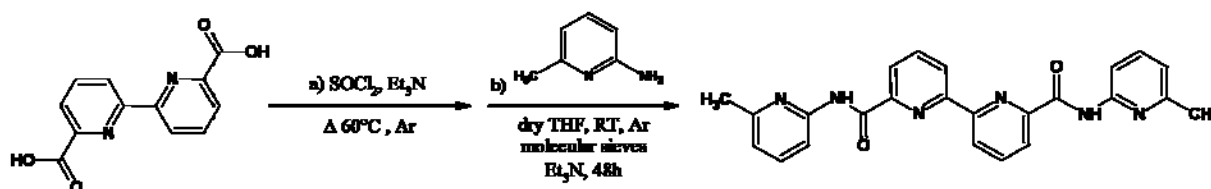
Calc. for C₂₄H₂₀N₆O₂*3/2H₂O: C, 63.84; N, 18.61; H, 5.13.

IR (KBr): 3350 (broad), 2923, 1692, 1608s, 1579, 1531 s, 1462, 1400s, 1301, 1240, 1067, 790, 688 cm⁻¹



Ligand 10

6,6'-Bis-[N-(6-methylpyridin-2-yl)carbamoyl]-2,2'-bipyridine - [6,6'-mpabpy]



Synthesis:

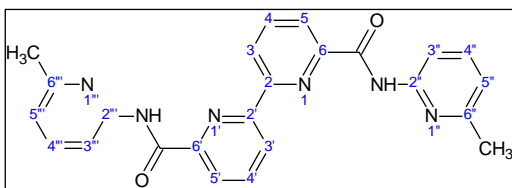
Under Ar, to a suspension of 6,6'-Dicarboxy-2,2'-bipyridine (210 mg; 0.85 mmol) in 20 ml of SOCl_2 , 250 μl of triethylamine was added and the solution was refluxed at 60 °C overnight. The orange solid was suspended quickly in 35 ml of dry THF stored on molecular sieves, 2-amino-6-methylpyridine (330 mg; 3 mmol) was added followed by 200 μl of triethylamine and the mixture was stirred under Ar atmosphere at r.t. for two days.

The formed precipitate was filtered, washed abundantly with CH_2Cl_2 and MeOH, dried under vacuum and recrystallized from MeOH to obtain 250 mg of a white powder. Yield: 70%

Characterization:

Molecular Formula: $\text{C}_{24}\text{H}_{20}\text{N}_6\text{O}_2$ **Molecular Weight:** 424.45

$^1\text{H-NMR}$ [CDCl_3 , 300MHz, 25°C, δ (ppm)]: 10.40 (s, 2H, NH), 8.85 (dd, 2H, $J_{3,4}=7.9\text{Hz}$, $J_{3,5}=1.1\text{Hz}$, H-3,3' bpy), 8.41 (dd, 2H, $J_{5,4}=7.7\text{Hz}$, $J_{3,5}=1.1\text{Hz}$, H-5,5' bpy), 8.29 (d, 2H, $J_{3',4''}=8.2\text{Hz}$, H-3'',3''' py), 8.16 (dd, 2H, $J_{3,4}=7.9\text{Hz}$, $J_{5,4}=7.7\text{Hz}$, H-4,4' bpy), 7.69 (dd, 2H, $J_{3',4''}=8.2\text{Hz}$, $J_{5',4'''}=7.5\text{Hz}$, H-4'',4''' py), 6.98 (d, 2H, $J_{5',4'''}=7.5\text{Hz}$, H-5'',5''' py), 2.55 (s, 6H, CH_3)



$^{13}\text{C-NMR}$ [CDCl_3 , 300MHz, 25°C, δ (ppm)]: 162.3(C=O), 157.2, 153.6, 150.3, 149.1, 138.9(CH), 138.7(CH), 124.6(CH), 123.2(CH), 119.6(CH), 111.0(CH), 24.1(CH_3)

HRMS (ESI +): m/z found: 425.171 $[\text{M}+\text{H}]^+$; calculated for $\text{C}_{24}\text{H}_{21}\text{N}_6\text{O}_2$: 425.172 $[\text{M}+\text{H}]^+$

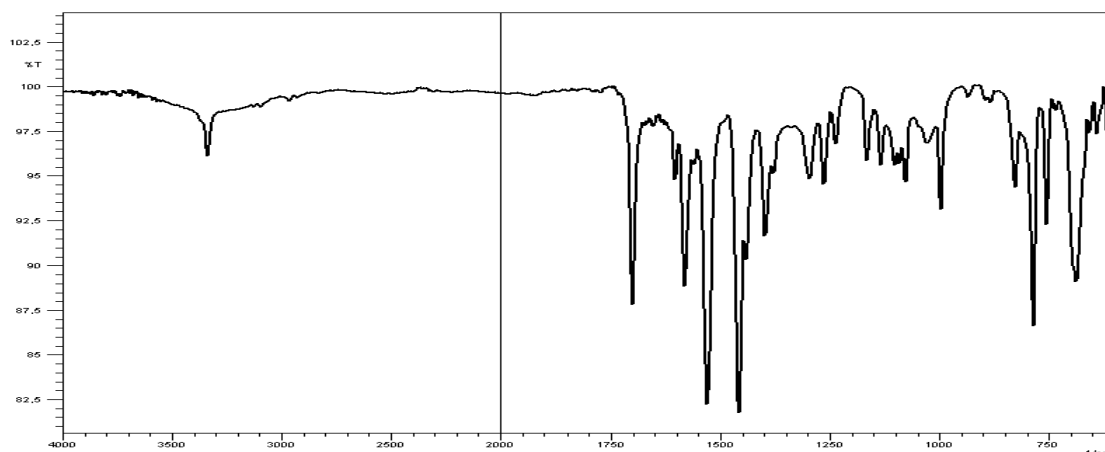
XRD - formula $[(\text{C}_{24}\text{H}_{20}\text{N}_6\text{O}_2) \cdot 2(\text{H}_2\text{O})]$, see structure **XXXVIII** in 'Annexes - Crystal structures'

mp (°C): 290-295 °C

Elemental analysis: Found: C, 60.36; N, 17.54; H, 5.38.

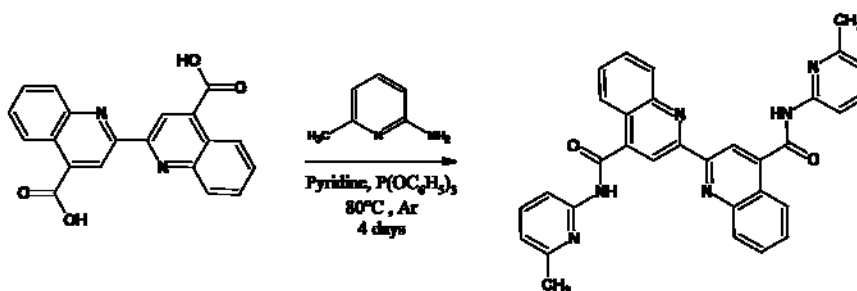
Calc. for $\text{C}_{24}\text{H}_{20}\text{N}_6\text{O}_2 \cdot 3\text{H}_2\text{O}$: C, 60.24; N, 17.56; H, 5.47.

IR (KBr): 3337,1701, 1581, 1530 s, 1458s, 1397, 997, 785m, 687 cm^{-1}



Ligand 11

4,4'-Bis-[N-(6-methylpyridin-2-yl)carbamoyl]-2,2'-biquinoline - [4,4'-mpaBQ]



Synthesis:

Commercially available 4,4'-Dicarboxy-2,2'-biquinoline (350 mg; 1.0 mmol) 300 mg of 2-amino-6-methylpyridine (2.7 mmol) were suspended in 10 ml of pyridine.

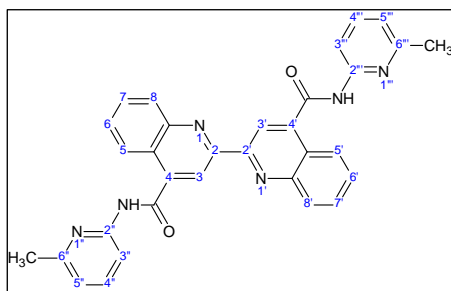
The mixture was heated at 50°C and stirred for 15 min before 0.8 ml of triethylphosphite (950 mg ; 3.0 mmol) was added under Ar. The temperature was raised to 80°C and, after 48 h, 5 ml of pyridine were added. The reaction was heated again, for 2 days, until the mixture turned coloured.

The brown solution was cooled at r.t. and the precipitate formed was collected, solvent was reduced to one half, 10 ml of methanol and 4 ml of water were added and the precipitate was filtered. The collected solid fractions were washed first with methanol, then with a 0.1 M NaOH solution and with water until pH=7. Finally, the white precipitate was further washed with dichloromethane to afford 230 mg of a white powder. Yield: 43 %

Characterization:

Molecular Formula: C₃₂H₂₄N₆O₂ **Molecular Weight:** 524.19

¹H-NMR [CDCl₃/TFA, 400MHz, 25°C, δ(ppm)]: 9.52 (s, 2H, N-H), 9.14 (s, 2H, Bq-H), 8.76 (d, 2H, J¹=8.7 Hz, py-H), 8.51 (dd, 2H, J¹=8.3 Hz, J⁵=0.8 Hz, Bq-H), 8.50 (dd, 2H, J²=8.5 Hz, J⁴=0.8 Hz, Bq-H), 8.27 (pseudo t, 2H, J¹=8.7 Hz, J²=7.8 Hz, py-H), 7.97 (ddd, 2H, J²=8.5 Hz, J³=7.4 Hz, J⁵=0.8 Hz, Bq-H), 7.81 (ddd, 2H, J¹=8.3 Hz, J³=7.4 Hz, J⁴=0.8 Hz, Bq-H), 7.86 (d, 2H, J²=7.8 Hz, py-H), 2.78 (s, 6H, CH₃)



¹³C-NMR [CDCl₃/TFA, 400MHz, 25°C, δ(ppm)]:

164.8 (C=O), 151.8, 148.8, 148.1, 146.9 (CH), 144.5, 142.6, 133.7 (CH), 131.4 (CH), 127.1 (CH), 125.6 (CH), 121.5 (CH), 120.4 (CH), 116.8, 115.2 (CH), 19.4 (CH₃)

Assignment is based on 2-D NMR studies; the product starts to decompose in the solvent mixture after one night.

MS (ESI +): m/z 525.2 (100, M⁺), 511.17 (70, M-N⁺)

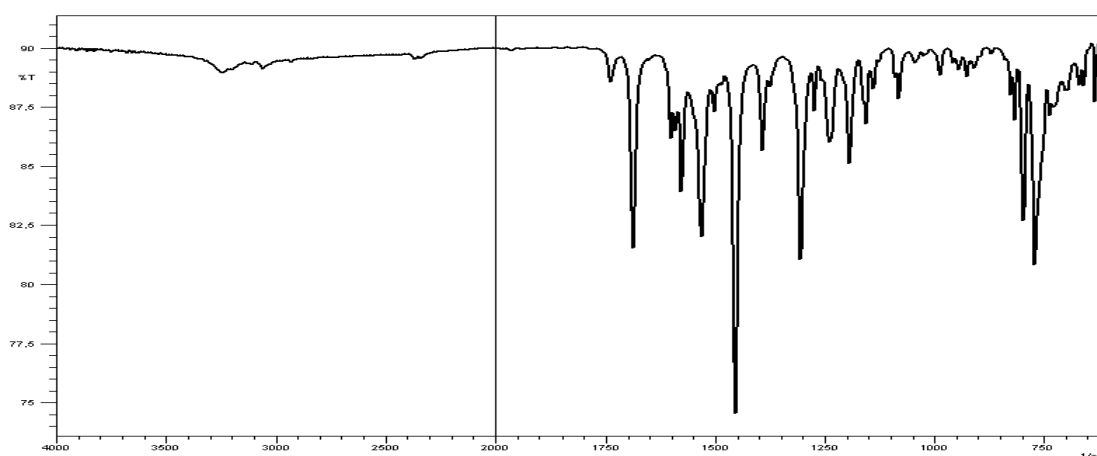
XRD: formula [(C₃₂H₂₆N₆O₂)*2(TFA)*2(CHCl₃)], see structure **XXXIX** in 'Annexes - Crystal structures'

mp (°C): >300 °C

Elemental analysis: Found: C, 73.26; N, 14.78; H, 4.62.

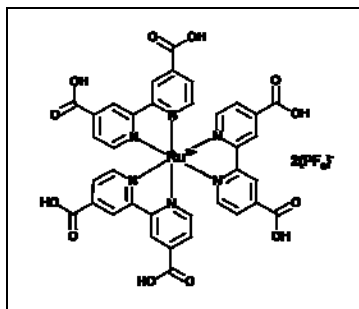
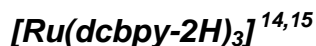
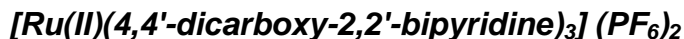
Calc. for C₃₂H₂₄N₆O₂ : C, 73.26; N, 16.02; H, 4.61.

IR (ATR): 3245 w, 1688 m, 1577 m, 1532 m, 1455 s, 1392 w, 1305 m, 1240 w, 1193 w, 795 m, 770 m cm⁻¹



VI.2 Synthesis of complexes

Complex 1



Synthesis:

A mixture of $\text{RuCl}_3 \cdot 3\text{H}_2\text{O}$ (120 mg, 0.53 mmol) and 4,4'-dicarboxy-2,2'-bipyridine (450 mg, 1.8 mmol) in 15 ml of DMF was refluxed overnight. The reaction flask was cooled to room temperature and the precipitate was filtered, washed with dichloromethane and vacuum-dried to obtain a dark brown powder $[\text{Ru}(\text{II})(4,4'\text{-dcbipy})_3\text{Cl}_2]$. The product was then converted into the hexafluorophosphate salt by stirring the chloride salt with a saturated aqueous solution of NH_4PF_6 for 3h. EtOH was added and the precipitate was recovered by filtration, washed with water and air-dried to obtain 450 mg of a red/brown product. Overall yield: 76%

Characterization:

Molecular Formula: $\text{C}_{36}\text{H}_{24}\text{N}_6\text{O}_{12}\text{F}_{12}\text{P}_2\text{Ru}$ **Molecular Weight:** 1123.60

$^1\text{H-NMR}$ [$\text{D}_2\text{O}/\text{NaOD}$, 300MHz, 25°C, $\delta(\text{ppm})$]: 8.75 (d, $J_{5,3}=1.6$ Hz, 6H, 3,3'-H), 7.75 (d, $J_{5,6}=5.8$ Hz, 6H, 6,6'-H), 7.55 (dd, $J_{5,6}=5.8$ Hz, $J_{5,3}=1.3$ Hz, 6H, 5,5'-H)

$^{13}\text{C-NMR}$ [$\text{D}_2\text{O}/\text{NaOD}$, 300MHz, 25°C, $\delta(\text{ppm})$]: 170.9 (COO), 157.2, 151.7(CH), 145.3, 126.0(CH), 123.0(CH)

MS (ESI +): m/z 416.9 [100, (1/2 M) $^+$]

XRD - formula $[\text{Ru} (\text{C}_{36}\text{H}_{22}\text{N}_6\text{O}_{12})^*1.5(\text{H}_2\text{O})]$, see structure **XII** in 'Annexes - Crystal structures'

Elemental analysis: Found: C, 41.20; N, 8.79; H, 3.14.

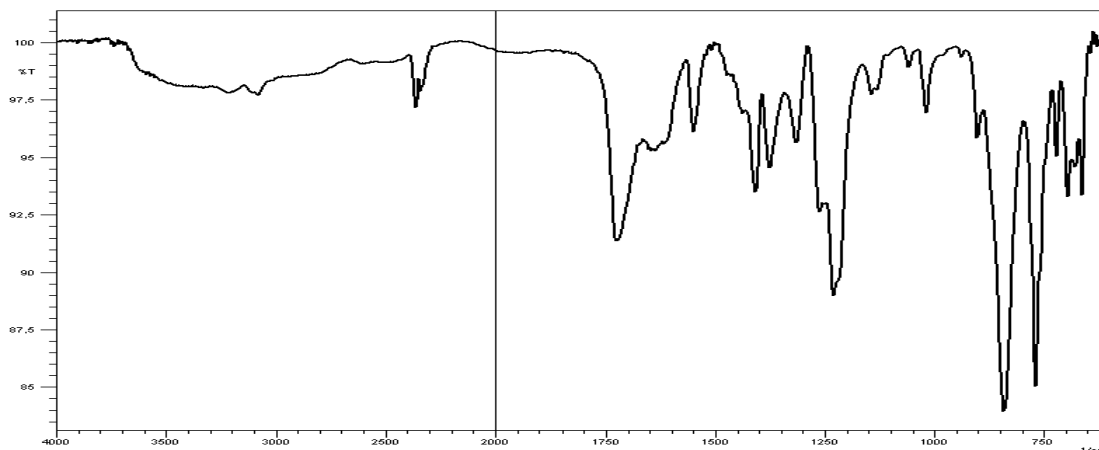
¹⁴ E. Eslinen, S. Luukkanen, M. Haukka, M. Ahlgrén, T. A. Pakkanen, ; *J. Chem. Soc., Dalton Trans.*; **2000**, 2745-2752

¹⁵ M. Zhou, G. P. Robertson, J. Roovers; *Inorg. Chem.*; **2005**, 8317-8325

Calc. for $C_3H_{24}N_6O_{12}ClF_6PRu^*(NH_4Cl)*(CH_3CH_2OH)$: C, 40.98; N, 8.80; H, 3.07.

UV-Vis : λ_{max} (H₂O-Et₃N) 269 (98690), 460 (21540) nm (ϵ)

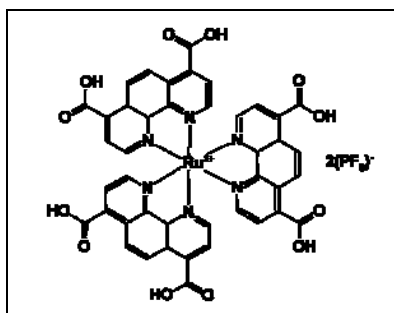
IR (KBr): 1727 (COOH), 1549, 1408, 1375, 1315, 1230, 1018, 840 s, 769 s cm^{-1}



Complex 2

$[Ru(II)(4,7\text{-dicarboxy-}1,10\text{-phenanthroline})_3] (PF_6)_2$

$[Ru(\text{dcphen-}2H)_3]^{16}$



Synthesis:

A mixture of $RuCl_3 \cdot 3H_2O$ (53 mg, 0.19 mmol) and 4,7-dicarboxy-1,10-phenanthroline (156 mg, 0.57 mmol) in 4 ml of water and 1 ml of concentrated HCl was placed in a sealed teflon coated stainless steel bomb and the latter placed hydrothermal apparatus. The temperature was raised to 220 °C and maintained for 12h. After slow cooling to room temperature over 4 days, the reaction mixture was filtered and washed with water affording 130 mg of a dark-brown product.

¹⁶ O. Schwarz, D. van Loyen, S. Jockusch, N. J. Turro, H. Dürr; *J. Photochem. Photobiol. A: Chemistry*; **2000**, *132*, 91-98

Ru(4,4'-dicarboxy-2,2'-bipyridine)₃Cl₂ (60 mg, 0.06 mmol) was suspended in a saturated solution of NH₄PF₆ and stirred for 24h. The precipitate was filtered and washed several times with ethanol and acetone to afford 41 mg of a red-brown powder. Yield: 56%

Characterization:

Molecular Formula: C₄₂H₂₄N₆O₁₂F₁₂P₂Ru **Molecular Weight:** 1195.67

¹H-NMR [D₂O/ NaOD, 300MHz, 25°C, δ(ppm)]: 8.27 (s, 6H, 5,6-H), 7.88 (d, J_{3,2}=5.4 Hz, 6H, 2,9-H), 7.55 (d, J_{2,3}=5.4 Hz, 6H, 3,8-H)

¹³C-NMR [D₂O/ NaOD, 300MHz, 25°C, δ(ppm)]: 172.8 (COO), 152.4 (CH), 148.2, 145.3, 126.8, 126.1 (CH), 122.5 (CH)

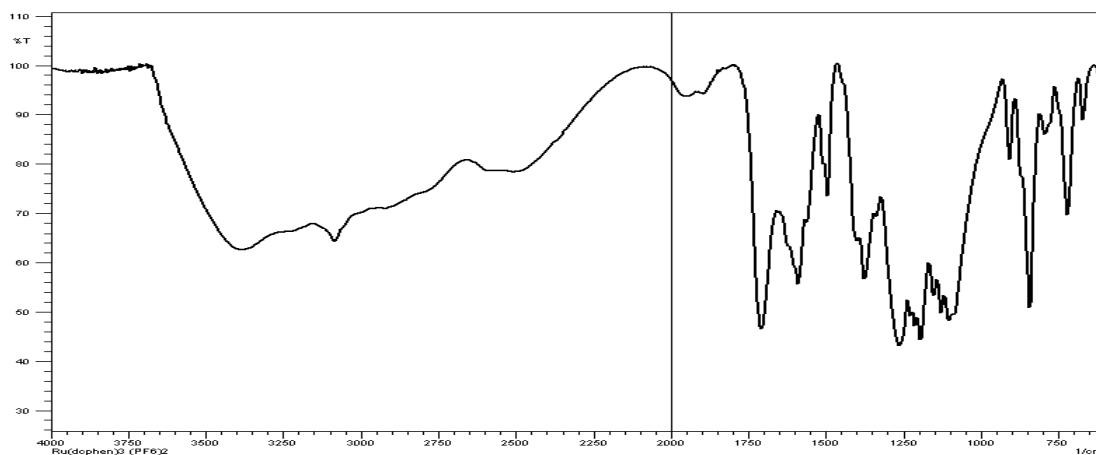
XRD: formula [Ru(C₄₂H₂₂N₆O₁₂)*2(H₂O)], see structure **XIII** in 'Annexes - Crystal structures'

Elemental analysis: Found: C, 42.88; N, 7.50; H, 2.49.

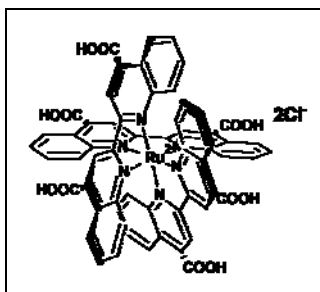
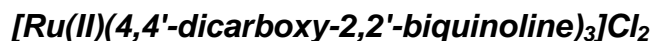
Calc. for C₄₂H₂₄N₆O₁₂F₁₂P₂Ru*(C₃H₆O)*1/3(NH₄Cl): C, 42.50; N, 6.97; H, 2.48.

UV: λ_{max} (H₂O-Et₃N) 246 (41387), 302 (88591), 466 (24514) nm(ε)

IR (KBr): 3381 (broad), 3083, 1710s (ν C=O), 1589s, 1494, 1375, 1261, 1227, 1212, 1194, 1152, 1129, 1102, 906, 839s, 790, 718, 670 cm⁻¹



Complex 3



Synthesis:

A mixture of the commercially available $\text{RuCl}_3 \cdot 3\text{H}_2\text{O}$ (50 mg, 0.19 mmol) and 4,4'-dicarboxy-2,2'-biquinoline (196 mg, 0.57 mmol) in 3 ml of water and 1.5 ml of concentrated HCl was placed in a sealed teflon coated stainless steel bomb. The temperature was raised to 200 °C and maintained for 6h. After slow cooling (10°C/h) to room temperature, the dark precipitate was filtered off and washed with water, methanol and CHCl_3 to give 180 mg of a brown powder. Yield: 80%

Characterization:

Molecular Formula: $\text{C}_{60}\text{H}_{36}\text{N}_6\text{O}_{12}\text{Cl}_2\text{Ru}$ **Molecular Weight:** 1204.08

$^1\text{H-NMR}$ [$\text{D}_2\text{O}/\text{NaOD}$, 300MHz, 25°C, $\delta(\text{ppm})$]: 8.20 (s, 6H, H-3,3'), 8.08 (t, 12H, H-5,5',8,8'), 7.78 (t, 6H, H-6,6'), 7.61 (t, 6H, H-7,7')

$^{13}\text{C-NMR}$ [$\text{D}_2\text{O}/\text{NaOD}$, 300MHz, 25°C, $\delta(\text{ppm})$]: 175.0 (COO), 155.7, 148.0, 147.4, 130.9 (CH), 128.4 (CH), 128.2 (CH), 125.7 (CH), 123.8, 116.2

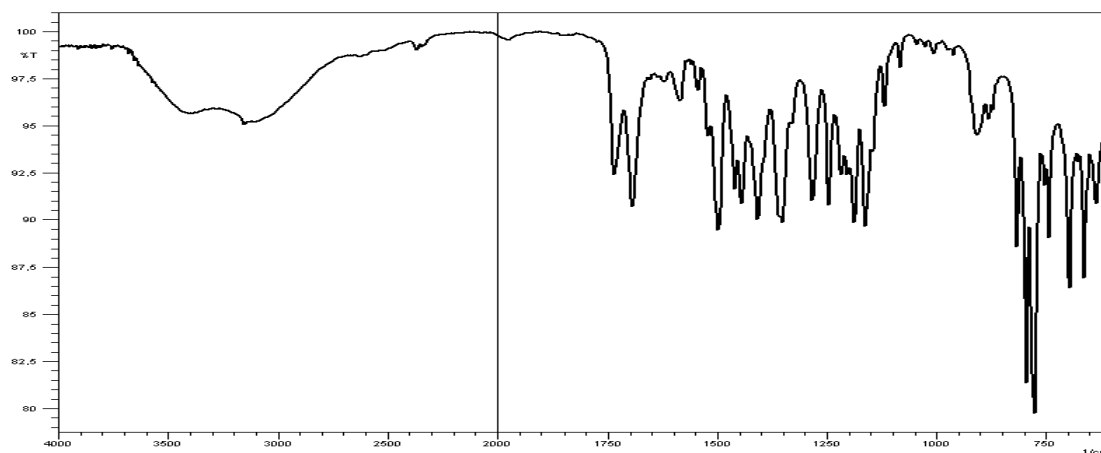
MS (MALDI): 1133.38 [M-H-2Cl]⁺

Elemental analysis: Found: C, 54.79; N, 6.25; H, 2.71.

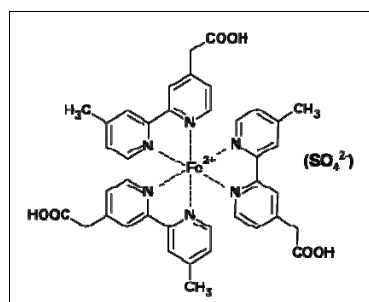
Calc. for $\text{C}_{60}\text{H}_{36}\text{N}_6\text{O}_{12}\text{Cl}_2\text{Ru} \cdot 1/2(\text{CHCl}_3)$: C, 54.66; N, 6.27; H, 2.78.

UV-Vis : λ_{max} ($\text{H}_2\text{O-Et}_3\text{N}$) 275 (87305), 322 (62660) nm(ϵ)

IR (ATR): 3150 (broad), 1735m, 1693m, 1497, 1460, 1445, 1408, 1352, 1282, 1247, 1187, 1163, 906, 815, 794s, 774s, 742, 696, 663 cm^{-1}



Complex 4



Synthesis:

4-Acetoxy-4'-Methyl-2,2'-bipyridine (218 mg, 0.95 mmol) and Iron(II)ammoniumsulfate hexahydrate (124 mg, 0.31 mmol) were dissolved in 15 ml of water and the solution was stirred overnight at r.t. The red-purple solution was filtered, reduced in volume and 30 ml of acetone was added. The precipitate was filtered off and the clear water-acetone solution was evaporated under reduced pressure. The powder was re-dissolved in ethanol and filtered to give a sparkling dark purple powder. The solid was redissolved in a minimum amount of water and chromatographed on Sephadex G-15 using MeOH as eluent. Yield: 60 %

Characterization:

Molecular Formula: $\text{C}_{39}\text{H}_{36}\text{N}_6\text{O}_{10}\text{SFe}$ **Molecular Weight:** 980.77

$^1\text{H-NMR}$ [D_2O , 300MHz, 25°C, δ (ppm)]: 8.24 (s, 2H), 7.33-7.04 (m, 4H), 3.61 (s, 2H, CH_2), 2.36 (s, 3H, CH_3)

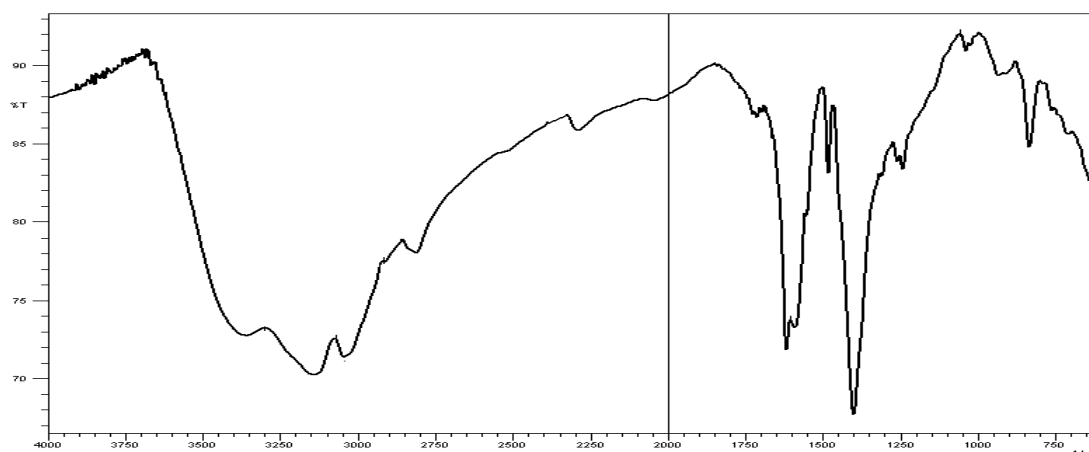
$^{13}\text{C-NMR}$ [D_2O , 500MHz, 25°C, $\delta(\text{ppm})$]: 159.2, 158.9, 158.5, 153.6 (CH), 153.4(CH), 152.9 (CH), 152.8, 150.8, 127.8 (CH), 127.5 (CH), 124.4 (CH), 42.7 (CH_2), 19.7 (CH_3)

MS (ESI +): m/z 370.13 [5, M^{++}], 511.13 [37, (M-L-H) $^+$], 547.11 [80, (M-L+Cl) $^+$], 739.23 [100, (M-H) $^+$]

Elemental analysis: Many submitted elemental analysis results were not satisfying.

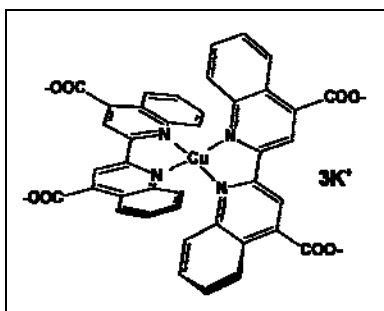
UV-Vis : λ_{max} (EtOH) 300 (27850), 356 (3726), 529 (4260) nm (ϵ)

IR (KBr): 3358 (broad), 3140 (broad), 1619s, 1590s, 1482w, 1400s, 1242w, 833w cm^{-1}



Complex 5

$[\text{Cu(I)}(4,4'\text{-dicarboxy-2,2'-biquinoline})_2]\text{K}_3 - [\text{Cu}(\text{dcBQ})_2]^{17}$



Synthesis:

Commercially available 4,4'-dicarboxy-2,2'-biquinoline dipotassium salt (500 mg, 1.05 mmol) was dissolved in 25 ml of distilled water and a solution of $\text{CuSO}_4 \cdot x\text{H}_2\text{O}$ (95 mg, 0.59 mmol) in 25 ml distilled water was added. Immediately a greenish precipitate was formed. The precipitate

¹⁷ R. D. Braun, K. J. Wiechelmann, A. A. Gallo; *Anal. Chim. Acta*, **1989**, 221, 223-238

was filtered, washed with water and again suspended in 40 ml of distilled water. The suspension was heated at 50 °C and a tip of spatula of hydroquinone was added under stirring. The mixture turned immediately into a purple solution which was reduced to 20 ml and the residual precipitate was filtered off. The solution was evaporated and the solid was redissolved in a minimum amount of methanol and chromatographed on Sephadex LH-20 using EtOH as eluent. Yield: 45%

Characterization:

Molecular Formula: $C_{40}H_{20}N_4O_8CuK_3$ **Molecular Weight:** 865.45

1H -NMR [MeOD, 500MHz, 25°C, δ (ppm)]: 8.99 (s, 4H, H-3,3'), 8.51 (dd, $J_{5,7}=1.3$ Hz, $J_{5,6}=8.4$ Hz, 4H, H-8,8'), 7.77 (dd, $J_{8,7}=8.5$ Hz, 4H, H-5,5'), 7.53 (ddd, $J_{6,8}=1.3$ Hz, $J_{7,6}=6.9$ Hz, $J_{5,6}=8.5$ Hz, 4H, H-6,6'), 7.35 (ddd, $J_{7,5}=1.3$ Hz, $J_{7,6}=6.9$ Hz, $J_{7,8}=8.4$ Hz, 4H, H-7,7')

Assignment is based on 1H - 1H -COSY spectrum.

^{13}C -NMR [MeOD, 500MHz, 25°C, δ (ppm)]: 174.1 (COO), 154.2 (C-2), 147.5 (C-8b), 132.0 (CH-7), 129.7 (CH-6), 128.9 (CH-5), 128.1 (CH-8), 127.8 (C-8a), 127.9 (C-3), 118.4 (CH-3)

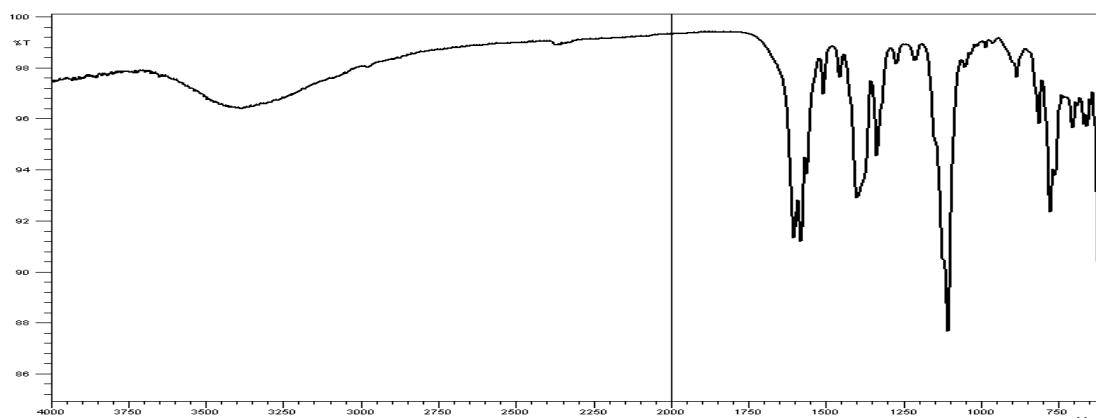
Assignment is based on 2-D NMR studies.

Elemental analysis: Found: C, 49.06; N, 5.59; H, 3.53.

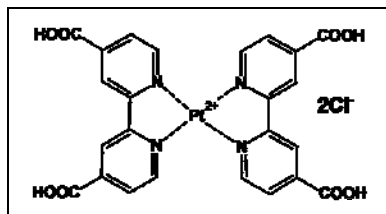
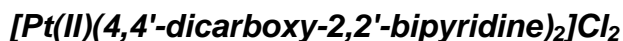
Calc. for $[CuC_{40}H_{20}N_4O_8]K_3 \cdot 6(H_2O)$: C, 49.34; N, 5.75; H, 3.31.

UV-Vis : λ_{max} (H₂O) 558 (77355) nm(ϵ)

IR (ATR): 3392 (broad), 1603 (s, ν_a COO), 1580(s, ν_s COO), 1508w, 1454w, 1397(s, δ COO), 1334m, 1271w, 1210w, 1120, 1106s, 883w, 812w, 775m, 702w, 616s cm^{-1}



Complex 6



Synthesis:

366 mg of 4,4'-dcbpy (1.5 mmol) was suspended in 20 ml of water, Et_3N (0.3 ml) was added and the yellow solution was heated to reflux for 2 h to evaporate the excess of base until pH=7 was reached. $\text{PtCl}_2(\text{bis-benzonitrile})$ was added (350 mg, 0.7 mmol) in 15 ml of methanol and the yellow suspension was heated to reflux overnight.

The mixture was filtrated and the grey precipitate was separated. The brown solution was evaporated to dryness, the solid was redissolved in 20 ml of water (pH=6/7) and 10 ml of methanol mixture and left at 4°C overnight. The precipitate was separated, the mixture was evaporated to obtain 150 mg of the neutral compound $[\text{Pt}(\text{C}_{24}\text{H}_{14}\text{N}_4\text{O}_8)]$. Alternatively, the compound could be precipitated as $[\text{Pt}(\text{C}_{24}\text{H}_{16}\text{N}_4\text{O}_8)\text{Cl}_2]$ upon adding a 0.1M HCl solution to reach pH=3-4 then by washing with methanol and drying in air. Yield: 36%

Characterization:

Molecular Formula: $[\text{C}_{24}\text{H}_{16}\text{N}_4\text{O}_8\text{Cl}_2\text{Pt}]$ or $[\text{C}_{24}\text{H}_{14}\text{N}_4\text{O}_8\text{Pt}]$

Molecular Weight: 752.99 or 681.04

$^1\text{H-NMR}$ [DMSO, 300MHz, 25°C, $\delta(\text{ppm})$]: 8.77 (s, 2H), 8.67 (s, 2H), 7.75 (s, 2H)

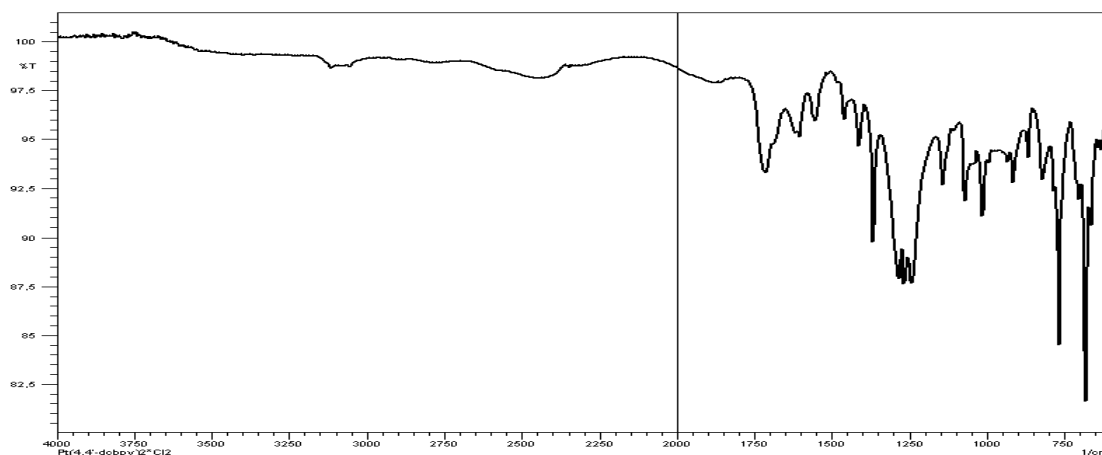
$^{13}\text{C-NMR}$ [DMSO, 300MHz, 25°C, $\delta(\text{ppm})$]: 168.5 (COO), 156.0, 149.6(CH), 147.7, 123.7(CH), 120.5 (CH)

MS (ESI +): m/z 553.03 [100, (M-L+Cl+DMSO) $^+$], 719.03 [10, (M+Cl) $^+$], 755.05 [30, (M+2Cl) $^+$]

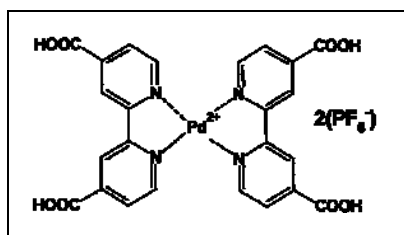
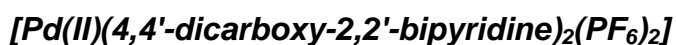
Elemental analysis : Found C, 35.31; H, 3.34; N, 6.55.

Calc. for $\text{C}_{24}\text{H}_{16}\text{N}_4\text{O}_8\text{Cl}_2\text{Pt}\cdot 3(\text{H}_2\text{O})$: C, 35.68; H, 2.74; N, 6.94

IR (ATR): 1712 m, 1604 w, 1552 w, 1412 w, 1365 m, 1283, 1266, 1243 s, 1141 w, 1070 w, 1012 w, 914 w, 866 w, 820 s, 765 s, 680 s cm^{-1}



Complex 7



Synthesis:

4,4'-dcbpy (244 mg, 1 mmol) was dissolved in 10 ml of water and stirred, 10 ml of a 0.1 M solution of NaOH (pH=7) and 230 mg (0.5 mmol) of $\text{Pd}(\text{CH}_3\text{CN})_4(\text{BF}_4)_2$ were added. Immediately a yellow-orange solution was formed, the pH was adjusted to 7 and the milky solution was filtered and heated to reflux for 8 h. The mixture was cooled to room temperature, the pH was adjusted to 6 by adding 0.1 M solution of HCl, the precipitate was filtered and washed with water (3x5 ml) and acetonitrile (3x5 ml).

The powder was redissolved in a minimum amount of 0.1 M NaOH (pH=10), stirred for 48 h for complete dissolution and purified on sephadex LH-20 as chromatographic support and water as eluent. Upon addition of HPF_6 , the desired compound was precipitated, filtered and washed with water (3x5 ml) and acetone (2x5 ml) affording a salmon powder. Yield: 55 %

Characterization:

Molecular Formula: $\text{C}_{24}\text{H}_{16}\text{N}_4\text{O}_8\text{F}_{12}\text{P}_2\text{Pd}$

Molecular Weight: 884.75

$^1\text{H-NMR}$ [DMSO, 300MHz, 25°C, δ (ppm)]: 8.91 (d, 2H, $J_{5,6}=4.4\text{Hz}$, H-6,6'), 8.84 (s, 2H, H-3,3'), 7.91 (d, 2H, $J_{5,6}=4.4\text{Hz}$, H-5,5')

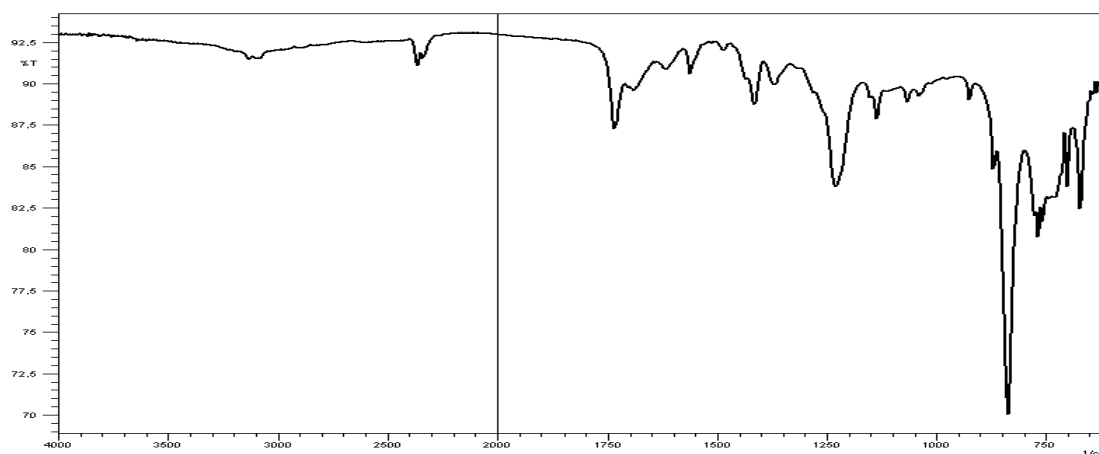
$^{13}\text{C-NMR}$ [DMSO, 300MHz, 25°C, δ (ppm)]: 166.4 (COO), 155.9, 151.1 (CH), 140.0, 123.9 (CH), 120.0 (CH)

Elemental analysis : Found: C, 34.61; H, 2.59; N, 6.53.

Calc. for $(\text{C}_{24}\text{H}_{16}\text{N}_4\text{O}_8\text{F}_{12}\text{P}_2\text{Pd})^*(\text{C}_3\text{H}_6\text{O})$: C, 34.39; H, 2.35; N, 5.94.

UV : λ_{max} ($\text{H}_2\text{O-Et}_3\text{N}$) 245 (28935), 303 (19815) nm(ϵ)

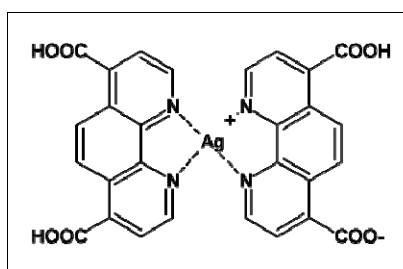
IR (ATR): 1375 m, 1415 m, 1229 m, 836 s, 767s (broad), 701 m, 672 m cm^{-1}



Complex 8

Ag(I)(4,7-dicarboxy-1,10-phenanthroline)₂

[Ag(4,7-dcphen)₂]



Synthesis:

4,7-dcphen (80 mg, 0.29 mmol) was added to a clear solution of AgPF_6 (37 mg, 0.15 mmol) in 30 ml of CH_3CN . The reaction mixture was protected from light and stirred overnight affording a yellow precipitate which was filtered and washed with ethanol (2x10 ml) and dried under vacuum giving 70 mg of a bright yellow powder. Yield: 75%

Characterization:

Molecular Formula: C₂₈H₁₅N₄O₈Ag **Molecular Weight:** 643.31

¹H-NMR [DMSO, 300MHz, 25°C, δ(ppm)]: 9.25 (d, 2H), 8.77 (s, 2H), 8.15 (d, 2H)

¹³C-NMR [DMSO, 300MHz, 25°C, δ(ppm)]: 167.9, 150.6 (CH), 146.5, 137.0, 125.2 (CH), 124.1 (CH)

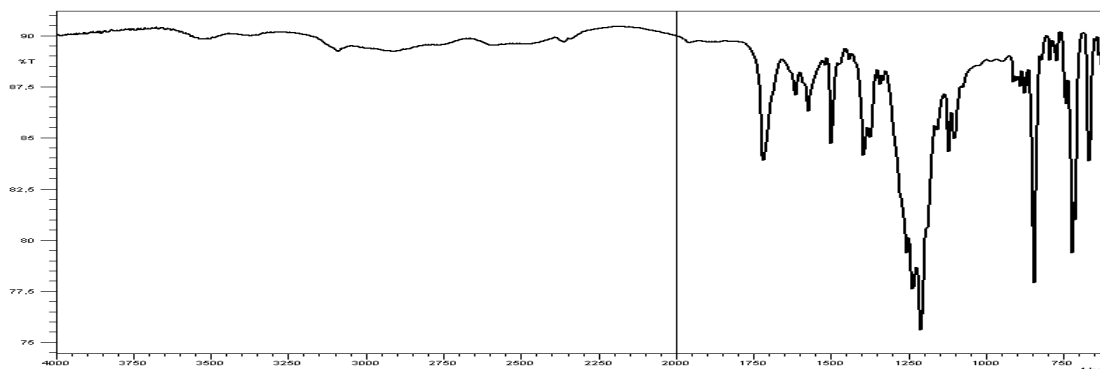
XRD: formula [Ag(C₁₄ H₁₅ N₄ O₂)*1.23(DMSO)*0.77(EtOH)], see structure **XV** in 'Annexes - Crystal structures'

Elemental analysis : Found C, 54.27; H, 3.18; N, 9.22.

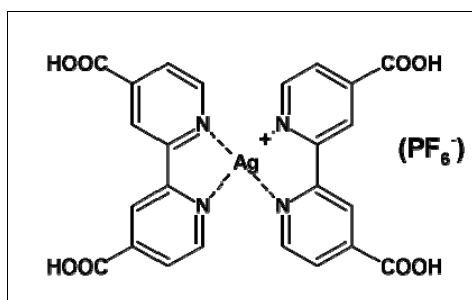
Calc. for (C₂₈H₁₅N₂O₄Ag)*(C₁₄H₈N₂O₄)*(H₂O): C, 54.30; H, 2.71; N, 9.05.

UV : λ_{max} (H₂O-Et₃N) 236.5 (56841), 270.5 (74033) nm(ε)

IR (ATR): 1718 s, 1614 w, 1497 m, 1393 m, 1373 m, 1253 s, 1234 s, 1210 s (broad), 1119 w, 1100 w, 843 s, 720 s, 665 m cm⁻¹



Complex 9

[Ag(I)(4,4'-dicarboxy-2,2'-bipyridine)₂ (PF₆)₂]**[Ag(4,4'-dcbipy-2H)₂]****Synthesis:**

4,4'-dcbpy (820 mg, 3.42 mmol) was stirred for 20 min in 2 ml of water and 8 ml of 0.1 M NaOH solution was added until pH=7 was reached, to afford a milky suspension.

AgPF₆ (450 mg; 1.71 mmol) in 10 ml of ethanol was added to the mixture and the flask was protected from light. The mixture was stirred at r.t. for 5 days then the precipitate was filtrated and carefully washed with water, then methanol and acetone to obtain 710 mg of an off-white powder. The product was suspended in 20 ml of water, 2 ml of HPF₆ were added until pH=2 and the mixture was stirred for 1h.

When the colour turned to bright yellow, the precipitate was filtered and washed with water to reach pH=7. The powder is sensitive towards basic pH which causes decomposition. The stability in air is not granted for long period. Yield: 70%

Characterization:

Molecular Formula: C₂₄H₁₅N₄O₈Ag or C₂₄H₁₆N₄O₈AgPF₆ **Molecular Weight:** 595.26 or 739.96

¹H-NMR [D₂O/Et₃N, 300MHz, 25°C, δ(ppm)]: 8.18 (d, J_{5,6}=4.5Hz, 2H, H-6,6'), 8.12 (s, 2H, H-3,3'), 7.51 (d, J_{5,6}=4.5Hz, 2H, H-5,5')

¹³C-NMR [D₂O/Et₃N, 300MHz, 25°C, δ(ppm)]: 170.8 (COO), 151.7, 150.8 (CH), 146.8, 124.4 (CH), 121.4 (CH)

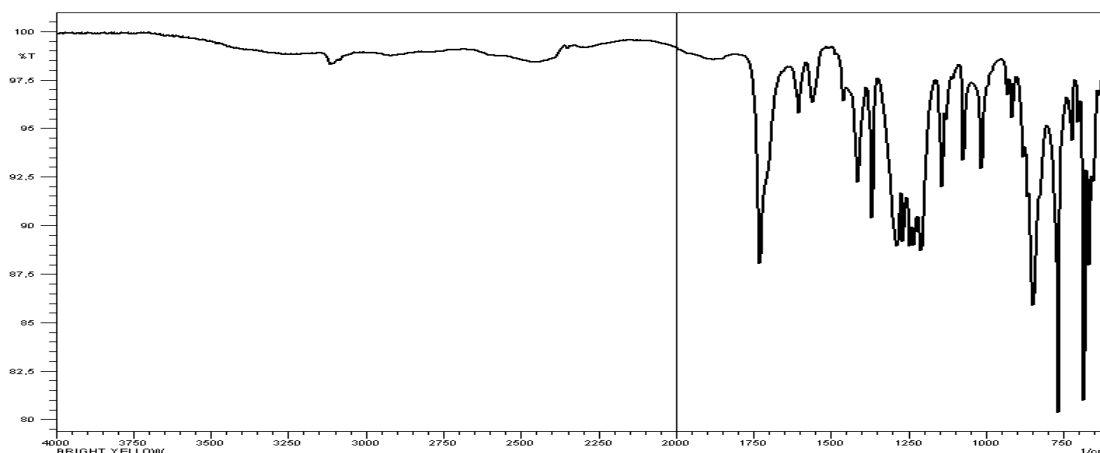
MS (ESI +): m/z 595.02 (100, M+H⁺)

Elemental analysis : Found C, 44.46; H, 3.08; N, 8.6.

Calc. for (C₂₄H₁₅N₄O₈Ag) (C₂₄H₁₅N₄O₈AgPF₆)*(CH₃CN)*(C₃H₃O): C, 44.38; H, 2.81; N, 8.79

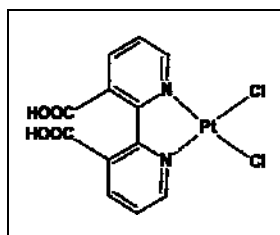
UV-Vis : λ_{max} (H₂O-Et₃N) 239 (20735), 298(24477) nm/(ε)

IR (ATR): 1728 s, 1603 m, 1556 m, 1412 m, 1365 m, 1285 s (broad), 1246 s, 1232 s, 1208 s, 1140 m, 1071 m, 1012 m, 846 s (broad), 765 s, 681 s, 666 m cm⁻¹



Complex 10

$Pt(II)(3,3'-dicarboxy-2,2'-bipyridine) Cl_2 - $[Pt(3,3'$ -dcbpy) $Cl_2]$ ¹⁸$



Synthesis:

In 30 ml of water, K_2PtCl_4 (235 mg, 0.55 mmol) and commercially available 3,3'-dicarboxy-2,2'-bipyridine (132 mg, 0.55 mmol) were refluxed for 20h. The orange suspension turned into a yellow solution and a precipitate was formed. The precipitate was filtered, washed with water (3x5 ml) and acetone (3x5 ml) and dried under vacuum affording 198 mg of a yellow powder. Yield: 70%

Characterization:

Molecular Formula: $C_{12}H_8N_2O_4Cl_2Pt$ **Molecular Weight:** 508.95

1H -NMR [D_2O/Et_3N , 300MHz, 25°C, δ (ppm)]: 8.66 (dd, 2H, $J_{4,6}=1.5$ Hz, $J_{6,5}=5.7$ Hz, H-6,6'), 8.22 (dd, 2H, $J_{4,6}=1.5$ Hz, $J_{4,5}=7.9$ Hz, H-4,4'), 7.48 (dd, 2H, $J_{6,5}=5.7$ Hz, $J_{4,5}=7.9$ Hz, H-5,5')

^{13}C -NMR [D_2O/Et_3N , 300MHz, 25°C, δ (ppm)]: 169.6 (COO), 156.3, 146.4 (CH), 140.0, 138.8 (CH), 126.1 (CH)

MS (ESI +): m/z 552.99 (100, M-2H+K+Li⁺)

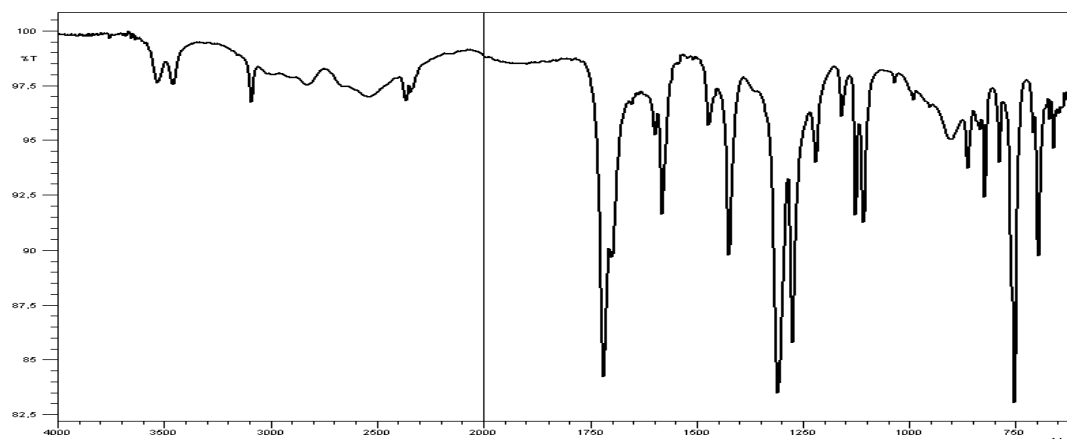
¹⁸ E. A. M. Geary, L. J. Yellowlees, L. A. Jack, I. D. H. Oswald, S. Parsons, N. Hirata, J. R. Durrant, N. Robertson; *Inorg. Chem.*; **2005**, *44*, 242-250

Elemental analysis: Found C, 26.93; H, 2.22; N, 5.18.

Calc. for $C_{12}H_8N_2O_4Cl_2Pt \cdot 2(H_2O)$: C, 26.38; H, 2.21; N, 5.13.

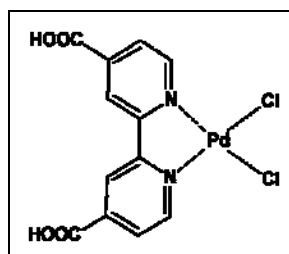
UV-Vis : λ_{max} (H_2O-Et_3N) 282 (14770), 399 (2732) nm (ϵ)

IR (ATR): 3529, 3088, 1719 (s, v C=O), 1581, 1424, 1309, 1274, 1126, 1107, 751, 696 cm^{-1}



Complex 11

$Pd(II)(4,4'$ -dicarboxy-2,2'-bipyridine) Cl_2 - $[Pd(4,4'$ -dcbpy) $Cl_2]^{19, 20}$



Synthesis:

4,4'-dicarboxy-2,2'-bipyridine (75 mg, 0.31 mmol) was added to a yellow solution of Bis(acetonitrile)dichloropalladium(II) (81 mg, 0.31 mmol) in 40 ml of acetone. The mixture was stirred overnight at r.t. leading to a pale yellow precipitate which was filtered and washed with acetone (10 ml) affording 110 mg of yellow powder. Yield: 84%

Characterization:

Molecular Formula: $C_{12}H_8N_2O_4Cl_2Pd$ **Molecular Weight:** 419.89

¹⁹ S. Meyer, s. Saborowski, B. Schäfer; *ChemPhysChem.*; **2006**, *7*, 572-574

²⁰ G.-J. Ten Brink, I.W. C. E. Arends, M. Hoogenraad, G. Verspui, R. A. Sheldon; *Adv. Synth. Catal.*, **2003**, *345*, 497-505

$^1\text{H-NMR}$ [DMSO, 300MHz, 25°C, $\delta(\text{ppm})$]: 9.27 (d, 2H, $J_{5,6}=5.5\text{Hz}$, H-6,6'), 8.99 (s, 2H, H-3,3'), 8.20 (d, 2H, $J_{5,6}=5.5\text{Hz}$, H-5,5')

$^{13}\text{C-NMR}$ [DMSO, 400MHz, 25°C, $\delta(\text{ppm})$]: 164.4 (COO), 156.7, 150.7 (CH), 142.3, 126.6 (CH), 123.5 (CH)

MS (ESI +): m/z 464.93 (100, $\text{M}+\text{CH}_3\text{CN}+\text{H}^+$)

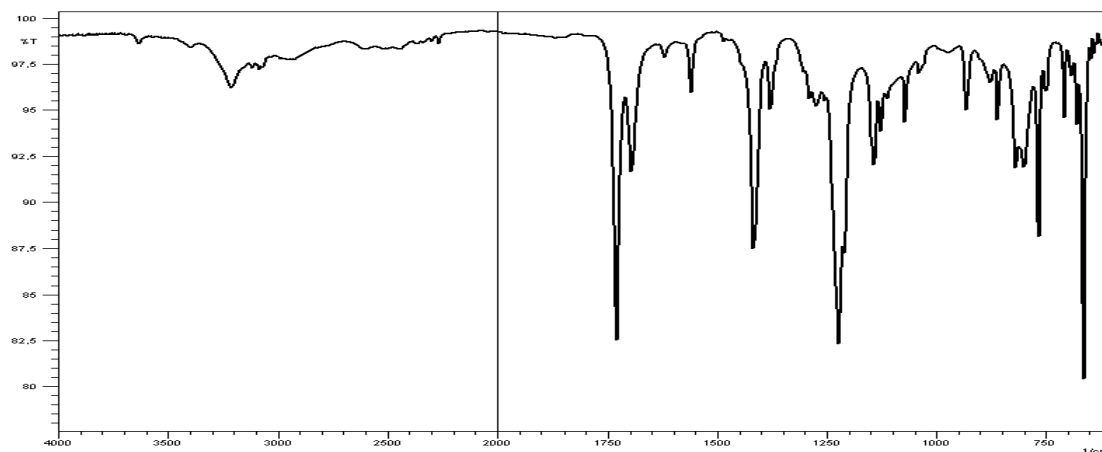
XRD: formula $\{[\text{Pd}(\text{C}_{12}\text{H}_8\text{N}_2\text{O}_4)\text{Cl}_2]^*(\text{DMSO})^*(\text{DMF})\}$, see structure **XIV** in 'Annexes - Crystal structures'

Elemental analysis : Found C, 31.97; H, 2.59; N, 6.12.

Calc. for $\text{C}_{12}\text{H}_8\text{N}_2\text{O}_4\text{Cl}_2\text{Pd}\cdot 2(\text{H}_2\text{O})$: C, 31.49; H, 2.64; N, 6.12.

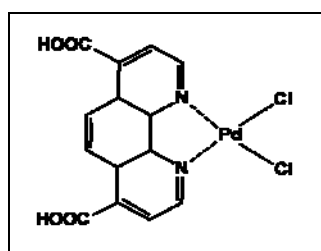
UV-Vis : λ_{max} ($\text{H}_2\text{O}-\text{Et}_3\text{N}$) 276 (10376), 322 (13162) nm/(ϵ)

IR (ATR) : 3633, 3209, 2360, 1730 (s, $\nu\text{C}=\text{O}$), 1697 m, 1560 w, 1417 m, 1379 w, 1222 s, 1210, 1141, 1126, 1071, 932, 860, 818, 799, 766, 707, 678, 663 s cm^{-1}



Complex 12

$\text{Pd}(\text{II})(4,7\text{-dicarboxy-1,10-phenanthroline})\text{Cl}_2$.- $[\text{Pd}(4,7\text{-dcphen})\text{Cl}_2]$



Synthesis:

Commercially available bis(benzonitrile)dichloropalladium(II) (80 mg, 0.20 mmol) was dissolved in 35 ml of acetone and 4,7-dicarboxy-1,10-phenanthroline (55 mg, 0.20 mmol) was added to the orange solution.

The mixture was stirred overnight at r.t. under Ar, the formed precipitate was filtered and the filtrate was washed with diethyl ether (2x5 ml) and acetonitrile (2x5 ml) and dried under vacuum. 80 mg of a yellow powder was obtained. Yield: 90%

Characterization:

Molecular Formula: $C_{14}H_8N_2O_4Cl_2Pd$ **Molecular Weight:** 445.55

1H -NMR [D_2O/Et_3N , 300MHz, 25°C, δ (ppm)]: 8.50 (d, $J_{3,2}=5.4$ Hz, 2H, H-2,9), 8.10 (s, 2H, H-5,6), 7.80 (d, $J_{2,3}=5.4$ Hz, 2H, H-3,8)

^{13}C -NMR [D_2O/Et_3N , 300MHz, 25°C, δ (ppm)]: 171.4 (COO), 148.2 (CH), 147.7, 146.2, 125.9, 125.3 (CH), 122.0 (CH)

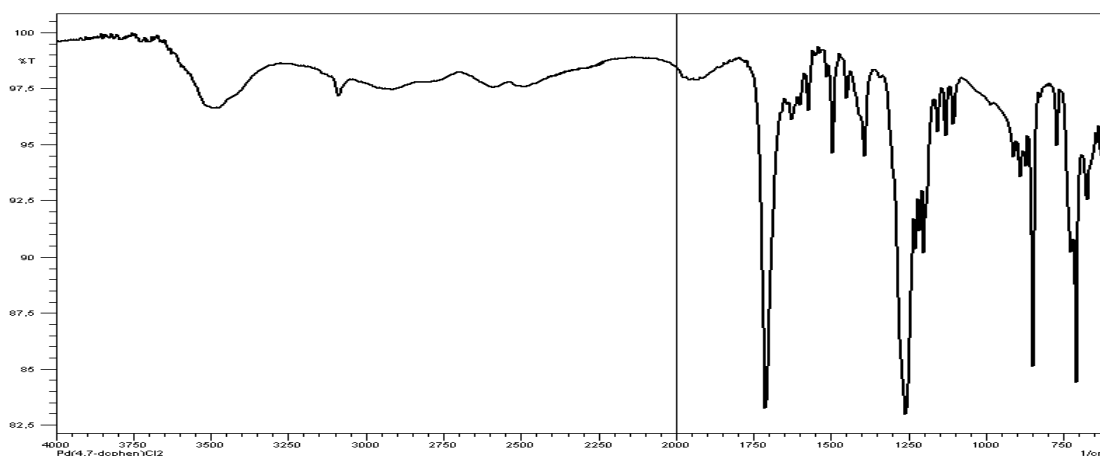
MS (ESI+): m/z 488.95 [100, (M-H-Cl+DMSO) $^+$], 524.92 [50, (M+2K) $^+$], 856.80 [45, (2M-2Cl-3H+K) $^+$]

Elemental analysis : Found C, 34.33; H, 2.64; N, 5.53.

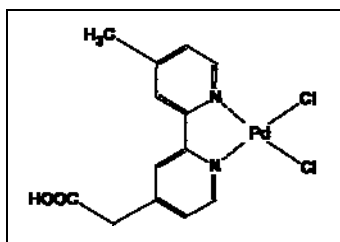
Calc. for $C_{14}H_{10}N_2O_4Cl_2Pd \cdot 2(H_2O)$: C, 34.86; H, 2.91; N, 5.81.

UV-Vis : λ_{max} (H_2O-Et_3N) 212 (26241), 246(23713), 333 (13307) nm/(ϵ)

IR (ATR): 3500 (broad), 3086, 1710 (s, $\nu C=O$) , 1493, 1391, 1257, 1199, 847, 707 cm^{-1}



Complex 13

Pd(II)(4-acetoxy-4'-methyl-2,2'-bipyridine)Cl₂***[Pd(4-ambpy)Cl₂]*****Synthesis:**

4-Acetoxy-4'-methyl-2,2'-bipyridine (296 mg, 1.30 mmol) and freshly prepared bis(acetonitrile)dichloropalladium(II) (338 mg, 1.31 mmol) were dissolved in 27 ml of methanol. The mixture was stirred at r.t. for two days turning to light brown. The precipitate was filtered off, washed with ethanol (2x10 ml) and air dried. The brown powder was dissolved in the a minimum amount of 0.1 M NaOH, the black residual solid was filtered, and the desired compound was purified on Sephadex LH-20 column using water as eluent.

The coloured solution was reduced in volume and acidified to pH=7 with 0.1 M HCl and filtered, the solution was again reduced in volume and acidified to pH=2 using 0.1 M HCl, the precipitate was filtered and washed well with water and air dried affording 120 mg of a light yellow powder. Yield: 20%

Characterization:

Molecular Formula: C₁₃H₁₂N₂O₂Cl₂Pd **Molecular Weight:** 405.57

¹H-NMR [DMSO, 300MHz, 25°C, δ(ppm)]: 12.90 (s, 1H, COOH), 8.94 (d, J_{6,5}=5.9 Hz, 1H, 6-H), 8.83 (d, J_{6',5'}=5.8 Hz, 1H, 6'-H), 8.49 (s, J_{5,3}=1.6 Hz, 1H, 3-H), 8.39 (s, J_{5',3'}=1.2 Hz, 1H, 3'-H), 7.69 (dd, J_{5,3}=1.6 Hz, J_{5,6}=5.9 Hz, 1H, 5-H), 7.59 (dd, J_{5',3'}=1.2 Hz, J_{5',6'}=5.0 Hz, 1H, 5'-H), 3.89 (s, 2H, CH₂), 2.52 (s, 3H, CH₃)

¹³C-NMR [DMSO, 300MHz, 25°C, δ(ppm)]: 171.0 (COO), 156.3, 155.9, 153.8, 150.2, 149.5 (CH), 149.2 (CH), 128.6 (CH), 128.2 (CH), 125.4 (CH), 124.9 (CH), 40.3 (CH₂), 21.5 (CH₃)

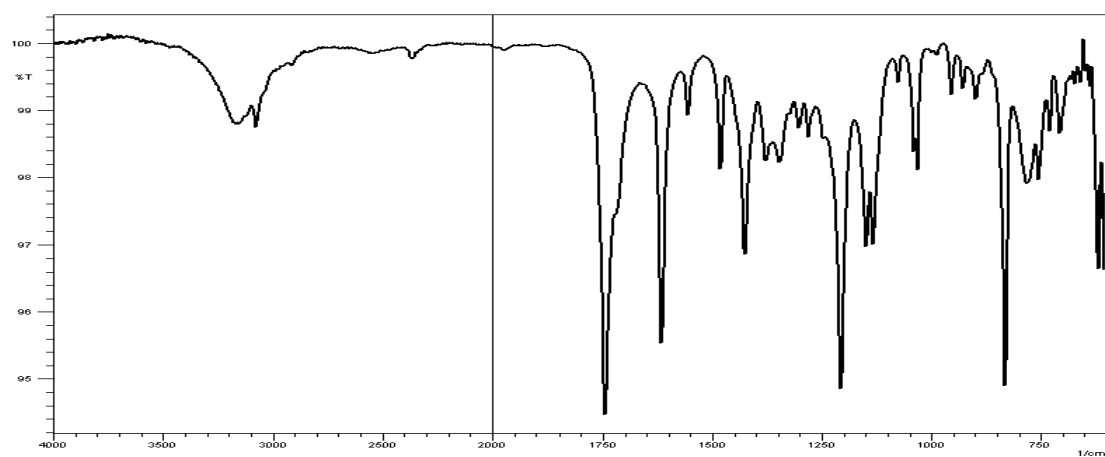
MS (ESI +): m/z 404.9 (95, M-H), 448.9 (100, M-Cl+DMSO)

Elemental analysis : Found C, 36.96; H, 3.20; N, 6.61.

Calc. for C₁₃H₁₂N₂O₂Cl₂Pd*(H₂O) : C, 36.86; H, 3.33; N, 6.61.

UV-Vis : λ_{max} (H₂O-Et₃N) 212 (26241), 252.5 (25026), 311.5 (20506) nm/(ε)

IR (ATR): 3164(broad), 3075 w, 1745 (s, ν C=O) , 1616 m, 1556 w, 1481 w 1426 m, 1378, 1347, 1206 s, 1148 m, 1133 m, 1031 m, 831s, 783 m, 619 m cm⁻¹

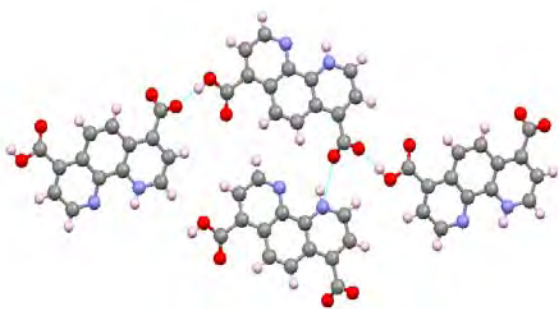


Annexes

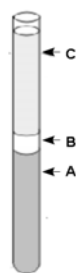
Crystal structures

Chapter II

**I. 4,7-Dicarboxy-1,10-phenanthroline
polymorphous α
(structure e1273)**



Crystallization conditions:



A stock solution was prepared dissolving 40 mg of 4,7-dcphen in 1 ml of a diluted aqueous solution of Et₃N (1 ml Et₃N in 24 ml H₂O) and adding water to a total volume of 8 ml. In a test tube ($\varnothing=1\text{cm}$), 0.3 ml THF (**B**) was layered carefully upon 1 ml DMSO (**A**) and, on top, 1 ml of the stock solution (**C**).

Colourless crystals were obtained after few days of slow diffusion.

[Polymorphous α and β were obtained in different crystallization batches]

Crystallographic data:

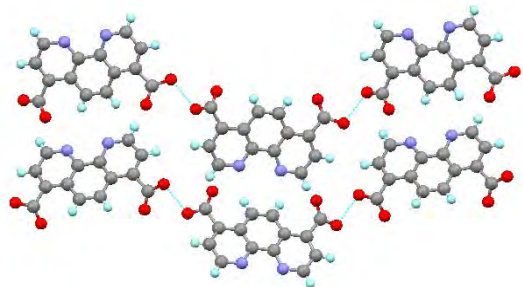
[C₁₄H₈N₂O₄]

Empirical formula
Formula weight
Temperature
Crystal system
Space group
Unit cell dimensions

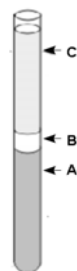
Volume
Z
Density (calculated)
Absorption coefficient(μ)
F(000)
Theta range for data collection
Index ranges
Reflections collected
Independent reflections
Completeness to theta = 27.47°
Max. and min. transmission
Data / restraints / parameters
Goodness-of-fit on F²
Final R indices [$I > 2\sigma(I)$]
Largest diff. peak and hole

C14 H8 N2 O4
268.22
173(2) K
Monoclinic
P2(1)/c
a = 9.7547(10) Å $\alpha = 90^\circ$.
b = 7.5702(6) Å $\beta = 104.189(3)^\circ$.
c = 15.2163(16) Å $\gamma = 90^\circ$.
3150.0(6) Å³
4
1.635 Mg/m³
0.123 mm⁻¹
552
2.15 to 27.47°.
-12 ≤ h ≤ 12, -9 ≤ k ≤ 6, -19 ≤ l ≤ 16
5993
2394 [R(int) = 0.0343]
96.0 %
0.9758 and 0.9711
2394 / 0 / 182
1.015
R1 = 0.0465, wR2 = 0.1143
0.251 and -0.241 e.Å⁻³

**II. 4,7-Dicarboxy-1,10-phenanthroline
polymorphous β
(structure e1274)**



Crystallization conditions:



A stock solution was prepared dissolving 40 mg of 4,7-dcphen with 1 ml of a diluted aqueous solution of Et_3N (1 ml Et_3N in 24 ml H_2O) and adding water to a total volume of 8 ml. In a test tube ($\varnothing=1\text{cm}$), 0.3 ml dioxane (**B**) was layered down upon 1 ml DMSO (**A**) and, on top, 1 ml of the stock solution (**C**). Colourless crystals were obtained after few days of slow diffusion.

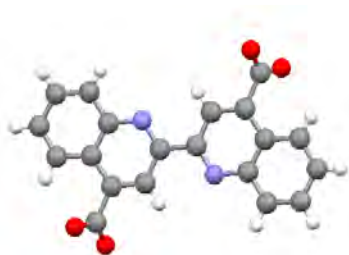
[Polymorphous α and β were obtained in different crystallization batches]

Crystallographic data:

[$\text{C}_{14}\text{H}_8\text{N}_2\text{O}_4$]

Empirical formula	$\text{C}_{14}\text{H}_8\text{N}_2\text{O}_4$
Formula weight	268.22
Temperature	173(2) K
Crystal system	Orthorhombic
Space group	$P2(1)2(1)2(1)$
Unit cell dimensions	$a = 7.4854(2) \text{ \AA}$ $\alpha = 90^\circ$. $b = 13.1928(4) \text{ \AA}$ $\beta = 90^\circ$. $c = 21.5958(7) \text{ \AA}$ $\gamma = 90^\circ$.
Volume	$2132.66(11) \text{ \AA}^3$
Z	8
Density (calculated)	1.671 Mg/m^3
Absorption coefficient(μ)	0.126 mm^{-1}
F(000)	1104
Theta range for data collection	1.81 to 27.52° .
Index ranges	$-8 < h < 9$, $-17 < k < 16$, $-28 < l < 28$
Reflections collected	20645
Independent reflections	4895 [R(int) = 0.0784]
Completeness to theta = 27.52°	99.7 %
Max. and min. transmission	0.9875 and 0.9851
Data / restraints / parameters	4895 / 0 / 362
Goodness-of-fit on F ²	1.115
Final R indices [$I > 2\sigma(I)$]	$R_1 = 0.0714$, $wR_2 = 0.1641$
Absolute structure (Flack) parameter	-0.6(19)
Largest diff. peak and hole	0.471 and $-0.295 \text{ e.\AA}^{-3}$

III. 4,4'-Dicarboxy-2,2'-biquinoline (structure e1594)

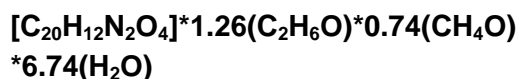


Crystallization conditions:



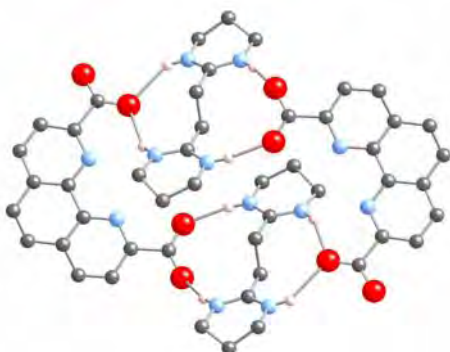
A stock solution was prepared dissolving 190 mg of 4,4'-dcBQ with 1 ml of a diluted aqueous solution of Et₃N (5 ml Et₃N in 24 ml H₂O) and adding water/EtOH 7:3 to a total volume of 80 ml. In a test tube (ø=1cm), 5 drops of ButOH (**B**) were layered down upon 3 ml of the stock solution (**A**) and on top 1.5 ml of water/EtOH 1:1 (**C**). Colourless crystals were obtained after some days of slow diffusion.

Crystallographic data:



Empirical formula	C _{23.26} H ₃₆ N ₂ O _{12.74}
Formula weight	544.74
Temperature	173(2) K
Crystal system	Monoclinic
Space group	C2/c
Unit cell dimensions	a = 31.676(2) Å α = 90° b = 4.7154(3) Å β = 120.882(3)° c = 21.3667(16) Å γ = 90°
Volume	2739.0(3) Å ³
Z	4
Density (calculated)	1.338 Mg/m ³
Absorption coefficient(μ)	0.110 mm ⁻¹
F(000)	1174
Theta range for data collection	1.94 to 27.58°
Index ranges	-40 ≤ h ≤ 40, -5 ≤ k ≤ 6, -27 ≤ l ≤ 27
Reflections collected	11843
Independent reflections	3158 [R(int) = 0.0393]
Completeness to theta = 27.58°	99.7 %
Max. and min. transmission	0.9913 and 0.9869
Data / restraints / parameters	3158 / 11 / 221
Goodness-of-fit on F ²	1.098
Final R indices [I > 2σ(I)]	R1 = 0.0645, wR2 = 0.2034
Largest diff. peak and hole	0.942 and -0.654 e.Å ⁻³

IV. **[BAD23][2,9-dcphen]**
(structure e1020)



Crystallization conditions:



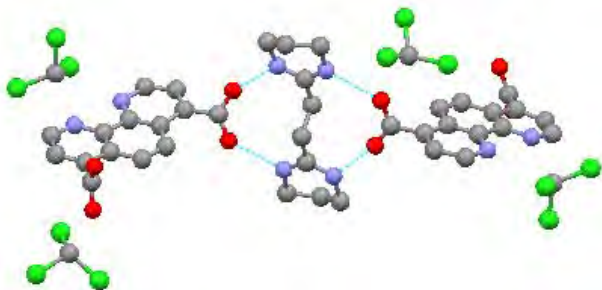
A suspension of 2,9-dcphen (100 mg) and BAD23 (72 mg) in 10 ml of ethanol 95% was refluxed for 40 min. After cooling the mixture was let evaporate in the air forming colourless crystals suitable for X-ray analysis in a couple of day.

Crystallographic data:

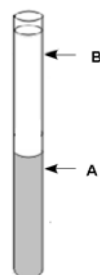


Empirical formula	C ₂₄ H ₃₆ N ₆ O ₉
Formula weight	552.59
Temperature	173(2) K
Crystal system	Monoclinic
Space group	C2/c
Unit cell dimensions	a = 24.6224(16) Å α = 90° b = 7.6323(7) Å β = 108.090(2)° c = 29.987(3) Å γ = 90°
Volume	5356.8(8) Å ³
Z	8
Density (calculated)	1.370 Mg/m ³
Absorption coefficient(μ)	0.106 mm ⁻¹
F(000)	2352
Theta range for data collection	1.88 to 29.51°
Index ranges	-20 ≤ h ≤ 34, -9 ≤ k ≤ 10, -42 ≤ l ≤ 24
Reflections collected	12864
Independent reflections	7397 [R(int) = 0.0581]
Completeness to theta = 29.51°	99.6 %
Max. and min. transmission	0.9843 and 0.9791
Data / restraints / parameters	7397 / 11 / 384
Goodness-of-fit on F ²	0.974
Final R indices [I > 2σ(I)]	R1 = 0.0603, wR2 = 0.0894
Largest diff. peak and hole	0.462 and -0.319 e.Å ⁻³

V. **[BAD23][4,7-dcphen]**
(structure e1618)



Crystallization conditions:



In a thin crystallization tube ($\varnothing=0.6\text{cm}$), were layered **(A)** a CHCl_3 solution (0.5ml , $1.5 \cdot 10^{-2}\text{M}$) of BAD23 (1.5 mg) and on top **(B)** a DMSO solution (0.5ml , $1 \cdot 10^{-2}\text{M}$) of 4,7-dcphen (2.7 mg).

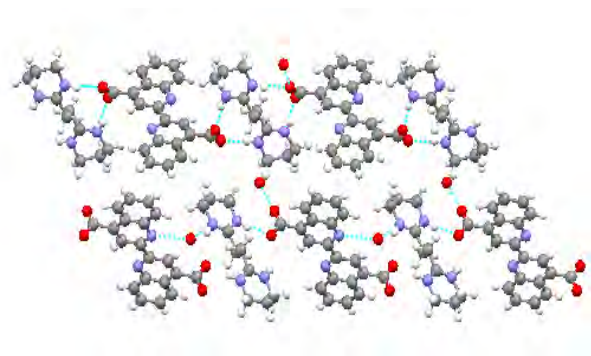
Colourless crystals were obtained by slow diffusion after some days.

Crystallographic data:



Empirical formula	$\text{C}_{26}\text{H}_{28}\text{Cl}_6\text{N}_6\text{O}_4$
Formula weight	701.24
Temperature	173(2) K
Crystal system	Orthorhombic
Space group	$P2(1)2(1)2(1)$
Unit cell dimensions	$a = 10.0015(12)\text{ \AA}$ $\alpha = 90^\circ$ $b = 14.7201(17)\text{ \AA}$ $\beta = 90^\circ$ $c = 21.396(2)\text{ \AA}$ $\gamma = 90^\circ$
Volume	$3150.0(6)\text{ \AA}^3$
Z	4
Density (calculated)	1.479 Mg/m^3
Absorption coefficient(μ)	0.588 mm^{-1}
F(000)	1440
Theta range for data collection	$1.68\text{ to }27.35^\circ$
Index ranges	$-12 \leq h \leq 9$, $-11 \leq k \leq 19$, $-27 \leq l \leq 27$
Reflections collected	19376
Independent reflections	6424 [R(int) = 0.0893]
Completeness to theta = 27.35°	97.4 %
Max. and min. transmission	0.9712 and 0.9656
Data / restraints / parameters	6424 / 0 / 379
Goodness-of-fit on F ²	1.241
Final R indices [$I > 2\sigma(I)$]	$R1 = 0.0672$, $wR2 = 0.1549$
Absolute structure (Flack) parameter	-0.04(11)
Largest diff. peak and hole	0.757 and -0.586 e.\AA^{-3}

**VI. [BAD23]/[4,4'-dcBQ]
(structure e1373)**



Crystallization conditions:

A suspension of 4,4'-dcbiquinoline (10.5 mg) and BAD23 (6 mg) in 5 ml of ethanol/H₂O 3:7 was heated for 1h at 80°C, after cooling the mixture was let evaporate slowly in the air. Single crystals (colourless) suitable for X-ray analysis were obtained in few days.

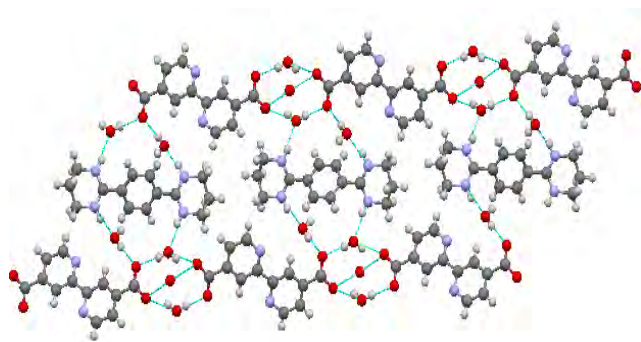


Crystallographic data:



Empirical formula	C ₃₀ H ₃₆ N ₆ O ₇
Formula weight	592.65
Temperature	173(2) K
Crystal system	Triclinic
Space group	P-1
Unit cell dimensions	a = 6.1466(12) Å α = 98.186(8)° b = 13.851(3) Å β = 91.165(9)° c = 16.891(4) Å γ = 97.594(6)°
Volume	1409.8(5) Å ³
Z	2
Density (calculated)	1.396 Mg/m ³
Absorption coefficient(μ)	0.101 mm ⁻¹
F(000)	628
Theta range for data collection	1.50 to 27.00°
Index ranges	-7<=h<=7, -17<=k<=17, -21<=l<=21
Reflections collected	12758
Independent reflections	6042 [R(int) = 0.1401]
Completeness to theta = 27.00°	98.7 %
Max. and min. transmission	0.9980 and 0.9950
Data / restraints / parameters	6042 / 0 / 388
Goodness-of-fit on F ²	1.034
Final R indices [I>2σ(I)]	R1 = 0.1169, wR2 = 0.2377
Largest diff. peak and hole	0.574 and -0.329 e.Å ⁻³

**VII. [BADbenz3][4,4'-dibpy]
(structure e1030)**



Crystallization conditions:



A solution of BADbenz3*2HCl (6 mg) in 2 ml of water and a solution of 4,4'-dcbpy-Na₂ (4 mg) in 2 ml of EtOH/H₂O (8:2) was mixed in a 10 ml flask. The solution was heated at 50°C and then cooled at 4°C in the refrigerator. Colourless crystals were obtained after cooling and slow evaporation in the refrigerator.

Crystallographic data:

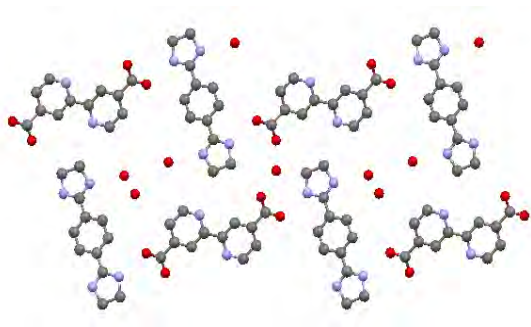
Empirical formula
Formula weight
Temperature
Crystal system
Space group
Unit cell dimensions

Volume
Z
Density (calculated)
Absorption coefficient(μ)
F(000)
Theta range for data collection
Index ranges
Reflections collected
Independent reflections
Completeness to theta = 27.47°
Max. and min. transmission
Data / restraints / parameters
Goodness-of-fit on F2
Final R indices [$I > 2\sigma(I)$]
Largest diff. peak and hole

[(C₁₂H₆N₂O₄)(C₁₄H₂₀N₄)] *5(H₂O)

C₂₆ H₃₆ N₆ O₉
576.61
173(2) K
Monoclinic
C2/c
a = 22.472(2) Å $\alpha = 90^\circ$.
b = 22.472(2) Å $\beta = 99.304(2)^\circ$.
c = 15.276(2) Å $\gamma = 90^\circ$.
2759.9(5) Å³
4
1.388 Mg/m³
0.106 mm⁻¹
1224
2.92 to 29.89°.
-30 ≤ h ≤ 29, -11 ≤ k ≤ 10, -21 ≤ l ≤ 21
16749
3933 [R(int) = 0.0389]
98.6 %
0.9758 and 0.9711
3933 / 5 / 201
1.031
R1 = 0.0435, wR2 = 0.1028
0.343 and -0.288 e.Å⁻³

**VIII. [BADbenz2][4,4'-dcbpy]
(structure e1183)**



Crystallization conditions:



A solution of BADbenz2*2TsOH (7 mg) in 2 ml of water and a solution of 4,4'-dcbpy-Na₂ (4 mg) in 2 ml of EtOH/H₂O (8:2) was mixed in a 10 ml flask. The solution was heated at 50°C and then cooled at 4°C in the refrigerator. Colourless crystals were obtained after cooling and slow evaporation in the refrigerator.

Crystallographic data:

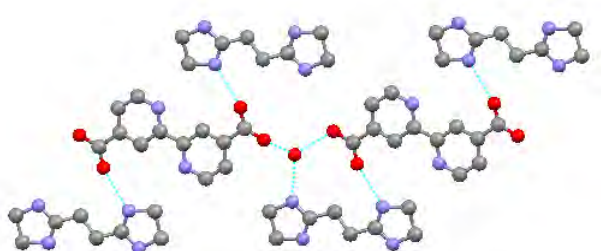
Empirical formula
Formula weight
Temperature
Crystal system
Space group
Unit cell dimensions

Volume
Z
Density (calculated)
Absorption coefficient(μ)
F(000)
Theta range for data collection
Index ranges
Reflections collected
Independent reflections
Completeness to theta = 27.47°
Max. and min. transmission
Data / restraints / parameters
Goodness-of-fit on F²
Final R indices [$I > 2\sigma(I)$]
Largest diff. peak and hole

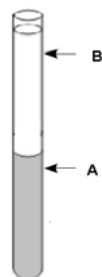
[(C₁₂H₆N₂O₄)(C₁₂H₁₆N₄)] *4(H₂O)

C₂₄ H₃₀ N₆ O₈
530.54
173(2) K
Monoclinic
P2(1)/c
a = 7.4015(3) Å $\alpha = 90^\circ$.
b = 14.1053(6) Å $\beta = 100.999(2)^\circ$.
c = 12.0348(4) Å $\gamma = 90^\circ$.
1233.36(8) Å³
2
1.429 Mg/m³
0.123 mm⁻¹
560
2.80 to 27.52°.
-9<=h<=9, -16<=k<=18, -15<=l<=15
10969
2822 [R(int) = 0.0371]
99.4 %
0.9946 and 0.9838
2822 / 4 / 184
1.052
R1 = 0.0490, wR2 = 0.1112
0.287 and -0.230 e.Å⁻³

**IX. [BAD22][4,4'-dcbpy]
(structure e1878)**



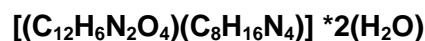
Crystallization conditions:



In a test tube ($\varnothing=1\text{cm}$), 1 ml of a 0.01M stock solution of 4,4'-dcbpy (**B**) (50 mg in 20 ml DMSO) was gently layered over 1 ml of a 0.01M stock solution of BAD22 (**A**) (35 mg in 20 ml of CHCl_3).

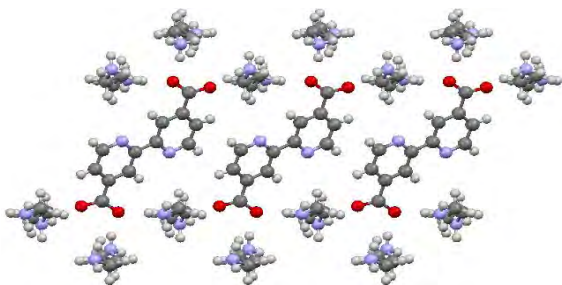
Colourless crystals were obtained after slow diffusion at room temperature in a few weeks.

Crystallographic data:



Empirical formula	$\text{C}_{20}\text{H}_{26}\text{N}_6\text{O}_6 \cdot \text{C}_8\text{H}_{16}\text{N}_4$
Formula weight	446.47
Temperature	173(2) K
Crystal system	Triclinic
Space group	P-1
Unit cell dimensions	$a = 6.7103(9) \text{ \AA}$ $\alpha = 110.018(7)^\circ$ $b = 7.7510(11) \text{ \AA}$ $\beta = 102.725(7)^\circ$ $c = 11.0673(12) \text{ \AA}$ $\gamma = 94.793(8)^\circ$
Volume	$519.57(12) \text{ \AA}^3$
Z	1
Density (calculated)	1.427 Mg/m^3
Absorption coefficient(μ)	0.108 mm^{-1}
F(000)	236
Theta range for data collection	2.03 to 27.00°
Index ranges	$-8 \leq h \leq 8, -10 \leq k \leq 9, -14 \leq l \leq 13$
Reflections collected	4954
Independent reflections	2201 [R(int) = 0.0470]
Completeness to theta = 27.47°	96.7 %
Max. and min. transmission	0.9979 and 0.9957
Data / restraints / parameters	2201 / 3 / 151
Goodness-of-fit on F ²	1.211
Final R indices [I > 2 σ (I)]	R1 = 0.1112, wR2 = 0.2745
Largest diff. peak and hole	0.544 and $-0.415 \text{ e. \AA}^{-3}$

**X. [4,4'-dcbpy][tmda]
(structure e1593)**

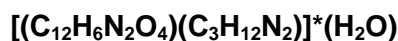


Crystallization conditions:



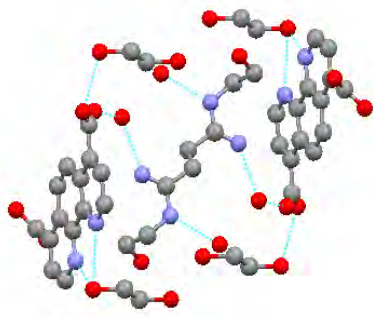
In a 10 ml flask, BAD23 (8 mg) and 1 eq. of 4,4'-dcbpy (10 mg) were dissolved in 5 ml of water. EtOH was added dropwise to obtain a cloudy solution that was heated at 40°C and turned clear. Colourless crystals were obtained after cooling and slow evaporation at 4°C in the refrigerator.

Crystallographic data:



Empirical formula	C ₁₅ H ₂₀ N ₄ O ₅
Formula weight	336.35
Temperature	173(2) K
Crystal system	Monoclinic
Space group	P2(1)/n
Unit cell dimensions	a = 8.2284(5) Å α = 90° b = 23.5695(12) Å β = 109.290(2)° c = 8.5495(4) Å γ = 90°
Volume	1565.00(14) Å ³
Z	4
Density (calculated)	1.428 Mg/m ³
Absorption coefficient(μ)	0.109 mm ⁻¹
F(000)	712
Theta range for data collection	2.67 to 27.51°
Index ranges	-10<=h<=10, -30<=k<=27, -8<=l<=11
Reflections collected	10907
Independent reflections	3505 [R(int) = 0.0277]
Completeness to theta = 27.47°	97.2 %
Max. and min. transmission	0.9957 and 0.9871
Data / restraints / parameters	3505 / 2 / 225
Goodness-of-fit on F ²	1.042
Final R indices [I>2σ(I)]	R1 = 0.0440, wR2 = 0.1145
Largest diff. peak and hole	0.443 and -0.254 e.Å ⁻³

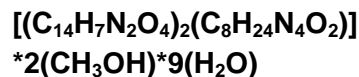
**XI. [4,7-dcphen][tmda]
(structure e1019)**



Crystallization conditions:

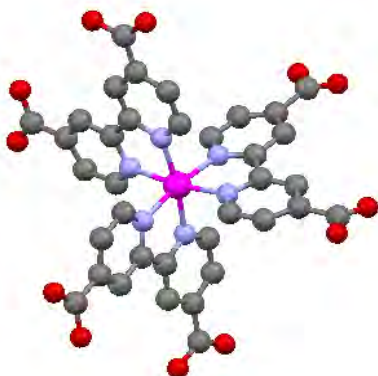
In a test tube ($\varnothing=1.5\text{cm}$) BAD22*2HCl (15 mg) and 1eq. of 4,7-dcphen- K_2 (21.5 mg) were dissolved in 5 ml of a 9:1 water/ethanol solution. The solution was placed in the refrigerator (4°C) for evaporation. Colourless crystals were obtained after few months.

Crystallographic data:

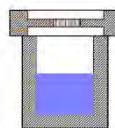


Empirical formula	C ₃₈ H ₆₄ N ₈ O ₂₁
Formula weight	962.92
Temperature	173(2) K
Crystal system	Triclinic
Space group	P-1
Unit cell dimensions	a = 10.3674(3) Å α = 96.862(2)° b = 10.4594(3) Å β = 91.819(2)° c = 12.1126(4) Å γ = 116.921(2)°
Volume	1157.25(6) Å ³
Z	1
Density (calculated)	1.382 Mg/m ³
Absorption coefficient(μ)	0.113 mm ⁻¹
F(000)	510
Theta range for data collection	1.70 to 30.07°
Index ranges	-14<=h<=14, -14<=k<=14, -17<=l<=17
Reflections collected	16729
Independent reflections	6771 [R(int) = 0.0373]
Completeness to theta = 27.47°	99.6 %
Max. and min. transmission	0.9887 and 0.9821
Data / restraints / parameters	6771 / 11 / 332
Goodness-of-fit on F ²	1.071
Final R indices [I>2σ(I)]	R1 = 0.1018, wR2 = 0.2317
Largest diff. peak and hole	1.562 and -0.872 e.Å ⁻³

**XII. [Ru(4,4'-dcbipy-2H)₂(4,4'-dcbipy)]
(structure e985)**



Crystallization conditions:



RuCl₃·3H₂O (50 mg, 0.19 mmol) with 4,4'-dicarboxy-2,2'-bipyridine (140 mg, 0.57 mmol) in 6 ml of water were sealed in a teflon coated stainless steel bomb and put into the hydrothermal apparatus. The temperature was raised to 200°C and maintained for 4h. Dark violet single crystals suitable for X-ray analysis were obtained after slow cooling (10°C/h).

[Polymorph of the structure published in: A. Pakkanen et al.; *J. Chem. Soc., Dalton. Trans.*, **2000**, 2745-2752]

Crystallographic data:

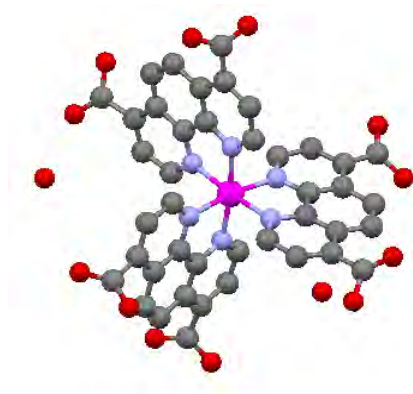
Empirical formula
Formula weight
Temperature
Crystal system
Space group
Unit cell dimensions

Volume
Z
Density (calculated)
Absorption coefficient(μ)
F(000)
Theta range for data collection
Index ranges
Reflections collected
Independent reflections
Completeness to theta = 27.87°
Max. and min. transmission
Data / restraints / parameters
Goodness-of-fit on F²
Final R indices [$I > 2\sigma(I)$]
Largest diff. peak and hole

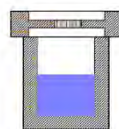
[Ru^{II}(C₃₆H₂₂N₆O₁₂)]*1.5(H₂O)

C72 H50 N12 O27 Ru2
1717.38
173(2) K
Monoclinic
C2/c
a = 16.2437(12) Å α = 90°.
b = 22.5502(12) Å β = 105.743(4)°.
c = 11.1149(6) Å γ = 90°.
3918.6(4) Å³
2
1.455 Mg/m³
0.472 mm⁻¹
1740
1.58 to 27.65°.
-20 ≤ h ≤ 21, -29 ≤ k ≤ 29, -14 ≤ l ≤ 14
15116
4435 [R(int) = 0.0989]
96.9 %
0.9814 and 0.9722
4435 / 0 / 268
1.073
R1 = 0.0808, wR2 = 0.2197
2.245 and -1.197 e.Å⁻³

**XIII. [Ru(4,7-dcphen-2H)₂(4,7-dcphen)]
(structure e983)**



Crystallization conditions:



RuCl₃·3H₂O (50 mg, 0.19 mmol) with 4,7-dicarboxy-1,10-phenanthroline (150 mg, 0.57 mmol) in 6 ml of water were sealed in a teflon coated stainless steel

bomb and put into the hydrothermal apparatus. The temperature was raised to 200°C and maintained for 4h. Dark red single crystals suitable for X-ray analysis were obtained after slow cooling (10°C/h).

Crystallographic data:

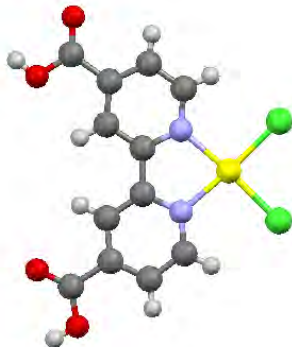
Empirical formula
Formula weight
Temperature
Crystal system
Space group
Unit cell dimensions

Volume
Z
Density (calculated)
Absorption coefficient(μ)
F(000)
Theta range for data collection
Index ranges
Reflections collected
Independent reflections
Completeness to theta = 27.87°
Max. and min. transmission
Data / restraints / parameters
Goodness-of-fit on F²
Final R indices [I > 2σ(I)]
Largest diff. peak and hole

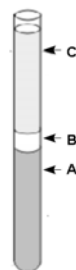
[Ru^{II}(C₄₂H₂₂N₆O₁₂)]·2(H₂O)

C₄₂ H₂₆ N₆ O₁₄ Ru
939.76
173(2) K
Triclinic
P-1
a = 10.9032(4) Å α = 104.483(3)°
b = 18.4013(7) Å β = 101.294(2)°
c = 19.3092(7) Å γ = 101.342(2)°
3553.1(2) Å³
4
1.757 Mg/m³
0.530 mm⁻¹
1904
1.37 to 26.50°
-14 ≤ h ≤ 14, -22 ≤ k ≤ 23, -24 ≤ l ≤ 25
29916
14422 [R(int) = 0.0883]
theta = 26.50° 98.7 %
0.9895 and 0.9740
14422 / 0 / 1136
1.006
R1 = 0.0773, wR2 = 0.1680
0.985 and -1.279 e.Å⁻³

**XIV. $[Pd(4,4'-dcbpy)Cl_2]$
(structure e1562)**



Crystallization conditions:



In a test tube ($\varnothing=1\text{cm}$) were gently layered in the order: **(A)** 1ml of CHCl_3 , **(B)** 0.5 ml of a $\text{CHCl}_3/\text{DMSO}$ 1:1 buffer solution and **(C)** 1 ml of a DMF solution containing 2 mg of $[Pd(II)(4,4'-dcbpy)Cl_2]$.

Yellow crystals suitable for XRD analysis were obtained after some days by slow diffusion.

Crystallographic data:

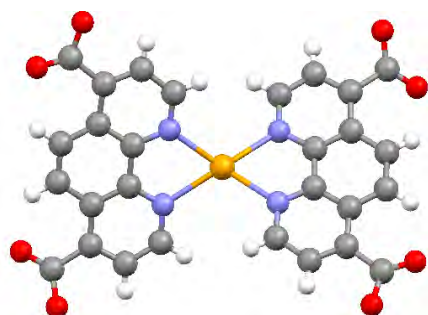
Empirical formula
Formula weight
Temperature
Crystal system
Space group
Unit cell dimensions

Volume
Z
Density (calculated)
Absorption coefficient(μ)
F(000)
Theta range for data collection
Index ranges
Reflections collected
Independent reflections
Completeness to theta = 27.47°
Max. and min. transmission
Data / restraints / parameters
Goodness-of-fit on F2
Final R indices [$I > 2\sigma(I)$]
Largest diff. peak and hole

$[Pd(C_{12}H_8N_2O_4)Cl_2] \cdot (DMSO) \cdot (DMF)$

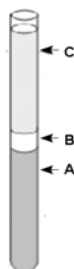
C17 H21 Cl2 N3 O6 Pd S
572.73
173(2) K
Triclinic
P-1
a = 9.0265(3) Å $\alpha = 75.8210(10)^\circ$
b = 10.1227(3) Å $\beta = 89.7050(10)^\circ$
c = 12.1927(4) Å $\gamma = 85.2560(10)^\circ$
1076.31(6) Å³
2
1.767 Mg/m³
1.247 mm⁻¹
576
2.08 to 30.15°
-12 ≤ h ≤ 12, -14 ≤ k ≤ 12, -16 ≤ l ≤ 16
13130
6158 [R(int) = 0.0208]
96.6 %
0.9518 and 0.9068
6158 / 0 / 277
1.018
R1 = 0.0244, wR2 = 0.0673
0.508 and -0.601 e.Å⁻³

**XV. [Ag(4,7-dcphen-2H)(4,7-dcphen-H)]
(structure e1619)**



Crystallization conditions:

In a thin crystallization tube ($\varnothing=0.6\text{cm}$) were layered in the following order: (A) a DMSO solution (0.5ml, $5 \cdot 10^{-3}\text{M}$) of 4,7-dcphen (1.3mg), (B) a DMSO/EtOH 1:1 buffer solution (0.5ml) and (C) an ethanolic solution (0.5ml, $2.7 \cdot 10^{-2}\text{M}$) of AgPF_6 (3.5mg). Yellow crystals were obtained by slow diffusion after few days.



Crystallographic data:

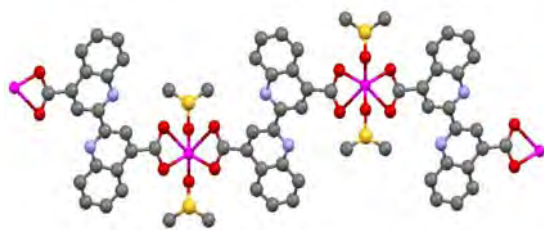
Empirical formula
Formula weight
Temperature
Crystal system
Space group
Unit cell dimensions

Volume
Z
Density (calculated)
Absorption coefficient(μ)
F(000)
Theta range for data collection
Index ranges
Reflections collected
Independent reflections
Completeness to theta = 27.47°
Max. and min. transmission
Data / restraints / parameters
Goodness-of-fit on F2
Final R indices [$I > 2\sigma(I)$]
Largest diff. peak and hole

[Ag(C₁₄H₁₅N₄O₂)]*1.23(DMSO)*0.77(EtOH)

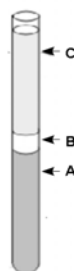
C32 H27 Ag N4 O10 S
767.51
173(2) K
Monoclinic
P2/c
a = 13.5409(10) Å $\alpha = 90^\circ$.
b = 7.4008(6) Å $\beta = 101.533(3)^\circ$.
c = 15.2713(9) Å $\gamma = 90^\circ$.
1499.49(19) Å³
2
1.700 Mg/m³
0.811 mm⁻¹
780
2.72 to 27.49°.
-17 ≤ h ≤ 17, -9 ≤ k ≤ 9, -19 ≤ l ≤ 19
12347
3438 [R(int) = 0.0448]
99.7 %
0.9840 and 0.8949
3438 / 5 / 236
1.030
R1 = 0.0716, wR2 = 0.1812
1.412 and -1.855 e.Å⁻¹

**XVI. $[\text{Zn}(4,4'\text{-dcBQ})(\text{DMSO})_2]$
(structure e1811)**



Crystallization conditions:

In a crystallisation tube ($\varnothing=0.6\text{cm}$), were gently layered in the order : **(A)** 0.5 ml of a 0.01M stock solution of 4,4'-dicarboxy-2,2'-biquinoline (24 mg in 7 ml of DMSO) in DMSO, **(B)** 0.3 ml of a DMSO/EtOH 1:1 buffer solution and **(C)** 0.5 ml of a methanolic solution of $\text{Zn}(\text{BF}_4)_2$ (6 mg/ml).



Colourless crystals suitable for XRD analysis were obtained after some weeks by slow diffusion.

Crystallographic data:

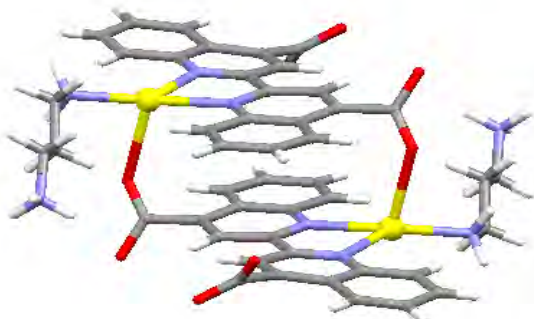
Empirical formula
Formula weight
Temperature
Crystal system
Space group
Unit cell dimensions

Volume
Z
Density (calculated)
Absorption coefficient(μ)
F(000)
Theta range for data collection
Index ranges
Reflections collected
Independent reflections
Completeness to theta = 27.63°
Max. and min. transmission
Data / restraints / parameters
Goodness-of-fit on F2
Final R indices [$I > 2\sigma(I)$]
Largest diff. peak and hole

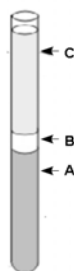
$[\text{Zn}(\text{C}_{20}\text{H}_{10}\text{N}_2\text{O}_4)(\text{C}_2\text{H}_6\text{SO})_2]$

C₂₄ H₂₂ N₂ O₆ S₂ Zn
563.93
173(2) K
Orthorhombic
Pnma
a = 8.2727(3) Å $\alpha = 90^\circ$
b = 22.3333(8) Å $\beta = 90^\circ$
c = 13.0135(4) Å $\gamma = 90^\circ$
2404.33(14) Å³
4
1.558 Mg/m³
1.239 mm⁻¹
1160
1.81 to 27.63°
-10 ≤ h ≤ 10, -22 ≤ k ≤ 29, -12 ≤ l ≤ 16
18503
2854 [R(int) = 0.1337]
99.5 %
0.9521 and 0.9074
2854 / 6 / 156
1.047
R1 = 0.1089, wR2 = 0.2819
1.718 and -1.279 e.Å⁻³

**XVII. $[Ag(I)(4,4'\text{-dcBQ})(en)]_2$
(structure e1531)**



Crystallization conditions:



A stock solution was prepared dissolving 50 mg (0.14 mmol) of 4,4'-dcBQ with 28 mg (0.14 mmol) of BAD23 in 115 ml of a 7:3 water/EtOH mixture ($1.25 \cdot 10^{-3}$ M) to obtain a clear solution at pH \approx 7. In a crystallisation tube ($\varnothing=0.6$ cm) were gently layered in the order: **(A)** 1 ml of the stock solution, **(B)** 0.3 ml of a H₂O/EtOH 1:1 buffer solution, 0.3 ml of dioxane and **(C)** 0.5 ml of an ethanolic solution of AgNO₃ (6 mg/ml). Pale yellow crystals suitable for XRD analysis were obtained after some weeks by slow diffusion followed by evaporation to the air.

Crystallographic data:

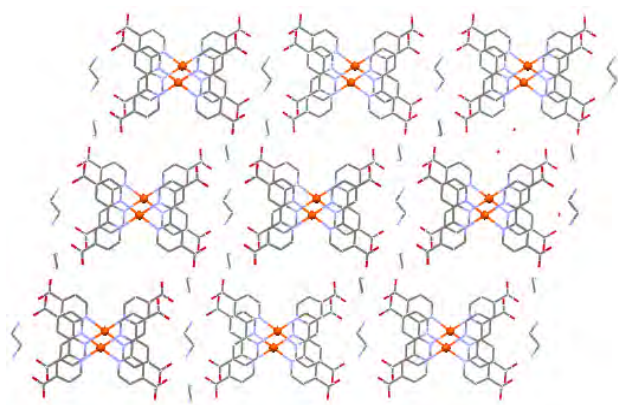
Empirical formula
Formula weight
Temperature
Crystal system
Space group
Unit cell dimensions

Volume
Z
Density (calculated)
Absorption coefficient(μ)
F(000)
Theta range for data collection
Index ranges
Reflections collected
Independent reflections
Completeness to theta = 27.51°
Max. and min. transmission
Data / restraints / parameters
Goodness-of-fit on F2
Final R indices [$I > 2\sigma(I)$]
Largest diff. peak and hole

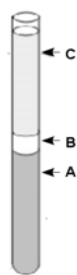
$[Ag(C_{20}H_{10}N_2O_4)(C_3H_{11}N_2)]_2 \cdot 8(H_2O)$

C₄₆ H₅₈ Ag₂ N₈ O₁₆
1194.74
173(2) K
Monoclinic
P2(1)/n
a = 13.0964(7) Å $\alpha = 90^\circ$.
b = 7.5877(5) Å $\beta = 104.251(2)^\circ$.
c = 25.4080(16) Å $\gamma = 90^\circ$.
2447.1(3) Å³
2
1.621 Mg/m³
0.880 mm⁻¹
1224
1.61 to 27.51°.
-10 \leq h \leq 17, -9 \leq k \leq 9, -29 \leq l \leq 33
19221
5585 [R(int) = 0.0629]
99.5 %
0.9573 and 0.9250
5585 / 0 / 326
1.153
R1 = 0.0490, wR2 = 0.1256
1.206 and -1.401 e.Å⁻³

**XVIII. $\{[Ag(I)(4,4'-dcbpy)_2](en)_{1.5}\}$
(structure e1251)**



Crystallization conditions:



BAD22 (6 mg) and 4,4'-dcbpy (8.8 mg) were mixed in 3 ml of water and 5 drops of butanol affording a clear solution (pH ca 7) (**A**). In a crystallisation tube ($\varnothing=1\text{cm}$) were gently layered in the order: (**A**) 3 ml of the solution, (**B**) 0.5 ml of a EtOH buffer and (**C**) 0.5 ml of an ethanolic solution of $AgSbF_6$ (7 mg/ml).

Yellow crystals suitable for X-ray diffraction on single crystals were obtained after several weeks.

Crystallographic data:

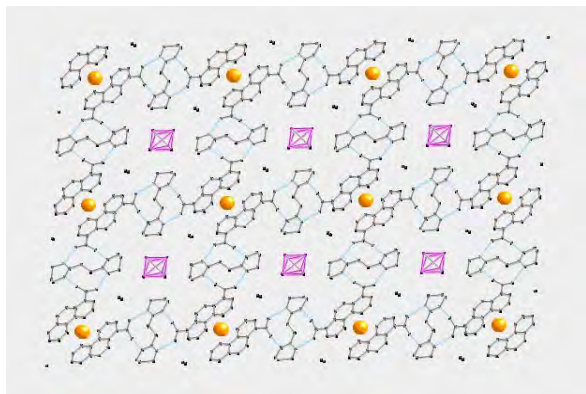
Empirical formula
Formula weight
Temperature
Crystal system
Space group
Unit cell dimensions

Volume
Z
Density (calculated)
Absorption coefficient(μ)
F(000)
Theta range for data collection
Index ranges
Reflections collected
Independent reflections
Completeness to theta = 27.47°
Max. and min. transmission
Data / restraints / parameters
Goodness-of-fit on F2
Final R indices [$I > 2\sigma(I)$]
Largest diff. peak and hole

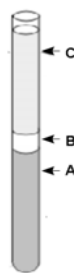
$\{[Ag(C_{12}H_6N_2O_4)_2][C_2H_{10}N_2]_{1.5}\} \cdot 4(H_2O)$

C27 H35 Ag N7 O12
757.49
173(2) K
Monoclinic
P2(1)/c
 $a = 13.2260(8) \text{ \AA}$ $\alpha = 90^\circ$
 $b = 7.0447(6) \text{ \AA}$ $\beta = 104.189(3)^\circ$
 $c = 33.600(3) \text{ \AA}$ $\gamma = 90^\circ$
 $3000.6(4) \text{ \AA}^3$
4
1.677 Mg/m^3
 0.749 mm^{-1}
1556
2.31 to 27.00°
 $-14 \leq h \leq 15, -9 \leq k \leq 9, -43 \leq l \leq 43$
18742
6089 [R(int) = 0.0817]
93.9 %
0.9852 and 0.9635
6089 / 8 / 451
1.128
 $R1 = 0.0728, wR2 = 0.1527$
 $0.532 \text{ and } -0.578 \text{ e.\AA}^{-3}$

**XIX. $\{Ag(I)(4,7-dcphen)_2(BAD23)_2\}SbF_6$
(structure e1149)**



Crystallization conditions:



BAD23 (6.4 mg) and 4,7-dcphen (8.8 mg) were mixed in 3 ml of water with 5 drops of butanol affording a clear solution (pH ca 7) (**A**). In a crystallisation tube ($\varnothing=1\text{cm}$) were gently layered in the order: (**A**) 3 ml of the solution, (**B**) 0.5 ml of a EtOH buffer and (**C**) 0.5 ml of an ethanolic solution of $AgSbF_6$ (7 mg/ml).

Yellow crystals suitable for X-ray diffraction on single crystals were obtained after several weeks.

Crystallographic data:

Empirical formula

Formula weight

Temperature

Crystal system

Space group

Unit cell dimensions

Volume

Z

Density (calculated)

Absorption coefficient(μ)

F(000)

Theta range for data collection

Index ranges

Reflections collected

Independent reflections

Completeness to theta = 27.54°

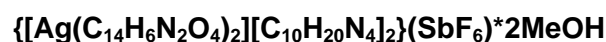
Max. and min. transmission

Data / restraints / parameters

Goodness-of-fit on F2

Final R indices [$I > 2\sigma(I)$]

Largest diff. peak and hole



C50 H60 Ag F6 N12 O10 Sb

1332.72

173(2) K

Monoclinic

C2/m

$a = 21.8809(18) \text{ \AA}$ $\alpha = 90^\circ$.

$b = 23.0194(18) \text{ \AA}$ $\beta = 98.574(4)^\circ$.

$c = 5.3675(5) \text{ \AA}$ $\gamma = 90^\circ$.

$2673.3(4) \text{ \AA}^3$

2

1.656 Mg/m^3

0.962 mm^{-1}

1352

1.29 to 27.54° .

$-28 \leq h \leq 28$, $-28 \leq k \leq 29$, $-6 \leq l \leq 6$

12061

99.0 %

3122 [R(int) = 0.0670]

0.9535 and 0.9357

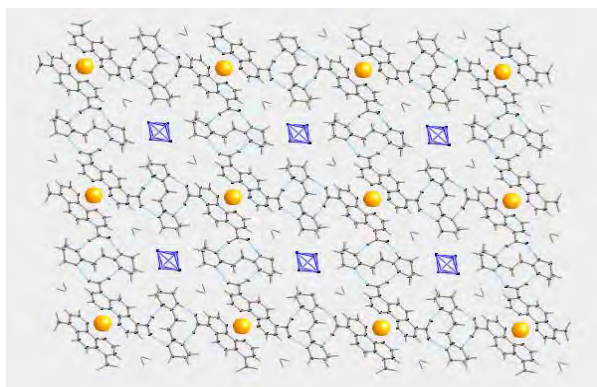
3122 / 0 / 197

1.053

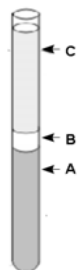
$R1 = 0.0824$, $wR2 = 0.2115$

0.724 and $-1.318 \text{ e.\AA}^{-3}$

**XX. $\{Ag(I)(4,7-dcphen)_2(BAD23)_2\}AsF_6$
(structure e1574)**



Crystallization conditions:



BAD23 (6.4 mg) and 4,7-dcphen (8.8 mg) were mixed in 3 ml of water with 5 drops of butanol affording a clear solution (pH ca 7) (**A**).

In a crystallisation tube ($\varnothing=1\text{cm}$) were gently layered in the order: (**A**) 3 ml of the solution, (**B**) 0.5 ml of a EtOH buffer and (**C**) 0.5 ml of an ethanolic solution of

$AgAsF_6$ (6 mg/ml).

Yellow crystals suitable for X-ray diffraction on single crystals were obtained after several weeks.

Crystallographic data:

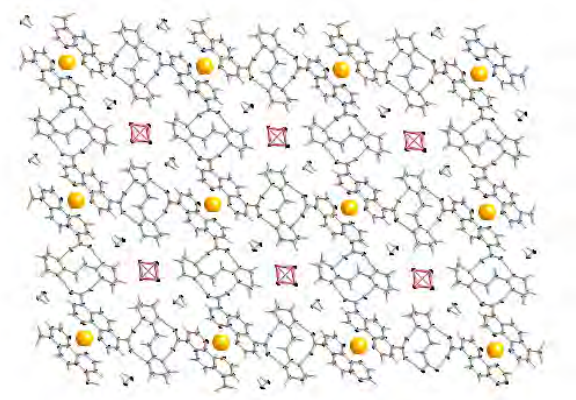
Empirical formula
Formula weight
Temperature
Crystal system
Space group
Unit cell dimensions

Volume
Z
Density (calculated)
Absorption coefficient(μ)
F(000)
Theta range for data collection
Index ranges
Reflections collected
Independent reflections
Completeness to theta = 27.56°
Max. and min. transmission
Data / restraints / parameters
Goodness-of-fit on F2
Final R indices [$I > 2\sigma(I)$]
Largest diff. peak and hole

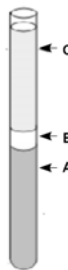
**$\{[Ag(C_{14}H_6N_2O_4)_2][C_{10}H_{20}N_4]_2\}(AsF_6)$
 $*2MeOH$**

C50 H60 Ag As F6 N12 O10
1285.89
173(2) K
Monoclinic
C2/m
a = 21.538(2) Å $\alpha = 90^\circ$
b = 23.019(2) Å $\beta = 98.638(5)^\circ$
c = 5.3934(5) Å $\gamma = 90^\circ$
2643.7(4) Å³
2
1.615 Mg/m³
1.094 mm⁻¹
1316
2.61 to 27.56°
-27 ≤ h ≤ 25, -28 ≤ k ≤ 29, -6 ≤ l ≤ 6
10656
3089 [R(int) = 0.0767]
99.0 %
0.9473 and 0.9273
3089 / 0 / 197
1.042
R1 = 0.0854, wR2 = 0.1778
1.809 and -1.839 e.Å⁻³

**XXI. $\{Ag(I)(4,7-dcphen)_2(BAD23)_2\}PF_6$
(structure e1348)**



Crystallization conditions:



BAD23 (6.4 mg) and 4,7-dcphen (8.8 mg) were mixed in 3 ml of water with 5 drops of butanol affording a clear solution (pH \approx 7) (**A**).

In a crystallisation tube ($\varnothing=1\text{cm}$) were gently layered in the order: (**A**) 3 ml of the solution, (**B**) 0.5 ml of a EtOH buffer and (**C**) 0.5 ml of an ethanolic solution of $AgAsF_6$ (7 mg/ml).

Yellow crystals suitable for X-ray diffraction on single crystals were obtained after several weeks.

Crystallographic data:

$\{[Ag(C_{14}H_6N_2O_4)_2][C_{10}H_{20}N_4]_2\}(PF_6)_2 \cdot 2MeOH$

Empirical formula

C₅₀ H₆₀ Ag F₆ N₁₂ O₁₀ P

Formula weight

1241.94

Temperature

173(2) K

Crystal system

Monoclinic

Space group

C2/m

Unit cell dimensions

$a = 21.4159(17) \text{ \AA}$ $\alpha = 90^\circ$.

$b = 23.109(3) \text{ \AA}$ $\beta = 99.117(6)^\circ$.

$c = 5.4593(6) \text{ \AA}$ $\gamma = 90^\circ$.

Volume

2667.7(5) \AA^3

Z

2

Density (calculated)

1.546 Mg/m³

Absorption coefficient(μ)

0.499 mm⁻¹

F(000)

1280

Theta range for data collection

1.93 to 27.87°.

Index ranges

$-27 \leq h \leq 26$, $-30 \leq k \leq 30$, $-7 \leq l \leq 3$

Reflections collected

10864

Independent reflections

3089 [R(int) = 0.1427]

Completeness to theta = 27.87°

94.6 %

Max. and min. transmission

0.9755 and 0.9659

Data / restraints / parameters

3089 / 0 / 197

Goodness-of-fit on F²

1.065

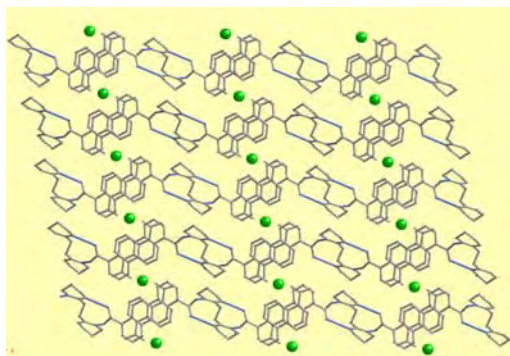
Final R indices [$I > 2\sigma(I)$]

R1 = 0.1026, wR2 = 0.2352

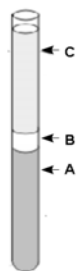
Largest diff. peak and hole

0.977 and -0.823 e. \AA^{-3}

**XXII. $\{Cu(II)(4,7-dcphen)_2(BAD23)\}$
(structure e1842)**

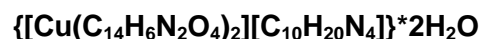


Crystallization conditions:



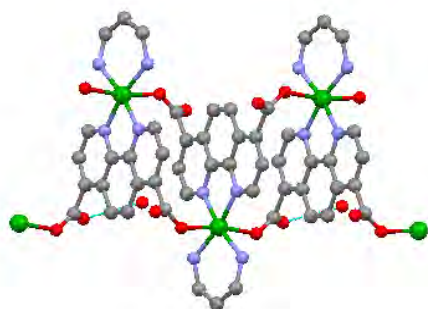
A stock solution was prepared dissolving 66 mg (0.34 mmol) of BAD23 with 91 mg (0.34 mmol) of 4,7-dcphen in 20 ml of water to obtain a clear solution (pH \approx 7). In a crystallisation tube ($\varnothing=1$ cm) were gently layered in the order: **(A)** 1 ml of the stock solution, **(B)** 1 ml of a H₂O/DMSO 9:1 buffer solution, 0.5ml of EtOH and **(C)** 0.5 ml of a 0.005 M solution of Cu(CF₃SO₃)₂ in EtOH. After slow diffusion, the tube was opened and left evaporate. Green crystals suitable for X-ray diffraction on single crystals were obtained from the green solution after ten months.

Crystallographic data:

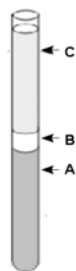


Empirical formula	C ₃₈ H ₃₆ Cu N ₈ O ₁₀
Formula weight	828.29
Temperature	173(2) K
Crystal system	Monoclinic
Space group	C2/c
Unit cell dimensions	a = 31.0216(15) Å $\alpha = 90^\circ$ b = 7.6724(3) Å $\beta = 103.3740(10)^\circ$ c = 14.6137(7) Å $\gamma = 90^\circ$
Volume	3383.9(3) Å ³
Z	4
Density (calculated)	1.626 Mg/m ³
Absorption coefficient(μ)	0.724 mm ⁻¹
F(000)	1716
Theta range for data collection	2.70 to 30.13°
Index ranges	-42 \leq h \leq 42, -8 \leq k \leq 10, -20 \leq l \leq 16
Reflections collected	26880
Independent reflections	4906 [R(int) = 0.0219]
Completeness to theta = 27.87°	98.3 %
Max. and min. transmission	0.9647 and 0.9312
Data / restraints / parameters	4906 / 3 / 264
Goodness-of-fit on F ²	1.023
Final R indices [I > 2 σ (I)]	R1 = 0.0482, wR2 = 0.1384
Largest diff. peak and hole	0.804 and -0.612 e.Å ⁻³

**XXIII. [Cu(II)(4,7-dcphen)(tmda)]
(structure 1863)**



Crystallization conditions:



A stock solution was prepared dissolving 232 mg (1.19 mmol) of BAD23 with 320 mg (1.19 mmol) of 4,7-dcphen in 120 ml of water to obtain a clear solution (pH \approx 7). In a crystallization tube ($\varnothing=1$ cm) were gently layered in the order: **(A)** 3 ml of the stock solution, **(B)** 0.3 ml of DMSO, 0.7 ml of a H₂O/EtOH 1:1 buffer solution and **(C)** 0.5 ml of a 0.02M solution of Cu(trf)₂ in EtOH. After slow diffusion, the tubes was opened and left evaporate.

Green crystals suitable for X-ray diffraction on single crystals were obtained after some months.

Crystallographic data:

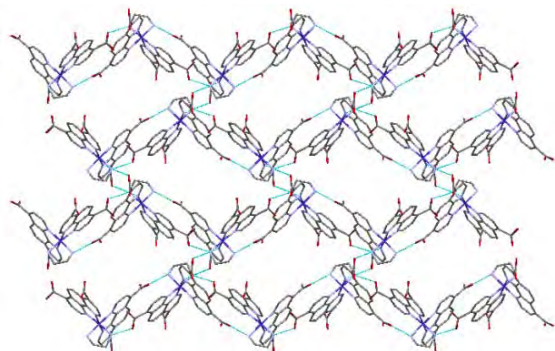
Empirical formula
Formula weight
Temperature
Crystal system
Space group
Unit cell dimensions

Volume
Z
Density (calculated)
Absorption coefficient(μ)
F(000)
Theta range for data collection
Index ranges
Reflections collected
Independent reflections
Completeness to theta = 27.53°
Max. and min. transmission
Data / restraints / parameters
Goodness-of-fit on F2
Final R indices [$I > 2\sigma(I)$]
Largest diff. peak and hole

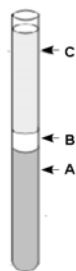
[Cu^{II}(C₁₄H₆N₂O₄)(C₃H₁₀N₂)]*2H₂O

C₃₈ H₃₆ Cu N₈ O₁₀
439.91
173(2) K
Monoclinic
C2/c
a = 15.0813(16) Å $\alpha = 90^\circ$.
b = 13.9906(16) Å $\beta = 116.243(4)^\circ$.
c = 8.8385(10) Å $\gamma = 90^\circ$.
1672.7(3) Å³
4
1.747 Mg/m³
1.354 mm⁻¹
908
2.09 to 27.53°.
-19 \leq h \leq 19, -18 \leq k \leq 13, -11 \leq l \leq 11
5652
1929 [R(int) = 0.0301]
99.6 %
0.8994 and 0.8544
1929 / 4 / 134
1.090
R1 = 0.0638, wR2 = 0.1683
1.196 and -0.839 e .Å⁻³

**XXIV. [Co(II)(4,7-dcphen)₂(tmda)] - squeezed
(structure 1959)**



Crystallization conditions:



A stock solution was prepared dissolving 68 mg (0.41 mmol) of BAD22 with 110 mg (0.41 mmol) of 4,7-dcphen in 14 ml of water to obtain a clear solution (pH ≈ 7). In a crystallization tube ($\varnothing=1\text{cm}$) were gently layered in the order: (A) 2 ml of the stock solution, (B) 0.5 ml of a H₂O/EtOH/DMSO 20:10:5 buffer solution and (C) 1.5 ml of a 0.02M solution of [Co(DMSO)₄(trf)₂] in EtOH. After slow diffusion, the tubes was opened and left evaporate. Red crystals suitable for X-ray diffraction on single crystals were obtained after some months.

Crystallographic data:

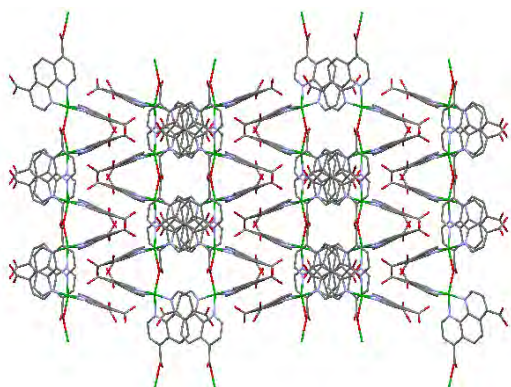
Empirical formula
Formula weight
Temperature
Crystal system
Space group
Unit cell dimensions

Volume
Z
Density (calculated)
Absorption coefficient(μ)
F(000)
Theta range for data collection
Index ranges
Reflections collected
Independent reflections
Completeness to theta = 27.58°
Max. and min. transmission
Data / restraints / parameters
Goodness-of-fit on F²
Final R indices [$I > 2\sigma(I)$]
Largest diff. peak and hole

[Cu^{II}(C₁₄H₇N₂O₄)₂(C₂H₈N₂)]

C₃₀ H₂₂ Co N₆ O₈
653.47
173(2) K
Monoclinic
P2(1)/c
a = 13.9046(4) Å $\alpha = 90^\circ$.
b = 17.4351(5) Å $\beta = 122.196(2)^\circ$.
c = 21.1603(6) Å $\gamma = 90^\circ$.
4341.0(2) Å³
4
1.000Mg/m³
0.437 mm⁻¹
1340
1.63 to 27.58°.
-18<=h<=15, 0<=k<=22, 0<=l<=271
31503
9941 [R(int) = 0.0443]
99.0 %
0.9659 and 0.9494
9941 / 5 / 394
1.034
R1 = 0.0843, wR2 = 0.2488
1.763 and -0.616 e .Å⁻³

**XXV. $[\text{Cu}(\text{II})(4,7\text{-dcphen})_2]$
(structure 1935)**



Crystallization conditions:



In a crystallisation tube ($\varnothing=1\text{cm}$), were gently layered in the order : **(A)** 1 ml of a 0.01M stock solution BAD22benz (40 mg in 15 ml of DMSO) with 1 ml of a 0.02M solution of 4,7.dcphen (45 mg in 8 ml of DMSO), **(B)** 1 ml of EtOH buffer and **(C)** 0.5 ml of a 0.02M solution of $\text{Cu}(\text{CF}_3\text{SO}_3)_2$ in MeOH.

After slow diffusion, the tube was opened and left evaporate. Blue crystals suitable for X-ray diffraction were obtained after some months.

Crystallographic data:

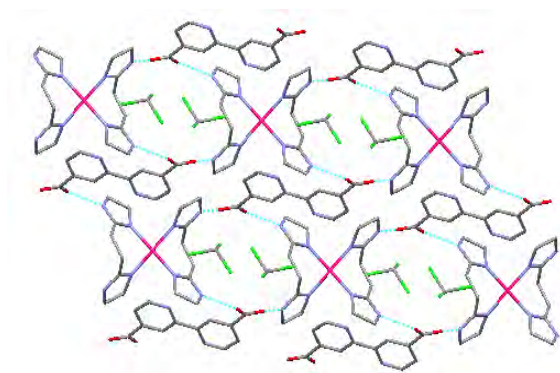
Empirical formula
Formula weight
Temperature
Crystal system
Space group
Unit cell dimensions

Volume
Z
Density (calculated)
Absorption coefficient(μ)
F(000)
Theta range for data collection
Index ranges
Reflections collected
Independent reflections
Completeness to theta = 27.00°
Max. and min. transmission
Data / restraints / parameters
Goodness-of-fit on F2
Final R indices [$I > 2\sigma(I)$]
Largest diff. peak and hole

$[\text{Cu}^{\text{II}}(\text{C}_{14}\text{H}_7\text{N}_2\text{O}_4)_2] \cdot \text{DMSO}$

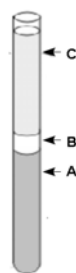
C58 H34 Cu2 N8 O17 S
1274.07
173(2) K
Monoclinic
C2/c
a = 31.308(2) Å $\alpha = 90^\circ$.
b = 8.7368(5) Å $\beta = 111.767(2)^\circ$.
c = 21.7356(14) Å $\gamma = 90^\circ$.
5521.5(6) Å³
4
1.533 Mg/m³
0.890 mm⁻¹
2592
1.40 to 27.00°.
-34 ≤ h ≤ 39, -11 ≤ k ≤ 11, -26 ≤ l ≤ 25
20169
5738 [R(int) = 0.0518]
96.2 %
0.9485 and 0.9084
5738 / 3 / 387
1.353
R1 = 0.1119, wR2 = 0.2648
1.692 and -0.849 e .Å⁻³

**XXVI. $\{[Pd(II)(BAD22)_2](4,4'-dcbpy)\}$
(structure 1946)**



Crystallization conditions:

In a crystallisation tube ($\varnothing=1\text{cm}$), were gently layered in the order : (A) 1 ml of a 0.01M stock solution BAD22 (42 mg in 25 ml of CHCl_3), (B) 0.2 ml of DMSO/EtOH 1:1 buffer solution and (C) 1 ml of a 0.005M solution of the complex $[Pd(4,4'-dcbpy)(\text{thiourea})_2]$ in DMSO.



After slow diffusion, the tube was opened and left evaporate. Pale yellow crystals suitable for X-ray diffraction were obtained after some months.

Crystallographic data:

Empirical formula
Formula weight
Temperature
Crystal system
Space group
Unit cell dimensions

Volume
Z
Density (calculated)
Absorption coefficient(μ)
F(000)
Theta range for data collection
Index ranges
Reflections collected
Independent reflections
Completeness to theta = 30.09°
Max. and min. transmission
Data / restraints / parameters
Goodness-of-fit on F2
Final R indices [$I > 2\sigma(I)$]
Largest diff. peak and hole

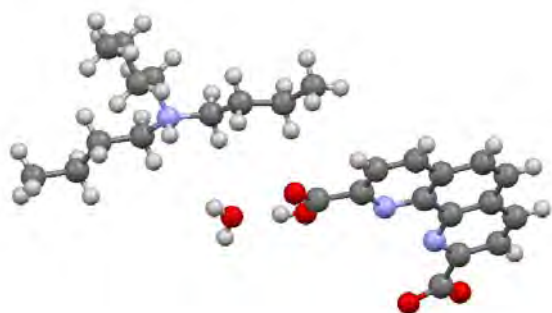
$\{[Pd^{II}(\text{C}_8\text{H}_{14}\text{N}_4)_2](\text{C}_{12}\text{H}_6\text{N}_2\text{O}_4)\} \cdot 2(\text{CHCl}_3)$

C30 H36 Cl6 N10 O4 Pd
919.79
173(2) K
Triclinic
P-1
a = 9.6249(2) Å $\alpha = 69.8090(10)^\circ$
b = 9.8585(2) Å $\beta = 73.8060(10)^\circ$
c = 10.8389(3) Å $\gamma = 85.7920(10)^\circ$
926.67(4) Å³
1
1.648 Mg/m³
0.984 mm⁻¹
466
2.46 to 30.09°
-13 ≤ h ≤ 13, -13 ≤ k ≤ 13, -15 ≤ l ≤ 15
18681
5342 [R(int) = 0.0209]
98.0 %
0.9343 and 0.8994
5342 / 0 / 232
1.002
R1 = 0.0307, wR2 = 0.0768
1.027 and -0.992 e . Å⁻³

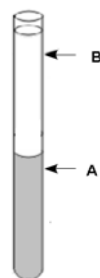
Crystal structures

Chapter III

**XXVII. [2,9-dcphen][But₃N]
(structure e1843)**



Crystallization conditions:



A stock solution (A) was prepared dissolving 160 mg of 2,9-dcphen with 5 ml of a diluted aqueous solution of But₃N (13 ml But₃N in 20 ml EtOH), in 30 ml of a mixture H₂O/EtOH/ButOH 15:5:5.

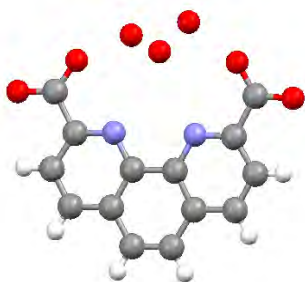
In a thin crystallization tube (ø=1cm), were layered (A) 2.5 ml of the stock solution of 2,9-dcphen*But₃N and on top (B) 0.5 ml of a H₂O/EtOH 1:1 solution followed by 2 ml of EtOH. Colourless crystals were obtained in few months of slow diffusion followed by evaporation to the air.

Crystallographic data:

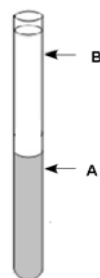
[(C₁₄H₇N₂O₄)(C₁₂H₂₈N)]*H₂O

Empirical formula	C ₂₆ H ₃₇ N ₃ O ₅
Formula weight	471.59
Temperature	173(2) K
Crystal system	Triclinic
Space group	P-1
Unit cell dimensions	a = 7.5823(8) Å α = 81.965(4)° b = 10.6417(12) Å β = 83.080(4)° c = 21.5958(7) Å γ = 76.042(3)°
Volume	1230.8(2) Å ³
Z	2
Density (calculated)	1.272 Mg/m ³
Absorption coefficient(μ)	0.088 mm ⁻¹
F(000)	508
Theta range for data collection	1.99 to 27.52°
Index ranges	-9<=h<=9, -13<=k<=12, -20<=l<=20
Reflections collected	10460
Independent reflections	5431 [R(int) = 0.0254]
Completeness to theta = 27.52°	96.1 %
Max. and min. transmission	0.9956 and 0.9921
Data / restraints / parameters	5431 / 4 / 320
Goodness-of-fit on F ²	1.009
Final R indices [I>2sigma(I)]	R1 = 0.0467, wR2 = 0.1120
Largest diff. peak and hole	0.383 and -0.242 e.Å ⁻³

**XXVIII. [2,9-dcphen]
(structure e1818)**



Crystallization conditions:



A 0.03M stock solution was prepared dissolving 110 mg of 2,9-dcphen with 1.5 ml of aqueous solution of Et₃N (1ml Et₃N in 24 ml H₂O) and adding 12 ml of H₂O.

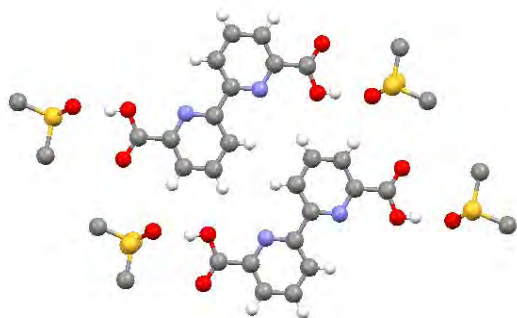
In a thin crystallization tube ($\varnothing=1\text{cm}$), were layered (A) 1 ml of the stock solution of 2,9-dcphen*Et₃N and on top (B) 1 ml of H₂O followed by 1.5 ml of EtOH. Colourless crystals were obtained in some weeks of slow diffusion followed by evaporation to the air.

Crystallographic data:

(C₁₄H₈N₂O₄)*2.5 (H₂O)

Empirical formula	C ₂₈ H ₂₆ N ₄ O ₁₃
Formula weight	626.53
Temperature	173(2) K
Crystal system	Orthorhombic
Space group	Fdd2
Unit cell dimensions	a = 37.551(7) Å α = 90° b = 10.2758(18) Å β = 90° c = 14.198(3) Å γ = 90°
Volume	5478.5(17) Å ³
Z	8
Density (calculated)	1.519 Mg/m ³
Absorption coefficient(μ)	0.123 mm ⁻¹
F(000)	2608
Theta range for data collection	2.17 to 27.69°
Index ranges	-30<=h<=48, -13<=k<=13, -18<=l<=17
Reflections collected	13537
Independent reflections	3019 [R(int) = 0.0389]
Completeness to theta = 27.52°	99.0 %
Max. and min. transmission	0.9951 and 0.9879
Data / restraints / parameters	3019 / 1 / 204
Goodness-of-fit on F ²	1.071
Final R indices [I>2σ(I)]	R1 = 0.0539, wR2 = 0.1530
Largest diff. peak and hole	0.475 and -0.238 e.Å ⁻³

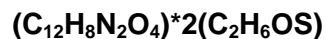
**XXIX. [6,6'-dcbpy]
(structure e1922)**



Crystallization conditions:

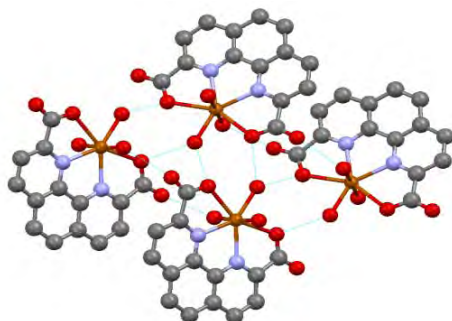
A saturated hot solution of the ligand 6,6'-dcbpy (8 mg) in 0.6 ml of DMSO at 100°C was deposited in a thin crystallisation tube ($\varnothing=0.5\text{cm}$). The solution was allowed to cool to room temperature and after few days colourless crystals suitable for XRD analysis appeared.

Crystallographic data:



Empirical formula	C ₁₆ H ₂₀ N ₂ O ₆ S ₂
Formula weight	400.46
Temperature	173(2) K
Crystal system	Monoclinic
Space group	P2(1)/n
Unit cell dimensions	a = 6.7525(2) Å α = 90° b = 7.2241(2) Å β = 91.138(2)° c = 18.9303(6) Å γ = 90°
Volume	923.25(5) Å ³
Z	2
Density (calculated)	1.441 Mg/m ³
Absorption coefficient(μ)	0.324 mm ⁻¹
F(000)	420
Theta range for data collection	2.15 to 27.47°
Index ranges	-8<=h<=8, -8<=k<=9, -24<=l<=24
Reflections collected	16988
Independent reflections	2102 [R(int) = 0.0227]
Completeness to theta = 27.47°	99.3 %
Max. and min. transmission	0.9777 and 0.9622
Data / restraints / parameters	2102 / 0 / 138
Goodness-of-fit on F ²	1.023
Final R indices [I>2σ(I)]	R1 = 0.0460, wR2 = 0.1440
Largest diff. peak and hole	0.843 and -0.359 e.Å ⁻³

**XXX. [Zn(II)(2,9-dcphen)(H₂O)₃]
(structure e1651)**



Crystallization conditions:



A 2×10^{-2} M stock solution (A) was prepared dissolving 118 mg of 2,9-dcphen with 3 ml of an aqueous solution of Et₃N (1 ml Et₃N in 24 ml H₂O) and adding 19 ml of H₂O.

In a test tube ($\varnothing=1$ cm), were layered (A) 2 ml of the stock solution of 2,9-dcphen*Et₃N, (B) 3 drops of ButOH, 0.5 ml of a H₂O/MeOH 1:1 buffer solution and on top (C) 1 ml of a solution of ZnSiF₆ (7 mg/ml, 3×10^{-2} M) in MeOH. Colourless crystals suitable for XRD analysis were obtained after some days by slow diffusion.

Crystallographic data:

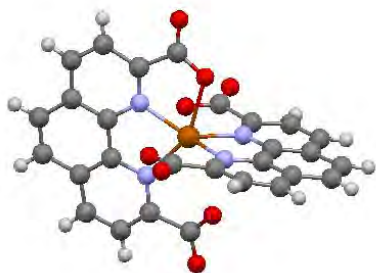
Empirical formula
Formula weight
Temperature
Crystal system
Space group
Unit cell dimensions

Volume
Z
Density (calculated)
Absorption coefficient(μ)
F(000)
Theta range for data collection
Index ranges
Reflections collected
Independent reflections
Completeness to theta = 27.47°
Max. and min. transmission
Data / restraints / parameters
Goodness-of-fit on F²
Final R indices [$I > 2\sigma(I)$]
Largest diff. peak and hole

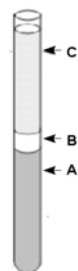
[Zn(C₁₄H₆N₂O₄)(H₂O)₃] * 2(H₂O)

C₁₄ H₁₆ N₂ O₉ Zn
421.67
173(2) K
Orthorhombic
Fddd
a = 7.39270(10) Å $\alpha = 90^\circ$
b = 18.7595(4) Å $\beta = 90^\circ$
c = 46.6794(8) Å $\gamma = 90^\circ$
6473.7(2) Å³
16
1.726 Mg/m³
1.572 mm⁻¹
3440
2.34 to 27.52°
-8 <= h <= 9, -23 <= k <= 24, -60 <= l <= 52
18510
1874 [R(int) = 0.0256]
99.8 %
0.9116 and 0.8337
1874 / 5 / 130
1.088
R1 = 0.0257, wR2 = 0.0714
0.628 and -0.431 e.Å⁻³

**XXXI. [Zn(II)(2,9-dphen)₂]
(structure e1604)**



Crystallization conditions:



In a thin crystallisation tube ($\varnothing=0.6\text{cm}$), were layered in the order (A) 1.5 ml of a $2 \times 10^{-2}\text{M}$ solution of 2,9-dcphen (5.5mg/ml) in DMF, (B) 0.3 ml of a DMF/EtOH 1:1 buffer solution and on top (C) 0.5 ml of a solution of ZnSiF_6 (6 mg/ml, $3 \times 10^{-2}\text{M}$) in MeOH. Colourless crystals suitable for XRD analysis were obtained after some months by slow diffusion.

Crystallographic data:

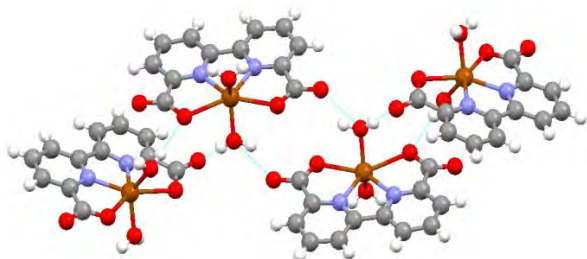
Empirical formula
Formula weight
Temperature
Crystal system
Space group
Unit cell dimensions

Volume
Z
Density (calculated)
Absorption coefficient(μ)
F(000)
Theta range for data collection
Index ranges
Reflections collected
Independent reflections
Completeness to theta = 27.61°
Max. and min. transmission
Data / restraints / parameters
Goodness-of-fit on F2
Final R indices [$I > 2\sigma(I)$]
Largest diff. peak and hole

[Zn(C₁₄H₇N₂O₄)₂]₂*(CH₃OH)*(H₂O)

C121 H190 N20 O36 Zn2
1247.65
173(2) K
Triclinic
P-1
a = 10.5252(5) Å $\alpha = 116.758(2)^\circ$
b = 17.2600(9) Å $\beta = 101.219(2)^\circ$
c = 17.2611(8) Å $\gamma = 100.185(2)^\circ$
2618.3(2) Å³
4
1.583 Mg/m³
1.003 mm⁻¹
1268
2.07 to 27.61° .
-13 $\leq h \leq 11$, -16 $\leq k \leq 22$, -22 $\leq l \leq 21$
16952
10434 [R(int) = 0.0308]
85.6 %
0.9151 and 0.8806
10434 / 3 / 744
1.037
R1 = 0.2109, wR2 = 0.4918
5.065 and -2.536 e.Å⁻³

**XXXII. $[Zn(II)(6,6'-dcbpy)(H_2O)_2]$
(structure e1847)**



Crystallization conditions:



A $3 \cdot 10^{-2} M$ stock solution (A) was prepared dissolving 150 mg of 6,6'-dcbpy with 4 ml of a aqueous solution of Et_3N (1ml Et_3N in 24 ml H_2O) and adding 16 ml of H_2O .

In a test tube ($\varnothing=1cm$), were layered (A) 2 ml of the stock solution of 6,6'-dcbpy* Et_3N , (B) 3 drops of ButOH, 0.5 ml of a $H_2O/MeOH$ 1:1 buffer solution and on top (C) 2 ml of a solution of $ZnSiF_6$ (6 mg/ml, $3 \cdot 10^{-2} M$) in MeOH. Colourless crystals suitable for XRD analysis were obtained after some weeks by slow diffusion.

Crystallographic data:

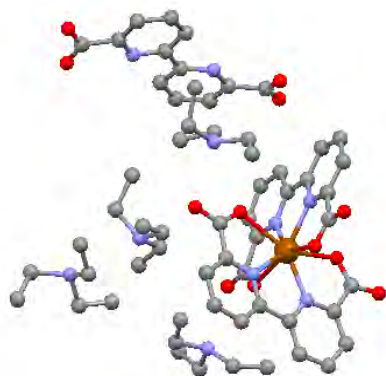
Empirical formula
Formula weight
Temperature
Crystal system
Space group
Unit cell dimensions

Volume
Z
Density (calculated)
Absorption coefficient(μ)
F(000)
Theta range for data collection
Index ranges
Reflections collected
Independent reflections
Completeness to theta = 30.02°
Max. and min. transmission
Data / restraints / parameters
Goodness-of-fit on F2
Final R indices [$I > 2\sigma(I)$]
Largest diff. peak and hole

$[Zn(C_{12}H_6N_2O_4)(H_2O)_2]$

$C_{12}H_{10}N_2O_6Zn$
343.59
173(2) K
Monoclinic
P2(1)/c
 $a = 8.2588(2) \text{ \AA}$ $\alpha = 90^\circ$
 $b = 21.8214(4) \text{ \AA}$ $\beta = 90^\circ$
 $c = 6.95600(10) \text{ \AA}$ $\gamma = 90^\circ$
 $1210.75(4) \text{ \AA}^3$
4
1.885 Mg/m^3
2.061 mm^{-1}
696
1.87 to 30.02° .
 $-11 \leq h \leq 11, -30 \leq k \leq 30, -9 \leq l \leq 9$
16623
3532 [R(int) = 0.0253]
99.8 %
0.9221 and 0.8692
3532 / 4 / 198
1.017
 $R_1 = 0.0248, wR_2 = 0.0622$
0.483 and $-0.342 e \cdot \text{\AA}^{-3}$

**XXXIII. $\{[Zn(II)(6,6'\text{-dcbpy})_2(Et_3N)_4][6,6'\text{-dcbpy}]\}$
(structure e1951)**



Crystallization conditions:



A 3×10^{-2} M stock solution (A) was prepared dissolving 150 mg of 6,6'-dcbpy with 4 ml of an aqueous solution of Et_3N (1 ml Et_3N in 24 ml H_2O) and adding 16 ml of H_2O .

In a test tube ($\varnothing=1$ cm), were layered (A) 2 ml of the stock solution of 6,6'-dcbpy* Et_3N , (B) 3 drops of ButOH, 0.5 ml of a $H_2O/MeOH$ 1:1 buffer solution and on top (C) 1 ml of a solution of $ZnSiF_6$ (6 mg/ml, 3×10^{-2} M) in MeOH. Colourless crystals suitable for XRD analysis were obtained after some months by slow diffusion.

Crystallographic data:

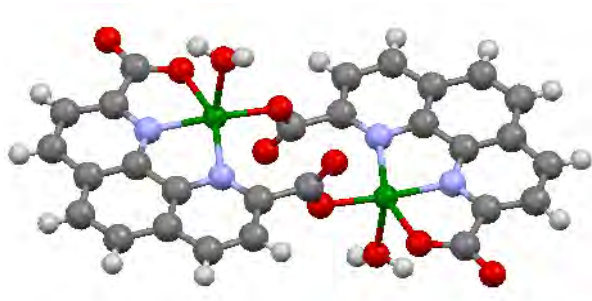
Empirical formula
Formula weight
Temperature
Crystal system
Space group
Unit cell dimensions

Volume
Z
Density (calculated)
Absorption coefficient (μ)
F(000)
Theta range for data collection
Index ranges
Reflections collected
Independent reflections
Completeness to theta = 27.52°
Max. and min. transmission
Data / restraints / parameters
Goodness-of-fit on F2
Final R indices [$I > 2\sigma(I)$]
Largest diff. peak and hole

**$\{[Zn(C_{12}H_6N_2O_4)_2(C_6H_{16}N)_4][C_{12}H_6N_2O_4]\}_2$
* CH_3OH * 11(H_2O)**

C121 H190 N20 O36 Zn2
2613.53
173(2) K
Monoclinic
C2/c
a = 43.9982(9) Å $\alpha = 90^\circ$
b = 10.7926(2) Å $\beta = 106.3140(10)^\circ$
c = 29.7102(5) Å $\gamma = 90^\circ$
13540.0(4) Å³
4
1.282 Mg/m³
0.437 mm⁻¹
5544
1.43 to 27.52°
-51 ≤ h ≤ 56, -14 ≤ k ≤ 13, -38 ≤ l ≤ 38
86622
15516 [R(int) = 0.0661]
99.6 %
0.9743 and 0.9495
15516 / 8 / 835
1.132
R1 = 0.0902, wR2 = 0.2346
1.746 and -0.819 e.Å⁻³

**XXXIV. $[(\text{Cu}(\text{II})(2,9\text{-dphen}))_2(\text{H}_2\text{O})]$
(structure e1642)**



Crystallization conditions:



A $2 \times 10^{-2}\text{M}$ stock solution (A) was prepared dissolving 118 mg of 2,9-dcphen with 3 ml of a aqueous solution of Et_3N (1ml Et_3N in 24 ml H_2O) and adding 19 ml of H_2O .

In a test tube ($\varnothing=1\text{cm}$), were layered (A) 2 ml of the stock solution of 2,9-dcphen* Et_3N , (B) 3 drops of ButOH, 0.5 ml of a $\text{CH}_3\text{CN}/\text{H}_2\text{O}$ 1:1 buffer solution and on top (C) 2 ml of a solution of $\text{Cu}(\text{CH}_3\text{CN})_4\text{PF}_6$ in CH_3CN (7mg/ml, $1.8 \times 10^{-2}\text{M}$). Green crystals suitable for XRD analysis were obtained after some days by slow diffusion.

Crystallographic data:

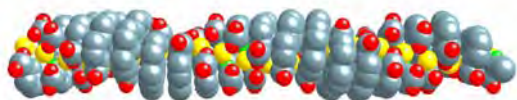
Empirical formula
Formula weight
Temperature
Crystal system
Space group
Unit cell dimensions

Volume
Z
Density (calculated)
Absorption coefficient(μ)
F(000)
Theta range for data collection
Index ranges
Reflections collected
Independent reflections
Completeness to theta = 27.47°
Max. and min. transmission
Data / restraints / parameters
Goodness-of-fit on F2
Final R indices [$I > 2\sigma(I)$]
Largest diff. peak and hole

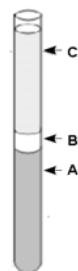
$[\text{Cu}_2(\text{C}_{14}\text{H}_6\text{N}_2\text{O}_4)_2(\text{H}_2\text{O})_2] \cdot 2(\text{H}_2\text{O})$

C28 H20 Cu2 N4 O12
731.56
173(2) K
Monoclinic
P2(1)/c
a = 9.3462(2) Å $\alpha = 90^\circ$.
b = 20.2918(5) Å $\beta = 93.8280(10)^\circ$.
c = 6.9301(2) Å $\gamma = 90^\circ$.
1311.37(6) Å³
2
1.853 Mg/m³
1.702 mm⁻¹
740
2.18 to 30.03°.
-13 ≤ h ≤ 12, -28 ≤ k ≤ 28, -9 ≤ l ≤ 9
32527
3792 [R(int) = 0.0253]
98.7 %
0.8619 and 0.7270
3792 / 4 / 218
1.044
R1 = 0.0263, wR2 = 0.0673
0.535 and -0.489 e.Å⁻¹

XXXV. [Ag(I)(2,9-dcphen)]₈ squeezed
(structure e1587)



Crystallization conditions:



A $3 \cdot 10^{-2}$ M stock solution (A) was prepared dissolving 67 mg of 2,9-dcphen with 49 mg of BAD23 in 8ml of water.

In a test tube ($\varnothing=1$ cm), were layered (A) 1 ml of the stock solution of 2,9-dcphen+BAD23, (B) 0.5 ml of a EtOH/H₂O 1:1 buffer solution and on top (C) 2 ml of a solution of Cu(CH₃CN)₄PF₆ in CH₃CN (7mg/ml, $1.8 \cdot 10^{-2}$ M). 0.5 ml solution of AgPF₆ in EtOH (7mg/ml, $2.7 \cdot 10^{-2}$ M). Off-white crystals suitable for XRD analysis were obtained after few months by slow evaporation.

Crystallographic data:

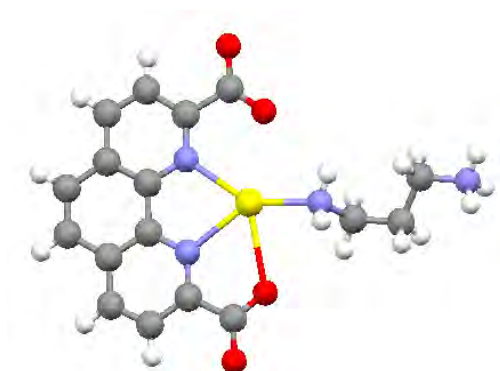
Empirical formula
Formula weight
Temperature
Crystal system
Space group
Unit cell dimensions

Volume
Z
Density (calculated)
Absorption coefficient(μ)
F(000)
Theta range for data collection
Index ranges
Reflections collected
Independent reflections
Completeness to theta = 27.47°
Max. and min. transmission
Data / restraints / parameters
Goodness-of-fit on F2
Final R indices [$I > 2\sigma(I)$]
Largest diff. peak and hole

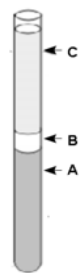
[Ag₈(C₁₄H₇N₂O₄)₇(C₁₄H₈N₂O₄)] (PF₆)

C112 H57 Ag8 F6 N16 O32 P
3146.67
173(2) K
Triclinic
P-1
a = 19.6017(4) Å α = 111.722(2)°
b = 20.8436(5) Å β = 106.382(2)°
c = 20.9263(8) Å γ = 108.8120(10)°
6689.5(3) Å³
2
1.562 Mg/m³
1.240 mm⁻¹
3084
1.68 to 27.54°
-12 ≤ h ≤ 12, -9 ≤ k ≤ 6, -19 ≤ l ≤ 16
79319
30544 [R(int) = 0.0344]
99.0 %
0.9293 and 0.8655
30544 / 1 / 1486
1.139
R1 = 0.0640, wR2 = 0.1895
1.575 and -1.531 e.Å⁻³

**XXXVI. [Ag(I)(2,9-dcphen)(tmda)]
(structure e1654)**



Crystallization conditions:



A $1.1 \cdot 10^{-2}$ M stock solution (A) was prepared dissolving 60 mg of 2,9-dcphen with 45 mg of BAD23 in 20 ml of water.

In a test tube ($\varnothing=1$ cm), were layered (A) 1 ml of the stock solution of 2,9-dcphen+BAD23, (B) 0.3 ml of a EtOH/H₂O 1:1 buffer solution and on top (C) 1 ml of a solution of Cu(CH₃CN)₄PF₆ in CH₃CN (7mg/ml, $1.8 \cdot 10^{-2}$ M). 0.5 ml solution of AgX₄ (X= BF₄, PF₆, AsF₆, SbF₆) in EtOH (2 mg/ml, $1 \cdot 10^{-2}$ M). Yellow needles suitable for XRD analysis were obtained after few days by slow diffusion.

Crystallographic data:

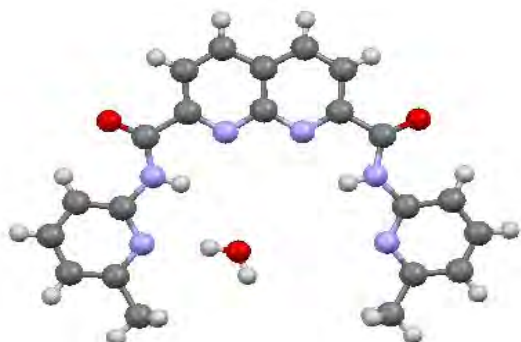
Empirical formula	C ₁₇ H ₂₄ Ag N ₄ O ₁₁
Formula weight	568.27
Temperature	173(2) K
Crystal system	Orthorhombic
Space group	P2(1)2(1)2(1)
Unit cell dimensions	a = 6.82400(10) Å α = 90° b = 15.8512(2) Å β = 90° c = 20.8159(3) Å γ = 90°
Volume	2251.63(5) Å ³
Z	4
Density (calculated)	1.676 Mg/m ³
Absorption coefficient(μ)	0.960 mm ⁻¹
F(000)	1156
Theta range for data collection	1.96 to 27.52°
Index ranges	-8<=h<=8, -20<=k<=13, -27<=l<=27
Reflections collected	18085
Independent reflections	5160 [R(int) = 0.0210]
Completeness to theta = 27.52°	99.6 %
Max. and min. transmission	0.9718 and 0.9101
Data / restraints / parameters	5160 / 0 / 299
Goodness-of-fit on F ²	1.036
Final R indices [I>2sigma(I)]	R1 = 0.0254, wR2 = 0.0771
Absolute structure (Flack) parameter	-0.02(2)
Largest diff. peak and hole	0.527 and -0.245 e.Å ⁻³

[Ag(C₁₄H₆N₂O₄)(C₃H₁₁N₂)] *7(H₂O)

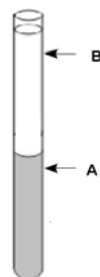
Crystal structures

Chapter IV

XXXVII. 2,7-mpanaphthy+H₂O
(structure e1203)



Crystallization conditions:

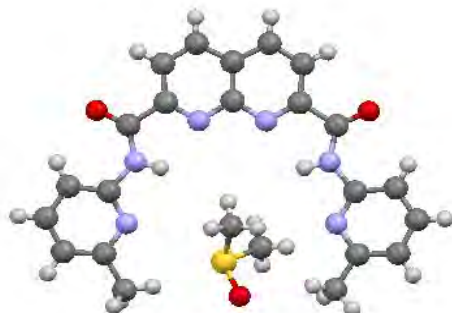


In a thin crystallization tube ($\varnothing=0.6\text{cm}$), were layered (A) a CHCl_3 solution (0.5ml) of 2,7-mpanaphthy (1.5 mg) and on top (B) 0.5 ml of methanol. Yellow crystals were obtained by slow diffusion after few days.

Crystallographic data:



Empirical formula	C ₂₂ H ₂₂ N ₆ O ₄
Formula weight	434.46
Temperature	173(2) K
Crystal system	Monoclinic
Space group	C2/c
Unit cell dimensions	a = 25.0626(13) Å $\alpha = 90^\circ$. b = 11.6160(7) Å $\beta = 96.935(3)^\circ$. c = 7.3518(5) Å $\gamma = 90^\circ$.
Volume	2124.6(2) Å ³
Z	4
Density (calculated)	1.358 Mg/m ³
Absorption coefficient(μ)	0.097 mm ⁻¹
F(000)	912
Theta range for data collection	3.02 to 27.50°.
Index ranges	-32<=h<=32, -15<=k<=12, -9<=l<=9
Reflections collected	7141
Independent reflections	2351 [R(int) = 0.0418]
Completeness to theta = 27.52°	96.2 %
Max. and min. transmission	0.9933 and 0.9894
Data / restraints / parameters	2351 / 3 / 153
Goodness-of-fit on F ²	1.014
Final R indices [I>2sigma(I)]	R1 = 0.0584, wR2 = 0.1484
Largest diff. peak and hole	0.285 and -0.240 e.Å ⁻³

XXXVIII. 2,7-mpanaphthy+DMSO
(structure e1708)**Crystallization conditions:**

In a thin crystallization tube ($\varnothing=0.6\text{cm}$), were layered (A) a DMSO solution (1ml) of 2,7-mpanaphthy (15 mg) and on top (B) 0.5 ml of methanol. Yellow crystals were obtained by slow diffusion after few weeks.

Crystallographic data:

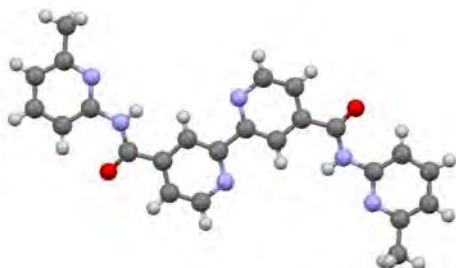
Empirical formula
Formula weight
Temperature
Crystal system
Space group
Unit cell dimensions

Volume
Z
Density (calculated)
Absorption coefficient(μ)
F(000)
Theta range for data collection
Index ranges
Reflections collected
Independent reflections
Completeness to theta = 27.55°
Max. and min. transmission
Data / restraints / parameters
Goodness-of-fit on F2
Final R indices [$I > 2\sigma(I)$]
Largest diff. peak and hole

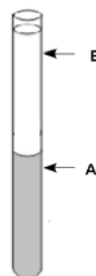
[C₂₂H₁₈N₆O₂]*DMSO

C₂₄ H₂₄ N₆ O₃ S
476.55
173(2) K
Triclinic
P-1
a = 10.2331(5) Å $\alpha = 111.926(2)^\circ$
b = 11.0490(3) Å $\beta = 105.734(2)^\circ$
c = 11.9488(3) Å $\gamma = 98.614(2)^\circ$
1157.66(7) Å³
2
1.367 Mg/m³
0.179 mm⁻¹
500
1.97 to 27.55°
-13 ≤ h ≤ 13, -14 ≤ k ≤ 14, -15 ≤ l ≤ 15
17918
2351 [R(int) = 0.0418]
98.7 %
0.9858 and 0.9788
5271 / 0 / 311
1.009
R1 = 0.0584, wR2 = 0.1549
0.568 and -0.568 e.Å⁻³

XXXIX. 4,4'-mpabpy
(structure e1793)



Crystallization conditions:



In a thin crystallization tube ($\varnothing=0.6\text{cm}$), were layered (A) an acetone solution (1ml) of 4,4'-mpabpy (2 mg) and on top (B) 0.7 ml of acetonitrile. Colourless crystals suitable for XRD analysis were obtained by slow diffusion after few days.

Crystallographic data:

[C₂₄H₂₀N₆O₂]

Empirical formula

C₂₄ H₂₀ N₆ O₂

Formula weight

424.46

Temperature

173(2) K

Crystal system

Orthorhombic

Space group

Pbca

Unit cell dimensions

$a = 12.0052(6) \text{ \AA}$ $\alpha = 90^\circ$.

$b = 10.0061(6) \text{ \AA}$ $\beta = 90^\circ$.

$c = 16.8547(8) \text{ \AA}$ $\gamma = 90^\circ$.

$2024.67(18) \text{ \AA}^3$

Volume

4

Z

1.392 Mg/m^3

Density (calculated)

0.093 mm^{-1}

Absorption coefficient(μ)

888

F(000)

$2.42 \text{ to } 27.24^\circ$.

Theta range for data collection

$-15 \leq h \leq 13, -12 \leq k \leq 11, -21 \leq l \leq 17$

Index ranges

8914

Reflections collected

2256 [R(int) = 0.0298]

Independent reflections

99.7 %

Completeness to theta = 27.52°

Max. and min. transmission

0.9981 and 0.9954

Data / restraints / parameters

2256 / 0 / 146

Goodness-of-fit on F²

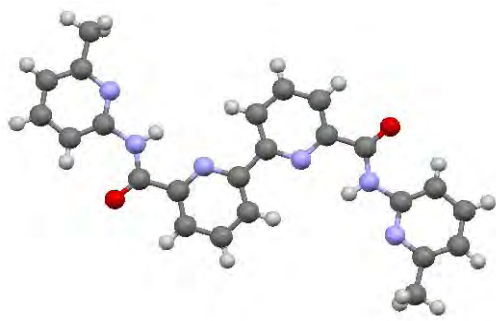
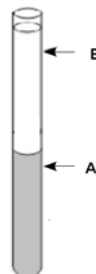
1.076

Final R indices [$I > 2\sigma(I)$]

$R1 = 0.0509, wR2 = 0.1194$

Largest diff. peak and hole

$0.269 \text{ and } -0.256 \text{ e.\AA}^{-3}$

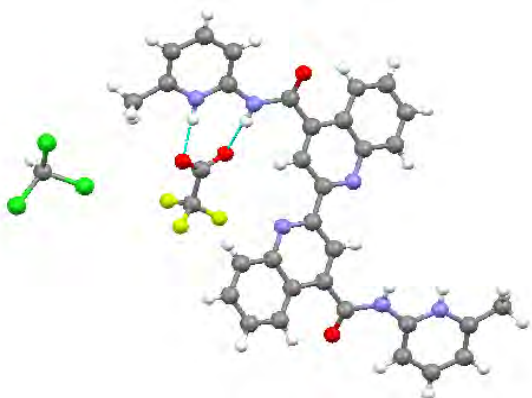
XL. 6,6'-mpabpy
(structure e1846)**Crystallization conditions:**

In a thin crystallization tube ($\varnothing=0.6\text{cm}$), were layered (A) a DMSO solution (2ml) of 6,6'-mpabpy (4 mg) and on top (B) 0.7 ml of ethanol. Colourless crystals suitable for XRD analysis were obtained by slow diffusion after few days.

Crystallographic data:**[C₂₄H₂₀N₆O₂]*4(H₂O)**

Empirical formula	C ₂₄ H ₂₈ N ₆ O ₆
Formula weight	460.49
Temperature	173(2) K
Crystal system	Monoclinic
Space group	C2/c
Unit cell dimensions	a = 29.9060(15) Å α = 90° b = 3.8196(2) Å β = 91.312(2)° c = 19.9862(10) Å γ = 90°
Volume	2282.4(2) Å ³
Z	4
Density (calculated)	1.340 Mg/m ³
Absorption coefficient(μ)	0.094 mm ⁻¹
F(000)	968
Theta range for data collection	2.04 to 27.00°
Index ranges	-38<=h<=38, -4<=k<=4, -23<=l<=24
Reflections collected	6805
Independent reflections	2406 [R(int) = 0.0263]
Completeness to theta = 27.52°	98.1 %
Max. and min. transmission	0.9953 and 0.9934
Data / restraints / parameters	2406 / 0 / 165
Goodness-of-fit on F ²	1.186
Final R indices [I>2σ(I)]	R1 = 0.0762, wR2 = 0.2272
Largest diff. peak and hole	0.661 and -0.461 e.Å ⁻³

**XLI. [4,4'-mpaBQ][CF₃COOH]
(structure e1888)**



Crystallization conditions:

The ligand 4,4'-mpaBQ (20 mg) was dissolved in a minimum amount of a CDCl₃/TFA 20:1 solution (1 ml) to and final pH≈6.

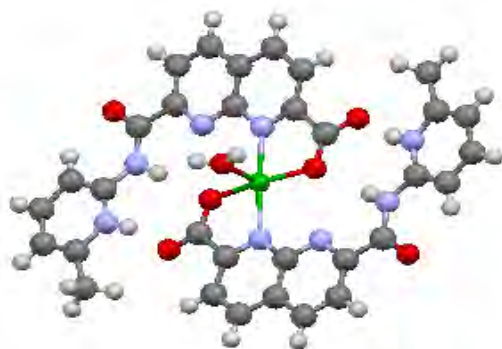
The yellow solution was transferred into a thin tube (ø=0.6cm) and left evaporate. Yellow crystals suitable for XRD analysis were obtained after three days.

Crystallographic data:

[C₃₂H₂₆N₆O₂]*2(C₂F₃O₂)*2(CHCl₃)

Empirical formula	C ₃₈ H ₂₈ Cl ₆ F ₆ N ₆ O ₆
Formula weight	991.36
Temperature	173(2) K
Crystal system	Triclinic
Space group	P-1
Unit cell dimensions	a = 8.1094(7) Å α = 103.533(4)° b = 10.4053(12) Å β = 106.933(4)° c = 13.3050(19) Å γ = 91.546(4)°
Volume	1038.72(19) Å ³
Z	1
Density (calculated)	1.585 Mg/m ³
Absorption coefficient(μ)	0.495mm ⁻¹
F(000)	502
Theta range for data collection	2.27 to 27.20°
Index ranges	-10<=h<=10, -13<=k<=13, -16<=l<=16
Reflections collected	13123
Independent reflections	4470 [R(int) = 0.0219]
Completeness to theta = 27.20°	98.8 %
Max. and min. transmission	0.9902 and 0.9568
Data / restraints / parameters	4470/ 0 / 281
Goodness-of-fit on F ²	1.040
Final R indices [I>2σ(I)]	R1 = 0.0739, wR2 = 0.1830
Largest diff. peak and hole	0.957 and -0.785 e.Å ⁻³

**XLII. $[\text{Cu}(\text{II})(2,7\text{-mono}(\text{mpanaphthy}))_2]$
(structure e1441)**



Crystallization conditions:



In a test tube ($\varnothing=1\text{cm}$) were gently layered in the order: **(A)** 0.5 ml of a solution of 2,7-mpanaphthy (1.5 mg) in of THF, **(B)** 0.2 ml of a THF/EtOH 1:1 buffer solution and **(C)** 0.5 ml of an ethanolic solution of $\text{Cu}(\text{II})(\text{CF}_3\text{SO}_3)_2$ (1 mg). Green crystals suitable for XRD analysis were obtained after few weeks by slow diffusion.

Crystallographic data:

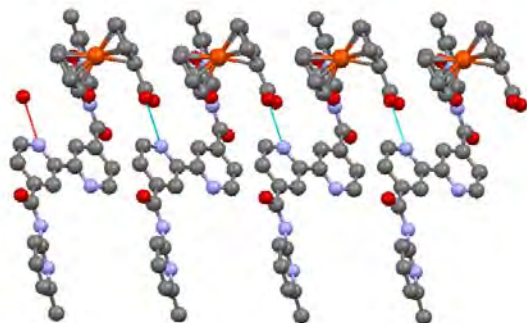
Empirical formula
Formula weight
Temperature
Crystal system
Space group
Unit cell dimensions

Volume
Z
Density (calculated)
Absorption coefficient(μ)
F(000)
Theta range for data collection
Index ranges
Reflections collected
Independent reflections
Completeness to theta = 27.47°
Max. and min. transmission
Data / restraints / parameters
Goodness-of-fit on F2
Final R indices [$I > 2\sigma(I)$]
Largest diff. peak and hole

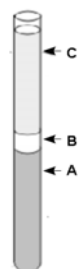
$[\text{Cu}(\text{C}_{16}\text{H}_{12}\text{N}_4\text{O}_3)_2(\text{H}_2\text{O})]^*2(\text{CF}_3\text{SO}_3)$

C34 H26 Cu F6 N8 O13 S2
996.29
173(2) K
Monoclinic
P2(1)/c
 $a = 16.899(2) \text{ \AA}$ $\alpha = 90^\circ$.
 $b = 14.720(2) \text{ \AA}$ $\beta = 111.770(4)^\circ$.
 $c = 16.558(2) \text{ \AA}$ $\gamma = 90^\circ$.
 $3825.4(9) \text{ \AA}^3$
4
1.730 Mg/m^3
 0.788 mm^{-1}
2020
2.02 to 27.54°.
 $-21 \leq h \leq 15, -17 \leq k \leq 19, -20 \leq l \leq 21$
25575
8757 [R(int) = 0.0556]
99.4 %
0.9324 and 0.9113
8757 / 2 / 583
0.987
 $R1 = 0.1087, wR2 = 0.2126$
1.509 and $-1.054 \text{ e.\AA}^{-3}$

**XLIII. [Ferroxdc][4,4'-mpabpy]
(structure e1810)**



Crystallization conditions:



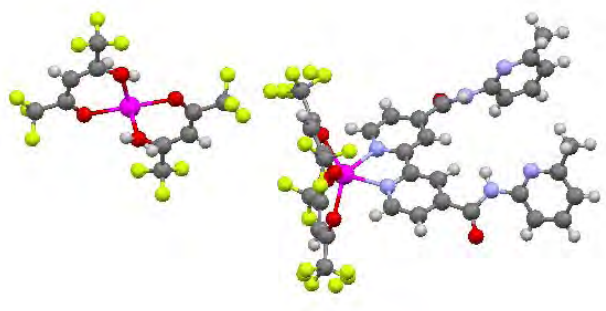
In a test tube ($\varnothing=0.6\text{cm}$) were gently layered in the order: **(A)** 0.5 ml of a 0.005M stock solution of 4,4'-mpabpy (42 mg in 20 ml of CHCl_3) in CHCl_3 , **(B)** 0.2 ml of a $\text{CHCl}_3/\text{EtOH}$ 1:1 buffer solution and **(C)** 0.5 ml of a 0.0025M solution of Ferrocenedicarboxylic acid in *iso*-propanol.

Orange, needle shaped crystals suitable for XRD analysis were obtained after some weeks by slow diffusion and evaporation.

Crystallographic data:

Empirical formula	$\text{C}_{36}\text{H}_{30}\text{Fe}_2\text{N}_6\text{O}_6$
Formula weight	698.51
Temperature	173(2) K
Crystal system	Monoclinic
Space group	$P2(1)/n$
Unit cell dimensions	$a = 7.7999(4) \text{ \AA}$ $\alpha = 90^\circ$ $b = 17.1760(7) \text{ \AA}$ $\beta = 91.70(2)^\circ$ $c = 22.7896(10) \text{ \AA}$ $\gamma = 90^\circ$
Volume	$3051.8(2) \text{ \AA}^3$
Z	4
Density (calculated)	1.520 Mg/m^3
Absorption coefficient(μ)	0.555 mm^{-1}
F(000)	1448
Theta range for data collection	2.37 to 27.54°
Index ranges	$-9 \leq h \leq 10$, $-21 \leq k \leq 21$, $-29 \leq l \leq 26$
Reflections collected	30930
Independent reflections	6872 [R(int) = 0.0431]
Completeness to theta = 27.54°	97.7 %
Max. and min. transmission	0.9890 and 0.9364
Data / restraints / parameters	6872 / 0 / 446
Goodness-of-fit on F ²	1.024
Final R indices [I > 2 σ (I)]	R1 = 0.0402, wR2 = 0.0976
Largest diff. peak and hole	0.404 and $-0.390 \text{ e.\AA}^{-3}$

**XLIV. $[\text{Mn}(\text{hfacac})_2(4,4'\text{-mpabpy})]$
 $[\text{Mn}(\text{hfacac})_2(\text{H}_2\text{O})]$
 (structure e1861)**



Crystallization conditions:



In a test tube ($\varnothing=0.6\text{cm}$) were gently layered in the order: **(A)** 1 ml of a 2.4×10^{-3} M stock solution of 4,4'-mpabpy (30 mg in 30 ml of CHCl_3), **(B)** 0.2 ml of a $\text{CHCl}_3/\text{MeOH}$ 1:1 buffer solution and **(C)** 0.5 ml of a 10^{-2} M solution of $\text{Mn}(\text{hfacac})_2$.

Yellow crystals suitable for XRD analysis were obtained after some weeks by slow diffusion and evaporation.

Crystallographic data:

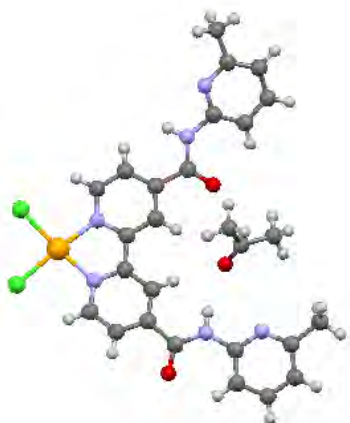
Empirical formula
 Formula weight
 Temperature
 Crystal system
 Space group
 Unit cell dimensions

 Volume
 Z
 Density (calculated)
 Absorption coefficient(μ)
 F(000)
 Theta range for data collection
 Index ranges
 Reflections collected
 Independent reflections
 Completeness to theta = 27.52°
 Max. and min. transmission
 Data / restraints / parameters
 Goodness-of-fit on F2
 Final R indices [$I > 2\sigma(I)$]
 Largest diff. peak and hole

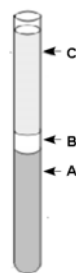
**$[\text{Mn}^{\text{II}}(\text{C}_{24}\text{H}_{20}\text{N}_6\text{O}_2)(\text{C}_5\text{HF}_6\text{O}_2)_2]_2$
 $[\text{Mn}^{\text{II}}(\text{C}_5\text{HF}_6\text{O}_2)_2(\text{H}_2\text{O})_2]$**

C78 H50 F36 Mn3 N12 O18
 2292.12
 173(2) K
 Triclinic
 P-1
 a = 11.5386(3) Å $\alpha = 100.0830(10)^\circ$.
 b = 11.6277(3) Å $\beta = 105.1310(10)^\circ$.
 c = 17.9883(4) Å $\gamma = 94.0770(10)^\circ$.
 2276.40(10) Å³
 1
 1.672 Mg/m³
 0.556 mm⁻¹
 1145
 1.20 to 27.52°.
 -14 ≤ h ≤ 9, -14 ≤ k ≤ 15, -23 ≤ l ≤ 23
 23177
 10216 [R(int) = 0.0289]
 97.5 %
 0.9674 and 0.9465
 10216 / 2 / 726
 1.059
 R1 = 0.0698, wR2 = 0.1684
 1.200 and -0.843 e.Å⁻³

**XLV. $[Pt(II)(4,4'-mpabpy)Cl_2]$
(structure e1972)**



Crystallization conditions:



In a test tube ($\varnothing=0.6\text{cm}$) were gently layered in the order: **(A)** 1 ml of a $2.4 \cdot 10^{-3}\text{M}$ stock solution of 4,4'-mpabpy (30 mg in 30 ml of acetone), **(B)** 0.2 ml of a acetone/MeOH 1:1 buffer solution and **(C)** 0.3 ml of a 10^{-2}M solution of $[Pt(\text{bis-benzonitrile})Cl_2]$.

Orange crystals suitable for XRD analysis were obtained after some weeks by slow diffusion and evaporation.

Crystallographic data:

Empirical formula
Formula weight
Temperature
Crystal system
Space group
Unit cell dimensions

Volume
Z
Density (calculated)
Absorption coefficient(μ)
F(000)
Theta range for data collection
Index ranges
Reflections collected
Independent reflections
Completeness to theta = 27.53°
Max. and min. transmission
Data / restraints / parameters
Goodness-of-fit on F2
Final R indices [$I > 2\sigma(I)$]
Largest diff. peak and hole

$[Pt^{II}(C_{24}H_{20}N_6O_2)Cl_2] \cdot (C_3H_6O)$

C₂₇ H₂₆ Cl₂ N₆ O₃ Pt
748.53
173(2) K
Orthorhombic
Pbca
a = 11.3684(3) Å $\alpha = 90^\circ$
b = 20.4043(5) Å $\beta = 90^\circ$
c = 23.2241(6) Å $\gamma = 90^\circ$
5387.2(2) Å³
8
1.846 Mg/m³
5.450 mm⁻¹
2928
2.18 to 27.53° .
 $-14 \leq h \leq 14, -23 \leq k \leq 26, -30 \leq l \leq 29$
60487
6199 [R(int) = 0.0283]
99.9 %
0.6696 and 0.6118
6199 / 0 / 356
1.059
R1 = 0.0261, wR2 = 0.0727
1.649 and -0.500 e.Å⁻³

Abbreviations:

Å	Angstrom
Ac	Acetate
But ₃ N	tributylamine
ButOH	butanol
°C.....	degree Celsius
CHCl ₃	chloroform
CH ₂ Cl ₂	dichloromethane
CH ₂ CN	acetonitrile
cm.....	centimeter
COSY.....	COrrrelation SpectroscopY
d.....	distance
δ.....	chemical shift
§	paragraph
DMF	dimethylformamide
DMSO.....	dimethylsulfoxide
Dpppe.....	1,5- bis(diphenylphosphino)pentane
en.....	Ethylenediamine
eq.....	equivalent
ESI-MS.....	Electro Spray Ionization Mass Spectrometry
Et.....	ethyl
Et ₃ N.....	triethylamine
EtOH.....	ethanol
Fig.....	figure
Ferroxdc.....	Ferrocene dicarboxylic acid
FTIR.....	Fourier Transform Infrared Spectroscopy
g, mg.....	gram, milligram
h	hour
hfac.....	hexafluoroacetylacetonate
HRMS.....	High Resolution Mass Spectrometry
Hz.....	Hertz
IR.....	Infra-Red spectroscopy
J.....	Joule
K.....	degree Kelvin
Kcal.....	Kilo calorie
KJ.....	Kilo Joule
L.....	Ligand
LDA.....	Lithium DiisopropylAmide
M.....	Metal
m/z.....	mass-to-charge ratio
Me.....	Methyl
MeOH.....	Methanol
MHz.....	Mega Hertz
ml.....	milliliter
	mm.....

mmol, mol.....	millimole, mole
nm.....	nanometer
NMR.....	Nuclear Magnetic Resonance
∅.....	diameter
ppm.....	parts per million
Ph.....	phenyl
Py.....	pyridine
r.t.....	room temperature
TFA.....	Trifluoroacetic acid
THF.....	Tetrahydrofuran
tmda.....	1,3-diaminopropane or trimethylenediamine
TMEDA.....	Tetramethylethylenediamine
TLC.....	Thin Layer Chromatography
Trf.....	Triflate
TsOH.....	tosylate
UV-vis.....	UltraViolet-visible

Communications

List of publications and communications

Publications :

1) Molecular tectonics: an example of design and not serendipity;

Cristina Carpanese, Sylvie Ferlay, Nathalie Kyritsakas Marc Henry and Mir Wais Hosseini;
Chem. Comm., **2009**, 6786-6788

Poster Communications:

1) H-bonded molecular networks based on metallic anionic carboxylate derivatives and bisamidinium cation; *Cristina Carpanese, Sylvie Ferlay, Nathalie Kyritsakas, Mir Wais Hosseini*, 1st International Conference on Metal-Organic Frameworks and Open Framework Compounds, 8-10th October 2008, Augsburg (Germany)

Oral Communications :

1) Strategy for H-bonded Networks; *Cristina Carpanese, Sylvie Ferlay, Mir Wais Hosseini*, First FuMaSSEC Meeting, 29-30th June 2007, Barcelona (Spain)

2) Progress in Hybrid H-bonded Molecular Networks, *Cristina Carpanese, Sylvie Ferlay, Mir Wais Hosseini*, Second FuMaSSEC Meeting, 26-27 November 2007, Strasbourg (France)

3) Progress in Hybrid H-bonded Molecular Networks, *Cristina Carpanese, Sylvie Ferlay, Mir Wais Hosseini*, Third FuMaSSEC Meeting, 30th June-1st July 2008, Nottingham (UK)

4) H-bonded molecular networks based on metallic anionic carboxylate derivatives and bisamidinium cation, *Cristina Carpanese, Sylvie Ferlay, Mir Wais Hosseini*, Second Karlsruhe-Strasbourg bilateral meetings on progress in Supramolecular Chemistry, 5th December 2008, Karlsruhe (Germany)

5) Playing with H-bond and coordination bond for building molecular networks, *Cristina Carpanese, Sylvie Ferlay, Mir Wais Hosseini*, Fourth FuMaSSEC Meeting, 19-20th April 2009, Barcelona (Spain)

Abstract

Based on concepts developed in the area of *molecular tectonics*, this work focused on the design, synthesis and structural investigations of supramolecular architectures generated under self-assembling conditions. In particular the design and generation of new functional hybrid organic/inorganic H-bonded networks based on coordination bond has attracted considerable interest in the recent years. On the other hand, owing to its selectivity, directivity as well as reversibility, hydrogen bonding is imposing itself as one of the most important strategy in crystal engineering. In particular, it has been shown that the simultaneous use of directional H-bonding and charge-charge electrostatic interactions leads to the formation of robust networks. The incorporation of transition metals into supramolecular architectures attracts interest because it offers the possibility of introducing redox, optical and magnetic properties.

In the first part of this work, new metallic complexes, based on mono- and di-carboxylate ligands derived from 2,2'-bipyridine or 4,7-phenanthroline, have been synthesized and employed as tectons for the preparation of hybrid networks. Following a one-pot strategy, a combination of charge-assisted H- and coordination-bonds, a tetra components system composed of a dicationic bis-amidinium tecton, the dianionic 1,10-phenanthroline-4,7-dicarboxylate, Ag^+ cation and XF_6^- ($\text{X} = \text{P}, \text{As}, \text{Sb}$) anion was shown to generate 2-D *isostructural* networks. Furthermore, a tri components system composed of a dicationic bis-amidinium tecton, the dianionic 1,10-phenanthroline-4,7-dicarboxylate and Cu^{2+} cation was shown to lead to the formation of 3-D three-fold interpenetrated network. In the second part, the formation of hybrid networks was explored upon combining ligands 2,2'-bipyridine-6,6'-dicarboxylic acid or 4,7-phenanthroline-2,9-dicarboxylic acid with Zn(II) , Cu(I/II) and Ag(I) cations in the presence or absence of an organic base. This strategy afforded an interesting 1D coordination network based on silver-silver interactions. In the third and final part, new bis-chelating symmetric ligands based on 2,2'-bipyridine, 2,2'-biquinoline or 1,8-naphthyridine backbones bearing polypyridyl moieties were designed and prepared. These ligands possessing both coordination sites for metal binding and recognition sites for carboxylic acid group, were used as building block for the construction of organic and hybrid networks.

Keywords

Molecular tectonics, crystal engineering, Supramolecular chemistry, self-assembly, coordination networks, hybrid networks, amidinium, bipyridine, phenanthroline.

Résumé

En utilisant les concepts de la "*tectonique moléculaire*", ce travail a été centré sur la conception, la synthèse ainsi que l'étude structurale d'architectures supramoléculaires obtenues dans des conditions d'auto-assemblage. La conception et l'obtention de réseaux moléculaires fonctionnels hybrides, organiques/inorganiques, obtenus à partir de motifs de reconnaissance basés sur les liaisons hydrogène ainsi que les liaisons de coordination, ont été particulièrement développés ces dernières années. Grâce à sa sélectivité, sa directionnalité, ainsi que sa réversibilité, la mise en place de la liaison hydrogène est une stratégie pertinente dans le domaine de l'ingénierie cristalline. Ainsi, en utilisant de manière simultanée la liaison hydrogène et des interactions électrostatiques, il est possible de créer des réseaux moléculaires robustes. L'introduction de métaux de transition dans de telles assemblées supramoléculaires est un atout, puisque cela permet d'apporter des propriétés nouvelles au système : redox, optiques et/ou propriétés magnétiques.

Dans la première partie de ce travail, de nouveaux complexes métalliques, obtenus à partir de ligands mono et di-carboxylate dérivés de 2,2'-bipyridine ou de 4,7-phenanthroline, ont été synthétisés et utilisés comme tectons pour la préparation de réseaux moléculaires hybrides. En suivant un mode de synthèse "one-pot" et en utilisant simultanément la liaison hydrogène assistée par des interactions charges-charge et la liaison de coordination, des architectures bidimensionnelles *isostructurales* à quatre composants ont été obtenues en combinant un tecton dianionique 1,10-phenanthroline-4,7-dicarboxylate, un dication de type bisamidinium, le cation Ag^+ ainsi que des anions XF_6^- ($\text{X} = \text{P}, \text{As}, \text{Sb}$). De plus, une architecture tridimensionnelle triplement interpénétrée a été formée à partir de trois composants (1,10-phenanthroline-4,7-dicarboxylate, dication bisamidinium et le cation Cu^{2+}). Dans la deuxième partie, la coordination des cations métalliques Zn(II) , Cu(I/II) and Ag(I) par les ligands 2,2'-bipyridine-6,6'-acide dicarboxylique ou 4,7-phenanthroline-2,9-acide dicarboxylique ainsi que la formation de réseaux moléculaires en présence ou non d'une base ont été étudiées. Cette investigation a conduit à la formation d'un réseau de coordination monodimensionnel basé sur des interactions Ag-Ag. Enfin, dans une troisième et dernière partie, nous nous sommes intéressés à une nouvelle famille de ligands symétriques basés sur des squelettes de type 2,2'-bipyridine, 2,2'-biquinoline ou 1,8-naphthyridine portant des groupes pyridyls. La particularité de ces ligands consiste en la présence simultanée de sites de coordination pour les métaux et un motif de reconnaissance pour le groupe carboxylique, particulièrement utile pour la formation de réseaux hybrides.

Mots clés

Tectonique moléculaire, ingénierie cristalline, chimie supramoléculaire, auto-assemblage, réseaux de coordination, architectures hybrides, amidinium, bipyridine, phenanthroline.